NANOPARTICLE DELIVERY OF DNA, SIRNA, AND MIRNA FOR THE TREATMENT OF GLIOBLASTOMA

by

Kristen L. Kozielski

A dissertation submitted to Johns Hopkins University in conformity with the requirements for the degree of Doctor of Philosophy

Baltimore, MD

September 2016

The overall goal of the thesis is to explore novel nanotechnologies for the treatment of brain cancer. In particular, we used nanoparticles to deliver nucleic acid cargoes to glioblastoma (GBM) with the goal of altering cancer gene expression in a way that can reduce the tumor's proliferative capacity, and ultimately kill the tumor cells. In **Aim 1**, we used poly(beta-amino ester) (PBAE) nanoparticles to deliver a plasmid encoding herpes simplex virus thymidine kinase (HSVtk) to the tumor cells. Our goal was to systemically deliver the inactive prodrug ganciclovir (GCV), which would be activated to its cell-killing form upon phosphorylation via HSVtk in the brain. We examined the ability of PBAE nanoparticles to deliver HSVtk to GBM *in vitro* and *in vivo*, and assessed the effect of the HSVtk/GCV therapeutic system to kill GBM and prolong survival in an orthotopic model of GBM. In **Aim 2**, our goal was to engineer PBAE nanoparticles for siRNA delivery by designing a novel, bioreducible PBAE nanoparticle that would biodegrade and release siRNA in the cytosol, its subcellular target location. We examined varying polymer properties to optimize siRNA delivery to GBM, and were able to show effective gene knockdown even with very low siRNA doses. This motivated the work presented in **Aim 3**, in which we used bioreducible PBAEs to codeliver multiple genes targeting GBM migration and proliferation. We also demonstrated that bioreducible PBAEs selectively deliver siRNA to brain cancer cells. We then used siRNA codelivery to show gene knockdown and a reduction in tumor growth *in vivo*. Finally in **Aim 4**, we use bioreducible PBAE nanoparticles to deliver microRNAs (miRNAs) to GBM. We were able to show that miRNA delivery was able to reduce GBM's stem like and tumor propogating phenotype both *in vitro* and *in vivo*, and that we can reduce tumor size and aggression.

Thesis Committee

Jordan J. Green (primary advisor, reader)
Assitant Professor, Departments of Biomedical Engineering, Materials Science and Engineering, Neurosurgery, Ophthalmology, and Oncology
Johns Hopkins University School of Medicine

Jennifer H. Elisseeff (reader)
Professor, Departments of Biomedical Engineering and Ophthalmology
Johns Hopkins University School of Medicine

Alfredo Quiñones-Hinojosa
Professor, Departments of Neurological Surgery and Oncology, Cellular and Molecular Medicine, and Neuroscience
Johns Hopkins University School of Medicine

Kevin Yarema
Associate Professor, Department of Biomedical Engineering
Johns Hopkins University School of Medicine

Hai-Quan Mao
Professor, Departments of Materials Science and Engineeirng, and Biomedical Engineering
Johns Hopkins University.

Acknowledgements

The work presented in this thesis has depended on collaboration with other members of the Green group as well as other collaborators within the Johns Hopkins community. I would first like to thank my primary advisor and mentor, Dr. Jordan J. Green. His encouragement and guidance as I began graduate school gave me the confidence to create the bioreducible polymers that make up the bulk of my thesis. I appreciate the trust and responsibility he gave me, which allowed me to take on roles not typical of graduate students. Throughout the last five years, I truly have felt that my training and professional development was a high priority to him, and I have no doubt this will benefit my career progression for years to come.

I would also like to thank Dr. Alfredo Quiñones-Hinojosa, or "Dr. Q." As a collaborator, Dr. Q went above and beyond, acting as a *de facto* secondary advisor. Dr. Q inspires me to address problems with a clinical setting in mind, and has given me invaluable experience in grant and fellowship writing. I will always cherish our shared group meetings, and appreciate how such an internationally prestigious neurosurgeon would genuinely listen and be excited to hear my ideas. Having Dr. Q as a secondary mentor also meant I was given a secondary lab, including Dr. Hugo Guerrero-Cazares, Dr. Paula Schiapparelli, Dr. Alejandro Ruiz-Valls, Sagar Shah, Akhila Denduluri, and Rawan Al-Kharboosh, Working in collaboration with brain cancer biologists enabled me to see our goals from a different perspective, and provided me with a great source of advice over the past years.

The completion of my thesis work would have not been possible without several other collaborators. Dr. John Laterra, Dr. Henry Brem, Betty Tyler, and the post-docs in their laboratories, Dr. Hernando Lopez-Bertoni, Dr. Bachchu Lal, Dr. Antonella Mangraviti, and Dr. Yuan Wang were integral to the aims within this thesis providing insight in the biological aspects

of brain cancer. In particular, I'd like to thank Hernando, whose work showing the activity of micro RNAs in glioblastoma led to the therapies designed and tested in Chapter 6.

Additionally, I have been fortunate to work with other collaborators whose projects extend beyond the scope of this thesis. I would like to thank Dr. Ben Hung in the laboratory of Dr. Warren Grayson, Dr. Xiaowei Li in the laboratory of Dr. Hai-Quan Mao, and Dr. Johan Karlsson, Dr. Yu-Ja Huang, and Dr. Amanda Levy in the laboratory of Dr. Peter Searson.

I would also like to thank the remaining members of my thesis committee for their advice and guidance throughout the development of my thesis. Dr. Hai-Quan Mao, Dr. Kevin Yarema, and in particular Dr. Jennifer Elisseeff, who was also my undergraduate principal investigator, all served as excellent teachers and sources of inspiration throughout my graduate years.

I could not have been luckier to have chosen the Green lab as my lab-family throughout the last five years. As a younger student, the earlier Green lab members, Dr. Nupura Bhise, Dr. Joel Sunshine, Dr. Stephany Tzeng, Dr. Ron Shmueli, and Dr. Corey Bishop were incredible mentors and friends. In particular, I'd like to thank Steph for being a close friend and one of my favorite people to ask questions and discuss experiments with. I'd also like to thank the graduate students who have succeeded me in the Green lab, Jayoung Kim, Randall Meyer, David Wilson, Dr. Camila Gadens Zamboni, Yuan Rui, and Elana Ben-Akiva. I am excited for the future of Green lab and to see how these students continue to improve upon our work. I would also like to thank the undergraduates who assisted me in completing the work of this thesis: Bolivia Hurtado de Mendoza, Barbara Kim, Hannah Vaughan, Casey Vantucci, Marisa Gionet-Gonzalez, and Teja Rao.

Finally, I would like to thank my family for their love and support throughout the progression of my career. I would like to thank my parents, Thomas and Carolyn Kozielski, my

sister, Ali Kozielski, my husband, Morgan Alexander, and my dogs, Frankenstein and Lucifer. Without those listed above this thesis work would not have been possible.

Table of Contents

List of Tables

List of Figures

Chapter 1

Introduction to the thesis

1.1 Outline of the thesis

The overall goal of the thesis is to explore novel nanotechnologies for the treatment of brain cancer. In particular, we used nanoparticles to deliver nucleic acid cargoes to glioblastoma (GBM) with the goal of altering cancer gene expression in a way that can reduce the tumor's proliferative capacity, and ultimately kill the tumor cells. In **Aim 1**, we used poly(beta-amino ester) (PBAE) nanoparticles to deliver a plasmid encoding herpes simplex virus thymidine kinase (HSVtk) to the tumor cells. Our goal was to systemically deliver the inactive prodrug ganciclovir (GCV), which would be activated to its cell-killing form upon phosphorylation via HSVtk in the brain. We examined the ability of PBAE nanoparticles to deliver HSVtk to GBM *in vitro* and *in vivo*, and assessed the effect of the HSVtk/GCV therapeutic system to kill GBM and prolong survival in an orthotopic model of GBM. In **Aim 2**, our goal was to engineer PBAE nanoparticles for siRNA delivery by designing a novel, bioreducible PBAE nanoparticle that would biodegrade and release siRNA in the cytosol, its subcellular target location. We examined varying polymer properties to optimize siRNA delivery to GBM, and were able to show effective gene knockdown even with very low siRNA doses. This motivated the work presented in **Aim 3**, in which we used bioreducible PBAEs to codeliver multiple genes targeting GBM migration and proliferation. We also demonstrated that bioreducible PBAEs selectively deliver siRNA to brain cancer cells. We then used siRNA codelivery to show gene knockdown and a reduction in tumor growth *in vivo*. Finally in **Aim 4**, we use bioreducible PBAE nanoparticles to deliver microRNAs (miRNAs) to GBM. We were able to show that miRNA delivery was able to reduce GBM's stem

like and tumor propogating phenotype both *in vitro* and *in vivo*, and that we can reduce tumor size and aggression.

1.2 Specific Aims

Aim 1. Use PBAE nanoparticles to deliver a tumor-killing gene to glioblastoma (GBM) as a cancer therapeutic.

Biodegradable polymeric nanoparticles have the potential to be safer alternatives to viruses for gene delivery; however, their use has been limited by poor efficacy *in vivo*. In this Aim, we synthesized and characterized polymeric gene delivery nanoparticles and evaluated their efficacy for DNA delivery of HSVtk combined with the prodrug GCV in a malignant glioma model. We investigated polymer structure for gene delivery in two rat glioma cell lines, 9L and F98, to discover nanoparticle formulations more effective than the leading commercial reagent Lipofectamine® 2000. The lead polymer structure, poly(1,4-butanediol diacrylate-co-4-amino-1-butanol) end-modified with 1-(3-aminopropyl)-4-methylpiperazine, is a PBAE and formed nanoparticles with HSVtk DNA that were 138 ± 4 nm in size and 13 ± 1 mV in zeta potential. These nanoparticles containing HSVtk DNA showed 100% cancer cell killing *in vitro* in the two glioma cell lines when combined with GCV exposure, while control nanoparticles encoding GFP maintained robust cell viability. For *in vivo* evaluation, tumor-bearing rats were treated with PBAE/HSVtk infusion via convection-enhanced delivery (CED) in combination with systemic administration of GCV. These treated animals showed a significant benefit in survival ($p=0.0012$ vs. control). Moreover, following a single CED infusion, labeled PBAE nanoparticles spread completely throughout the tumor. This study highlights a new nanomedicine approach that is highly promising for the treatment of malignant glioma.

Aim 2. Synthesize, characterize, and optimize a novel polymer and assess its ability to deliver siRNA to GBM cells in vitro.

siRNA nanomedicines can potentially treat many human diseases, but safe and effective delivery remains a challenge. DNA delivery polymers such as PBAEs were in the past unable to effectively deliver siRNA and require chemical modification to enable siRNA encapsulation and delivery. An optimal siRNA delivery nanomaterial needs to be able to bind and self-assemble with siRNA molecules that are shorter and stiffer than plasmid DNA in order to form stable nanoparticles, and needs to promote efficient siRNA release upon entry to the cytoplasm. To address these concerns, we designed, synthesized, and characterized an array of bioreducible PBAEs that self-assemble with siRNA in aqueous conditions to form nanoparticles of approximately 100 nm and that exhibit environmentally triggered siRNA release upon entering the reducing environment of the cytosol. By tuning polymer properties, including bioreducibility and hydrophobicity, we were able to fabricate polymeric nanoparticles capable of efficient gene knockdown in primary human glioblastoma cells without significant cytotoxicity. We were also able to achieve significantly higher knockdown using these polymers with a low dose of 5 nM siRNA compared to commercially available reagent Lipofectamine™ 2000 with a four-fold higher dose of 20 nM siRNA. These bioreducible PBAEs also enabled 63 ± 16% gene knockdown using an extremely low 1 nM siRNA dose, highlighting their potential as efficient carriers for siRNA-based nanomedicine.

Aim 3. Assess cancer-selective delivery siRNA via bioreducible PBAE nanoparticles in primary human GBM, and deliver functional siRNAs to combinatorially target genes responsible for tumor cell proliferation, migration, and invasion.

The goal of this Aim is to create a novel siRNA delivery nanotechnology capable of treating and preventing the recurrence of GBM, the most malignant primary human brain cancer. There is increasing evidence that brain tumor recurrence is due to the presence of brain tumor initiating cells. These cells are believed to be able to survive conventional treatments and to be able to migrate away from the primary tumor site and form new tumors. RNA interference (RNAi), a natural cellular process that can prevent the expression of genes in a sequence-specific manner, can be induced by the introduction of short interfering RNA (siRNA) into the cells. Using siRNA to turn off the genes that allow GBMs to survive treatment, to migrate, and to form new tumors has the potential to prevent tumor recurrence following treatment. However, siRNA delivery is challenging. Viral siRNA delivery has many potential problems such as tumorigenicity and immunogenicity, and is generally limited to carrying one type of siRNA, as multiple doses could increase the risks of using them in patients.

For work completing Aim 2, we synthesized a novel, bioreducible PBAE-based nanoparticle capable of safe and effective delivery of siRNA to primary human glioblastoma cells. We were also able to show that we can achieve near complete gene knockdown of a fluorescent marker gene using only a fraction of the siRNA that we can load into the nanoparticles. In Aim 3, this motivated us to explore our ability to load several different siRNAs within the same nanoparticle. In particular, we wanted to use this technology to codeliver multiple genes that enable GBM cells to grow and migrate. We will also show that bioreducible PBAEs selectively deliver siRNA to brain cancer cells while avoiding transfection of healthy human brain cells. Finally, we will demonstrate that using siRNA codelivery via nanoparticles enables us to slow tumor cell growth *in vivo*. This has allowed us to optimize and characterize a combinatorial, tumor-specific technology for the delivery of brain cancer therapeutics.

Aim 4. Deliver therapeutic microRNAs (miRNAs) to human GBM with the goal of reducing GBM stem-like properties and sensitizing tumors to radiation treatment.

Despite our growing molecular understanding of GBM, treatment modalities remain limited. Recent developments in nanomedicine provide new avenues to treat and manage brain tumors. Gene delivery via a novel bioreducible PBAE is of particular interest since these types of polymers are have high delivery efficacy and provide subcellularly-targeted cargo release. In this Aim, we combined bioreducible PBAE nanoparticles with newly discovered stem cell inhibiting miRNAs to develop miRNA nanoparticles to treat gliomas. We show these nano/miRs can effectively deliver miRNA mimics and inhibit the stem cell phenotype of GBM cells *in vitro*. These miRNA nanoparticles efficiently distribute throughout an established tumor *in vivo,* and more importantly, inhibit the growth of established orthotopic GBM tumor in mouse models. Additionally, we were able to combine our miRNA nanoparticle technology with a conventional cancer therapy, radiation treatment. We were able to show that miRNA delivery sensitized the tumor to radiation, which on its own was ineffective at slowing tumor growth. Our findings demonstrate that combining cancer stem cell-inhibitory miRNAs with advanced nanoparticle technology can impact the development of novel therapies for treating GBM.

Chapter 2

State of the Art

2.1 Nanotechnology for nucleic acid delivery

2.1.1. Introduction

The delivery of nucleic acids to manipulate gene regulation can be both a therapeutic and a scientific tool. Diseases caused by missing or defective genes could potentially be cured by replacing these genes, such as upregulating tumor suppressor genes in cancer.[1-3] The immune system can be modulated by the introduction of DNA-based vaccines,[4, 5] or by introducing genes that would allow the immune system to better recognize or fight cancer.[6, 7] Additionally, suicide genes can be introduced to kill cancer cells.[8] *Ex vivo*, gene therapy can be used to manipulate stem cells for targeted differentiation,[9] or to reprogram induced pluripotent stem cells from differentiated cells.[10] Turning off or downregulating genes could treat diseases caused by gene overexpression.[11, 12] Technology to selectively turn genes off is also a valuable biological tool to elucidate the function of genes within a cell and in the context of a disease.[13]

Viral gene delivery vectors, although effective, come with risks such as tumorigenicity and immunogenicity.[14] Adenovirus-mediated gene delivery studies have found that dosage repeatability and concentrations can be limited by toxicity and humoral immune response.[15] Although non-viral nucleic acid delivery can avoid these issues, it is typically less effective.[16]

This chapter contains material modified from the following articles previously published or awating publication as:
Kim, J.J.;* Kozielski, K.L.;* Wilson, D.R.;* Green, J.J.: Biodegradable polymeric nanoparticles for gene delivery. In *Perspectives in Micro and Nanotechnology for Biomedical Applications*. Xu, C. and Chan, J.M. eds.; Imperial College Press: London, UK, 2015, *In press*.
Kozielski, K.L.;* Tzeng, S.Y;* Green, J.J.: Bioengineered nanoparticles for siRNA delivery. *WIREs Nanomedicine and Nanobiotechnology* **2013**, *5,* 449-468.

Lipid-based and inorganic delivery vehicles have previously been examined for their potential to deliver nucleic acids. Lipid-based delivery is well-characterized,[17-19] and commercially-available lipid-based delivery vehicles are available for *in vitro* delivery of DNA[20, 21] and siRNA.[22] Lipid-based nanoparticles can potentially generate off-target and immunogenic effects,[20] but there are strategies to attenuate these unwanted interactions such as the introduction of poly(ethylene glyocol) (PEG) shielding.[23, 24] Calcium phosphate crystals,[25-27] gold nanoparticles, quantum-dots and other inorganic materials have also been employed for non-viral gene delivery. Gold is advantageous because it's biocompatible, easy to functionalize, and has malleable physical properties.[28-32] Quantum dots are useful for fluorescent imaging as they are brighter and less prone to photobleaching than typical fluorophores.[33, 34] Several lipid-based and inorganic nanoparticle systems have also been combined with polymeric materials for enhanced gene delivery, particularly through the incorporation of PEG coatings[24, 35, 36] for nanoparticulate shielding or polyamines for improved interaction with DNA and intracellular delivery.[37, 38]

Biodegradable polymeric gene delivery systems are a relatively newer class of materials for non-viral gene therapy. They are promising due to key features such as safety mediated by their biodegradability, design flexibility due to their tunable structure, large cargo capacity, and relative ease in manufacture. This chapter will focus on biodegradable polymeric nanoparticles for gene delivery. They will be discussed in the context of systemic and intracellular barriers to gene delivery and how polymer design can be utilized to overcome these barriers. New developments in the field of biodegradable polymeric gene delivery and an outlook for the future will be highlighted.

2.1.2. Obstacles to gene delivery

The central limitation of non-viral vectors for gene delivery is inefficient gene transfection arising from the natural mechanisms of the human body to protect itself against foreign substances.[39] These barriers to biomaterial-mediated gene transfection span a spectrum from the systemic level to the cellular level (**Figure 2.1**).[40] Different biomaterial properties and modifications to gene carriers are important for each step of the delivery process leading to successful expression of exogenous delivered nucleic acid. We will discuss seven major biological barriers to gene transfer using non-viral vectors and strategies to overcome each of these barriers. It is also important to note that the design properties seemingly optimal for one of the delivery obstacles could pose a challenge to other obstacles; hence further effort is needed to globally optimize polymeric nanoparticles to balance these potential trade-offs.

Nucleic acid binding / encapsulation

An efficient gene delivery vector must condense or encapsulate the nucleic acid to prevent enzymatic degradation and facilitate its cellular entry.[41] As DNA is a strongly negatively charged material, early work in the field of non-viral gene delivery focused on the use of naturally occurring biological materials with significant positive charge that could electrostatically bind to the DNA. In this manner, DNA could be condensed into a smaller size, be made more resistant to potential enzymatic degradation, and have improved ability to enter cells. Polycation poly(*L*-lysine) (PLL) was observed to bind to nucleohistones,[42, 43] and was later investigated as one of the earliest polymers to form nanocomplexes with DNA.[44-46] PLL is capable of complexing with DNA to form nanoparticles that successfully undergo cellular uptake but fail to escape from the endosome.[47] To overcome this challenge, PLL has been used in combination with other materials that aid in endosomal escape including other peptide molecules and pH sensitive moieties that make use of the proton sponge effect.[48-50] To improve delivery in

comparison to PLL, alternative gene delivery materials needed to be discovered. An off-the-shelf commercially produced polymer with very high charge density, polyethylenimine (PEI), was first reported for use in transfection in 1995 by Boussif *et al.,* who attributed its high transfection efficiency to its ability to undergo endosomal escape via the proton sponge effect.[51] Unfortunately, while transfection efficacy is correlated with the molecular weight of PEI, cytotoxicity is similarly correlated, making unmodified high MW PEI largely unsuitable for *in vivo* applications. PEI is a non-biodegradable polycation that requires excess polymer to effectively transfect cells amd can lead to accumulation upon repeated administration.[52, 53] To overcome this first obstacle to non-viral gene delivery, other biomaterials can encapsulate nucleic acids into particulates. Amphiphilic lipids, such as N-[1-(2,3-dioleyloxy)propylJ-N,N,N-trimethylammonium chloride (DOTMA), and relatively hydrophobic polymers, including poly(lactide-*co*-glycolide) polymer (PLG), form DNA-encapsulated nanoparticles by either phase separation alone or in combination with electrostatic interaction.[54, 55]

Polymeric vectors are able to deliver different types of nucleic acids. For DNA, standard double-stranded plasmids as well as minicircles, which are plasmids that have had prokaryote sequences such as the CpG islands removed, are widely used to introduce exogenous genes that encode for proteins of interest.[56] Because of the large size of DNA molecules, they are able to bind to cationic polymers such as PEI and poly(β-amino ester)s (PBAE) and form stable nanoparticles.[57, 58] Small interfering RNA (siRNA), through the RNA interference pathway, causes mRNA to be broken down and inhibits translation.[59] As an siRNA molecule is dramatically shorter (~20 bp vs > 1,000 bp) and stiffer than a plasmid DNA molecule, stable particle formulation through electrostatic interactions with cationic polymers is more difficult.[60, 61] Therefore, siRNA-delivering nanoparticles can require more complex engineering solutions to

form effective particles, such as making siRNA more multivalent by introducing short complementary overhangs[62] or multimerizing siRNA molecules with cleavable disulfide linkages.[63] More recently, an enzymatic RNA polymerization technique has been used to condense RNA structures into self-assembled RNAi-microsponges.[64] While siRNA binding and encapsulation can be challenging, siRNA delivery overall is not necessarily more difficult than DNA delivery, as unlike DNA, siRNA does not require nuclear import to function.[65]

Systemic circulation

Both viral-based and non-viral based vectors face the problem of rapid clearance from the systemic circulation on the order of minutes.[66, 67] While viruses often suffer from specific antibody-mediated immune response, non-viral platforms are quickly cleared by several non-specific mechanisms. Most polymeric gene delivery materials are positively charged as electrostatic interaction is the prevalent driving force in forming many types of nanoparticles for gene delivery. The resulting positive surface charge of nanoparticles provides colloidal stability in aqueous solutions and facilitates interaction with cellular membrane. However, it also attracts anionic counter ions in physiological salt and serum proteins that cause opsonization and aggregation, leading to increased clearance by the mononuclear phagocyte system (MPS) and the reticuloendothelial system (RES).[68-70]

Several strategies have been employed to minimize clearance from the systemic circulation, including charge shielding and shape control. One common "stealth" technology involves coating nanoparticles with PEG which provides a relatively inert surface due to its neutral and hydrophilic structure.[71, 72] Conjugation of PEG or "PEGylation" to gene delivery particles composed of cationic polymers,[73, 74] lipids,[75, 76] dextran-spermine,[77] and other materials have been reported demonstrating beneficial effects. An alternative approach is the

neutralization of excess positive surface charge of particles through coatings with anionic biomacromolecules such as negatively charged polypeptides.[78] More recently, engineering of particle shape has also been shown to be an important parameter to extend circulation time. Nanoparticles for drug delivery with higher aspect ratios had longer circulation half-lives than spherical particles,[79] and this strategy has begun to be utilized for gene delivery nanoparticles.[80]

Tissue and cell targeting

Tissue targeting can be accomplished through design of a targeted systemically administered nanoparticle, through a tissue-specific promoter, or through a local injection. Nanoparticles can be injected into anatomically accessible sites to enhance delivery in the local region of interest while reducing non-specific transfection at other sites. For example, intracerebroventricular delivery grants direct access to the brain, retrograde intrabiliary infusion to the liver, and intratumoral injection to tumors.[81-83]

Nanoparticles that are administered intravenously must have mechanisms to exit the circulation at the target tissue. The application of nanoparticles to solid tumors is often benefited by passive targeting. The formation of new blood vessels near rapidly growing solid tumors allows nanoparticles with diameters of 400 nm or less to passively leak out of the neovasculature and distribute to the tumor tissue. Therefore, prolonging systemic circulation by the aforementioned strategies, such as PEGylation, can increase the accumulation of nanoparticles at a tumor site, and this enhanced permeability and retention (EPR) effect has become an important tool in nanoparticle-mediated gene delivery for cancer therapy.[84] On the other hand, molecular ligands and chemical moieties that bind specifically to overexpressed receptors on the vascular endothelial cells' surface near a solid tumor have been conjugated to various nanoparticles as an active targeting mechanism. For example, arginine-glycine-aspartic acid (RGD) peptide

sequence and other chemical antagonists to various integrin isoforms have been covalently conjugated or electrostatically bound via negatively charged polypeptides to biomaterials target tumor vasculature.[85-89] Another emerging method of conferring tissue-specificity to nanoparticles utilizes aptamers as targeting ligands.[90]

Nanoparticles with targeting ligands can be used to target many additional cell types as well. This is important as, when cell-specific RNA interference or therapeutic exogenous DNA expression is critical, nucleic acid delivery nanoparticles with cell-specific targeting can increase efficacy and reduce potential off-target side effects. Overexpressed receptors on the surface of specific cell types of interest are good candidates to target with ligands. The gene delivery and nanomedicine literature show that modification of nanoparticles ligands of many different types can be effective including: galactosylated PEI targeting hepatocytes, antibodies specific to the insulin receptor to target cancer cells in brain, synthetic peptides that bind to integrin α5β1 on neuroblastoma cells, small molecules targeting CD40 on ovarian cancer cells, and leukocyte function-associated antigen-1 to bind to melanoma cells.[91-95]

Other methods for cell-specific gene delivery are also possible. Following a polymer library approach, a recent study by Guerrero-Cázares *et al.* showed that the specific chemical structure of a polymer that comprises a polymer/DNA gene delivery nanoparticle can confer cell specificity to one type of cell over another such as primary brain tumor initiating cells over healthy neural progenitor cells.[96] Similar results have also been shown for polymeric nanoparticles that can target liver cancer cells[97] and endothelial cells.[98, 99] A final approach is including a cell type-specific promoter in the plasmid to promote targeting of specific cells such as cancer cells.[100] In this manner, even if some of the polymeric nanoparticles are delivered to

off-target cells, there is only successful expression of the exogenous gene in the targeted cells where the specific promoter is active.

Cellular uptake

Once nanoparticles reach the cells of interest, they must overcome several barriers at the cellular level before successful transfection is achieved. First, gene carriers need to cross the cellular membrane, for which exist both non-specific and specific mechanisms. Macropinocytosis is a non-specific cellular uptake mechanism, where cells engulf extracellular fluid through actin-driven evagination.[101] However, gene vectors entered via macropinocytosis result in poor transfection efficacy due to high rate of recycling.[102] Also, positive surface charge on nanoparticles formulated with cationic polymers or lipids promotes electrostatic interaction with relatively negative cell surface, which in turn triggers another non-specific pathway, adsorptive endocytosis.[103] It should be noted that positive surface charge is shielded with PEGylation, which prevents electrostatic interaction with cellular membrane.

On the other hand, specific uptake mechanisms are mediated by receptors on the cellular membrane, which can recognize various molecular ligands as well as chemical moieties of the vector. In the case of PEGylated nanoparticles, ligands can be conjugated to the PEG chain, and chemical moieties can be exposed upon environment-stimulated PEG cleavage.[104, 105] There are two major specific uptake routes for gene carriers. Clathrin-mediated endocytosis is initiated with clathrin-coated pits of about 100 – 150 nm in size that pinch off from the plasma membrane to form endosomes.[106] Nanoparticles modified with MC1SP-peptide and transferrin that target melanocortin receptor-1 and transferrin receptor respectively, and unmodified lipoplexes and liposomes are found to be endocytosed via this pathway.[107-109] In comparison, caveolae-mediated endocytosis is characterized by flask-shaped invaginations of about 50 – 100 nm in diameter.[110]

Folic acid hat bind with folate receptors as well as unmodified polymeric nanoparticles are directed to caveolae-mediated uptake.[109, 111]

Different uptake pathways lead to different intracellular fate, which underscores the importance of the cellular uptake on successful transfection.[112] For example, the major route of uptake for PBAE nanoparticles does not necessarily lead to high transfection efficiency.[113] Therefore, nanoparticles can be modified take an uptake pathway different from its major route to improve the intracellular fate of the plasmid.

Endosomal escape

Once endocytosed, nanoparticles must escape the endosomal compartment and reach the cytoplasm. A common mechanism of endosomal escape for polymeric nanoparticles is the proton sponge effect.[114] Reversibly protonated biomaterial vector can act as a buffer as the endosome gradually become acidic, thereby protecting the cargo. Subsequently, chloride ions enter the endosomes to neutralize the charge, creating osmotic pressure that eventually leads to endosomal burst and cargo release. PLL, owing to its primary amines that are easily protonated at pH 7, is unable to provide buffering capacity at endosomal pH. In order to neutralize the acidic pH, researchers have either co-delivered PLL with amphiphatic amines, such as chloroquine, or substituted its lysine residues with histidine or arginine that has titratable amines. [48, 115] PEI and PBAE, on the other hand, have weakly basic tertiary amines in their structure that allows for the proton sponge effect.[51, 116] Although the hypothesis is the most widely believed mechanism of endosomal escape, it has been challenged and remains to be clearly elucidated.[117]

Nanoparticles can also escape the endosome by destabilizing endosomal membrane. For example, amphiphatic, fusogenic peptides, such as GALA (repeats of Glu-Ala-Leu-Ala) and KALA (repeats of Lys-Ala-Leu-Ala), have been utilized as the vector itself or associated non-

covalently with nanoparticles.[118, 119] These fusogenic peptides are able to form alpha-helical structure at lower pH that can be inserted and destabilize the membrane. Other amphiphatic lipids, such as dioleoylphosphatidylethanolamine (DOPE), that assume non-bilayer structure can also facilitate endosomal membrane destabilization when associated with liposomes.[120, 121]

Dissociation of nucleic acid and nuclear transport of DNA

Although strong binding or encapsulation of nucleic acid is necessary to form stable particles, nucleic acid must be able to dissociate from the vector once the particles escape endosomes. This is necessary in order to enable the nucleic acid to have a biological effect, as DNA that isn't released from its carrier is unable to be transcribed as efficiently. [122, 123] This was illustrated by a recent study showing that the binding constant between polycations and DNA is biphasic with the transfection efficiency.[124] Additionally, polymer degradability imparts decreased cytoxicity, as polymer molecular weight has been shown to positively correlate with toxicity.[125] Lack of degradability contributes to the toxicity of conventional polymers such as 25 kDa branched PEI.[126, 127] Below, we will discuss methods that allow for the chemical modification of conventional polymers in order to enable them to degrade (**Figure 2.2**), in addition to the design of polymers with degradable moieties inherent in their chemical structure.

2.1.3. Degradable polymeric moieties for cargo release and transport

Hydrolysis

The release of nanoparticle cargo can be achieved through polymer hydrolysis via the cleavage of ester, urethane, imine, and orthoester linkages. Poly[alpha-(4 aminobutyl)-L-glycolic acid] (PAGA) is a hydrolysable analog of PLL in which the amides linking conventional PLL monomers are replaced with ester linkages. PAGA based DNA delivery has been shown to lead to better transfection efficacy and lower toxicity versus conventional PLL.[128] Hydrolytically

cleavable PEI can be synthesized using by linking shorter PEI polymers with ester-containing crosslinkers. Diacrylate monomers used to crosslink 800 Da PEI were shown to create nanoparticles with the same size, shape, charge, and DNA binding versus 25 kDa PEI while achieving 16-fold transfection efficacy with no measureable toxicity.[129] PBAE polymers are formed via Michael addition of amine-containing monomers with diacrylate monomers and therefore contain esters within the polymer backbone.[130] Combining various amine and acrylate monomers enables for the creating of large libraries of PBAEs with various chemical properties,[131] and whose binding constants are affected by polymer molecular weight.[124] Other poly(amino ester)s can be synthesized to have a similar chemical structure and transfection efficacy as 25 kDa PEI but with reduced toxicity (**Figure 2.4**).[132] Poly(lactic-*co*-glycolic) acid (PLGA)-based nanoparticles can encapsulate nucleic acids, particularly using a double emulsion method and polyamines, and successfully deliver nucleic acids.[133] PLGA chemically modified with amine-containing molecules grafted onto their polymer backbone has also been shown to effectively deliver DNA and siRNA.[134, 135] Other hydrolytically cleavable polymer linkages have been explored for biodegrable polymer design. Amine containing polyurethanes can be designed to deliver DNA.[136] Polyimines, which specifically allow for acid-labile hydrolysis, can be used to link short chain PEI.[137] Additionally, polyorthoester polymers can form stable nanoparticles at neutral pH, but are acid-labile and release DNA at pH 5. [138, 139]

Reduction

Polymer bioreducibility via the inclusion of disulfide bonds enables cargo release targeted to the cytoplasm. Cytosolic reduction potential is mainly due to glutathione, a molecule present in concentrations roughly 1000 times higher in the cytosol versus extracellular space.[140] This targeted release makes bioreducible polymers particularly useful for delivery of siRNA,

mRNA, and miRNA whose site of action is within the cytosol. Conversely, DNA delivery via disulfide-containing polymers has sometimes been found to be less-effective.[141] As with hydrolytic linkages, reducible linkages can improve delivery efficacy and reduce cytotoxicity of conventional polymers. PLL linked with disulfides has shown improved nucleic acid delivery.[142] Methods to crosslink PLL with disulfides, either by incorporating cysteines into the polypeptide backbone,[143] or by chemically modifying the lysine sidechains to contain thiols,[144, 145] has led to improved siRNA and DNA delivery. Linear PEI linked with disulfides also showed improved siRNA delivery with lower toxicity than 25 kDa PEI.[146] The KALA fusogenic peptide has also been modified with cysteines to allow for crosslinking.[147]

Polymer bioreducibility can also be imparted by synthesizing polymers from disulfide-containing monomers. Poly(amido amine)s (PAAs) are synthesized with diacrylamide and amine-containing monomers, and are therefore not biodegradable. However, disulfide-containing diacrylamides can also form PAAs and impart targeted cargo release to the cytoplasm. Disulfide-containing PAAs have been extensively studied for both DNA and siRNA delivery. [146, 148-151] PBAEs can also be bioreducible, either by end-capping with disulfide-containing monomers,[9, 152] or using diacrylate monomers with disulfides to incorporate them into the polymer backbone.[153] Bioreducible PBAEs have been shown to be very successful siRNA delivery vehicles, often achieving near-complete gene knockdown with little toxicity,[154] even using very low siRNA doses.[141]

Other modes of degradation

Other modes of degradability can also enable targeted delivery. Enzyme-cleavable linkages, specifically matrix-metalloproteinase (MMP)-cleavable groups, can allow for release

within tumor space.[155] Light-induced degradation, although not biodegradable, allows for user-controlled release and could allow for spatially controlled cargo release.[156]

Nuclear transport

Lastly, unlike siRNA, DNA has to be transported to the nuclear membrane and enter the nucleus for transcription to occur. The simian virus 40 large T antigen nuclear localization signal (NLS), which is a peptide sequence rich of lysine amino acid, is known to facilitate the nuclear transport.[157] Many vectors, including cationic peptides and lipids, or the DNA itself have been modified with variant forms of NLS in order to enhance transfection.[158-160]

2.1.4. Degradable polymeric gene delivery vectors

Peptides

Poly(L-lysine)

While PLL, shown in **Figure 2.3a**, had low efficacy for gene delivery by itself, multicomponent nanoparticles utilizing PLL as the polycation to bind the nucleic acid have been more successful. Notably, PEG modified PLL nanoparticles created by Meyer *et al.* for the delivery of siRNA utilized the lytic peptide melittin (Mel) shielded by pH cleavable dimethylmaleic anhydride (DMMAn) to only expose the lytic peptides for endosomal escape once a pH of 5.[50] In addition to the pH sensitive lytic peptide exposure, siRNA release was achieved via disulfide cleavage between the siRNA and polymer.[50] These PEG-PLL-DMMAn-Mel nanoparticles were shown to achieve 90% knockdown *in vitro* but at only 70% metabolic activity measured by an MTT cytotoxicity assay.[50] While results of this nanoparticle formulation were promising for siRNA delivery *in vitro*, *in vivo* testing revealed a high level of toxicity in health mice and tumor bearing mice alike requiring sacrifice of the animals shortly after application.[50]

More recent uses of PLL for nucleic acid delivery have included pH cleavable PEGylated PLL-cholic acid nanoparticles shown to have a nine-fold reduction in gene expression *in vitro* equal to that of INTERFERin with cell viability over 90%.[161] *In vivo* results of PEGylated PLL-chlolic acid nanoparticle delivery of VEFG siRNA achieved a tumor size reduction of 41% with a measured 70% qPCR knockdown of VEGF mRNA without a significant weight reduction in treated mice.[161] Another PLL nanoparticle formulation utilizing dendritic PLL for the knockdown of Apolipoprotein B to reduce serum low-density lipoprotein levels was shown to achieve significant knockdown *in vivo* leading to a 40% reduction in serum LDL.[162] PLL has been shown to be an effective polycation when modified to enable endosomal escape and cellular targeting but its current use is limited as it lacks the versatility of many other polycations for the delivery of nucleic acids.

Cell-penetrating peptides

Peptides have been incorporated in many other nanoparticles designs as both the backbone structure and as surface molecules. Amphipathic endosomal escape peptides such as GALA and KALA, as mentioned previously, are well documented for improving transfection among many different cell types and with many different nanoparticle formulations.[118, 163] Other CPPs have been used in the creation nanoparticles for the delivery of siRNA with the residue lysine often being used to increase the cationic nature of the peptides.[164] Peptides have also been incorporated into nanoparticles for purposes of endosomal release. The use of sHGP, a 15 amino acid oligopeptides from HIV gp41, has been shown to improve endosomal release.[165] Peptide sequences from influenza, specifically Inf7, have also been utilized in the design of nanoparticles to aid in endosomal escape and has been shown to improve efficacy of transfection with siRNA.[166] Control over enzymatic degradation rate of peptide based nanoparticles has also been

achieved by Chu *et al*. who designed nanoparticles utilizing both *D* and *L* amino acids for controlled cleavage by Cathepsin B.[167] In this way stereospecific enzymatic degradation was shown to offer excellent stability extracellularly with rate controlled intracellular degradation and release of nucleic acids.[167]

CPP based nanoparticles termed PF6 for the delivery of siRNA created by Andaloussi *et al.* were demonstrated to be able to knockdown a reporter gene up to 90% in serum containing media with minimal cytotoxicity and inflammatory effects.[164] Importantly, PF6 nanoparticles were shown to be stable over a span of weeks in water as well as being stable over a short term in serum containing media at a diameter between 125-200 nm and zeta potential of approximately -10 mV.[164] Intravenous administration of PF6 with luc-siRNA to transgenic mice with bioluminescent liver cells showed effective knockdown peaking on day 5 at a 75% reduction.[164] PF6 knockdown of the functional protein HPRT1 was observed to be greatest in the liver, but was followed closely by silencing of greater than 60% in the kidneys, which the authors note is likely due to blood supply similarities between the organs.[164] Further modification of PF6 for targeting of organs or tumors or local injection will be required for functional siRNA delivery. Particularly since PF6 is known to have a negative zeta potential, targeting organs other than the liver may prove to be a challenge.

Synthetic polymers

Poly(ethylene imine)

High molecular weight 25 kDa PEI, shown in **Figure 2.3b**, has previously been shown to condense DNA to form nanoparticles, undergo endosomal escape, and successfully deliver DNA.[51, 168] Unfortunately while transfection efficacy is correlated with the molecular weight of PEI, cytotoxicity is likewise correlated making unmodified 25 kDa PEI largely unsuitable for *in*

vivo applications.[168] Related to issues of immediate cytotoxicity, PEI is a non-biodegradable polycation that requires excess polymer to effectively transfect cells that can lead to accumulation upon repeated administration.[52, 53] The 50 kDa and 800 kDa PEI initially used was quickly replaced in use by lower molecular weight PEI of approximately 25 kDa, which was shown to have higher transfection efficiency but still suffered from cytotoxicity *in vivo* in mice.[51, 169] To further minimize the cytotoxicity of non-biodegradable PEI, even lower molecular weight branched PEI was initially used followed shortly after by partially biodegradable crosslinked PEI and hyperbranched oligoethyleneimine.[170-173] Biodegradable linkages between low molecular weight PEI segments have primarily included bioreducible disulfides and hydrolysable esters, both of which have been shown to improve transfection efficacy as well as decrease cytotoxicity compared to 25 kDa PEI.[129, 172] In 2003, Forrest *et al.* created hydrolysable PEI polymers 800 Da PEI and diol-diacrylate monomers that improved transfection efficiency and reduce cytotoxicity.[129] Using disulfide cross-linked 1.8 kDa low molecular weight PEI, Liu *et al*. were able to achieve greater than 60% transfection with 90% cell viability in serum containing media in 2010.[174]

These improvements to the polymer structure have made PEI much less toxic *in vitro* but fail to avoid problems of polycation accumulation *in vivo* that plague non-biodegradable polymeric delivery systems. Even with that limitation, a PEI based nanoparticle formulation for the delivery of a plasmid encoding interleukin-12 for 13 patients with recurrent ovarian cancer was tested in an initial Phase I clinical trial with favorable results for safety published in 2009.[175] The nanoparticle composed of lipopolymer, PEG-PEI-cholesterol was administered in a series of four increasing doses every 4 weeks intrapleurally.[175]

Poly(beta-amino ester)s

The development of PBAEs, shown in **Figure 2.3c**, as a material for transfection has been greatly advanced by high throughput screening of PBAE polymer libraries in which monomers and end cap groups are varied.[131, 176-178] This rapid screening technique has allowed for a large variety of PBAEs to be tested and patterns in transfection to be determined. Transfection by PBAEs has been shown to be largely cell type specific with cellular uptake and transfection differences between healthy cells and tumor cells able to be screened for to determine polymer candidates targeted to only the cell population of interest.[96, 97, 179] Using polymer libraries and high throughput screening, PBAE nanoparticle formulations for the delivery of siRNA and DNA to glioblastoma cells have been achieved up to 85% and 90% respectively *in vitro*, significantly greater than Lipofectamine or any commercial transfection reagent (**Figure 2.4**).[153] While most PBAE nanoparticles for the delivery of nucleic acids have used linear PBAEs for rapid intracellular degradation and release of DNA polyplexes, cross-linked PBAEs formed by Michael addition using triacrylate monomers and N,N-dimethylethylenediamine have been created to reduce the rate of degradation and DNA release.[180]

In vivo results of PBAE nanoparticle delivery in mice of both siRNA and DNA have demonstrated transfection or knockdown with reporter genes as well as functional transfection for treating diseases such as ovarian cancer.[181] Transfection of brain tumor-initiating cells (BTICs) in 3D oncospheres with pDNA has been accomplished with PBAE nanoparticles at up to 76% transfection *in vitro*.[96] In this work, PBAE nanoparticle specificity of transfection for BTICs over fetal neural progenitor cells (fNPCs) has been demonstrated both *in vitro* and *in vivo*, supporting the notion that *in vitro* monolayer culture screening of PBAE nanoparticles has relevance for *in vivo* efficacy. Transfection of ovarian tumor bearing mice via intratumoral

injection of PBAE nanoparticles containing a plasmid encoding diphtheria toxin showed a mean tumor load reduction greater than that of administration with dual chemotherapeutics.[181] The intrapleural injection route used in this study mirrors the current injection route of chemotherapeutics for advanced ovarian cancer, supporting the clinical relevance of the work.[181] Of greater importance to clinical relevance, PBAE nanoparticles with pDNA have been demonstrated to be stable when stored at -20°C for up to two years upon lyophilization with sucrose as a cryoprotectant.[96]

PBAEs have also been used as a cationic polymer to supplement other materials in the creation of nanoparticles for the delivery of siRNA. Cohen *et al.* have created acetalated-dextran nanoparticles with 10 wt% PBAE that showed pH sensitive degradation and release of DNA.[182] PBAE has been used as a cationic polymer for binding DNA in conjunction with PLGA to form microspheres capable of transfecting macrophages to express a tumor specific antigen and induce an adaptive immune response in mice.[183]

For localized delivery of DNA and siRNA amenable to tissue engineering applications, PBAEs have been used in the development of multilayer polyelectrolyte films shown to enable contact dependent transfection.[184] These multilayered films developed in the lab of David Lynn rely on charge association between layers of polycation, specifically a PBAE, and DNA to respond in a pH and temperature dependent way for localized transfection.[185] DNA release was shown to be largely dependent multilayer film degradation and released DNA in a relaxed conformation compared to the typical supercoiled conformation resulting from nanoparticle delivery.[184] Multilayered polyelectrolyte films have been further developed for localized delivery of siRNA with release shown to be subject to diffusion out of the film instead of due to film

degradation[186] Notably, the multilayer film design allowed for sustained release of DNA 30 hours, while siRNA was released in a burst manner.[184, 186]

Poly(amido amine)s

Dendrimers are symmetrically branched polymer structures that have been used as base units to encapsulate and deliver various materials through charge interactions or conjugation. Many dendrimers, including poly(amidoamine) (PAA or PAMAM) shown in **Figure 2.3d**, are synthesized by a series of Michael addition reactions, allowing for great specificity of size and nitrogen content for complexation with nucleic acids by a fine-tuned N:P ratio. The exterior surface of dendrimer molecules can also be modified with hydrophilic groups to allow for improved solubility in water or with targeting ligands for attempted improved active cellular uptake. The most frequently used dendrimer for nucleic acid delivery to date has been PAMAM, although peptide dendrimers have also been utilized with some success.[187] Bioreducible PAMAM nanoparticles for the delivery of DNA have been created with very high cell viability and transfection efficiency up to 200 times that of branched PEI.[188] The degree to which the structure of these hyperbranched PAMAM particles were able to be reduce was able to be finely tuned by the changing the monomer molar ratios used in the Michael addition reactions used to create the polymer.[188] Beyond PAMAM, Barnard *et al.* developed an ester hydrolysable dendrimer with surface amine groups capable transfection of *in vitro* up to 10 times more efficiently than PEI.[189]

Poly(lactide-co-glycolide) and poly(caprolactone)

PLGA microparticles containing 25 w% PBAE were used to transfect macrophages with reporter gene DNA both *in vitro* and *in vivo*.[183] *In vivo* results showed that these microparticles containing a plasmid for the expression of a tumor antigen were able to induce rejection of the

transplanted tumor specific antigen.[183] The resulting adaptive immune response was sufficient to cause a reduction in measured tumor growth by day 11 following transfection.[183] In another nanoparticle formulation, copolymer hybrid poly(ester amine) nanoparticle formulations of polycaprolactone and PEI have been formulated with improved transfection over 25 kDa PEI for a number of cell lines.[190]

Polysaccharides

Chitosan

Chitosan, a linear polysaccharide derived from chitin and shown in **Figure 2.3e**, has been used in the delivery of pDNA and siRNA but generally has had low transfection efficiency due to chitosan's low performance as a proton sponge.[191] Chitosan varies by the degree of deacetylation from chitin expressed as a ratio of β-(1–4)-linked D-Glucosamine to N- acetylated-D-glucosamine.[192] Highly deacetylated chitosan has been used more frequently for nucleic acid delivery due to its greater cationic nature and corresponding ability to complex with the negatively charged backbone of DNA or RNA. In 2001, Mao *et al.* created PEGylated chitosan DNA nanoparticles with the targeting molecule transferrin capable of transfection, but only at a fraction of the efficiency of Lipofectamine A.[193] Since then, chitosan thiamine pyrophosphate nanoparticles for the delivery of siRNA have been shown to achieve knockdown up to 70% with cell viability above 90% *in vitro* for hepatocarcinoma cells, notably greater than Lipofectamine.[194] Trimethyl chitosan has also been used in conjunction with the polysaccharide polysialic acid (PSA) for the delivery of transcription factor decoy oligonucleotides resulting in a reduction of inflammation measured by excreted cytokines *in vitro*.[195]

Hyaluronic acid

Hyaluronic acid (HA), shown in **Figure 2.3f**, has been utilized in nanoparticles for the delivery of nucleic acids as well as a targeting molecule for the CD44 cell receptor often overexpressed on the surface of tumor cells.[196, 197] HA chitosan-PEG nanoparticles synthesized for the delivery of pDNA and siRNA have been shown to have transfection efficiency equivalent to that of Lipofectamine 2000 *in vitro* in 2010.[196] Nanoparticles for siRNA delivery composed of HA-spermine and HA-PEI have achieved above 90% knockdown *in vitro* with specificity for the CD44 receptor.[197] When the HA-PEI particles were tested *in vivo* for targeting of a metastatic lung cancer model implanted subcutaneously in mice, knockdown measured by qPCR up to 55% was observed.[197] Improving serum stability of nanoparticles is another area in which HA has been utilized in combination with polycations such as PEI, functioning in much the same way as glycosylation of proteins *in vivo*.[198] HA has also been utilized in the creation of hydrogels capable of delivering DNA at controlled rates for *in vivo* tissue engineering applications.[199]

Cyclodextrin

β-Cyclodextrin, shown in **Figure 2.3g**, is a three-dimensionally stable oligomer of glucose that forms cup like structures with a hydrophobic core. Chemical modification of β-cyclodextrin with acetyl groups enables the polymer structure to complex with nucleic acids as a cationic polymer. Cyclodextrin based nanoparticles developed in the lab of Mark Davis for the intravenous delivery of siRNA have notably reached clinical trials. These nanoparticles, shown in **Figure 2.5a**, are formulated from β-cyclodextrin, adamantine-PEG and the targeting ligand transferrin and have been shown to have many favorable characteristics for the delivery of siRNA including a size between 60-80 nm, a zeta potential +10-20 mV and the ability to protect siRNA from nuclease activity in the presence of serum for at least 4 hours.[200] In 2009 following animal trials in monkeys this nanoparticle formulation for the delivery of RRM2-siRNA was

tested in FDA Phase I clinical trials as a cancer therapeutic.[201] The Phase I trial involving 24 patients has since concluded with favorable results for the nanoparticle safety, including evidence for the lack of a complement response.[202] Additionally, RRM2 mRNA levels intratumorally were shown to have been reduced up to 77% and a 32% partial knockdown of RRM2 was measured for RRM2 protein levels in the tissue and shown in **Figure 2.5b**.[203] While this level of knockdown is unlikely to be effective as a solitary treatment for tumors, it provides the first evidence that siRNA can be targeted to tumor cells *in vivo* with measurable knockdown of a specific protein.

Dextran

Dextran, shown in **Figure 2.3h**, a branched polysaccharide of repeating glucose units, has been used in the formation of many nanoparticles for the delivery of siRNA and pDNA. Dextran is often acetelated to improve solubility in organic solvents and allow for pH dependent degradation.[204] While the structure of unmodified dextran does not fit the requirements of an ideal material for the delivery of nucleic acids, its status as an easily modified biocompatible and biodegradable polymer does allow for it to be utilized for other materials in the formulation of nanoparticles for nucleic acid delivery. Acetalated dextran has been used in conjunction with PBAE and spermine for the delivery of both siRNA and DNA.[182, 205] The Ac-DEX/PBAE particles created for the delivery of DNA were shown to undergo endosomal pH dependent degradation and also coated with cell penetrating peptides for improved endosomal escape.[182]

Spermine

Spermine, shown in **Figure 2.3i**, is a natural oligoamine that has been used primarily as an oligomer grafted onto non-cationic polymers to allow for the polymer to have a charge association with DNA. Biodegradable polysaccharide based particles using spermine as the

polycation have been explored with varying degrees of success. In 2002, a library of over 300 polysaccharide-oligoamine particles were created with some polysaccharide-spermine particles reaching transfection efficiency equal to that of Transfast cationic lipids.[206] Since then, acetalated-dextran spermine nanoparticles have been created for siRNA as well and shown to cause up to 60% knockdown of GFP in HeLa cells.[205]

Nucleic acid based particles

Nanoparticles composed entirely of nucleic acids have been created for the delivery of siRNA. Lee *et al.* used six 30 bp segments of DNA with complementary overhanging siRNA segments to create self-assembling tetrahedral oligonucleotide nanoparticles by complementation between the DNA and overhanging siRNA as shown in **Figure 2.3j**.[207] These particles, each carrying six siRNA molecules, were shown to have a circulation time four times longer than unprotected siRNA.[207] Oligonucleotide nanoparticles improved siRNA delivery for the knockdown of luciferase both *in vitro* and *in vivo* with a 60% reduction in bioluminescence of luciferase expressing tumors in a rat model two days after treatment.[207] These initial studies, particularly for improved *in vivo* delivery of siRNA have indicated that nucleic acid origami particles are a high capacity siRNA delivery method that deserves further study.[207]

2.1.5. Conclusion

Gene therapy holds great promise in treating various diseases of genetic origin by introducing exogenous nucleic acid to express desired proteins or knock down the expression of undesirable genes. A key challenge to gene therapy is effective delivery, and significant effort has been invested into developing biomaterials that can form nanoparticles to deliver genes to specific targets safely and efficiently. As highlighted in this chapter, a number of non-viral, biodegradable polymers have been developed to form biodegradable nanoparticles for gene

delivery and are promising due to their ease of synthesis, low toxicity, and efficacy at transfection. Importantly, strategies for polymer modifications have been identified to overcome major biological barriers to gene delivery. While a polymeric nanoparticle system for human gene therapy has yet to be FDA-approved, numerous systems for polymeric DNA and siRNA delivery are in preclinical and clinical trials. These systems, or their future derivatives, may be able to achieve the promise of genetic medicine.

2.2. Nanotechnology optimized for siRNA delivery

2.2.1. Introduction

Since its discovery in 1998,[208] the RNA interference (RNAi) gene silencing pathway has been a focus of many major areas of research. Chief among these are the natural mechanism of viral defense in plants and insects,[209-211] the discovery of endogenous protein function by reducing its production,[13] and the treatment of diseases that are caused by overproduction of a specific gene.[212, 213] The last of these applications in particular requires safe and effective methods for siRNA delivery in order to maximize the clinical potential of RNAi.

The natural RNAi pathway begins with double-stranded RNA (dsRNA) that is cleaved by the protein Dicer into ~21-base pair dsRNA known as short interfering RNA (siRNA). The antisense strand of siRNA is incorporated into the RNA-induced silencing complex (RISC), which binds and subsequently cleaves, in a catalytic fashion, strands of mRNA complementary to the siRNA. This prevents protein production and results in sequence-specific gene knockdown (for review, see Hannon[214]). Early methods to non-virally induce RNAi included direct injection of dsRNA[215-217] or mechanical agitation of cells in the presence of dsRNA.[218] However, these methods are not clinically translatable, and introduction of dsRNA longer than 30 base pairs has

been shown to induce an interferon (IFN) response.[219] As a result, delivery of siRNA to circumvent IFN is more frequently employed.

Although very effective, viral methods for nucleic acid delivery have been associated with immunogenicity and tumorigenicity.[14] Non-viral nucleic acid delivery systems are traditionally less effective[16] but can be designed to avoid issues typical of viruses. Several types of materials have been used for delivery of nucleic acids and of siRNA in particular. Because many early efforts at siRNA delivery used materials that were already well-studied in the context of DNA delivery, we first discuss properties of these materials that make them suitable for nucleic acid delivery in general and then describe their utility for overcoming barriers to siRNA delivery (**Figure 2.6**) in particular.

2.2.2. General properties of nucleic acid delivery nanoparticles

Nucleic acid binding or encapsulation ability

The biomaterial transfection agent must have sufficient ability to bind to or encapsulate the nucleic acid. Because nucleic acids are negatively charged, positively charged biomaterials are commonly used. Poly(L-lysine) (PLL)'s ability to bind DNA was discovered through studies of DNA-histone binding and conformation,[43] and it was later explored for delivery of exogenous DNA.[220, 221] PLL, however, lacks the ability to escape the endosome, an essential step in intracellular delivery through the endocytic internalization route.[222, 223] Other biomaterials such as liposomes are able to encapsulate nucleic acids within their aqueous interior. These artificial vesicles can be made with tight control over physical properties by changing the amphiphilic lipids that compose them as well as by varying fabrication methods.[18, 19, 224] Nucleic acid binding or encapsulation is generally a necessary, but not sufficient, biomaterial attribute to prevent

degradation of the nucleic acid and to facilitate the entry of such highly negatively charged molecules into the cell.

Shielding

Liposomes, as well as other types of nanoparticles (NPs), often suffer from quick clearance from the circulation by cells of the mononuclear phagocyte system (MPS).[225, 226] Chemical structure of specific materials aside, most NPs for nucleic acid delivery rely at least partially on ionic interactions for cellular uptake and carry charge on their surface. Although electrostatic repulsion contributes to NP colloidal stability in aqueous suspension, physiological salt[225, 226] and serum[227] conditions are often enough to coat the NPs non-specifically with proteins, and cause aggregation, leading to decreased delivery efficiency and increased clearance by MPS cells. One way to overcome this potential problem is to coat the NP surface with a shielding molecule, commonly poly(ethylene glycol) (PEG), whose hydrated structure can prevent non-specific interactions with biomolecules.[228] This strategy, dubbed "PEGylation," has been employed in a number of gene delivery systems, including NPs based on chitosan,[229] gelatin,[230] cationic polymers,[231] lipids,[232] and metallic NPs.[233]

It should be noted that PEGylation has also been found to prevent desirable interactions, such as those leading to intracellular delivery to target cells. As a result, researchers have explored the use of cleavable PEG chains on NP surfaces to increase circulation time but also allow effective transfection.[104]

Targeting and cellular internalization

A number of methods can be used to promote uptake of nucleic acids by cells of interest. For example, taking advantage of the properties of the lipid bilayer of cell membranes, cationic lipids can facilitate cellular uptake by interacting with anionic cell surface molecules.[234-236]

Similarly, other cationic materials, such as polymers, also show high uptake into cells compared to neutral or anionic materials due to interactions with the relatively negative cell surface.[103] Unfortunately, these interactions with NPs and the cell membrane can also contribute to cytotoxicity.[237]

Various chemical moieties and biological ligands can also be incorporated into the material or into the NP as an alternative or additional method of increasing cellular internalization. For instance, the amphipathic peptide GALA (30 residue polypeptide containing 4 Glu-Ala-Leu-Ala repeats) forms an alpha-helical structure that promotes interaction with lipid bilayers,[163] as does the KALA peptide (30 residue polypeptide containing 3 Lys-Ala-Leu-Ala repeats),[238] which has the additional advantage of being positively-charged at neutral or low pH for binding to nucleic acids. The transition from random coil to alpha helix, and therefore the ability to disrupt membranes, is pH-dependent for both of these peptides, making them potentially useful specifically for environmentally triggered membrane fusion.[239, 240] Other cell-penetrating peptides (CPPs) used for this purpose include the trans-activating transcriptional activator (TAT) peptide derived from the human immunodeficiency virus (HIV).[241, 242] This strategy can be combined with a disassembly approach by synthesizing a high molecular-weight form of TAT peptide, linked with disulfide bridges, that can be degraded by bioreduction to reduce potential cytotoxicity.[243]

In addition to general, non-specific cellular uptake, it is often desirable to be able to deliver siRNA to a specific cell or tissue type. Ligands such as sugars, aptamers, peptides, and proteins for cell- or tissue-specific cell surface proteins can also be coated on[89, 244] or conjugated to[245, 246] a biomaterial or NP to enhance uptake and delivery in a targeted manner.

Endosomal Escape

For successful intracellular delivery of nucleic acids, it is critical that that the NP be able to reach the cytoplasm safely and efficiently. A common method of overcoming the endosomal escape barrier is the proton sponge mechanism, in which a reversibly protonated material is believed to act as a buffer. This not only protects the cargo from acidification of the endosomal compartment but also causes a water influx that leads to endosome lysis and release of the cargo into the cytosol. This mechanism was proposed to explain the effectiveness of polyethylenimine (PEI) for gene transfer, as PEI contains reversibly protonated tertiary amines,[247] and while its validity has not been incontrovertibly proven and has been challenged,[248] it nonetheless remains the most widely believed hypothesis.[114, 249] Other materials like PLL can be modified to contain titratable amines, such as by substituting histidine or arginine for lysine residues,[48, 250] leading to improved transfection. Other materials like poly(amidoamine) (PAA) dendrimers are also reversibly protonated at physiologically relevant pH.[251] However, while these materials increased DNA delivery efficacy, some, like PAAs, bind siRNA less tightly, compromising their ability to act as siRNA delivery agents without additional modifications.[149]

Other methods for endosomal escape include hydrophobic biomaterials that can fuse with the membrane, such as dioleoylphosphatitylethanolamine (DOPE) in lipid-based particles.[252, 253] Polyanionic biomaterials have also been employed to promote membrane destabilization, often in a pH-dependent manner that allows triggered endosomal escape when NPs are in certain environments.[254] Membrane-disruptive peptides, such as GALA and KALA, can also be conjugated to or non-covalently associated with NPs to cause endosomal escape.[221, 239, 240] KALA in particular maintains α-helical character even at low pH (4.5), thus making it capable of membrane disruption and leakage even in lower pH environments comparable to late endosomes. KALA was shown to cause nearly 100% leakage of endosomal contents over pH range 4.5-8.[238]

Degradability and nucleic acid release

Release of a NP into the cytoplasm after endosomal escape is not necessarily sufficient for biological effect. It was shown that DNA plasmids must unbind sufficiently from a delivery vehicle for transfection to occur.[122, 123] However, while DNA must be trafficked to the nucleus, siRNA must be released in the cytoplasm, its principal site of action.[255] A number of factors can affect material degradation and cargo release rate; for example, poly(beta-amino ester)s (PBAE)s are hydrolytically degradable,[130] with their degradation and complex disassociation rate dependent on the local pH and the polymer conformation.[256] Because hydrolytic degradation of free PBAEs in solution takes place in hours at pH 7 at 37°C, these nanoparticles can diffuse or be convected to cells and release their cargo shortly thereafter. Moreover, the polymers showed slowed degradation at the lower pH (5-6) found in endosomal compartments, which could provide some protection for nucleic acids until after endosomal escape to the cytoplasm.

Aside from hydrolysis, as is characteristic of PBAEs and other polyesters, another mode of degradation useful in siRNA delivery is bioreduction due to disulfide linkages (for review, see Son *et al.*[257]). The latter mechanism takes advantage of the reducing cytoplasmic environment to cause quick, environmentally-triggered degradation and siRNA release into the correct cellular compartment.

NPs that do not have a mechanism to stimulate siRNA release may cause low knockdown. Gold NPs, for example, without an siRNA release mechanism may achieve lower knockdown or require higher siRNA doses[37] versus similar delivery vehicles that contain an efficient release mechanism.[38]

Biocompatibility

It is critical that materials administered to a patient be biocompatible. Although cationic lipids have been studied often for nucleic acid delivery, their disruption of the membrane, while an advantage for cellular uptake, can also cause excessive cytotoxicity.[258] Biomaterial degradation is one mechanism of increasing biocompatibility. Degradation of a biomaterial can reduce cytotoxicity, as molecular weight of cationic polymers has been positively correlated with cytotoxicity.[125] For instance, poly[alpha-(4-aminobutyl)-l-glycolic acid] (PAGA), a hydrolytically degradable PLL analogue containing ester bonds in place of the amide bond of the polypeptide, showed not only increased transfection efficacy but also negligible toxicity *in vitro* compared to unmodified PLL.[128] A hydrolytically degradable form of branched PEI showed a similar increase in biocompatibility[129] compared to the typically high cytotoxicity of unmodified PEI.[126, 259]

Stability

Although many of the above biomaterials have been explored for siRNA delivery, and most continue to be investigated for this purpose, several challenges remain to be overcome. Many of these biomaterials and NPs were initially developed for DNA delivery. Aside from differences in the site of action of these two nucleic acids, there are also biophysical differences between them. Although both are composed of similar anionic bases, siRNA molecules are much smaller in size than DNA plasmids. In addition, dsRNA is stiffer than dsDNA,[61, 260] and segments as short as siRNA act as rigid rods. This has important implications for nucleic acid binding properties[261, 262]: there is less multivalency in siRNA than in DNA when interacting with a cationic polymer because of fewer binding sites per molecule. In addition, the stiff RNA molecule, which is expected to condense very little, may not be able to bend to the

conformations ideal for high affinity binding and encapsulation, and this can lead to weak stability of siRNA-containing NPs.

In addition to low binding affinity, instability of the RNA cargo itself is a major problem in many of the delivery systems currently investigated. siRNA is more prone to enzymatic degradation than DNA, though less so than single-stranded RNA. Therefore, protection from the extracellular and endosomal environments is necessary for successful delivery. Stability is a challenge for lipid-based materials as well since lipid-based colloids often exhibit low stability.[263]

2.2.3. Nanoparticles for siRNA delivery

Examples of broad classes of biomaterials used for siRNA delivery are presented in **Figure 2.7**. Below and in **Table 2.1**, we will discuss illustrative examples of next-generation materials that address many of the challenges listed here, including siRNA binding and protection, particle stability, cellular internalization and targeting, material biocompatibility and efficacy, endosomal escape and intracellular targeting, and siRNA release.

Lipid-based nanoparticles

Lipid-based materials are the most widely-used biomaterials for nanoparticulate siRNA delivery. Of over 20 siRNA phase I clinical trials, nearly half use NPs as the delivery vehicle, and almost all of these are lipid-based.[264] Many of the leading commercially available reagents are lipid-based, including Lipofectamine™ 2000,[21] 1,2-dioleoyl-3-trimethylammonium-propane (DOTAP),[20] RNAifect,[20] and TransIT-TKO and TransIT-siQuest.[22] It has become clear, however, that careful controls are necessary for the successful interpretation of results, as siRNA in combination with cationic lipids can cause off-target effects. For example, an *in vivo* study in mice showed that intravenous injection of naked siRNA had no measurable effect; however,

injection of liposomal siRNA NPs based on 1,2-dioleoyl-3-trimethylammonium-propane (DOTAP), a commonly used cationic lipid for nucleic acid delivery, induced a potent IFN response, including the upregulation of downstream molecule STAT1 (signal transducer and activator of transcription 1).[20] Although the greatest effect was seen with DOTAP/siRNA complexes, including several different siRNA sequences, DOTAP alone did cause an IFN and STAT1 response, emphasizing the importance of careful design of the material used for lipid-based NPs to avoid potentially adverse side effects as well as careful interpretation of results. Some researchers have focused on overcoming this problem in particular; for example, Chono *et al.*[23] used the additional components of hyaluronic acid, a polysaccharide with low immunogenicity, PEG, and a targeting ligand, and found that their liposome elicited no significant immunotoxicity, measured by cytokine expression, within their therapeutic range. Other strategies have been employed to reduce the off-target immunological response to siRNAs, particularly when delivered within liposomes; for instance, 2'-O-methyl-modified siRNAs were designed and delivered in stable nucleic acid lipid particles (SNALPs)[265] with less unwanted immune stimulation observed.

To bypass problematic toxicity and particle instability and to maximize siRNA delivery and gene knockdown, several strategies can be employed. Akinc *et al.* used a combinatorial library to link acrylate esters or acrylamides containing 9- to 18-carbon hydrocarbon tails via one of many different amine-containing small molecules,[266] thereby creating a wide range of lipidoid materials with slightly varying structure (**Figure 2.8**). These lipidoid molecules were mixed with cholesterol and a PEG-lipid (polyethylene glycol conjugated to a lipid moiety for incorporation into liposomes via hydrophobic interactions) and loaded with siRNA. Using this method, the authors optimized nanocomplex stability and efficacy *in vitro*, then used top materials to achieve

>90% knockdown *in vivo* after two daily intravenous injections of 2 mg siRNA/kg mouse. A follow-up study showed increased efficacy of their material to nearly 100% when the siRNA dose was increased to 10 mg/kg, though high toxicity associated with cationic lipids necessitated a lower lipid concentration to be tolerable. The authors improved the biocompatibility by maximizing siRNA loading, thereby reducing the total lipid content delivered, and optimized the PEG chain length to improve *in vivo* particle stability.[267]

Lipid material optimization and selection has also been done to examine very specific aspects of transfection. For example, one reason for the use of cholesterol in liposome formulations is to increase fusion with the cell membrane for internalization,[268, 269] in addition to affecting the fluidity or rigidity of the liposome bilayer. Other lipids have also been found to promote fusion of the liposome with the endosomal membrane because their structure requires less energy to transition to a non-lamellar phase, forming tubular structures with hydrophobic tails exposed and promoting siRNA release into the cytoplasm.[270, 271] While many groups have incorporated fusogenic lipids into their NP formulations and some trends had been implicated in increasing fusogenicity, Heyes *et al.* specifically studied the effect of saturation and chain length on fusogenic phase transition as well as on transfection efficacy.[272] They and others have investigated siRNA delivery from SNALPs by selecting the best fusogenic lipid for the endosomal escape step. Semple *et al.* used *in vivo* screening in mice to develop siRNA-containing SNALPs that could be administered i.v. to non-human primates and cause 80% knockdown of a target gene.[273]

The *in vivo* studies described, while showing high efficacy, required ~1 mg/kg of siRNA to achieve knockdown. By using a similar combinatorial method to that mentioned above, Love *et al.* identified a linker molecule, *N*-(2-(4-(2-aminoethyl)piperazin-1-yl)ethyl)ethane-1,2-

diamine, that, after reaction with the 12-carbon epoxide 1,2-epoxydodecane, formed lipid-based NPs that were primarily taken up by macropinocytosis rather than endocytosis, as with their previously-studied materials.[29] They were able to achieve one to two orders of magnitude better efficiency (0.03-0.3 mg/kg dose) in non-human primates with up to ~75% knockdown at the lowest dose, possibly because their internalization route allowed their particles to avoid the endosome. The authors note that lower siRNA doses, while causing the same initial effect, had lower knockdown duration compared to high siRNA doses. This high nucleic acid efficiency allowed the authors to reduce the total amount of lipidoid material needed for therapeutic benefit, lowering potential toxicity, and also allowed them to knock down several genes in a single combined dose.

In addition to nanomaterial composition, siRNA delivery efficacy *in vivo* can also depend heavily on the route of administration. Leconet *et al.*, using commercially available reagents (the lipid-based Invivofectamine 2.0 and the polymeric JET-PEI), achieved transient knockdown in diabetic mice, with a single injection of siRNA/lipid-based carrier able to knock down a target gene for at least seven days in their system.[274] In particular, they found that pancreatic immune cells were transfected with much greater efficacy after intraperitoneal injection compared with intravenous injection. All of these various factors, therefore--specific siRNA sequence and chemical modification, material composition, dose of siRNA and/or material, additives into the liposome, route of cellular entry, and route of *in vivo* administration--can each have enormous effects on RNAi mediated by lipid-based nanocarriers.

The ability of lipid-based materials to stably encapsulate siRNA has led to their prolific use in ongoing clinical trials relative to other siRNA delivery technologies (for review, see Forbes and Peppas[264]). In particular, the decreased immunogenicity and enhanced *in vivo*

stability and shielding promoted by the PEG layers surrounding SNALPs has enabled multiple clinical trials involving SNALPs. Drug TKM-080301 sponsored by Tekmira Pharmaceuticals Corporation and Alnylam Pharmaceuticals is a SNALP containing siRNA targeting polo-like kinase-1 (PLK-1). This drug has completed a Phase I trial administered via hepatic arterial infusion for primary or secondary liver cancer, and is currently undergoing an additional Phase I trial targeting solid tumors via intravenous infusion.[275, 276] SNALP-based siRNA drug ALN-TTR01, also sponsored by Alnylam Pharmaceuticals, has completed a Phase I trial using siRNA targeting transthyretin in an effort to treat Transthyretin-Mediated Amyloidosis.[277] Cationic lipid nanoparticle-based siRNA drug Atu027 sponsored by Silence Therapeutics AG has completed a dose-escalation, Phase I clinical trial to assess toxicity.[278] These and other lipid-based siRNA delivery technologies represent the class of material nearest to reaching the clinic for siRNA delivery.

Polymeric nanoparticles

Although lipid-based nanoparticles have been historically more widely used for nucleic acid delivery, polymer-based nanoparticles are very promising newer class of materials for the delivery of nucleic acids and are an active subject of ongoing research. Because many of the polymers used for siRNA delivery were originally investigated as DNA delivery materials, many of them have gone through iterations of modification as various hurdles specific to siRNA delivery were discovered. Key classes of materials are described below, along with examples of the bottlenecks encountered and the strategies used to sidestep them.

Poly(l-lysine)- and polyethylenimine-based materials

PLL and PEI, as mentioned above, were early candidate materials for siRNA delivery, with PEI still used frequently in research today. Derivatives of both polymers continue to be

developed and optimized and are the basis of many of the polymeric systems being studied for siRNA delivery. Because PLL/nucleic acid complexes can be taken up by cells but cannot efficiently escape the endosome, Meyer *et al.* developed PLL- and PEI- based materials by conjugating the polycation to an endosomolytic mellitin peptide sequence modified with pH-labile protecting groups (dimethylmaleic anhydride), which restrict the lytic activity of the peptide until they are cleaved at acidic pH.[279] However, because the peptide was negatively charged and was necessary in high number for effective endosomal escape, this covalent modification destabilized the polymer/siRNA complex, precluding the formation of sufficiently small NPs for cell uptake. As a solution for this, the authors grafted PEG to the polycation before modification with the peptide, which increased the stability of the complex and caused gene knockdown *in vitro* in human neuroblastoma cells.

Miyata *et al.* used a previously-developed[280, 281] PEG-*b*-PLL copolymer to deliver nucleic acids.[145] By modifying some of the lysine sidechains with thiol-containing functional groups, they could form micelles via electrostatic interactions with anionic DNA and then oxidize the complexes, forming disulfide bridges to stabilize the particles.[145] This method was also effective for *in vitro* siRNA delivery to Huh7 human hepatoma cells, with ~80% knockdown seen after delivery of 100 nM siRNA to Huh7 cells in the presence of serum. Because of weaker binding seen in siRNA polyplexes compared with DNA polyplexes, the authors further modified their polymer with 2-iminothiolane to increase the cationic character and thus strengthen siRNA binding.[144] Because of the difference in redox potential between the cytoplasm and extracellular environment, this system carries with it the advantage of quick siRNA release once in the desired cellular compartment. Further improvements on this system included the conjugation of cyclic RGD peptide to the PEG block, thereby providing a method to target tissues *in vivo* (**Figure**

2.9a).[282] These siRNA-containing micelles accumulated in tumor tissue and the surrounding vasculature in a subcutaneous HeLa tumor model. Delivery of 24 μg siRNA per mouse (~0.5-1 mg/kg) against vascular endothelial growth factor (VEGF) and VEGF receptor 2 (VEGFR-2) two times every four days for 12 days showed ~50% decreased in measured VEGF mRNA levels in the tumor and significantly slowed tumor growth (~60-70% smaller tumor volume after 12 days compared to control) without apparent toxic side effects on the animal. Similar strategies have also been employed with PEI, using PEGylated siRNA against VEGF to form PEI-based micelles that caused VEGF knockdown in an *in vivo* PC-3 prostate cancer model.[283]

With toxicity as a major problem limiting the use of PEI, forms of degradable PEI have been studied extensively for siRNA as well as DNA delivery. Breunig *et al.* linked low-molecular weight linear PEI segments with disulfide bridges to form a bioreducible PEI.[146] Combining the efficacy of high-molecular PEI with the biocompatibility of shorter polymer chains, they delivered 100 nM siRNA *in vitro* to Chinese hamster ovary cells (CHO-K1) in serum-free medium and were able to achieve *in vitro* RNAi of green fluorescent protein (GFP) expression (~50% knockdown) that was comparable in efficacy to that of high-molecular weight branched PEI (bPEI) while being less cytotoxic. This design carried with it the additional benefit of targeted siRNA release into the cytoplasm, as disulfide bridges would be expected to be reduced to thiols.

Other classes of polymers

Also capitalizing on bioreducible linkages for targeted release, Jeong *et al.* described the use of a bioreducible PAA, designated SS-PAEI [poly(amido ethylenimine)], for siRNA delivery.[148] Having found previously that SS-PAEI had higher buffering capacity than PEI,[284] they further demonstrated that their bioreducible polymer could cause significant knockdown of

vascular endothelial growth factor (VEGF) expression from human prostate cancer cells *in vitro* with 30 nM siRNA delivered in serum-free medium. Their polymer was more effective (up to ~80% less mRNA expression) and less toxic than the linear PEI used as a comparison. Because there was not a significant increase in cellular uptake of SS-PAEI/siRNA particles compared to PEI/siRNA, the authors concluded that intracellular events, likely the disulfide reduction step, was the main reason for the increased efficacy. The siRNA binding efficiency of SS-PAEI is lower than that of PEI; therefore, SS-PAEI was copolymerized with a polymer block containing ethylene diamine.[149] The increased amine content and therefore increased positive charge caused tighter siRNA binding and, at optimized ratios, better *in vitro* knockdown efficiency in human head and neck carcinoma cells (UM-SCC-14C) and non-small-cell lung carcinoma (H1299).

Further optimization of this system included PEGylation by adding PEG-amine into the SS-PAEI synthesis, then mixing PEG-containing SS-PAEI with PEG-free SS-PAEI in order to improve particle stability in the presence of blood components like serum.[285] However, while particles with higher PEG content were more stable against aggregation in serum or salt, they were also more easily dissociated in the presence of heparin, suggesting less stable binding interactions between siRNA and highly PEGylated polymers. Toxicity in erythrocytes as well as H1299 cells decreased with increasing PEG content, although this came at the cost of strongly compromised knockdown efficacy as well.

Similar to PAAs are poly(ester amine)s (PEAs) or poly(beta-amino ester)s (PBAEs), which are hydrolytically degradable through their ester groups. Initially studied primarily for DNA delivery, some early attempts to use PBAEs for siRNA delivery fell short without additionally conjugating siRNA to solid particles.[286] As with other cationic polymers, this class of materials faced obstacles in polymer-siRNA binding efficiency and intracellular release. By

increasing the ratio of PBAE to siRNA (100:1 or greater PBAE:nucleic acid ratio by weight, compared to ~50:1 for DNA delivery), better particle formation and siRNA complexation was achieved, resulting in successful knockdown (~70%) in human umbilical vein endothelial cells when 60 nM siRNA was delivered in medium with 2% serum.[141]

Other groups were able to show ~70% *in vitro* knockdown in hepatoma cells in serum-free medium with lower PBAE:siRNA weight ratios when using PBAEs of similar chemical structure.[287] Interestingly, the PBAE molecular weight reported was higher than that of the previous two studies cited and this may have enabled the increased efficacy at lower PBAE:siRNA weight ratios. Trends in PBAE structure with siRNA delivery efficacy have since been further examined,[256] confirming the general trend of increasing knockdown efficacy with increasing PBAE molecular weight, as well as other polymer properties like hydrophobicity. This study also showed that the siRNA dose could be decreased by a factor of twelve (as low as 5 nM) without negatively affecting the knockdown efficacy (~90% knockdown in serum-free medium) as long as the total polymer concentration was not altered. Transfection in 10% serum-containing medium was lower (~70%), which the authors believed was due to some destabilization of the nanoparticles in the presence of serum proteins. In particular, this was observed with the top PBAEs in the study, most of which contained a primary amine terminal functional group that could be cleaved in a reducing environment. By utilizing disulfide bonds, this study and others[9, 288] have found bioreducible linkages can be a key attribute for successful non-viral siRNA delivery. In another study, poly(ethylene oxide) (PEO)-*b*-PBAE NPs were made for siRNA delivery in combination with PEO-*b*-poly(ε-caprolactone) (PCL) NPs loaded with paclitaxel.[213] This study showed successful knockdown of MDR-1, a cause of multiple drug

resistance in cancer cells, and consequently increased efficacy of a chemotherapeutic *in vitro* in SKOV3 ovarian cancer cells.

The combination of PEGylation with disulfide linkages has also been applied to polypeptides, including KALA.[147] Mok *et al.* conjugated PEG to siRNA via a disulfide bridge. Cysteine-containing KALA was then self-crosslinked to form a high-molecular weight, but bioreducible polymer, which electrostatically complexed with siRNA-PEG. This system was able to achieve nearly 50% gene knockdown in MDA-MB-435 melanoma cells, cultured *in vitro* in the presence of 10% serum with siRNA concentration of ~60 nM.

Woodrow *et al.* had an interesting finding while investigating the effectiveness of poly(lactic-*co*-glycolic acid) (PLGA) NPs at siRNA-mediated silencing *in vivo*.[289] Although a positively-charged component, spermidine, was included in the encapsulation formulation, it was used as an excipient rather than as a primary delivery agent. The PLGA/siRNA NPs themselves were small enough for cellular internalization, and siRNA released over time from the particles could be isolated and delivered separately without loss of function. Using these particles, the authors delivered siRNA across the vaginal mucosal barrier and effected knockdown in cells in the vaginal tract. A major advantage of this system is the biocompatibility of PLGA and related polyesters, which have been used in a number of FDA-approved devices. In addition, being solid particles, this delivery system does not suffer from unstable binding interactions as do many polymeric electrostatic complexes. Researchers are interested in adding cationic materials, such as chitosan or the above spermidine, as part of PLGA-based NPs to increase siRNA loading into anionic PLGA NPs and increase knockdown efficacy.[290]

A study by Zhou *et al.*[291] provides an example of how several components can be combined in a NP design to incorporate many different functions and properties. The authors

used as its base material a PEG-grafted PLGA-*b*-PLL block copolymer previously developed for fabrication of surface-functionalized NPs.[292, 293] DNA or siRNA was loaded into the NPs during synthesis, along with palmitoyl-avidin, allowing biotinylated peptides to be conjugated to the NP surface. In this way, the authors were able to design NPs containing polycations for nucleic acid complexation; PLGA as a biocompatible matrix; PEG to improve stability and circulation time; two encapsulated drugs to enhance delivery efficacy and siRNA processing; and three peptides to promote cellular uptake, endosomal escape, and tissue homing (**Figure 2.10**). While this type of drug delivery vehicle is more complex than some of the other examples described here, it provides flexibility in formulation and design details and was effective *in vitro* for ~91% knockdown in A549 lung cancer cells in culture medium.

Other elegant polymer designs for siRNA delivery, including a multifunctional, cyclodextrin-based vehicle, have had successful siRNA delivery preclinical studies and have moved forward to clinical testing.[294] This formulation, denoted CALAA-01, is a self-assembled complex of siRNA with a multi-component delivery vehicle, consisting of (i) a cyclodextrin-containing polymer, which also contains positive charges for siRNA binding; (ii) adamantane-conjugated PEG, with PEG added for particle stability and adamantine used to bind to cyclodextrin; and (iii) an adamantine-PEG-transferrin conjugate for targeting. This polymeric siRNA formulation, designed for good *in vivo* stability and site-specific delivery, is currently in a phase I trial.

Inorganic NPs

Calcium Phosphate

Calcium phosphate (CaP) crystals were originally developed for DNA delivery and were fabricated by highly saturated solutions of DNA and CaP that resulted in spontaneous

coprecipitation.[25-27] In an effort to limit the rapid and often difficult-to-control growth of CaP crystals, Kakisawa *et al.* developed an inorganic-organic NP hybrid for DNA delivery in which polyaspartate segments of polyaspartate-PEG block copolymers could adsorb onto the expanding crystal surface, thereby limiting continued growth.[35] The PEG segments impart biocompatibility and particle stability.

This NP formulation was eventually used for *in vitro* siRNA delivery to human embryonic kidney 293 cells and was able to achieve roughly 50% gene knockdown using a 125 nM siRNA dose in serum-containing media.[295] However, these particles required chloroquine for efficient endosomal escape, so the same researchers replaced polyaspartate with poly(methacrylic acid) (PMA), as PMA becomes more hydrophobic in pH 4-6 and could disrupt the endosomal membrane. To assess the siRNA delivery of this CaP-PMA-PEG system to 293 cells in a more physiologically relevant way *in vitro*, the group incubated all siRNA transfection agents in serum-containing media for 30 min prior to transfection. They were able to show significantly lower toxicity than Lipofectamine™ 2000 and a significantly higher gene knockdown of 65% versus RNAifect™ at 42%.[295]

siRNA loading into CaP based NPs was improved five-fold versus previously described systems by Zhang *et al.* via the covalent linkage of PEG to siRNA before precipitation with CaP. These NPs achieved roughly 60% gene knockdown in HeLa cells with 100 nM siRNA in serum-containing media.[296]

Gold

Gold-based nanoparticles (AuNPs) are attractive drug delivery candidates due to their low cytotoxicity,[32] easily tunable physical properties,[31] and readily functionalizable surface chemistry.[28, 30, 297] Elbakry *et al.* used AuNPs and the ionic layer-by-layer (LbL)[298] surface

modification process for siRNA delivery. These researchers took advantage of sulfur-gold binding to coat AuNPs with 11-mercaptoundecanoic acid (MUA), then used electrostatic interactions to coat the particles with a layer of PEI, followed by siRNA and another layer of PEI. *In vitro* delivery to CHO-K1 cells using 290 nM siRNA in serum-containing media resulted in approximately 80% knockdown.[37] However, this particular NP formulation required a high siRNA dose most likely because it included no siRNA release mechanism. Cytoplasmically-targeted siRNA release was achieved by Lee *et al.* in a AuNP formulation in which siRNA was attached to AuNPs via a PEG linker and bioreducible disulfide bonds, then coated with PBAEs. This formulation achieved near-complete gene knockdown in HeLa cells when a 90 nM dose of siRNA was delivered in serum-containing media.[38] Giljohann *et al.* have also demonstrated transfection agent-free delivery of siRNA through the use of AuNPs densely functionalized with RNA oligonucleotides.[299] In this study, ~100 nM of RNA duplex (3 nM AuNPs) caused 73% knockdown in HeLa cells. In an intriguing recent development, spherical nucleic acids, consisting of 13 nm AuNP cores and 30 siRNAs per particle densely functionalized around the surfaces, were able to penetrate skin and cause functional knockdown in hairless mice following topical treatment *in vivo*.[300]

Silica

As NP-based siRNA therapeutics are developed for clinical use, an important obstacle will be to create optimal dosing regimens, ideally those that minimize dosing frequency. Multistage release vectors were developed to address this issue by using nanosized lipid-based siRNA carriers loaded into micron sized, porous silicon particles.[301] In an *in vivo* study of orthotopic mouse ovarian carcinoma, this systemic delivery system extended gene knockdown from a few days to more than three weeks and effectively reduced angiogenesis, cell

proliferation, and tumor burden. Another formulation was developed in which porous silicon nanoparticles were loaded with the chemotherapeutic doxorubicin and siRNA targeting a drug efflux transporter, and then coated with siRNA. *In vitro* delivery of these particles to multidrug-resistant KB-V1 cells showed knockdown of the drug transporter, resulting in increased intracellular and intranuclear doxorubicin levels.[302]

Quantum Dots

Quantum dots (QDs) are inorganic semiconductor nanoparticles and can be used as fluorophores. QDs with easily tunable emission properties, such as CdSe/ZnS nanoparticles, are promising candidates for imaging purposes in that they are brighter,[34, 303] less susceptible to photobleaching,[33] are easier to detect amongst *in vivo* background fluorescence versus most fluorescent dyes,[34] and are able to be made biocompatible enough to be used with cells.[304, 305] Chen *et al.* first codelivered siRNA and QDs in order to trace the delivered siRNA *in vitro*.[306] This concept was extended to make QDs part of the delivery system itself by Derfus *et al.*, in which QDs were covalently modified with PEG, siRNA, and a tumor homing peptide (F3) to deliver siRNA to HeLa cells.[36] They were able to show that cell uptake was facilitated by F3 conjugation, and the NPs achieved approximately 30% gene knockdown in serum conditions with a 50 nM dose of siRNA. Although the NPs could not improve upon the knockdown achieved by Lipofectamine™ 2000, this delivery system showed an exciting proof-of-concept for a method to deliver and specifically track siRNA molecules using QDs.

Engineered RNA-based NPs

As gene knockdown via direct delivery of siRNA is a transient, dose-dependent process, siRNA loading into the delivery system is critical for complete and long-lasting gene suppression. Delivery systems in which siRNA is conjugated directly to a biomaterial or in

which engineered RNA is the delivery material itself present exciting strategies to maximize loading. An example of increased loading was examined earlier in this review when siRNA was directly conjugated to PEG and coprecipitated with CaP to improve siRNA loading five-fold.[296] Additionally, particle stability can be enhanced with the use of multimeric siRNAs, a class of material created by either covalently or noncovalently linking siRNA molecules. These multimeric siRNAs promote multivalent biomaterial-nucleic acid interactions similar to those seen with plasmid DNA, resulting in improved NP stability with RNA. Strategies for modifying siRNA while maintaining its biological activity are discussed below.

siRNA Conjugates

Important considerations for chemically modifying siRNA include assuring that the modification will not interfere with RNAi,[307] and, for modifications where multiple siRNAs are attached to each other, that the long chain of RNA will not induce an IFN response.[219] Singh *et al.* examined the former issue using the PEGylated siRNA-QD conjugates described earlier in this review. The authors found that decreasing the length of the siRNA-QD linker resulted in less RNAi, while lengthening this linker promoted more RNAi. They also found that the site of conjugation on the siRNA molecule, 5' versus 3', sense versus antisense, did not seem to effect RNAi.[308] These results confirmed what an earlier study had concluded with conjugation to magnetic NPs.[309]

Another investigation into PEG-siRNA conjugation utilized a disulfide linker and formed NPs using PEG-siRNA and PEI. These NPs were able to achieve 80% and 96.5% gene knockdown in serum and serum-free conditions, respectively, in human prostate carcinoma PC-3 cells using a 100 nM siRNA dose.[310] The same material in an *in vivo* study using subcutaneous PC-3 tumors and IV injection of NPs with 1.5 nmol VEGF-targeting siRNA showed 86 ± 4%

decreased VEGF expression, resulting in a 78 ± 9% reduction in microvessel formation and a ten-fold decrease in tumor volume.[283]

An alternative siRNA conjugation strategy involves conjugating the 3' end of the sense strand of siRNA to cholesterol. Such a system can cause 50% knockdown in HeLa cells with a ~200 nM siRNA dose without using any additional transfection agent or nanoparticle.[311] Cholesterol-siRNA, but not unmodified siRNA, has improved pharmacokinetic properties and can mediate knockdown in mice following i.v. administration. Other lipophilic modifications to siRNA can also enhance *in vivo* knockdown.[312]

Multimeric siRNA

While most strategies focus on tuning vector material properties to make DNA delivery vehicles work for siRNA delivery, another approach is to adjust the siRNA itself to make it physically more like DNA. Multimeric siRNA allows for increased multivalent interactions in addition to lending the geometric flexibility that is favorable for higher affinity binding. An interesting method to form multimeric siRNA was introduced by Bolcato-Bellemin *et al.* in which they synthesized siRNA strands with 5-8 bp overhangs to yield "sticky siRNA ends" that would reversibly concatemerize to form long repeats of siRNA.[313] When delivered with linear PEI to A549 human lung carcinoma cells in serum-free conditions, these NPs achieved 80% gene knockdown with 50 nM siRNA and 70% knockdown with as little as 20 nM siRNA. The authors also showed that this material triggered no IFN response. This concept was later expanded upon by covalently linking siRNA strands with either a bioreducible or non-degrading linkage.[314] When complexed with linear PEI, both the cleavable and non-cleavable siRNA NPs achieved near complete gene knockdown in PC3 cells with a 90 nM siRNA dose in serum-free conditions. However, when using rapid amplification of cDNA ends to look for the specific

cleaved target mRNA, the authors only found a significant concentration of the expected fragment in the samples treated with the disulfide-linked siRNA.

A unique method to create an siRNA-based material was recently suggested by Lee *et al.*[315] The group employed rolling circle transcription[316] to make connected repeats of hairpin RNAs, which then crystallized into growing sheets to eventually form microsponges. From these microsponges, micron-sized, spherical particles could be pinched off and coated with bPEI to compact them into roughly 200 nm sized particles. These particles achieved such incredibly high siRNA loading that the authors were able to show comparable knockdown to commercially available siRNA delivery systems using three orders of magnitude fewer particles. *In vitro* delivery of these particles to T22 cells achieved nearly 60% knockdown with 100 nM siRNA, and an *in vivo* intratumoral injection to T22 cells showed significant gene knockdown at 4 days post-transfection.

An additional class of three-dimensional nucleic acid-only structures for RNA delivery are polyvalent nucleic acid nanostructures. These have been synthesized by Chad Mirkin and his research group by constructing intra-crosslinked spherical nucleic acids with an inorganic nanoparticle core and then subsequent dissolution of this core.[317] These polyvalent nucleic acid nanostructures share many of the characteristics of spherical nucleic acids including being able to cause comparable efficient gene knockdown.

2.2.4. Conclusion

Despite its clinical potential, use of siRNA as a therapeutic has been hampered by a lack of effective and safe methods of delivery. Many different materials have been explored in the laboratory, with some, mostly lipid-based, having been translated to the clinic in early-phase trials. It is important to note, however, that both the siRNA molecule itself and also the delivery

vehicle can have off-target effects that may confound results and affect the translation of this technology.

As each biomaterial is developed, challenges in siRNA delivery are illuminated, aiding in the design of improved carrier NPs. New biomaterials have now been developed to fit the chemistry, biophysical structure, and biological function of siRNA. Many research groups are exploiting the benefits of increased siRNA binding affinity, for example, by increasing the positive charge of a biomaterial or by synthesizing multimeric siRNA molecules, to improve stability and delivery efficacy. Similarly, other researchers are investigating triggered release properties, such as disulfide bonds to cause siRNA release upon entering the cytoplasm, to improve delivery efficacy and reduce cytotoxicity. These next-generation materials have shown promise in the laboratory both *in vitro* and *in vivo*. As better ways for siRNA delivery are discovered, the wide range of therapeutic benefits to using siRNA will more fully come to light.

2.3. Tables

Table 2.1. Types of biomaterials used for siRNA delivery and the challenges they pose.

Biomaterial type	Major Challenges	Strategies to overcome	Examples
Lipid-based nanoparticles	Off-target immunogenicity	Surface-coating with non-immunogenic materials	DOTAP-based nanoparticles surface-modified with hyaluronic acid and PEG[23]
	Toxicity	Low lipid-to-siRNA ratio	Amine-containing lipidoid synthesized from 12-C acrylamides was complexed with siRNA at different ratios to find maximum siRNA loading efficiency[267]
		Empirical testing of different compounds	Screening of a combinatorial library of synthetic lipidoids and test for toxicity and efficacy[266]
	Cellular uptake	Fusogenic lipids	Addition of cholesterol to liposome[266-269]
			Lipid structure engineered to promote fusogenic phase transition[272]
		Other lipid interaction with membrane	Screening of lipid polar headgroups with different size, charge, and acid-dissociation constant[318]
	Liposome instability	Surface modification	Incorporation of PEG into liposome formulation[266, 267, 273]
Polymeric nanoparticles	Endosomal escape	Proton-sponge effect (buffering capacity)	Reversibly protonated tertiary amines (e.g. PEI,[247] PAA,[251] PBAE[130])
		Fusogenic peptides	PLL conjugated to pH-sensitive endosomolytic peptide[279]
			PLGA-b-PLL nanoparticles non-covalently coated with endosomolytic peptide[291]
			Membrane-penetrating peptide KALA crosslinked into an siRNA-binding polymer[147]
	siRNA binding	High polymer cationic character	Primary polymer blended or doped with polycation (e.g. chitosan[290])
			Addition of a small molecule with primary amines[144, 149, 319]
			Copolymerization with polycation[291]
		Crosslinked particles	Oxidation of thiol-functionalized polymers to form disulfides throughout nanoparticle[144, 282]
	Toxicity	Degradation	Hydrolytically-cleavable ester moieties (e.g. PBAEs)[9, 141, 213, 287]
			Bioreducible disulfide bridges[9, 141, 146-149, 284, 285, 319]
	Cellular targeting	Tissue-specific ligands	Conjugation of ligand to polymer[282]
			Non-covalent coating of nanoparticle surface with ligand[291]
Inorganic NPs	Long-term efficacy	Controlled release	Porous silica particles that can be loaded with siRNA-containing NPs[301]
	Toxicity	Gold-based NPs	Gold NPs coated with PEI and siRNA using LbL process[37, 38]
			Gold NPs functionalized with PEG and siRNA, then coated with PBAEs[38]
			Gold NPs functionalized with polyvalent siRNA[299] and made into spherical nucleic acids[300]
	Particle tracking	Quantum dot-based NPs	Quantum dots covalently modified with siRNA, PEG, and a tumor homing peptide[36]
	Particle instability	Multimeric siRNA	siRNA strands with "sticky" overhangs that reversibly concatamerize[261, 283, 308, 310]

Engineered RNA-based NPs			RNAi microsponges containing densely packed, multimeric siRNA[315]
	Interferon response	Control over RNA size	Disulfide-linked multimeric siRNA[261, 314]
			siRNA strands with “sticky” overhangs[261, 314]
	Loss of siRNA biological activity	Labile, long, or crosslinked linkages	Disulfide linkages[283, 308, 310] or long, non-labile linkages[308]
			Polyvalent nucleic acid nanostructures[317]

2.4. Figures

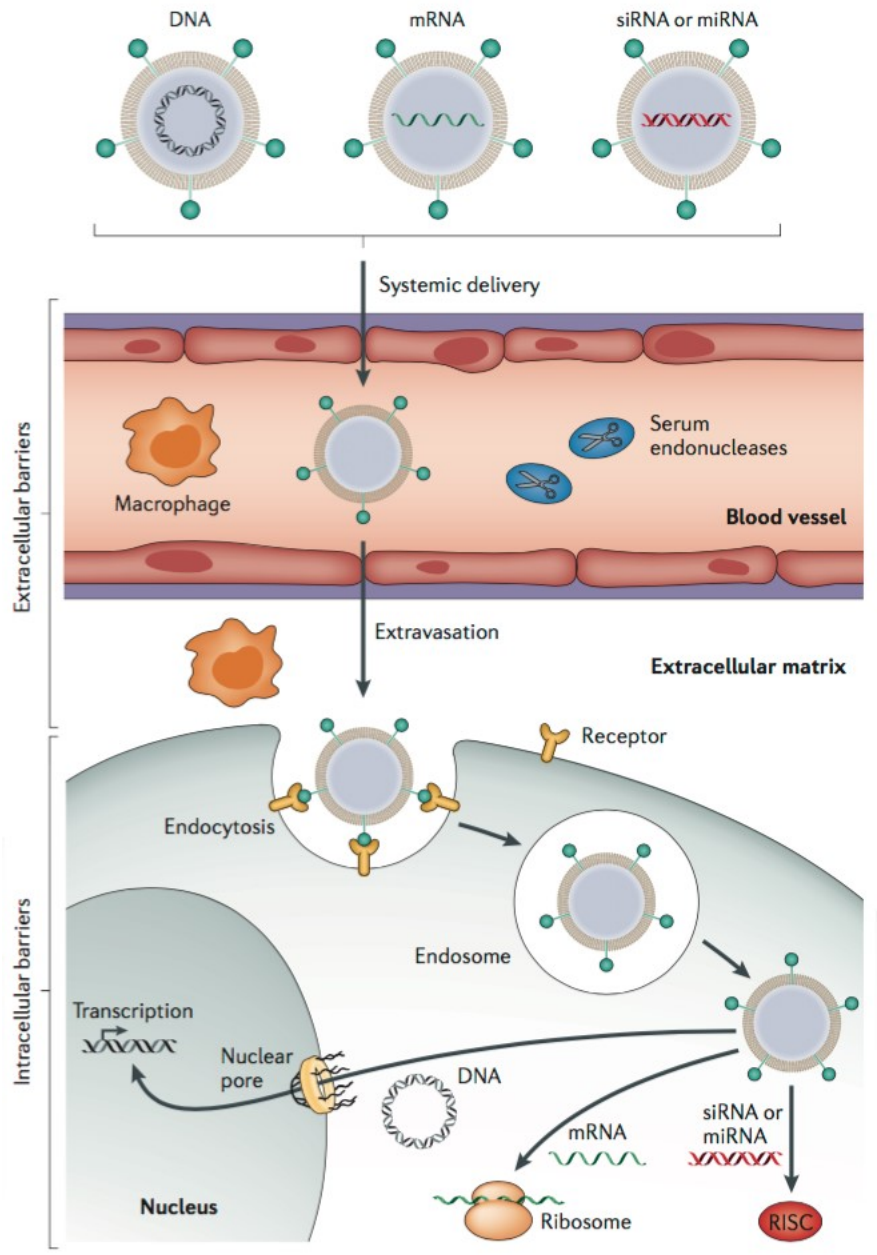

Figure 2.1. Major barriers to nucleic acid delivery using nanoparticles include stable particle formation, systemic circulation, tissue and cell targeting, cellular uptake, endosomal escape, and release of nucleic acid. Reprinted by permission from Macmillan Publishers Ltd: *Nature reviews. Genetics* **2014**, 15, 541-55, copyright 2014.[40]

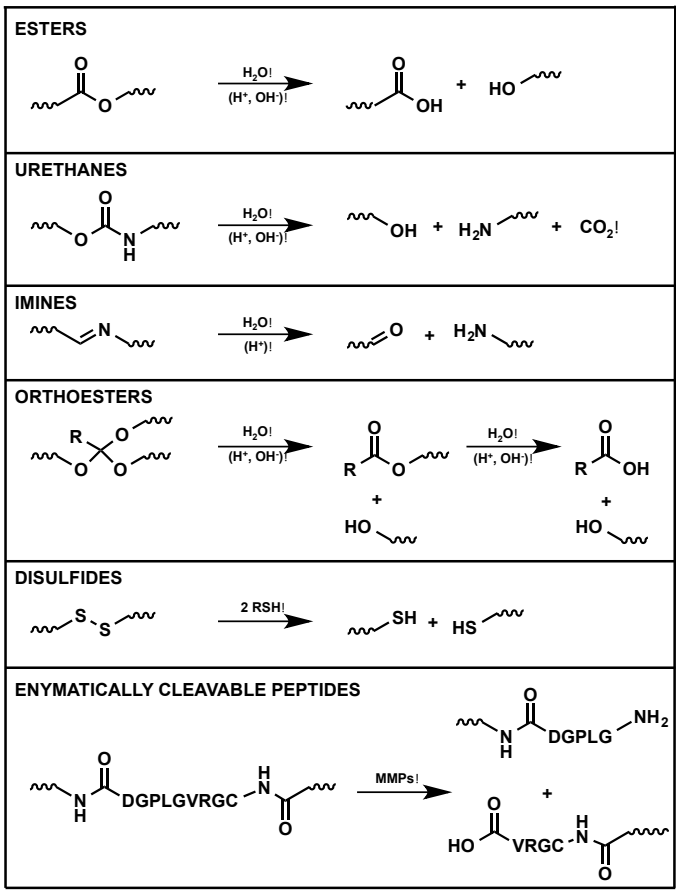

Figure 2.2. Commonly used chemical moieties for the creation of degradable polymers. Chemicals listed above the reaction scheme arrow indicate those necessary for the reaction, while chemicals listed below indicate reaction catalysts.

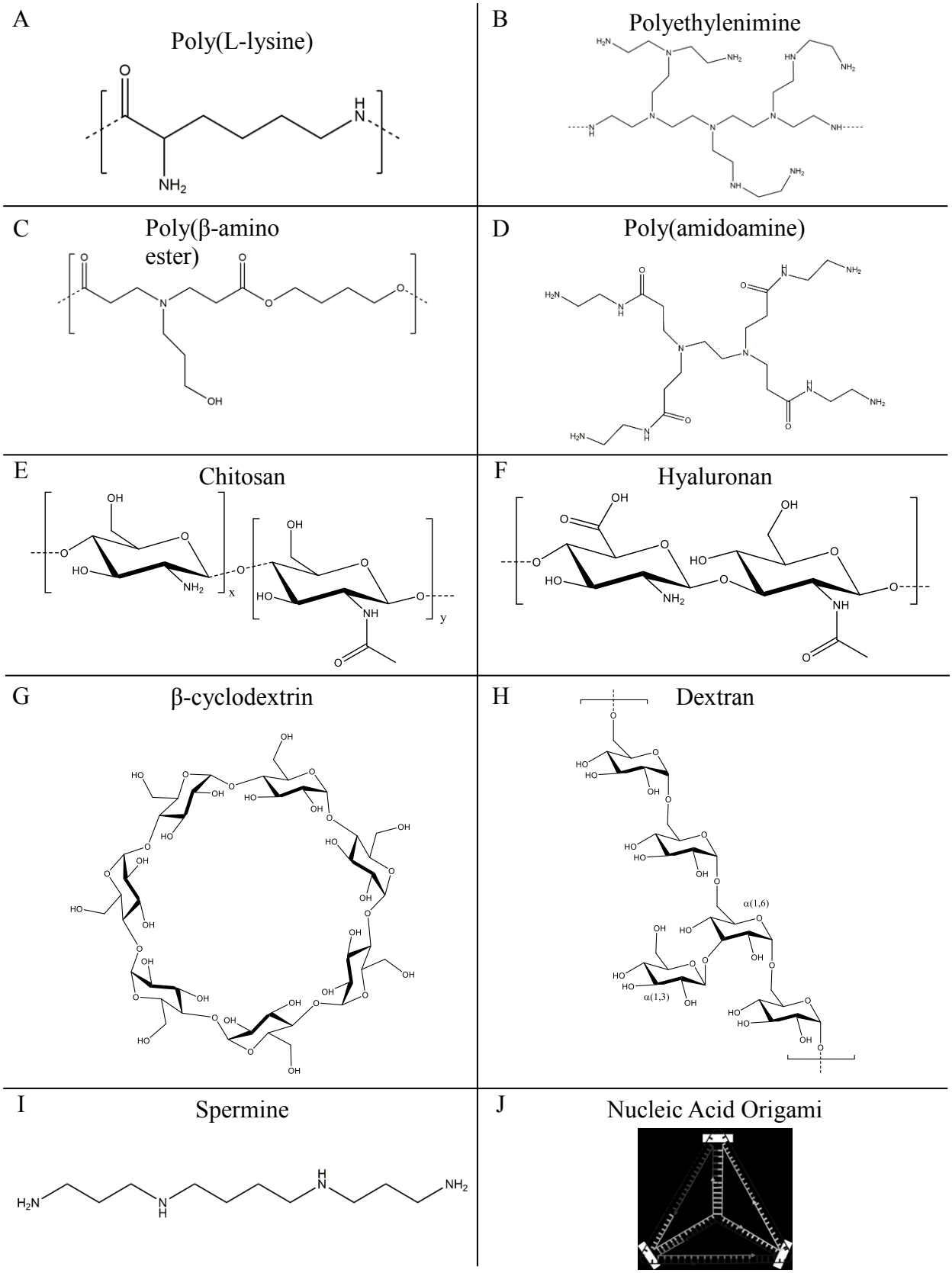

Figure 2.3. Characteristic chemical structures for polymers used in gene delivery

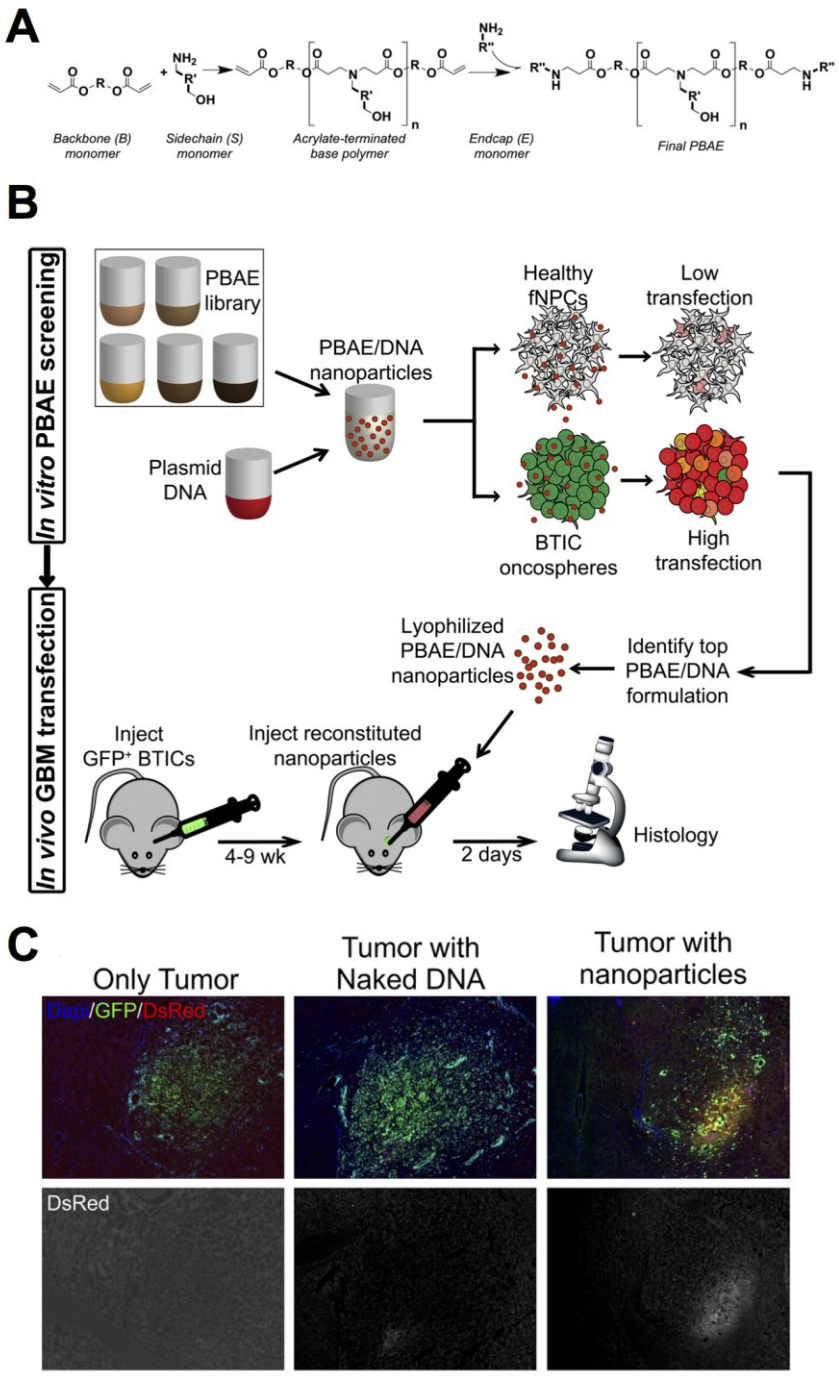

Figure 2.4. Large libraries of PBAEs can be generated by combining different acrylate and amine-containing monomers (A). DNA-containing nanoparticles can be lyophilized and stored prior to *in vivo* administration (B). PBAE DNA nanoparticles selectively transfect tumor cells while avoiding healthy tissue (C). Reprinted with permission from *ACS Nano*. **2014**, 8, 5141-5153, copyright 2014 American Chemical Society.[96]

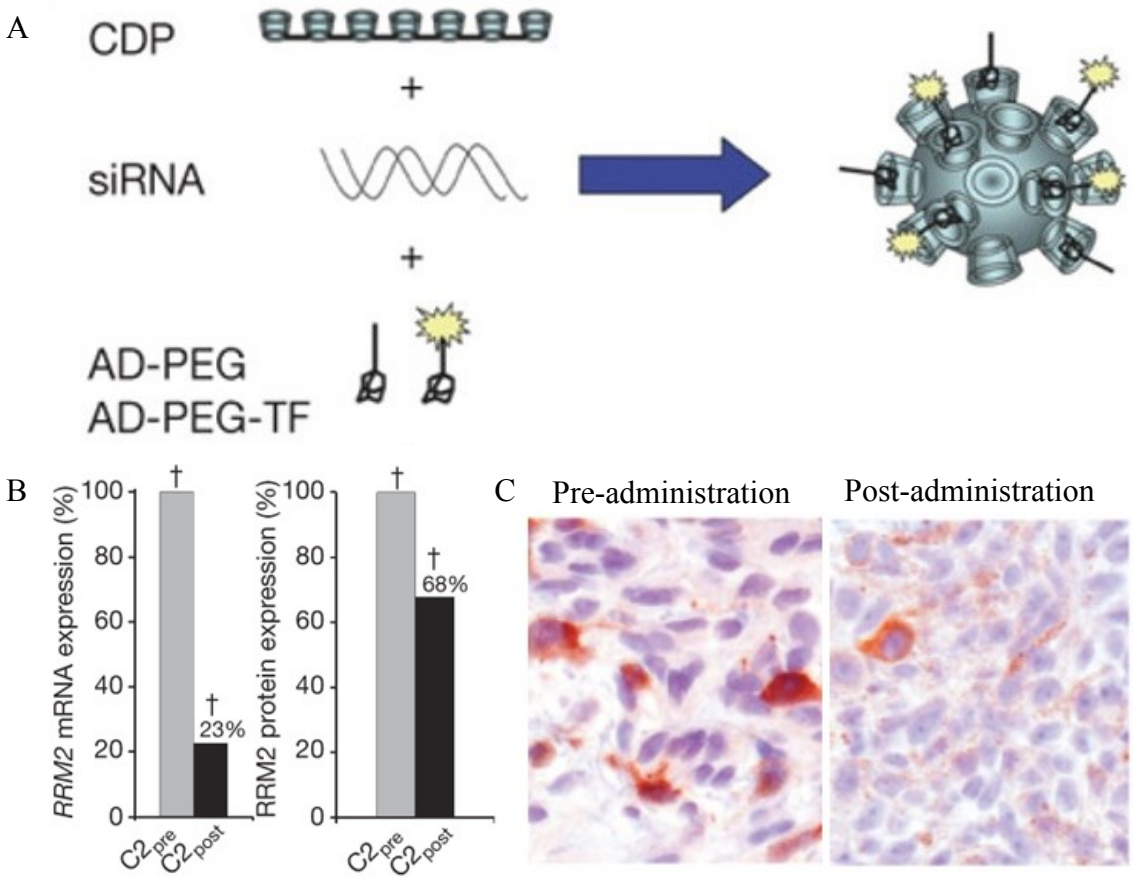

Figure 2.5. (A) The formulation of CALAA-01, a cyclodextrin containing nanoparticle for RRM2 RNAi tested in FDA phase I clinical trials (B) mRNA and protein levels of RRM2 in the targeted tissue of one patient (C) RRM2 staining (red) of human tumor tissue comparing tissue from before and after systemic administration of CALAA-01. . Reprinted by permission from Nature Publishing Group: *Nature.* **2010**, 464, 1067-70, copyright 2010.[203]

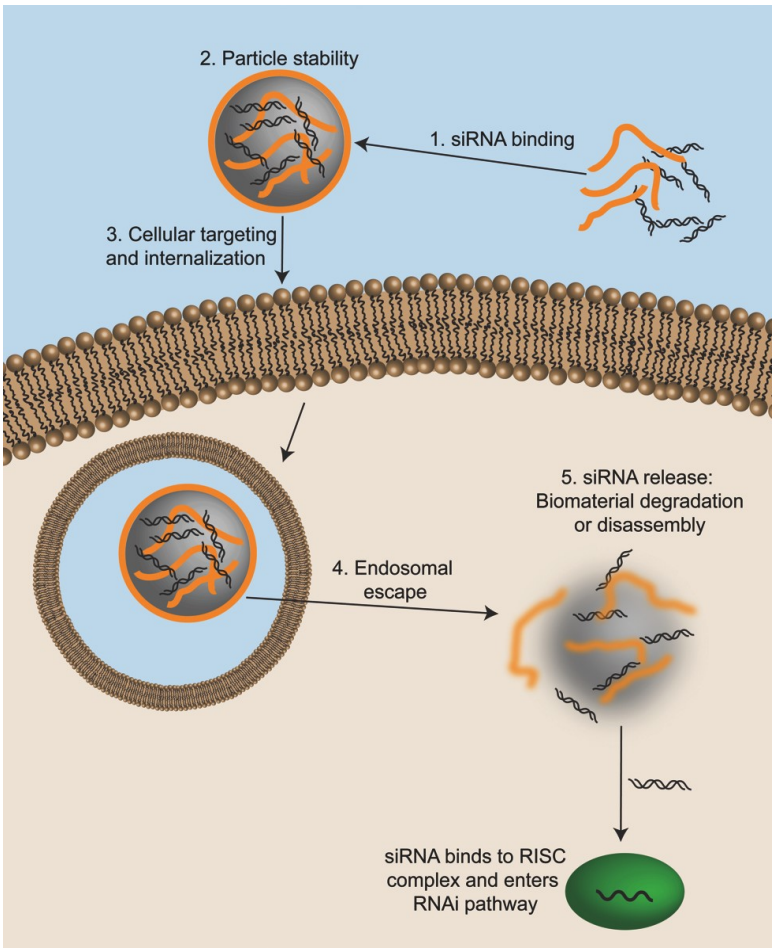

Figure 2.6. siRNA faces several barriers during intracellular delivery. Representative biomaterials that are able to overcome these barriers are shown above, along with the particular strategy employed by that material.

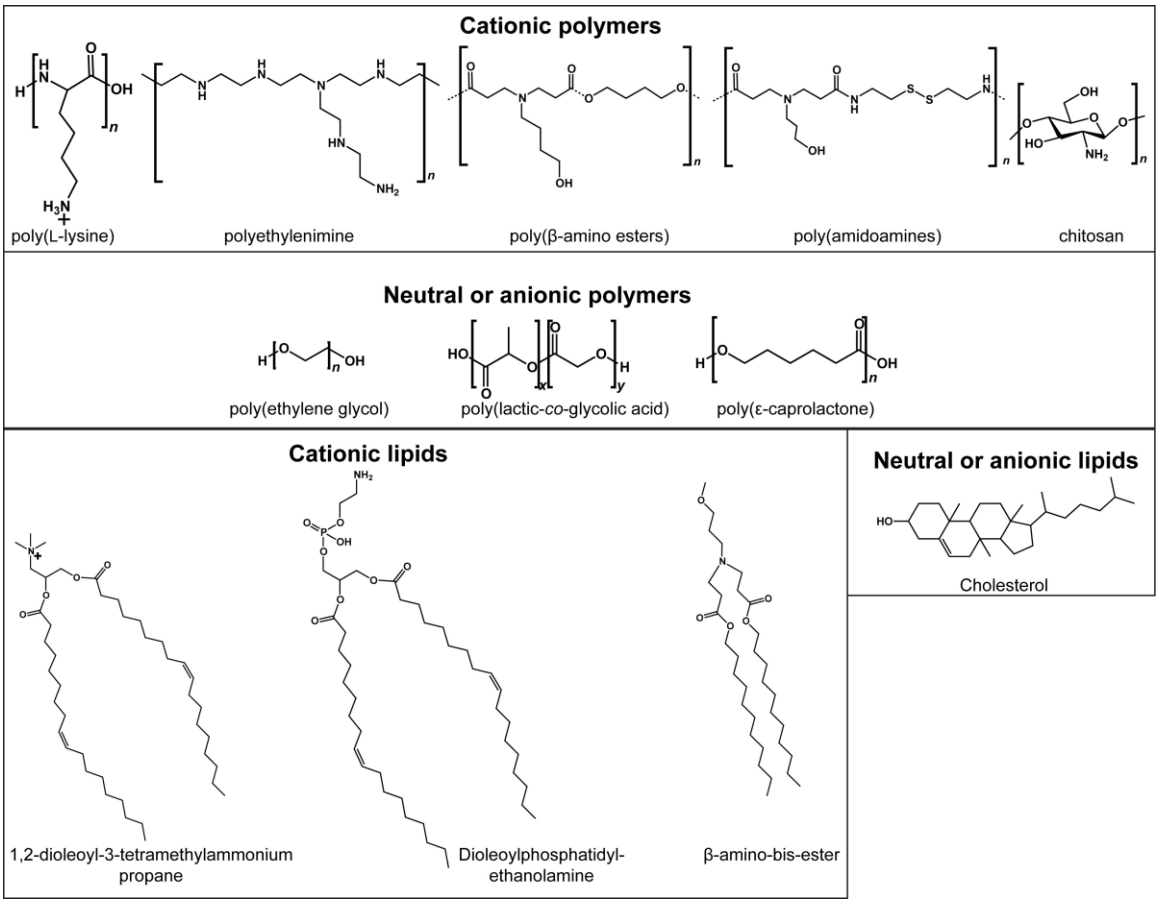

Figure 2.7. Examples of classes of polymeric and lipidic biomaterials used for siRNA delivery.

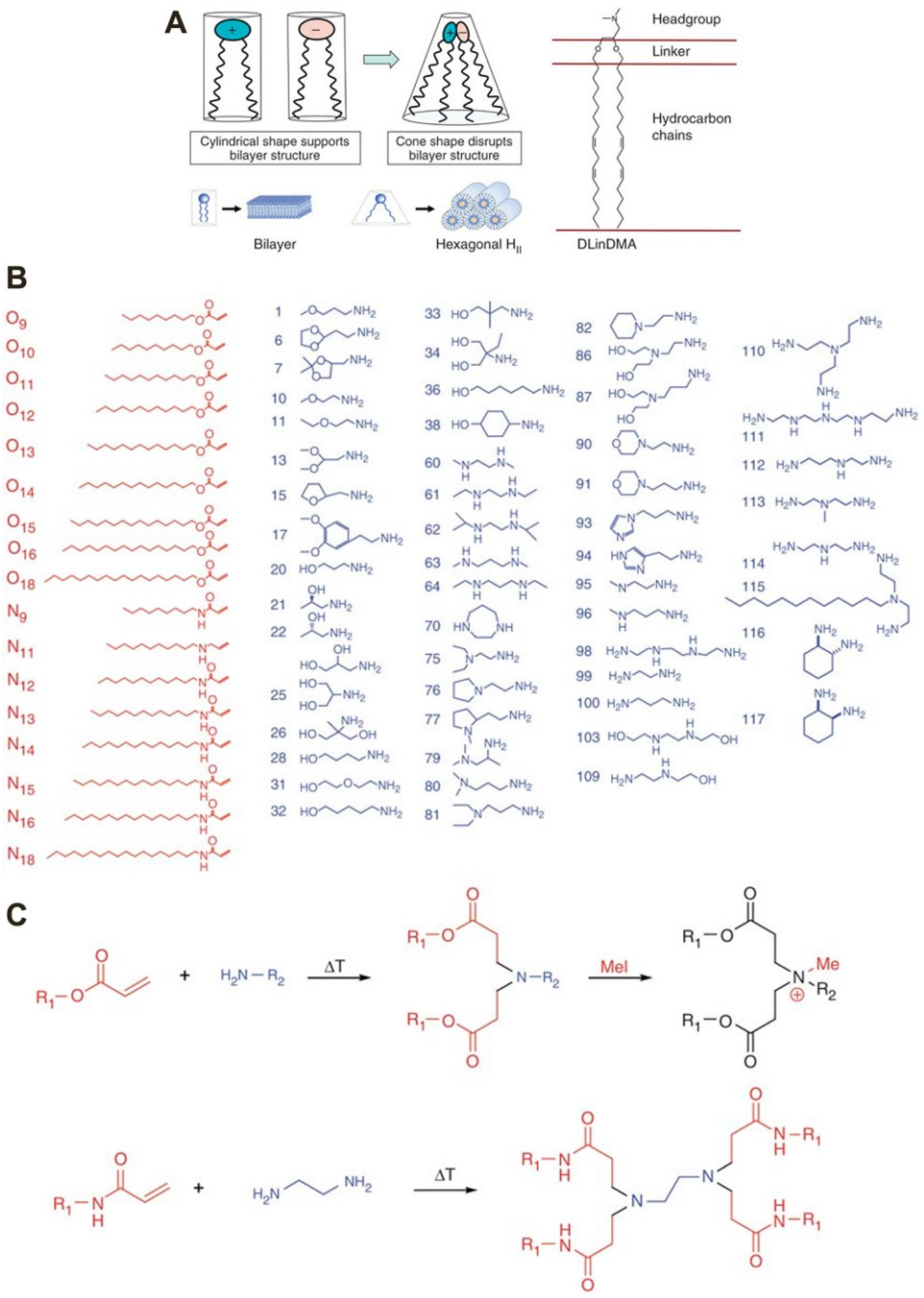

Figure 2.8. Various approaches have been taken to lipid-based siRNA delivery. While some groups use rational design and focus on specific delivery aspects, such as lipid polymorphism leading to membrane fusion (A), others have employed high-throughput methods to screen through a wide array of different molecules to empirically determine the best structures (B-C). Reprinted by permission from Macmillan Publishers Ltd: *Nature Biotechnology*,[266, 318] copyright (2010) (A) and copyright (2008) (B-C).

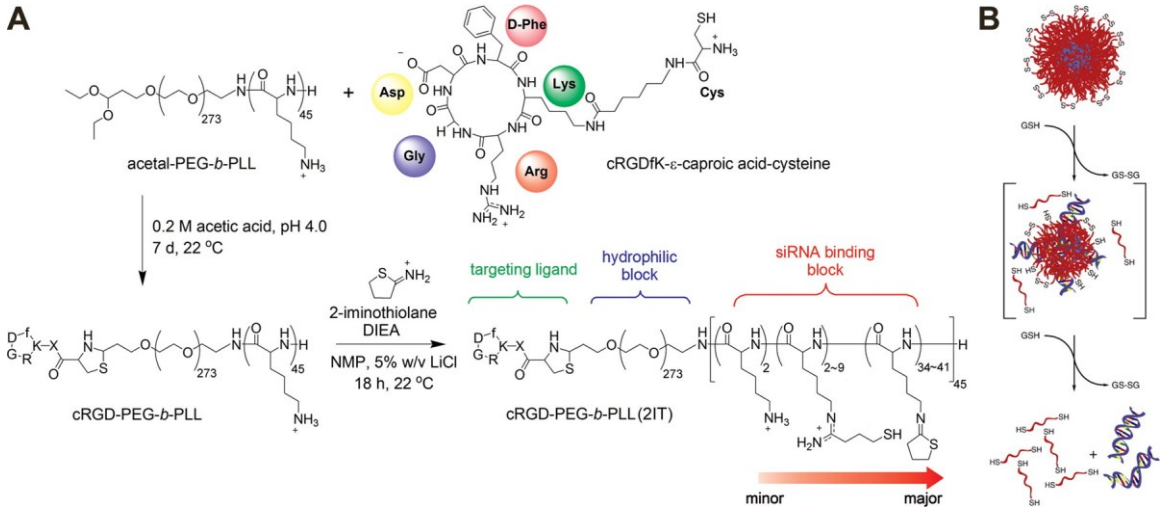

Figure 2.9. Widely-used approaches to improving polymeric siRNA delivery include conjugation to PEG and targeting ligands (A) and introduction of disulfide bridges for controlled cytoplasmic release (B). Part A reprinted with permission from Christie, R. J.; Matsumoto, Y.; Miyata, K.; Nomoto, T.; Fukushima, S.; Osada, K.; Halnaut, J.; Pittella, F.; Kim, H. J.; Nishiyama, N.; Kataoka, K.: Targeted Polymeric Micelles for siRNA Treatment of Experimental Cancer by Intravenous Injection. *ACS Nano* **2012**, *6*, 5174-5189.[282] Copyright (2012) American Chemical Society. Part B reprinted from *Journal of Controlled Release*, 150/2, van der Aa et al, Optimization of poly(amido amine)s as vectors for siRNA delivery, 177-186,[150] Copyright (2011), with permission from Elsevier.

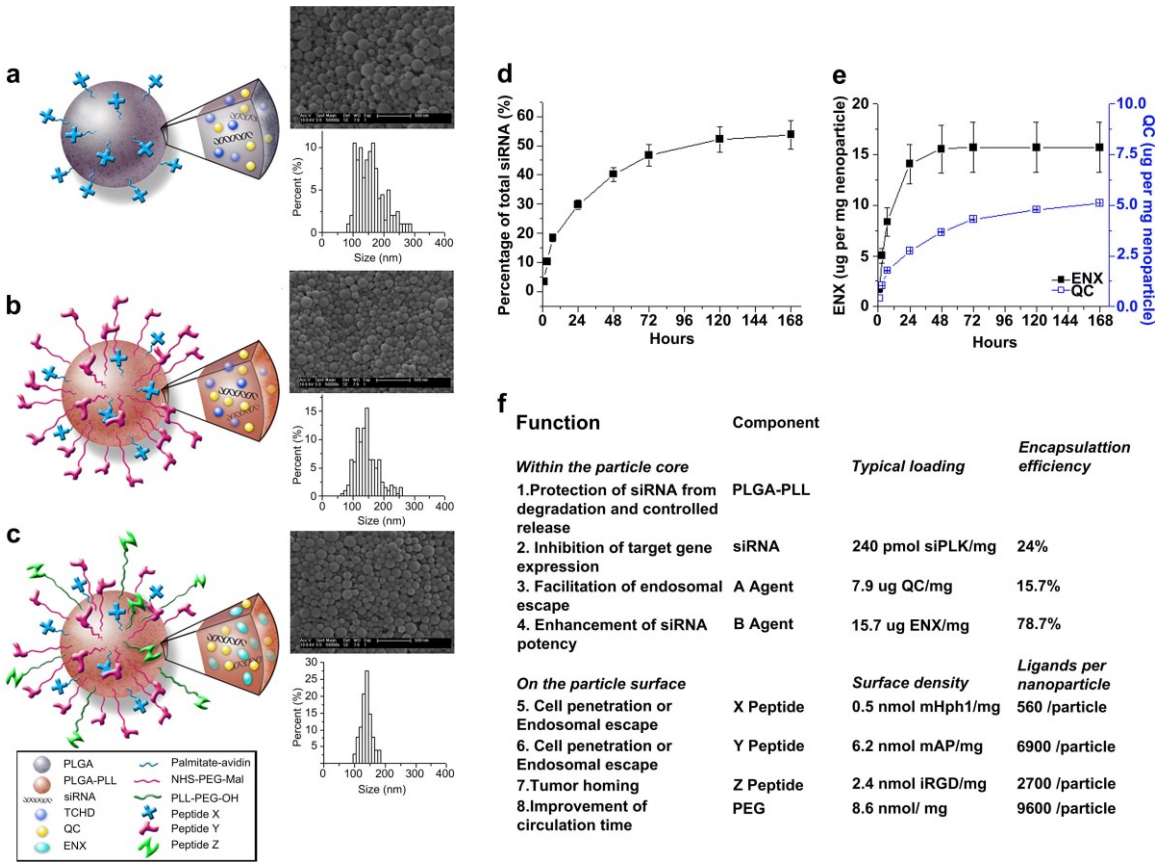

f

Function	Component		
Within the particle core		*Typical loading*	*Encapsulattion efficiency*
1.Protection of siRNA from degradation and controlled release	PLGA-PLL		
2. Inhibition of target gene expression	siRNA	240 pmol siPLK/mg	24%
3. Facilitation of endosomal escape	A Agent	7.9 ug QC/mg	15.7%
4. Enhancement of siRNA potency	B Agent	15.7 ug ENX/mg	78.7%
On the particle surface		*Surface density*	*Ligands per nanoparticle*
5. Cell penetration or Endosomal escape	X Peptide	0.5 nmol mHph1/mg	560 /particle
6. Cell penetration or Endosomal escape	Y Peptide	6.2 nmol mAP/mg	6900 /particle
7.Tumor homing	Z Peptide	2.4 nmol iRGD/mg	2700 /particle
8.Improvement of circulation time	PEG	8.6 nmol/ mg	9600 /particle

Figure 2.10. PLGA-b-PLL-g-PEG NPs contain siRNA, two drugs, and three ligands for targeting, cell penetration, and trafficking. Reprinted from *Biomaterials*, 33/2, Zhou et al, Octa-functional PLGA nanoparticles for targeted and efficient siRNA delivery to tumors, 177-186,[291] Copyright (2012), with permission from Elsevier.

2.6. References

1. Lang, F. F.; Bruner, J. M.; Fuller, G. N.; Aldape, K.; Prados, M. D.; Chang, S.; Berger, M. S.; McDermott, M. W.; Kunwar, S. M.; Junck, L. R.; Chandler, W.; Zwiebel, J. A.; Kaplan, R. S.; Yung, W. K. A. Phase I Trial of Adenovirus-Mediated P53 Gene Therapy for Recurrent Glioma: Biological and Clinical Results. *Journal of Clinical Oncology* **2003,** 21, 2508-2518.
2. Tolcher, A. W.; Hao, D.; de Bono, J.; Miller, A.; Patnaik, A.; Hammond, L. A.; Smetzer, L.; Van Wart Hood, J.; Merritt, J.; Rowinsky, E. K.; Takimoto, C.; Von Hoff, D.; Eckhardt, S. G. Phase I, Pharmacokinetic, and Pharmacodynamic Study of Intravenously Administered Ad5cmv-P53, an Adenoviral Vector Containing the Wild-Type P53 Gene, in Patients with Advanced Cancer. *Journal of Clinical Oncology* **2006,** 24, 2052-2058.
3. Prabha, S.; Labhasetwar, V. Nanoparticle-Mediated Wild-Type P53 Gene Delivery Results in Sustained Antiproliferative Activity in Breast Cancer Cells. *Mol. Pharm.* **2004,** 1, 211-219.
4. Gurunathan, S.; Klinman, D. M.; Seder, R. A. DNA Vaccines: Immunology, Application, and Optimization*. *Annual Review of Immunology* **2000,** 18, 927-974.
5. Rice, J.; Ottensmeier, C. H.; Stevenson, F. K. DNA Vaccines: Precision Tools for Activating Effective Immunity against Cancer. *Nat Rev Cancer* **2008,** 8, 108-120.
6. King, G. D.; Muhammad, A. K. M. G.; Larocque, D.; Kelson, K. R.; Xiong, W.; Liu, C.; Sanderson, N. S. R.; Kroeger, K. M.; Castro, M. G.; Lowenstein, P. R. Combined Flt3l/Tk Gene Therapy Induces Immunological Surveillance Which Mediates an Immune Response against a Surrogate Brain Tumor Neoantigen. *Mol. Ther.* **2011,** 19, 1793-1801.
7. Okada, H.; Villa, L.; Attanucci, J.; Erff, M.; Fellows, W. K.; Lotze, M. T.; Pollack, I. F.; Chambers, W. H. Cytokine Gene Therapy of Gliomas: Effective Induction of Therapeutic Immunity to Intracranial Tumors by Peripheral Immunization with Interleukin-4 Transduced Glioma Cells. *Gene Ther.* **2001,** 8, 1157-1166.
8. Zarogoulidis, P.; Darwiche, K.; Sakkas, A.; Yarmus, L.; Huang, H.; Li, Q.; Freitag, L.; Zarogoulidis, K.; Malecki, M. Suicide Gene Therapy for Cancer - Current Strategies. *J Genet Syndr Gene Ther* **2013,** 9, 16849.
9. Tzeng, S. Y.; Hung, B. P.; Grayson, W. L.; Green, J. J. Cystamine-Terminated Poly(Beta-Amino Ester)S for Sirna Delivery to Human Mesenchymal Stem Cells and Enhancement of Osteogenic Differentiation. *Biomaterials* **2012,** 33, 8142-8151.
10. Bhise, N. S.; Wahlin, K.; Zack, D.; Green, J. J. Evaluating the Potential of Poly(Beta-Amino Ester) Nanoparticles for Reprogramming Human Fibroblasts to Become Induced Pluripotent Stem Cells. *International Journal of Nanomedicine* **2013,** 8, 4641-4658.
11. Wu, W.; Sun, M.; Zou, G. M.; Chen, J. Microrna and Cancer: Current Status and Prospective. *Int. J. Cancer* **2007,** 120, 953-960.
12. Yadav, S.; van Vlerken, L. E.; Little, S. R.; Amiji, M. M. Evaluations of Combination Mdr-1 Gene Silencing and Paclitaxel Administration in Biodegradable Polymeric Nanoparticle Formulations to Overcome Multidrug Resistance in Cancer Cells. *Cancer Chemother. Pharmacol.* **2009,** 63, 711-722.
13. Kuwabara, P. E.; Coulson, A. Rnai--Prospects for a General Technique for Determining Gene Function. *Parasitol. Today* **2000,** 16, 347-349.
14. Thomas, C. E.; Ehrhardt, A.; Kay, M. A. Progress and Problems with the Use of Viral Vectors for Gene Therapy. *Nat. Rev. Genet.* **2003,** 4, 346-358.

15. Goodman, J. C.; Trask, T. W.; Chen, S. H.; Woo, S. L.; Grossman, R. G.; Carey, K. D.; Hubbard, G. B.; Carrier, D. A.; Rajagopalan, S.; Aguilar-Cordova, E.; Shine, H. D. Adenoviral-Mediated Thymidine Kinase Gene Transfer into the Primate Brain Followed by Systemic Ganciclovir: Pathologic, Radiologic, and Molecular Studies. *Hum Gene Ther* **1996,** 7, 1241-1250.
16. Pack, D. W.; Hoffman, A. S.; Pun, S.; Stayton, P. S. Design and Development of Polymers for Gene Delivery. *Nat. Rev. Drug Discov.* **2005,** 4, 581-593.
17. Alving, C. R.; Steck, E. A.; Chapman, W. L., Jr.; Waits, V. B.; Hendricks, L. D.; Swartz, G. M., Jr.; Hanson, W. L. Therapy of Leishmaniasis: Superior Efficacies of Liposome-Encapsulated Drugs. *Proc Natl Acad Sci U S A.* **1978,** 75, 2959-2963.
18. Scherphof, G. L.; Dijkstra, J.; Spanjer, H. H.; Derksen, J. T.; Roerdink, F. H. Uptake and Intracellular Processing of Targeted and Nontargeted Liposomes by Rat Kupffer Cells in Vivo and in Vitro. *Ann N Y Acad Sci.* **1985,** 446, 368-384.
19. Vadiei, K.; Lopez-Berestein, G.; Perez-Soler, R.; Luke, D. R. In Vitro Evaluation of Liposomal Cyclosporine. *Int. J. Pharm* **1989,** 57, 133-138.
20. Ma, Z.; Li, J.; He, F. T.; Wilson, A.; Pitt, B.; Li, S. Cationic Lipids Enhance Sirna-Mediated Interferon Response in Mice. *Biochem. Biophys. Res. Commun.* **2005,** 330, 755-759.
21. Dalby, B.; Cates, S.; Harris, A.; Ohki, E. C.; Tilkins, M. L.; Price, P. J.; Ciccarone, V. C. Advanced Transfection with Lipofectamine 2000 Reagent: Primary Neurons, Sirna, and High-Throughput Applications. *Methods* **2004,** 33, 95-103.
22. Palliser, D.; Chowdhury, D.; Wang, Q. Y.; Lee, S. J.; Bronson, R. T.; Knipe, D. M.; Lieberman, J. An Sirna-Based Microbicide Protects Mice from Lethal Herpes Simplex Virus 2 Infection. *Nature* **2006,** 439, 89-94.
23. Chono, S.; Li, S. D.; Conwell, C. C.; Huang, L. An Efficient and Low Immunostimulatory Nanoparticle Formulation for Systemic Sirna Delivery to the Tumor. *J. Control. Release* **2008,** 131, 64-69.
24. Judge, A. D.; Bola, G.; Lee, A. C. H.; MacLachlan, I. Design of Noninflammatory Synthetic Sirna Mediating Potent Gene Silencing in Vivo. *Mol. Ther.* **2006,** 13, 494-505.
25. Chen, C.; Okayama, H. High-Efficiency Transformation of Mammalian Cells by Plasmid DNA. *Mol. Cell. Biol.* **1987,** 7, 2745-2752.
26. Jordan, M.; Schallhorn, A.; Wurm, F. M. Transfecting Mammalian Cells: Optimization of Critical Parameters Affecting Calcium-Phosphate Precipitate Formation. *Nucleic Acids Res.* **1996,** 24, 596-601.
27. Tolou, H. Administration of Oligonucleotides to Cultured Cells by Calcium Phosphate Precipitation Method. *Anal. Biochem.* **1993,** 215, 156-158.
28. Ghosh, P. S.; Kim, C. K.; Han, G.; Forbes, N. S.; Rotello, V. M. Efficient Gene Delivery Vectors by Tuning the Surface Charge Density of Amino Acid-Functionalized Gold Nanoparticles. **2008**.
29. Love, K. T.; Mahon, K. P.; Levins, C. G.; Whitehead, K. A.; Querbes, W.; Dorkin, J. R.; Qin, J.; Cantley, W.; Qin, L. L.; Racie, T.; Frank-Kamenetsky, M.; Yip, K. N.; Alvarez, R.; Sah, D. W. Y.; de Fougerolles, A.; Fitzgerald, K.; Koteliansky, V.; Akinc, A.; Langer, R.; Anderson, D. G. Lipid-Like Materials for Low-Dose, in Vivo Gene Silencing. *Proc. Natl. Acad. Sci.* **2010,** 107, 1864-1869.
30. Mirkin, C. A.; Letsinger, R. L.; Mucic, R. C.; Storhoff, J. J. A DNA-Based Method for Rationally Assembling Nanoparticles into Macroscopic Materials. **1996**.

31. Daniel, M. C.; Astruc, D. Gold Nanoparticles: Assembly, Supramolecular Chemistry, Quantum-Size-Related Properties, and Applications toward Biology, Catalysis, and Nanotechnology. *Chemical Reviews-Columbus* **2004,** 104, 293.
32. Connor, E. E.; Mwamuka, J.; Gole, A.; Murphy, C. J.; Wyatt, M. D. Gold Nanoparticles Are Taken up by Human Cells but Do Not Cause Acute Cytotoxicity. *Small* **2005,** 1, 325-327.
33. Derfus, A. M.; Chan, W. C. W.; Bhatia, S. N. Intracellular Delivery of Quantum Dots for Live Cell Labeling and Organelle Tracking. *Adv. Mater.* **2004,** 16, 961-966.
34. Gao, X.; Cui, Y.; Levenson, R. M.; Chung, L. W. K.; Nie, S. In Vivo Cancer Targeting and Imaging with Semiconductor Quantum Dots. *Nat. Biotechnol.* **2004,** 22, 969-976.
35. Kakizawa, Y.; Kataoka, K. Block Copolymer Self-Assembly into Monodispersive Nanoparticles with Hybrid Core of Antisense DNA and Calcium Phosphate. *Langmuir* **2002,** 18, 4539-4543.
36. Derfus, A. M.; Chen, A. A.; Min, D. H.; Ruoslahti, E.; Bhatia, S. N. Targeted Quantum Dot Conjugates for Sirna Delivery. *Bioconjugate Chem.* **2007,** 18, 1391-1396.
37. Elbakry, A.; Zaky, A.; Liebl, R.; Rachel, R.; Goepferich, A.; Breunig, M. Layer-by-Layer Assembled Gold Nanoparticles for Sirna Delivery. *Nano Lett.* **2009,** 9, 2059-2064.
38. Lee, J. S.; Green, J. J.; Love, K. T.; Sunshine, J.; Langer, R.; Anderson, D. G. Gold, Poly (Beta-Amino Ester) Nanoparticles for Small Interfering Rna Delivery. *Nano Lett.* **2009,** 9, 2402-2406.
39. Kaneda, Y. Gene Therapy: A Battle against Biological Barriers. *Curr Mol Med* **2001,** 1, 493-499.
40. Yin, H.; Kanasty, R. L.; Eltoukhy, A. A.; Vegas, A. J.; Dorkin, J. R.; Anderson, D. G. Non-Viral Vectors for Gene-Based Therapy. *Nat. Rev. Genet.* **2014,** 15, 541-555.
41. Kawabata, K.; Takakura, Y.; Hashida, M. The Fate of Plasmid DNA after Intravenous Injection in Mice: Involvement of Scavenger Receptors in Its Hepatic Uptake. *Pharm Res* **1995,** 12, 825-830.
42. Chang, C.; Weiskopf, M.; Li, H. J. Conformational Studies of Nucleoprotein. Circular Dichroism of Deoxyribonucleic Acid Base Pairs Bound by Polylysine. *Biochemistry* **1973,** 12, 3028-3032.
43. Li, H. J.; Chang, C.; Weiskopf, M. Helix-Coil Transition in Nucleoprotein-Chromatin Structure. *Biochemistry* **1973,** 12, 1763-1772.
44. Laemmli, U. K. Characterization of DNA Condensates Induced by Poly(Ethylene Oxide) and Polylysine. *Proc Natl Acad Sci U S A* **1975,** 72, 4288-4292.
45. Wagner, E.; Cotten, M.; Foisner, R.; Birnstiel, M. L. Transferrin-Polycation-DNA Complexes: The Effect of Polycations on the Structure of the Complex and DNA Delivery to Cells. *Proc Natl Acad Sci U S A* **1991,** 88, 4255-4259.
46. Wu, G. Y.; Wu, C. H. Receptor-Mediated in Vitro Gene Transformation by a Soluble DNA Carrier System. *The Journal of biological chemistry* **1987,** 262, 4429-4432.
47. Midoux, P.; Monsigny, M. Efficient Gene Transfer by Histidylated Polylysine/Pdna Complexes. *Bioconjugate chemistry* **1999,** 10, 406-411.
48. Okuda, T.; Sugiyama, A.; Niidome, T.; Aoyagi, H. Characters of Dendritic Poly(L-Lysine) Analogues with the Terminal Lysines Replaced with Arginines and Histidines as Gene Carriers in Vitro. *Biomaterials* **2004,** 25, 537-544.
49. Wagner, E.; Plank, C.; Zatloukal, K.; Cotten, M.; Birnstiel, M. L. Influenza Virus Hemagglutinin Ha-2 N-Terminal Fusogenic Peptides Augment Gene Transfer by Transferrin-

Polylysine-DNA Complexes: Toward a Synthetic Virus-Like Gene-Transfer Vehicle. *Proc Natl Acad Sci U S A* **1992,** 89, 7934-7938.
50. Meyer, M.; Dohmen, C.; Philipp, A.; Kiener, D.; Maiwald, G.; Scheu, C.; Ogris, M.; Wagner, E. Synthesis and Biological Evaluation of a Bioresponsive and Endosomolytic Sirna−Polymer Conjugate. *Molecular Pharmaceutics* **2009,** 6, 752-762.
51. Boussif, O.; Lezoualc'h, F.; Zanta, M. A.; Mergny, M. D.; Scherman, D.; Demeneix, B.; Behr, J.-P. A Versatile Vector for Gene and Oligonucleotide Transfer into Cells in Culture and in Vivo: Polyethylenimine. *Proc. Natl. Acad. Sci.* **1995,** 92, 7297-7301.
52. Boeckle, S.; Katharina von, G.; Silke van der, P.; Culmsee, C.; Wagner, E.; Ogris, M. Purification of Polyethylenimine Polyplexes Highlights the Role of Free Polycations in Gene Transfer. *J. Gene. Med.* **2004,** 6, 1102-1111.
53. Kunath, K.; von Harpe, A.; Fischer, D.; Petersen, H.; Bickel, U.; Voigt, K.; Kissel, T. Low-Molecular-Weight Polyethylenimine as a Non-Viral Vector for DNA Delivery: Comparison of Physicochemical Properties, Transfection Efficiency and in Vivo Distribution with High-Molecular-Weight Polyethylenimine. *J. Control. Release* **2003,** 89, 113-125.
54. Felgner, P. L.; Gadek, T. R.; Holm, M.; Roman, R.; Chan, H. W.; Wenz, M.; Northrop, J. P.; Ringold, G. M.; Danielsen, M. Lipofection: A Highly Efficient, Lipid-Mediated DNA-Transfection Procedure. *Proc Natl Acad Sci U S A* **1987,** 84, 7413-7417.
55. Cohen, H.; Levy, R. J.; Gao, J.; Fishbein, I.; Kousaev, V.; Sosnowski, S.; Slomkowski, S.; Golomb, G. Sustained Delivery and Expression of DNA Encapsulated in Polymeric Nanoparticles. *Gene Ther.* **2000,** 7, 1896-1905.
56. Chen, Z. Y.; He, C. Y.; Ehrhardt, A.; Kay, M. A. Minicircle DNA Vectors Devoid of Bacterial DNA Result in Persistent and High-Level Transgene Expression in Vivo. *Mol. Ther.* **2003,** 8, 495-500.
57. Keeney, M.; Ong, S. G.; Padilla, A.; Yao, Z.; Goodman, S.; Wu, J. C.; Yang, F. Development of Poly(Beta-Amino Ester)-Based Biodegradable Nanoparticles for Nonviral Delivery of Minicircle DNA. *ACS Nano* **2013,** 7, 7241-7250.
58. Zhang, C.; Gao, S.; Jiang, W.; Lin, S.; Du, F.; Li, Z.; Huang, W. Targeted Minicircle DNA Delivery Using Folate-Poly(Ethylene Glycol)-Polyethylenimine as Non-Viral Carrier. *Biomaterials* **2010,** 31, 6075-6086.
59. Fire, A.; Xu, S.; Montgomery, M. K.; Kostas, S. A.; Driver, S. E.; Mello, C. C. Potent and Specific Genetic Interference by Double-Stranded Rna in Caenorhabditis Elegans. *Nature* **1998,** 391, 806-811.
60. Hagerman, P. J. Flexibility of Rna. *Annual review of biophysics and biomolecular structure* **1997,** 26, 139-156.
61. Kebbekus, P.; Draper, D. E.; Hagerman, P. Persistence Length of Rna. *Biochemistry* **1995,** 34, 4354-4357.
62. Bolcato-Bellemin, A. L.; Bonnet, M. E.; Creusat, G.; Erbacher, P.; Behr, J. P. Sticky Overhangs Enhance Sirna-Mediated Gene Silencing. *Proc Natl Acad Sci U S A* **2007,** 104, 16050-16055.
63. Mok, H.; Lee, S. H.; Park, J. W.; Park, T. G. Multimeric Small Interfering Ribonucleic Acid for Highly Efficient Sequence-Specific Gene Silencing. *Nature materials* **2010,** 9, 272-278.
64. Lee, J. B.; Hong, J.; Bonner, D. K.; Poon, Z.; Hammond, P. T. Self-Assembled Rna Interference Microsponges for Efficient Sirna Delivery. *Nature materials* **2012,** 11, 316-322.

65. Kawasaki, H.; Taira, K. Short Hairpin Type of Dsrnas That Are Controlled by Trna(Val) Promoter Significantly Induce Rnai-Mediated Gene Silencing in the Cytoplasm of Human Cells. *Nucleic acids research* **2003,** 31, 700-707.
66. Alemany, R.; Suzuki, K.; Curiel, D. T. Blood Clearance Rates of Adenovirus Type 5 in Mice. *J Gen Virol* **2000,** 81, 2605-2609.
67. Mahato, R. I.; Anwer, K.; Tagliaferri, F.; Meaney, C.; Leonard, P.; Wadhwa, M. S.; Logan, M.; French, M.; Rolland, A. Biodistribution and Gene Expression of Lipid/Plasmid Complexes after Systemic Administration. *Hum Gene Ther* **1998,** 9, 2083-2099.
68. Miyata, K.; Nishiyama, N.; Kataoka, K. Rational Design of Smart Supramolecular Assemblies for Gene Delivery: Chemical Challenges in the Creation of Artificial Viruses. *Chem Soc Rev* **2012,** 41, 2562-2574.
69. Ogris, M.; Steinlein, P.; Kursa, M.; Mechtler, K.; Kircheis, R.; Wagner, E. The Size of DNA/Transferrin-Pei Complexes Is an Important Factor for Gene Expression in Cultured Cells. *Gene Ther* **1998,** 5, 1425-1433.
70. Dash, P. R.; Read, M. L.; Barrett, L. B.; Wolfert, M. A.; Seymour, L. W. Factors Affecting Blood Clearance and in Vivo Distribution of Polyelectrolyte Complexes for Gene Delivery. *Gene Ther.* **1999,** 6, 643-650.
71. Davis, F. F. The Origin of Pegnology. *Adv. Drug Deliv. Rev.* **2002,** 54, 457-458.
72. Veronese, F. M.; Harris, J. M. Introduction and Overview of Peptide and Protein Pegylation. *Adv. Drug Deliv. Rev.* **2002,** 54, 453-456.
73. Ogris, M.; Brunner, S.; Schuller, S.; Kircheis, R.; Wagner, E. Pegylated DNA/Transferrin-Pei Complexes: Reduced Interaction with Blood Components, Extended Circulation in Blood and Potential for Systemic Gene Delivery. *Gene Ther* **1999,** 6, 595-605.
74. Itaka, K.; Yamauchi, K.; Harada, A.; Nakamura, K.; Kawaguchi, H.; Kataoka, K. Polyion Complex Micelles from Plasmid DNA and Poly(Ethylene Glycol)-Poly(L-Lysine) Block Copolymer as Serum-Tolerable Polyplex System: Physicochemical Properties of Micelles Relevant to Gene Transfection Efficiency. *Biomaterials* **2003,** 24, 4495-4506.
75. MacKay, J. A.; Deen, D. F.; Szoka, F. C., Jr. Distribution in Brain of Liposomes after Convection Enhanced Delivery; Modulation by Particle Charge, Particle Diameter, and Presence of Steric Coating. *Brain Res* **2005,** 1035, 139-153.
76. Tseng, Y. C.; Mozumdar, S.; Huang, L. Lipid-Based Systemic Delivery of Sirna. *Adv. Drug Deliv. Rev.* **2009,** 61, 721-731.
77. Hosseinkhani, H.; Azzam, T.; Tabata, Y.; Domb, A. J. Dextran-Spermine Polycation: An Efficient Nonviral Vector for in Vitro and in Vivo Gene Transfection. *Gene Ther.* **2004,** 11, 194-203.
78. Trubetskoy, V. S.; Wong, S. C.; Subbotin, V.; Budker, V. G.; Loomis, A.; Hagstrom, J. E.; Wolff, J. A. Recharging Cationic DNA Complexes with Highly Charged Polyanions for in Vitro and in Vivo Gene Delivery. *Gene Ther.* **2003,** 10, 261-271.
79. Geng, Y.; Dalhaimer, P.; Cai, S.; Tsai, R.; Tewari, M.; Minko, T.; Discher, D. E. Shape Effects of Filaments Versus Spherical Particles in Flow and Drug Delivery. *Nat Nanotechnol* **2007,** 2, 249-255.
80. Jiang, X.; Qu, W.; Pan, D.; Ren, Y.; Williford, J. M.; Cui, H.; Luijten, E.; Mao, H. Q. Plasmid-Templated Shape Control of Condensed DNA-Block Copolymer Nanoparticles. *Adv. Mater.* **2013,** 25, 227-232.
81. Chauhan, N. B. Trafficking of Intracerebroventricularly Injected Antisense Oligonucleotides in the Mouse Brain. *Antisense Nucleic Acid Drug Dev* **2002,** 12, 353-357.

82. Dai, H.; Jiang, X.; Tan, G. C.; Chen, Y.; Torbenson, M.; Leong, K. W.; Mao, H. Q. Chitosan-DNA Nanoparticles Delivered by Intrabiliary Infusion Enhance Liver-Targeted Gene Delivery. *Int. J. Nanomedicine* **2006,** 1, 507-522.
83. Coll, J. L.; Chollet, P.; Brambilla, E.; Desplanques, D.; Behr, J. P.; Favrot, M. In Vivo Delivery to Tumors of DNA Complexed with Linear Polyethylenimine. *Hum Gene Ther* **1999,** 10, 1659-1666.
84. Zhang, Y.; Satterlee, A.; Huang, L. In Vivo Gene Delivery by Nonviral Vectors: Overcoming Hurdles? *Mol. Ther.* **2012,** 20, 1298-1304.
85. Suh, W.; Han, S. O.; Yu, L.; Kim, S. W. An Angiogenic, Endothelial-Cell-Targeted Polymeric Gene Carrier. *Mol. Ther.* **2002,** 6, 664-672.
86. Reynolds, A. R.; Moein Moghimi, S.; Hodivala-Dilke, K. Nanoparticle-Mediated Gene Delivery to Tumour Neovasculature. *Trends Mol Med* **2003,** 9, 2-4.
87. Ogris, M.; Walker, G.; Blessing, T.; Kircheis, R.; Wolschek, M.; Wagner, E. Tumor-Targeted Gene Therapy: Strategies for the Preparation of Ligand-Polyethylene Glycol-Polyethylenimine/DNA Complexes. *J. Control. Release* **2003,** 91, 173-181.
88. Green, J. J.; Chiu, E.; Leshchiner, E. S.; Shi, J.; Langer, R.; Anderson, D. G. Electrostatic Ligand Coatings of Nanoparticles Enable Ligand-Specific Gene Delivery to Human Primary Cells. *Nano Lett.* **2007,** 7, 874-879.
89. Shmueli, R. B.; Anderson, D. G.; Green, J. J. Electrostatic Surface Modifications to Improve Gene Delivery. *Expert Opin Drug Deliv* **2010,** 7, 535-550.
90. Farokhzad, O. C.; Karp, J. M.; Langer, R. Nanoparticle-Aptamer Bioconjugates for Cancer Targeting. *Expert Opin Drug Deliv* **2006,** 3, 311-324.
91. Kunath, K.; von Harpe, A.; Fischer, D.; Kissel, T. Galactose-Pei-DNA Complexes for Targeted Gene Delivery: Degree of Substitution Affects Complex Size and Transfection Efficiency. *J. Control. Release* **2003,** 88, 159-172.
92. Zhang, Y.; Jeong Lee, H.; Boado, R. J.; Pardridge, W. M. Receptor-Mediated Delivery of an Antisense Gene to Human Brain Cancer Cells. *J. Gene. Med.* **2002,** 4, 183-194.
93. Lee, L. K.; Siapati, E. K.; Jenkins, R. G.; McAnulty, R. J.; Hart, S. L.; Shamlou, P. A. Biophysical Characterization of an Integrin-Targeted Non-Viral Vector. *Med Sci Monit* **2003,** 9, BR54-61.
94. Hakkarainen, T.; Hemminki, A.; Pereboev, A. V.; Barker, S. D.; Asiedu, C. K.; Strong, T. V.; Kanerva, A.; Wahlfors, J.; Curiel, D. T. Cd40 Is Expressed on Ovarian Cancer Cells and Can Be Utilized for Targeting Adenoviruses. *Clin Cancer Res* **2003,** 9, 619-624.
95. Jaafari, M. R.; Foldvari, M. Targeting of Liposomes to Melanoma Cells with High Levels of Icam-1 Expression through Adhesive Peptides from Immunoglobulin Domains. *J Pharm Sci* **2002,** 91, 396-404.
96. Guerrero-Cázares, H.; Tzeng, S. Y.; Young, N. P.; Abutaleb, A. O.; Quiñones-Hinojosa, A.; Green, J. J. Biodegradable Polymeric Nanoparticles Show High Efficacy and Specificity at DNA Delivery to Human Glioblastoma in Vitro and in Vivo. *ACS Nano* **2014,** 8, 5141-5153.
97. Kozielski, K. L.; Tzeng, S. Y.; Green, J. J. Sirna Nanomedicine: The Promise of Bioreducible Materials. *Expert Rev Med Devices* **2013,** 10, 7-10.
98. Shmueli, R. B.; Sunshine, J. C.; Xu, Z.; Duh, E. J.; Green, J. J. Gene Delivery Nanoparticles Specific for Human Microvasculature and Macrovasculature. *Nanomedicine : nanotechnology, biology, and medicine* **2012,** doi:10.1016/j.nano.2012.01.006.
99. Green, J. J. 2011 Rita Schaffer Lecture: Nanoparticles for Intracellular Nucleic Acid Delivery. *Annals of Biomedical Engineering* **2012,** 40, 1408-1418.

100. Haase, R.; Magnusson, T.; Su, B.; Kopp, F.; Wagner, E.; Lipps, H.; Baiker, A.; Ogris, M. Generation of a Tumor- and Tissue-Specific Episomal Non-Viral Vector System. *BMC Biotechnol* **2013,** 13, 49.
101. Amyere, M.; Mettlen, M.; Van Der Smissen, P.; Platek, A.; Payrastre, B.; Veithen, A.; Courtoy, P. J. Origin, Originality, Functions, Subversions and Molecular Signalling of Macropinocytosis. *Int J Med Microbiol* **2002,** 291, 487-494.
102. Goncalves, C.; Mennesson, E.; Fuchs, R.; Gorvel, J. P.; Midoux, P.; Pichon, C. Macropinocytosis of Polyplexes and Recycling of Plasmid Via the Clathrin-Dependent Pathway Impair the Transfection Efficiency of Human Hepatocarcinoma Cells. *Mol. Ther.* **2004,** 10, 373-385.
103. Verma, A.; Stellacci, F. Effect of Surface Properties on Nanoparticle-Cell Interactions. *Small* **2010,** 6, 12-21.
104. Meyer, M.; Wagner, E. Ph-Responsive Shielding of Non-Viral Gene Vectors. *Expert Opin Drug Deliv* **2006,** 3, 563-571.
105. Kursa, M.; Walker, G. F.; Roessler, V.; Ogris, M.; Roedl, W.; Kircheis, R.; Wagner, E. Novel Shielded Transferrin-Polyethylene Glycol-Polyethylenimine/DNA Complexes for Systemic Tumor-Targeted Gene Transfer. *Bioconjug Chem* **2003,** 14, 222-231.
106. Marsh, M.; McMahon, H. T. The Structural Era of Endocytosis. *Science* **1999,** 285, 215-220.
107. Rejman, J.; Conese, M.; Hoekstra, D. Gene Transfer by Means of Lipo- and Polyplexes: Role of Clathrin and Caveolae-Mediated Endocytosis. *J Liposome Res* **2006,** 16, 237-247.
108. Durymanov, M. O.; Beletkaia, E. A.; Ulasov, A. V.; Khramtsov, Y. V.; Trusov, G. A.; Rodichenko, N. S.; Slastnikova, T. A.; Vinogradova, T. V.; Uspenskaya, N. Y.; Kopantsev, E. P.; Rosenkranz, A. A.; Sverdlov, E. D.; Sobolev, A. S. Subcellular Trafficking and Transfection Efficacy of Polyethylenimine-Polyethylene Glycol Polyplex Nanoparticles with a Ligand to Melanocortin Receptor-1. *J. Control. Release* **2012,** 163, 211-219.
109. Gabrielson, N. P.; Pack, D. W. Efficient Polyethylenimine-Mediated Gene Delivery Proceeds Via a Caveolar Pathway in Hela Cells. *J. Control. Release* **2009,** 136, 54-61.
110. Pelkmans, L.; Helenius, A. Endocytosis Via Caveolae. *Traffic* **2002,** 3, 311-320.
111. van der Aa, M. A.; Huth, U. S.; Hafele, S. Y.; Schubert, R.; Oosting, R. S.; Mastrobattista, E.; Hennink, W. E.; Peschka-Suss, R.; Koning, G. A.; Crommelin, D. J. Cellular Uptake of Cationic Polymer-DNA Complexes Via Caveolae Plays a Pivotal Role in Gene Transfection in Cos-7 Cells. *Pharm Res* **2007,** 24, 1590-1598.
112. Conner, S. D.; Schmid, S. L. Regulated Portals of Entry into the Cell. *Nature* **2003,** 422, 37-44.
113. Kim, J.; Sunshine, J. C.; Green, J. J. Differential Polymer Structure Tunes Mechanism of Cellular Uptake and Transfection Routes of Poly(Beta-Amino Ester) Polyplexes in Human Breast Cancer Cells. *Bioconjug Chem* **2014,** 25, 43-51.
114. Sonawane, N. D.; Szoka, F. C., Jr.; Verkman, A. S. Chloride Accumulation and Swelling in Endosomes Enhances DNA Transfer by Polyamine-DNA Polyplexes. *The Journal of biological chemistry* **2003,** 278, 44826-44831.
115. Midoux, P.; Mendes, C.; Legrand, A.; Raimond, J.; Mayer, R.; Monsigny, M.; Roche, A. C. Specific Gene Transfer Mediated by Lactosylated Poly-L-Lysine into Hepatoma Cells. *Nucleic Acids Res.* **1993,** 21, 871-878.

116. Sunshine, J. C.; Peng, D. Y.; Green, J. J. Uptake and Transfection with Polymeric Nanoparticles Are Dependent on Polymer End-Group Structure, but Largely Independent of Nanoparticle Physical and Chemical Properties. *Mol Pharm* **2012,** 9, 3375-3383.
117. Benjaminsen, R. V.; Mattebjerg, M. A.; Henriksen, J. R.; Moghimi, S. M.; Andresen, T. L. The Possible "Proton Sponge " Effect of Polyethylenimine (Pei) Does Not Include Change in Lysosomal Ph. *Mol. Ther.* **2013,** 21, 149-157.
118. Wyman, T. B.; Nicol, F.; Zelphati, O.; Scaria, P. V.; Plank, C.; Szoka, F. C. Design, Synthesis, and Characterization of a Cationic Peptide That Binds to Nucleic Acids and Permeabilizes Bilayers†. *Biochemistry* **1997,** 36, 3008-3017.
119. Alhakamy, N. A.; Nigatu, A. S.; Berkland, C. J.; Ramsey, J. D. Noncovalently Associated Cell-Penetrating Peptides for Gene Delivery Applications. *Ther Deliv* **2013,** 4, 741-757.
120. Maitani, Y.; Igarashi, S.; Sato, M.; Hattori, Y. Cationic Liposome (Dc-Chol/Dope=1:2) and a Modified Ethanol Injection Method to Prepare Liposomes, Increased Gene Expression. *Int. J. Pharm* **2007,** 342, 33-39.
121. Farhood, H.; Serbina, N.; Huang, L. The Role of Dioleoyl Phosphatidylethanolamine in Cationic Liposome Mediated Gene Transfer. *Biochimica et biophysica acta* **1995,** 1235, 289-295.
122. Gary, D. J.; Puri, N.; Won, Y. Y. Polymer-Based Sirna Delivery: Perspectives on the Fundamental and Phenomenological Distinctions from Polymer-Based DNA Delivery. *J. Control. Release* **2007,** 121, 64-73.
123. Luo, D.; Saltzman, W. M. Synthetic DNA Delivery Systems. *Nat. Biotechnol.* **2000,** 18, 33-37.
124. Bishop, C. J.; Ketola, T. M.; Tzeng, S. Y.; Sunshine, J. C.; Urtti, A.; Lemmetyinen, H.; Vuorimaa-Laukkanen, E.; Yliperttula, M.; Green, J. J. The Effect and Role of Carbon Atoms in Poly(Beta-Amino Ester)S for DNA Binding and Gene Delivery. *J Am Chem Soc* **2013,** 135, 6951-6957.
125. Hill, I. R.; Garnett, M. C.; Bignotti, F.; Davis, S. S. In Vitro Cytotoxicity of Poly(Amidoamine)S: Relevance to DNA Delivery. *Biochim. Biophys. Acta* **1999,** 1427, 161-174.
126. Grayson, A. C. R.; Doody, A. M.; Putnam, D. Biophysical and Structural Characterization of Polyethylenimine-Mediated Sirna Delivery in Vitro. *Pharmaceut. Res.* **2006,** 23, 1868-1876.
127. Sutton, D.; Kim, S.; Shuai, X.; Leskov, K.; Marques, J. T.; Williams, B. R.; Boothman, D. A.; Gao, J. Efficient Suppression of Secretory Clusterin Levels by Polymer-Sirna Nanocomplexes Enhances Ionizing Radiation Lethality in Human Mcf-7 Breast Cancer Cells in Vitro. *Int. J. Nanomedicine* **2006,** 1, 155-162.
128. Lim, Y. B.; Han, S. O.; Kong, H. U.; Lee, Y.; Park, J. S.; Jeong, B.; Kim, S. W. Biodegradable Polyester, Poly[Alpha-(4 Aminobutyl)-L-Glycolic Acid], as a Non-Toxic Gene Carrier. *Pharmaceut. Res.* **2000,** 17, 811-816.
129. Forrest, M. L.; Koerber, J. T.; Pack, D. W. A Degradable Polyethylenimine Derivative with Low Toxicity for Highly Efficient Gene Delivery. *Bioconjugate Chem.* **2003,** 14, 934-940.
130. Lynn, D. M.; Langer, R. Degradable Poly (Beta-Amino Esters): Synthesis, Characterization, and Self-Assembly with Plasmid DNA. *J. Am. Chem. Soc.* **2000,** 122, 10761-10768.
131. Green, J. J.; Langer, R.; Anderson, D. G. A Combinatorial Polymer Library Approach Yields Insight into Nonviral Gene Delivery. *Accounts of chemical research* **2008,** 41, 749-759.

132. Wu; Liu, Y.; Jiang, X.; Chen, L.; He; Goh, S. H.; Leong, K. W. Evaluation of Hyperbranched Poly(Amino Ester)S of Amine Constitutions Similar to Polyethylenimine for DNA Delivery. *Biomacromolecules* **2005,** 6, 3166-3173.
133. Woodrow, K. A.; Cu, Y.; Booth, C. J.; Saucier-Sawyer, J. K.; Wood, M. J.; Mark Saltzman, W. Intravaginal Gene Silencing Using Biodegradable Polymer Nanoparticles Densely Loaded with Small-Interfering Rna. *Nat Mater* **2009,** 8, 526-533.
134. Nguyen, J.; Steele, T. W. J.; Merkel, O.; Reul, R.; Kissel, T. Fast Degrading Polyesters as Sirna Nano-Carriers for Pulmonary Gene Therapy. *J. Control. Release* **2008,** 132, 243-251.
135. Oster, C.; Wittmar, M.; Unger, F.; Barbu-Tudoran, L.; Schaper, A.; Kissel, T. Design of Amine-Modified Graft Polyesters for Effective Gene Delivery Using DNA-Loaded Nanoparticles. *Pharmaceut. Res.* **2004,** 21, 927-931.
136. Yang, T.-f.; Chin, W.-k.; Cherng, J.-y.; Shau, M.-d. Synthesis of Novel Biodegradable Cationic Polymer: N,N-Diethylethylenediamine Polyurethane as a Gene Carrier. *Biomacromolecules* **2004,** 5, 1926-1932.
137. Kim, Y. H.; Park, J. H.; Lee, M.; Kim, Y.-H.; Park, T. G.; Kim, S. W. Polyethylenimine with Acid-Labile Linkages as a Biodegradable Gene Carrier. *J. Control. Release* **2005,** 103, 209-219.
138. Wang, C.; Ge, Q.; Ting, D.; Nguyen, D.; Shen, H.-R.; Chen, J.; Eisen, H. N.; Heller, J.; Langer, R.; Putnam, D. Molecularly Engineered Poly(Ortho Ester) Microspheres for Enhanced Delivery of DNA Vaccines. *Nat Mater* **2004,** 3, 190-196.
139. Heller, J.; Barr, J.; Ng, S. Y.; Abdellauoi, K. S.; Gurny, R. Poly(Ortho Esters): Synthesis, Characterization, Properties and Uses. *Adv. Drug Deliv. Rev.* **2002,** 54, 1015-1039.
140. Griffith, O. W. Biologic and Pharmacologic Regulation of Mammalian Glutathione Synthesis. *Free Radical Bio. Med.* **1999,** 27, 922-935.
141. Tzeng, S. Y.; Yang, P. H.; Grayson, W. L.; Green, J. J. Synthetic Poly(Ester Amine) and Poly(Amido Amine) Nanoparticles for Efficient DNA and Sirna Delivery to Human Endothelial Cells. *Int. J. Nanomedicine* **2012,** 6, 3309-3322.
142. Trubetskoy, V. S.; Loomis, A.; Slattum, P. M.; Hagstrom, J. E.; Budker, V. G.; Wolff, J. A. Caged DNA Does Not Aggregate in High Ionic Strength Solutions. *Bioconjugate Chem.* **1999,** 10, 624-628.
143. McKenzie, D. L.; Smiley, E.; Kwok, K. Y.; Rice, K. G. Low Molecular Weight Disulfide Cross-Linking Peptides as Nonviral Gene Delivery Carriers. *Bioconjugate Chem.* **2000,** 11, 901-909.
144. Matsumoto, S.; Christie, R. J.; Nishiyama, N.; Miyata, K.; Ishii, A.; Oba, M.; Koyama, H.; Yamasaki, Y.; Kataoka, K. Environment-Responsive Block Copolymer Micelles with a Disulfide Cross-Linked Core for Enhanced Sirna Delivery. *Biomacromolecules* **2009,** 10, 119-127.
145. Miyata, K.; Kakizawa, Y.; Nishiyama, N.; Harada, A.; Yamasaki, Y.; Koyama, H.; Kataoka, K. Block Catiomer Polyplexes with Regulated Densities of Charge and Disulfide Cross-Linking Directed to Enhance Gene Expression. *J. Am. Chem. Soc.* **2004,** 126, 2355-2361.
146. Breunig, M.; Hozsa, C.; Lungwitz, U.; Watanabe, K.; Umeda, I.; Kato, H.; Goepferich, A. Mechanistic Investigation of Poly (Ethylene Imine)-Based Sirna Delivery: Disulfide Bonds Boost Intracellular Release of the Cargo. *J. Control. Release* **2008,** 130, 57-63.
147. Mok, H.; Park, T. G. Self-Crosslinked and Reducible Fusogenic Peptides for Intracellular Delivery of Sirna. *Biopolymers* **2008,** 89, 881-888.

148. Jeong, J. H.; Christensen, L. V.; Yockman, J. W.; Zhong, Z. Y.; Engbersen, J. F. J.; Kim, W. J.; Feijen, J.; Kim, S. W. Reducible Poly(Amido Ethylenimine) Directed to Enhance Rna Interference. *Biomaterials* **2007,** 28, 1912-1917.
149. Vader, P.; van der Aa, L. J.; Engbersen, J. F. J.; Storm, G.; Schiffelers, R. M. Disulfide-Based Poly(Amido Amine)S for Sirna Delivery: Effects of Structure on Sirna Complexation, Cellular Uptake, Gene Silencing and Toxicity. *Pharmaceut. Res.* **2011,** 28, 1013-1022.
150. van der Aa, L. J.; Vader, P.; Storm, G.; Schiffelers, R. M.; Engbersen, J. F. J. Optimization of Poly(Amido Amine)S as Vectors for Sirna Delivery. *J. Control. Release* **2011,** 150, 177-186.
151. Emilitri, E.; Ranucci, E.; Ferruti, P. New Poly(Amidoamine)S Containing Disulfide Linkages in Their Main Chain. *Journal of Polymer Science Part a-Polymer Chemistry* **2005,** 43, 1404-1416.
152. Tzeng, S. Y.; Green, J. J. Subtle Changes to Polymer Structure and Degradation Mechanism Enable Highly Effective Nanoparticles for Sirna and DNA Delivery to Human Brain Cancer. *Adv. Healthcare Mater.* **2013,** 2, 468-480.
153. Kozielski, K. L.; Tzeng, S. Y.; Green, J. J. A Bioreducible Linear Poly(Beta-Amino Ester) for Sirna Delivery. *Chem. Commun.* **2013,** 49, 5319 - 5321.
154. Kozielski, K. L.; Tzeng, S. Y.; Mendoza, B. A. H. d.; Green, J. J. Bioreducible Cationic Polymer-Based Nanoparticles for Efficient and Environmentally Triggered Cytoplasmic Sirna Delivery to Primary Human Brain Cancer Cells. *ACS Nano* **2014,** 8, 3232-3241.
155. Kim, H. S.; Yoo, H. S. Mmps-Responsive Release of DNA from Electrospun Nanofibrous Matrix for Local Gene Therapy: In Vitro and in Vivo Evaluation. *J. Control. Release* **2010,** 145, 264-271.
156. Li, H.-J.; Wang, H.-X.; Sun, C.-Y.; Du, J.-Z.; Wang, J. Shell-Detachable Nanoparticles Based on a Light-Responsive Amphiphile for Enhanced Sirna Delivery. *Royal Society of Chemistry Advances* **2014,** 4, 1961-1964.
157. Zanta, M. A.; Belguise-Valladier, P.; Behr, J. P. Gene Delivery: A Single Nuclear Localization Signal Peptide Is Sufficient to Carry DNA to the Cell Nucleus. *Proc Natl Acad Sci U S A* **1999,** 96, 91-96.
158. Collas, P.; Husebye, H.; Alestrom, P. The Nuclear Localization Sequence of the Sv40 T Antigen Promotes Transgene Uptake and Expression in Zebrafish Embryo Nuclei. *Transgenic Res* **1996,** 5, 451-458.
159. Remy, J. S.; Kichler, A.; Mordvinov, V.; Schuber, F.; Behr, J. P. Targeted Gene Transfer into Hepatoma Cells with Lipopolyamine-Condensed DNA Particles Presenting Galactose Ligands: A Stage toward Artificial Viruses. *Proc Natl Acad Sci U S A* **1995,** 92, 1744-1748.
160. Moffatt, S.; Wiehle, S.; Cristiano, R. J. A Multifunctional Pei-Based Cationic Polyplex for Enhanced Systemic P53-Mediated Gene Therapy. *Gene Ther.* **2006,** 13, 1512-1523.
161. Guo, J.; Cheng, W. P.; Gu, J.; Ding, C.; Qu, X.; Yang, Z.; O'Driscoll, C. Systemic Delivery of Therapeutic Small Interfering Rna Using a Ph-Triggered Amphiphilic Poly-L-Lysine Nanocarrier to Suppress Prostate Cancer Growth in Mice. *European Journal of Pharmaceutical Sciences* **2012,** 45, 521-532.
162. Watanabe, K.; Harada-Shiba, M.; Suzuki, A.; Gokuden, R.; Kurihara, R.; Sugao, Y.; Mori, T.; Katayama, Y.; Niidome, T. In Vivo Sirna Delivery with Dendritic Poly (L-Lysine) for the Treatment of Hypercholesterolemia. *Molecular BioSystems* **2009,** 5, 1306-1310.

163. Subbarao, N. K.; Parente, R. A.; Szoka Jr, F. C.; Nadasdi, L.; Pongracz, K. The Ph-Dependent Bilayer Destabilization by an Amphipathic Peptide. *Biochemistry* **1987,** 26, 2964-2972.
164. EL Andaloussi, S.; Lehto, T.; Mäger, I.; Rosenthal-Aizman, K.; Oprea, I. I.; Simonson, O. E.; Sork, H.; Ezzat, K.; Copolovici, D. M.; Kurrikoff, K.; Viola, J. R.; Zaghloul, E. M.; Sillard, R.; Johansson, H. J.; Said Hassane, F.; Guterstam, P.; Suhorutšenko, J.; Moreno, P. M. D.; Oskolkov, N.; Hälldin, J.; Tedebark, U.; Metspalu, A.; Lebleu, B.; Lehtiö, J.; Smith, C. I. E.; Langel, Ü. Design of a Peptide-Based Vector, Pepfect6, for Efficient Delivery of Sirna in Cell Culture and Systemically in Vivo. *Nucleic Acids Res.* **2011,** 39, 3972-3987.
165. Schellinger, J. G.; Pahang, J. a.; Shi, J.; Pun, S. H. Block Copolymers Containing a Hydrophobic Domain of Membrane-Lytic Peptides Form Micellar Structures and Are Effective Gene Delivery Agents. *ACS macro letters* **2013,** 2, 725-730.
166. Dohmen, C.; Edinger, D.; Fröhlich, T.; Schreiner, L.; Lächelt, U.; Troiber, C.; Rädler, J.; Hadwiger, P.; Vornlocher, H.-P.; Wagner, E. Nanosized Multifunctional Polyplexes for Receptor-Mediated Sirna Delivery. *ACS nano* **2012,** 6, 5198-5208.
167. Chu, D. S. H.; Johnson, R. N.; Pun, S. H. Cathepsin B-Sensitive Polymers for Compartment-Specific Degradation and Nucleic Acid Release. *Journal of controlled release : official journal of the Controlled Release Society* **2012,** 157, 445-454.
168. Breunig, M.; Lungwitz, U.; Liebl, R.; Goepferich, A. Breaking up the Correlation between Efficacy and Toxicity for Nonviral Gene Delivery. *Proc. Natl. Acad. Sci.* **2007,** 104, 14454-14459.
169. Abdallah, B.; Hassan, A.; Benoist, C.; Goula, D.; Behr, J. P.; Demeneix, B. A. A Powerful Nonviral Vector for in Vivo Gene Transfer into the Adult Mammalian Brain: Polyethylenimine. *Human gene therapy* **1996,** 7, 1947-1954.
170. Fischer, D.; Bieber, T.; Li, Y.; Elsasser, H.-P.; Kissel, T. A Novel Non-Viral Vector for DNA Delivery Based on Low Molecular Weight, Branched Polyethylenimine: Effect of Molecular Weight on Transfection Efficiency and Cytotoxicity. *Pharmaceut. Res.* **1999,** 16, 1273-1279.
171. Gosselin, M. A.; Guo, W.; Lee, R. J. Efficient Gene Transfer Using Reversibly Cross-Linked Low Molecular Weight Polyethylenimine. *Bioconjugate Chem.* **2001,** 12, 989-994.
172. Kloeckner, J.; Wagner, E.; Ogris, M. Degradable Gene Carriers Based on Oligomerized Polyamines. *European Journal of Pharmaceutical Sciences* **2006,** 29, 414-425.
173. Russ, V.; Elfberg, H.; Thoma, C.; Kloeckner, J.; Ogris, M.; Wagner, E. Novel Degradable Oligoethylenimine Acrylate Ester-Based Pseudodendrimers for in Vitro and in Vivo Gene Transfer. *Gene Ther.* **2007,** 15, 18-29.
174. Liu, J.; Jiang, X.; Xu, L.; Wang, X.; Hennink, W. E.; Zhuo, R. Novel Reduction-Responsive Cross-Linked Polyethylenimine Derivatives by Click Chemistry for Nonviral Gene Delivery. *Bioconjugate Chem.* **2010,** 21, 1827-1835.
175. Anwer, K.; Barnes, M. N.; Fewell, J.; Lewis, D. H.; Alvarez, R. D. Phase-I Clinical Trial of Il-12 Plasmid/Lipopolymer Complexes for the Treatment of Recurrent Ovarian Cancer. *Gene Ther.* **2010,** 17, 360-369.
176. Anderson, D. G.; Lynn, D. M.; Langer, R. Semi-Automated Synthesis and Screening of a Large Library of Degradable Cationic Polymers for Gene Delivery. *Angewandte Chemie International Edition* **2003,** 42, 3153-3158.

177. Greenland, J. R.; Liu, H.; Berry, D.; Anderson, D. G.; Kim, W.-K.; Irvine, D. J.; Langer, R.; Letvin, N. L. [Beta]-Amino Ester Polymers Facilitate in Vivo DNA Transfection and Adjuvant Plasmid DNA Immunization. *Mol. Ther.* **2005,** 12, 164-170.
178. Jere, D.; Xu, C.-X.; Arote, R.; Yun, C.-H.; Cho, M.-H.; Cho, C.-S. Poly(B-Amino Ester) as a Carrier for Si/Shrna Delivery in Lung Cancer Cells. *Biomaterials* **2008,** 29, 2535-2547.
179. Tzeng, S. Y.; Guerrero-Cázares, H.; Martinez, E. E.; Sunshine, J. C.; Quiñones-Hinojosa, A.; Green, J. J. Non-Viral Gene Delivery Nanoparticles Based on Poly(B-Amino Esters) for Treatment of Glioblastoma. *Biomaterials* **2011,** 32, 5402-5410.
180. Kim, T.-i.; Seo, H. J.; Choi, J. S.; Yoon, J. K.; Baek, J.-u.; Kim, K.; Park, J.-S. Synthesis of Biodegradable Cross-Linked Poly(B-Amino Ester) for Gene Delivery and Its Modification, Inducing Enhanced Transfection Efficiency and Stepwise Degradation. *Bioconjugate Chem.* **2005,** 16, 1140-1148.
181. Huang, Y.-H.; Zugates, G. T.; Peng, W.; Holtz, D.; Dunton, C.; Green, J. J.; Hossain, N.; Chernick, M. R.; Padera, R. F.; Langer, R.; Anderson, D. G.; Sawicki, J. a. Nanoparticle-Delivered Suicide Gene Therapy Effectively Reduces Ovarian Tumor Burden in Mice. *Cancer Res.* **2009,** 69, 6184-6191.
182. Cohen, J. a.; Beaudette, T. T.; Cohen, J. L.; Broaders, K. E.; Bachelder, E. M.; Fréchet, J. M. J. Acetal-Modified Dextran Microparticles with Controlled Degradation Kinetics and Surface Functionality for Gene Delivery in Phagocytic and Non-Phagocytic Cells. *Advanced materials (Deerfield Beach, Fla.)* **2010,** 22, 3593-3597.
183. Little, S. R.; Lynn, D. M.; Ge, Q.; Anderson, D. G.; Puram, S. V.; Chen, J.; Eisen, H. N.; Langer, R. Poly-B Amino Ester-Containing Microparticles Enhance the Activity of Nonviral Genetic Vaccines. *Proc. Natl. Acad. Sci.* **2004,** 101, 9534-9539.
184. Zhang, J.; Chua, L. S.; Lynn, D. M. Multilayered Thin Films That Sustain the Release of Functional DNA under Physiological Conditions. *Langmuir* **2004,** 20, 8015-8021.
185. Jewell, C. M.; Zhang, J.; Fredin, N. J.; Lynn, D. M. Multilayered Polyelectrolyte Films Promote the Direct and Localized Delivery of DNA to Cells. *J. Control. Release* **2005,** 106, 214-223.
186. Flessner, R. M.; Jewell, C. M.; Anderson, D. G.; Lynn, D. M. Degradable Polyelectrolyte Multilayers That Promote the Release of Sirna. *Langmuir* **2011,** 27, 7868-7876.
187. Bayele, H. K.; Sakthivel, T.; O'Donell, M.; Pasi, K. J.; Wilderspin, A. F.; Lee, C. A.; Toth, I.; Florence, A. T. Versatile Peptide Dendrimers for Nucleic Acid Delivery. *Journal of Pharmaceutical Sciences* **2005,** 94, 446-457.
188. Chen, J.; Wu, C.; Oupicky, D. Bioreducible Hyperbranched Poly (Amido Amine) S for Gene Delivery. *Biomacromolecules* **2009,** 10, 2921-2927.
189. Barnard, A.; Posocco, P.; Pricl, S.; Calderon, M.; Haag, R.; Hwang, M. E.; Shum, V. W. T.; Pack, D. W.; Smith, D. K. Degradable Self-Assembling Dendrons for Gene Delivery: Experimental and Theoretical Insights into the Barriers to Cellular Uptake. *J. Am. Chem. Soc.* **2011,** 133, 20288-20300.
190. Arote, R.; Kim, T.-H.; Kim, Y.-K.; Hwang, S.-K.; Jiang, H.-L.; Song, H.-H.; Nah, J.-W.; Cho, M.-H.; Cho, C.-S. A Biodegradable Poly(Ester Amine) Based on Polycaprolactone and Polyethylenimine as a Gene Carrier. *Biomaterials* **2007,** 28, 735-744.
191. Lai, W.-F.; Lin, M. C.-M. Nucleic Acid Delivery with Chitosan and Its Derivatives. *Journal of controlled release : official journal of the Controlled Release Society* **2009,** 134, 158-168.

192. Yuan, X.; Shah, B. A.; Kotadia, N. K.; Li, J.; Gu, H.; Wu, Z. The Development and Mechanism Studies of Cationic Chitosan-Modified Biodegradable Plga Nanoparticles for Efficient Sirna Drug Delivery. *Pharmaceut. Res.* **2010,** 27, 1285-1295.
193. Mao, H.-Q.; Roy, K.; Troung-Le, V. L.; Janes, K. A.; Lin, K. Y.; Wang, Y.; August, J. T.; Leong, K. W. Chitosan-DNA Nanoparticles as Gene Carriers: Synthesis, Characterization and Transfection Efficiency. *Journal of Controlled Release* **2001,** 70, 399-421.
194. Rojanarata, T.; Opanasopit, P.; Techaarpornkul, S.; Ngawhirunpat, T.; Ruktanonchai, U. Chitosan-Thiamine Pyrophosphate as a Novel Carrier for Sirna Delivery. *Pharmaceut. Res.* **2008,** 25, 2807-2814.
195. Wardwell, P. R.; Bader, R. a. Immunomodulation of Cystic Fibrosis Epithelial Cells Via Nf-Kb Decoy Oligonucleotide-Coated Polysaccharide Nanoparticles. *Journal of biomedical materials research. Part A* **2014**, 1-10.
196. Raviña, M.; Cubillo, E.; Olmeda, D.; Novoa-Carballal, R.; Fernandez-Megia, E.; Riguera, R.; Sánchez, A.; Cano, A.; Alonso, M. J. Hyaluronic Acid/Chitosan-G-Poly(Ethylene Glycol) Nanoparticles for Gene Therapy: An Application for Pdna and Sirna Delivery. *Pharmaceut. Res.* **2010,** 27, 2544-2555.
197. Ganesh, S.; Iyer, A. K.; Morrissey, D. V.; Amiji, M. M. Hyaluronic Acid Based Self-Assembling Nanosystems for Cd44 Target Mediated Sirna Delivery to Solid Tumors. *Biomaterials* **2013,** 34, 3489-3502.
198. Park, K.; Lee, M.-Y.; Kim, K. S.; Hahn, S. K. Target Specific Tumor Treatment by Vegf Sirna Complexed with Reducible Polyethyleneimine–Hyaluronic Acid Conjugate. *Biomaterials* **2010,** 31, 5258-5265.
199. Tokatlian, T.; Cam, C.; Segura, T. Non-Viral DNA Delivery from Porous Hyaluronic Acid Hydrogels in Mice. *Biomaterials* **2014,** 35, 825-835.
200. Bartlett, D. W.; Davis, M. E. Physicochemical and Biological Characterization of Targeted, Nucleic Acid-Containing Nanoparticles. *Bioconjugate Chem.* **2007,** 18, 456-468.
201. Davis, M. E. The First Targeted Delivery of Sirna in Humans Via a Nanoparticle : From Concept to Clinic. **2009,** 6, 659-668.
202. Zuckerman, J. E.; Gritli, I.; Tolcher, a.; Heidel, J. D.; Lim, D.; Morgan, R.; Chmielowski, B.; Ribas, a.; Davis, M. E.; Yen, Y. Correlating Animal and Human Phase Ia/Ib Clinical Data with Calaa-01, a Targeted, Polymer-Based Nanoparticle Containing Sirna. *Proc. Natl. Acad. Sci.* **2014,** 111.
203. Davis, M. E.; Zuckerman, J. E.; Choi, C. H. J.; Seligson, D.; Tolcher, A.; Alabi, C. a.; Yen, Y.; Heidel, J. D.; Ribas, A. Evidence of Rnai in Humans from Systemically Administered Sirna Via Targeted Nanoparticles. *Nature* **2010,** 464, 1067-1070.
204. Bachelder, E. M.; Beaudette, T. T.; Broaders, K. E.; Dashe, J.; Fréchet, J. M. J. Acetal-Derivatized Dextran: An Acid-Responsive Biodegradable Material for Therapeutic Applications. *J. Am. Chem. Soc.* **2008,** 130, 10494-10495.
205. Cohen, J. L.; Schubert, S.; Wich, P. R.; Cui, L.; Cohen, J. a.; Mynar, J. L.; Fréchet, J. M. J. Acid-Degradable Cationic Dextran Particles for the Delivery of Sirna Therapeutics. *Bioconjugate Chem.* **2011,** 22, 1056-1065.
206. Azzam, T.; Eliyahu, H.; Shapira, L.; Linial, M.; Barenholz, Y.; Domb, A. J. Polysaccharide−Oligoamine Based Conjugates for Gene Delivery. *Journal of Medicinal Chemistry* **2002,** 45, 1817-1824.
207. Lee, H.; Lytton-Jean, A. K.; Chen, Y.; Love, K. T.; Park, A. I.; Karagiannis, E. D.; Sehgal, A.; Querbes, W.; Zurenko, C. S.; Jayaraman, M.; Peng, C. G.; Charisse, K.; Borodovsky,

A.; Manoharan, M.; Donahoe, J. S.; Truelove, J.; Nahrendorf, M.; Langer, R.; Anderson, D. G. Molecularly Self-Assembled Nucleic Acid Nanoparticles for Targeted in Vivo Sirna Delivery. *Nature nanotechnology* **2012,** 7, 389-393.
208. Fire, A.; Xu, S. Q.; Montgomery, M. K.; Kostas, S. A.; Driver, S. E.; Mello, C. C. Potent and Specific Genetic Interference by Double-Stranded Rna in Caenorhabditis Elegans. *Nature* **1998,** 391, 806-811.
209. Baulcombe, D. Rna Silencing in Plants. *Nature* **2004,** 431, 356-363.
210. Sanchez-Vargas, I.; Travanty, E. A.; Keene, K. M.; Franz, A. W. E.; Beaty, B. J.; Blair, C. D.; Olson, K. E. Rna Interference, Arthropod-Borne Viruses, and Mosquitoes. *Virus research* **2004,** 102, 65-74.
211. Voinnet, O. Induction and Suppression of Rna Silencing: Insights from Viral Infections. *Nat. Rev. Genet.* **2005,** 6, 206-220.
212. Wu, W.; Sun, M.; Zou, G. M.; Chen, J. Microrna and Cancer: Current Status and Prospective. *Int. J. Cancer* **2007,** 120, 953-960.
213. Yadav, S.; van Vlerken, L. E.; Little, S. R.; Amiji, M. M. Evaluations of Combination Mdr-1 Gene Silencing and Paclitaxel Administration in Biodegradable Polymeric Nanoparticle Formulations to Overcome Multidrug Resistance in Cancer Cells. *Cancer Chemother. Pharmacol.* **2009,** 63, 711-722.
214. Hannon, G. J. Rna Interference. *nature* **2002,** 418, 244-251.
215. Boxem, M.; Srinivasan, D. G.; van den Heuvel, S. The Caenorhabditis Elegans Gene Ncc-1 Encodes a Cdc2-Related Kinase Required for M Phase in Meiotic and Mitotic Cell Divisions, but Not for S Phase. *Development* **1999,** 126, 2227-2239.
216. Longman, D.; Johnstone, I. L.; Caceres, J. F. Functional Characterization of Sr and Sr-Related Genes in Caenorhabditis Elegans. *EMBO J.* **2000,** 19, 1625-1637.
217. Svoboda, P.; Stain, P.; Hayashi, H.; Schultz, R. M. Selective Reduction of Dormant Maternal Mrnas in Mouse Oocytes by Rna Interference. *Development* **2000,** 127, 4147-4156.
218. Clemens, J. C.; Worby, C. A.; Simonson-Leff, N.; Muda, M.; Maehama, T.; Hemmings, B. A.; Dixon, J. E. Use of Double-Stranded Rna Interference in Drosophila Cell Lines to Dissect Signal Transduction Pathways. *Proc. Natl. Acad. Sci.* **2000,** 97, 6499-6503.
219. Stark, G. R.; Kerr, I. M.; Williams, B. R. G.; Silverman, R. H.; Schreiber, R. D. How Cells Respond to Interferons. *Annu. Rev. Biochem.* **1998,** 67, 227-264.
220. Wu, G. Y.; Wu, C. H. Receptor-Mediated in Vitro Gene Transformation by a Soluble DNA Carrier System. *J. Biol. Chem.* **1987,** 262, 4429-4432.
221. Wagner, E.; Plank, C.; Zatloukal, K.; Cotten, M.; Birnstiel, M. L. Influenza-Virus Hemagglutinin-Ha-2 N-Terminal Fusogenic Peptides Augment Gene-Transfer by Transferrin Polylysine DNA Complexes - toward a Synthetic Virus-Like Gene-Transfer Vehicle. *Proc. Natl. Acad. Sci.* **1992,** 89, 7934-7938.
222. Curiel, D. T.; Agarwal, S.; Wagner, E.; Cotten, M. Adenovirus Enhancement of Transferrin Polylysine-Mediated Gene Delivery. *Proc. Natl. Acad. Sci.* **1991,** 88, 8850-8854.
223. Midoux, P.; Monsigny, M. Efficient Gene Transfer by Histidylated Polylysine Pdna Complexes. *Bioconjugate Chem.* **1999,** 10, 406-411.
224. Alving, C. R.; Steck, E. A.; Chapman, W. L., Jr.; Waits, V. B.; Hendricks, L. D.; Swartz, G. M., Jr.; Hanson, W. L. Therapy of Leishmaniasis: Superior Efficacies of Liposome-Encapsulated Drugs. *Proc. Natl. Acad. Sci.* **1978,** 75, 2959-2963.

225. Wightman, L.; Kircheis, R.; Rossler, V.; Carotta, S.; Ruzicka, R.; Kursa, M.; Wagner, E. Different Behavior of Branched and Linear Polyethylenimine for Gene Delivery in Vitro and in Vivo. *J. Gene. Med.* **2001,** 3, 362-372.
226. Ogris, M.; Steinlein, P.; Kursa, M.; Mechtler, K.; Kircheis, R.; Wagner, E. The Size of DNA/Transferrin-Pei Complexes Is an Important Factor for Gene Expression in Cultured Cells. *Gene Ther.* **1998,** 5, 1425-1433.
227. Ward, C. M.; Read, M. L.; Seymour, L. W. Systemic Circulation of Poly(L-Lysine)/DNA Vectors Is Influenced by Polycation Molecular Weight and Type of DNA: Differential Circulation in Mice and Rats and the Implications for Human Gene Therapy. *Blood* **2001,** 97, 2221-2229.
228. Ogris, M.; Brunner, S.; Schuller, S.; Kircheis, R.; Wagner, E. Pegylated DNA/Transferrin-Pei Complexes: Reduced Interaction with Blood Components, Extended Circulation in Blood and Potential for Systemic Gene Delivery. *Gene Ther.* **1999,** 6, 595-605.
229. Mao, H. Q.; Roy, K.; Troung-Le, V. L.; Janes, K. A.; Lin, K. Y.; Wang, Y.; August, J. T.; Leong, K. W. Chitosan-DNA Nanoparticles as Gene Carriers: Synthesis, Characterization and Transfection Efficiency. *J. Control. Release* **2001,** 70, 399-421.
230. Kaul, G.; Amiji, M. Tumor-Targeted Gene Delivery Using Poly(Ethylene Glycol)-Modified Gelatin Nanoparticles: In Vitro and in Vivo Studies. *Pharmaceut. Res.* **2005,** 22, 951-961.
231. Suk, J. S.; Suh, J.; Choy, K.; Lai, S. K.; Fu, J.; Hanes, J. Gene Delivery to Differentiated Neurotypic Cells with Rgd and Hiv Tat Peptide Functionalized Polymeric Nanoparticles. *Biomaterials* **2006,** 27, 5143-5150.
232. Hatakeyama, H.; Akita, H.; Kogure, K.; Oishi, M.; Nagasaki, Y.; Kihira, Y.; Ueno, M.; Kobayashi, H.; Kikuchi, H.; Harashima, H. Development of a Novel Systemic Gene Delivery System for Cancer Therapy with a Tumor-Specific Cleavable Peg-Lipid. *Gene Ther.* **2007,** 14, 68-77.
233. Kawano, T.; Yamagata, M.; Takahashi, H.; Niidome, Y.; Yamada, S.; Katayama, Y.; Niidome, T. Stabilizing of Plasmid DNA in Vivo by Peg-Modified Cationic Gold Nanoparticles and the Gene Expression Assisted with Electrical Pulses. *J. Control. Release* **2006,** 111, 382-389.
234. Hafez, I.; Maurer, N.; Cullis, P. On the Mechanism Whereby Cationic Lipids Promote Intracellular Delivery of Polynucleic Acids. *Gene Therapy* **2001,** 8, 1188-1196.
235. Xu, Y.; Szoka Jr, F. C. Mechanism of DNA Release from Cationic Liposome/DNA Complexes Used in Cell Transfection. *Biochemistry* **1996,** 35, 5616-5623.
236. Zelphati, O.; Szoka Jr, F. C. Mechanism of Oligonucleotide Release from Cationic Liposomes. *Proc. Natl. Acad. Sci.* **1996,** 93, 11493-11498.
237. Lockman, P. R.; Koziara, J. M.; Mumper, R. J.; Allen, D. D. Nanoparticle Surface Charges Alter Blood-Brain Barrier Integrity and Permeability. *J. Drug Target.* **2004,** 12, 635-641.
238. Wyman, T. B.; Nicol, F.; Zelphati, O.; Scaria, P.; Plank, C.; Szoka Jr, F. C. Design, Synthesis, and Characterization of a Cationic Peptide That Binds to Nucleic Acids and Permeabilizes Bilayers. *Biochemistry* **1997,** 36, 3008-3017.
239. Niidome, T.; Ohmori, N.; Ichinose, A.; Wada, A.; Mihara, H.; Hirayama, T.; Aoyagi, H. Binding of Cationic Alpha-Helical Peptides to Plasmid DNA and Their Gene Transfer Abilities into Cells. *J. Biol. Chem.* **1997,** 272, 15307-15312.

240. Plank, C.; Oberhauser, B.; Mechtler, K.; Koch, C.; Wagner, E. The Influence of Endosome-Disruptive Peptides on Gene-Transfer Using Synthetic Virus-Like Gene-Transfer Systems. *J. Biol. Chem.* **1994,** 269, 12918-12924.
241. Frankel, A. D.; Pabo, C. O. Cellular Uptake of the Tat Protein from Human Immunodeficiency Virus. *Cell* **1988,** 55, 1189-1193.
242. Green, M.; Loewenstein, P. M. Autonomous Functional Domains of Chemically Synthesized Human Immunodeficiency Virus Tat *Trans*-Activator Protein. *Cell* **1988,** 55, 1179-1188.
243. Manickam, D. S.; Bisht, H. S.; Wan, L.; Mao, G. Z.; Oupicky, D. Influence of Tat-Peptide Polymerization on Properties and Transfection Activity of Tat/DNA Polyplexes. *J. Control. Release* **2005,** 102, 293-306.
244. Harris, T. J.; Green, J. J.; Fung, P. W.; Langer, R.; Anderson, D. G.; Bhatia, S. N. Tissue-Specific Gene Delivery Via Nanoparticle Coating. *Biomaterials* **2010,** 31, 998-1006.
245. Cheng, C. J.; Saltzman, W. M. Enhanced Sirna Delivery into Cells by Exploiting the Synergy between Targeting Ligands and Cell-Penetrating Peptides. *Biomaterials* **2011,** 32, 6194-6203.
246. Zhou, J.; Neff, C. P.; Swiderski, P.; Li, H.; Smith, D. D.; Aboellail, T.; Remling-Mulder, L.; Akkina, R.; Rossi, J. J. Functional in Vivo Delivery of Multiplexed Anti-Hiv-1 Sirnas Via a Chemically Synthesized Aptamer with a Sticky Bridge. *Mol Ther* **2013,** 21, 192-200.
247. Boussif, O.; Lezoualch, F.; Zanta, M. A.; Mergny, M. D.; Scherman, D.; Demeneix, B.; Behr, J. P. A Versatile Vector for Gene and Oligonucleotide Transfer into Cells in Culture and in-Vivo - Polyethylenimine. *Proc. Natl. Acad. Sci.* **1995,** 92, 7297-7301.
248. Benjaminsen, R. V.; Mattebjerg, M. A.; Henriksen, J. R.; Moghimi, S. M.; Andresen, T. L. The Possible "Proton Sponge" Effect of Polyethylenimine (Pei) Does Not Include Change in Lysosomal Ph. *Mol. Ther.* **2013,** 21, 149-157.
249. Nel, A. E.; Madler, L.; Velegol, D.; Xia, T.; Hoek, E. M. V.; Somasundaran, P.; Klaessig, F.; Castranova, V.; Thompson, M. Understanding Biophysicochemical Interactions at the Nano-Bio Interface. *Nature Mater.* **2009,** 8, 543-557.
250. Benns, J. M.; Choi, J. S.; Mahato, R. I.; Park, J. S.; Kim, S. W. Ph-Sensitive Cationic Polymer Gene Delivery Vehicle: N-Ac-Poly(L-Histidine)-Graft-Poly(L-Lysine) Comb Shaped Polymer. *Bioconjugate Chem.* **2000,** 11, 637-645.
251. Haensler, J.; Szoka Jr, F. C. Polyamidoamine Cascade Polymers Mediate Efficient Transfection of Cells in Culture. *Bioconjugate Chem.* **1993,** 4, 372-379.
252. Felgner, J. H.; Kumar, R.; Sridhar, C. N.; Wheeler, C. J.; Tsai, Y. J.; Border, R.; Ramsey, P.; Martin, M.; Felgner, P. L. Enhanced Gene Delivery and Mechanism Studies with a Novel Series of Cationic Lipid Formulations. *J. Biol. Chem.* **1994,** 269, 2550-2561.
253. El Ouahabi, A.; Thiry, M.; Pector, V.; Fuks, R.; Ruysschaert, J. M.; Vandenbranden, M. The Role of Endosome Destabilizing Activity in the Gene Transfer Process Mediated by Cationic Lipids. *FEBS Lett.* **1997,** 414, 187-192.
254. Drummond, D. C.; Zignani, M.; Leroux, J. C. Current Status of Ph-Sensitive Liposomes in Drug Delivery. *Prog Lipid Res* **2000,** 39, 409-460.
255. Kawasaki, H.; Taira, K. Short Hairpin Type of Dsrnas That Are Controlled by Trnaval Promoter Significantly Induce Rnai-Mediated Gene Silencing in the Cytoplasm of Human Cells. *Nucleic Acids Res.* **2003,** 31, 700-707.

256. Tzeng, S. Y.; Green, J. J. Subtle Changes to Polymer Structure and Degradation Mechanism Enable Highly Effective Nanoparticles for Sirna and DNA Delivery to Human Brain Cancer. *Adv. Healthcare Mater.* **2013,** 2, 467.
257. Son, S.; Namgung, R.; Kim, J.; Singha, K.; Kim, W. J. Bioreducible Polymers for Gene Silencing and Delivery. *Accounts of Chemical Research* **2012,** 45.
258. Spagnou, S.; Miller, A. D.; Keller, M. Lipidic Carriers of Sirna: Differences in the Formulation, Cellular Uptake, and Delivery with Plasmid DNA. *Biochemistry* **2004,** 43, 13348-13356.
259. Sutton, D.; Kim, S. J.; Shuai, X. T.; Leskov, K.; Marques, J. T.; Williams, B. R. G.; Boothman, D. A.; Gao, J. M. Efficient Suppression of Secretory Clusterin Levels by Polymer-Sirna Nanocomplexes Enhances Ionizing Radiation Lethality in Human Mcf-7 Breast Cancer Cells in Vitro. *International Journal of Nanomedicine* **2006,** 1, 155-162.
260. Hagerman, P. J. Flexibility of Rna. *Annu. Rev. Biophys. Biomol. Struct.* **1997,** 26, 139-156.
261. Bolcato-Bellemin, A. L.; Bonnet, M. E.; Creusatt, G.; Erbacher, P.; Behr, J. P. Sticky Overhangs Enhance Sirna-Mediated Gene Silencing. *Proc. Natl. Acad. Sci.* **2007,** 104, 16050-16055.
262. Li, S. D.; Chen, Y. C.; Hackett, M. J.; Huang, L. Tumor-Targeted Delivery of Sirna by Self-Assembled Nanoparticles. *Mol. Ther.* **2008,** 16, 163-169.
263. Adair, J. H.; Parette, M. P.; Altinoglu, E. I.; Kester, M. Nanoparticulate Alternatives for Drug Delivery. *ACS Nano* **2010,** 4, 4967-4970.
264. Forbes, D. C.; Peppas, N. A. Oral Delivery of Small Rna and DNA. *J. Control. Release* **2012,** 162, 438-435.
265. Judge, A. D.; Bola, G.; Lee, A. C. H.; Maclachlan, I. Design of Noninflammatory Synthetic Sirna Mediating Potent Gene Silencing in Vivo. *Mol. Ther.* **2006,** 13, 494-505.
266. Akinc, A.; Zumbuehl, A.; Goldberg, M.; Leshchiner, E. S.; Busini, V.; Hossain, N.; Bacallado, S. A.; Nguyen, D. N.; Fuller, J.; Alvarez, R.; Borodovsky, A.; Borland, T.; Constien, R.; de Fougerolles, A.; Dorkin, J. R.; Jayaprakash, K. N.; Jayaraman, M.; John, M.; Koteliansky, V.; Manoharan, M.; Nechev, L.; Qin, J.; Racie, T.; Raitcheva, D.; Rajeev, K. G.; Sah, D. W. Y.; Soutschek, J.; Toudjarska, I.; Vornlocher, H. P.; Zimmermann, T. S.; Langer, R.; Anderson, D. G. A Combinatorial Library of Lipid-Like Materials for Delivery of Rnai Therapeutics. *Nat. Biotechnol.* **2008,** 26, 561-569.
267. Akinc, A.; Goldberg, M.; Qin, J.; Dorkin, J. R.; Gamba-Vitalo, C.; Maier, M.; Jayaprakash, K. N.; Jayaraman, M.; Rajeev, K. G.; Manoharan, M.; Koteliansky, V.; Rohl, I.; Leshchiner, E. S.; Langer, R.; Anderson, D. G. Development of Lipidoid-Sirna Formulations for Systemic Delivery to the Liver. *Mol. Ther.* **2009,** 17, 872-879.
268. Lu, J. J.; Langer, R.; Chen, J. Z. A Novel Mechanism Is Involved in Cationic Lipid-Mediated Functional Sirna Delivery. *Mol. Pharm.* **2009,** 6, 763-771.
269. Umeda, M.; Nojima, S.; Inoue, K. Effect of Lipid Composition on Hvj-Mediated Fusion of Glycophorin Liposomes to Erythrocytes. *J. Biochem.* **1985,** 97, 1301-1310.
270. Litzinger, D. C.; Huang, L. Phosphatidylethanolamine Liposomes - Drug Delivery, Gene-Transfer and Immunodiagnostic Applications. *Biochim. Biophys. Acta* **1992,** 1113, 201-227.
271. Hafez, I. M.; Cullis, P. R. Roles of Lipid Polymorphism in Intracellular Delivery. *Adv. Drug Deliv. Rev.* **2001,** 47, 139-148.
272. Heyes, J.; Palmer, L.; Bremner, K.; MacLachlan, I. Cationic Lipid Saturation Influences Intracellular Delivery of Encapsulated Nucleic Acids. *J. Control. Release* **2005,** 107, 276-287.

273. Semple, S. C.; Akinc, A.; Chen, J.; Sandhu, A. P.; Mui, B. L.; Cho, C. K.; Sah, D. W. Y.; Stebbing, D.; Crosley, E. J.; Hafez, I. M. Rational Design of Cationic Lipids for Sirna Delivery. *Nat. Biotechnol.* **2010,** 28, 172-176.
274. Leconet, W.; Petit, P.; Peraldi-Roux, S.; Bresson, D. Nonviral Delivery of Small Interfering Rna into Pancreas-Associated Immune Cells Prevents Autoimmune Diabetes. *Mol. Ther.* **2012,** 20, 2315-2325.
275. Zaidi, H., A; DiMeco, F.; Quinones-Hinojosa, A. Brain Tumor Stem Cells. In *Youman's Neurological Surgery*, 2009.
276. Bao, S.; Wu, Q.; McLendon, R. E.; Hao, Y.; Shi, Q.; Hjelmeland, A. B.; Dewhirst, M. W.; Bigner, D. D.; Rich, J. N. Glioma Stem Cells Promote Radioresistance by Preferential Activation of the DNA Damage Response. *Nature* **2006,** 444, 756-760.
277. Mohyeldin, A.; Garzon-Muvdi, T.; Quinones-Hinojosa, A. Oxygen in Stem Cell Biology: A Critical Component of the Stem Cell Niche. *Cell Stem Cell* **2010,** 7, 150-161.
278. Putnam, D. Polymers for Gene Delivery across Length Scales. *Nature Mater.* **2006,** 5, 439-451.
279. Meyer, M.; Philipp, A.; Oskuee, R.; Schmidt, C.; Wagner, E. Breathing Life into Polycations: Functionalization with Ph-Responsive Endosomolytic Peptides and Polyethylene Glycol Enables Sirna Delivery. *J. Am. Chem. Soc.* **2008,** 130, 3272-+.
280. Kakizawa, Y.; Harada, A.; Kataoka, K. Environment-Sensitive Stabilization of Core-Shell Structured Polyion Complex Micelle by Reversible Cross-Linking of the Core through Disulfide Bond. *J. Am. Chem. Soc.* **1999,** 121, 11247-11248.
281. Kakizawa, Y.; Harada, A.; Kataoka, K. Glutathione-Sensitive Stabilization of Block Copolymer Micelles Composed of Antisense DNA and Thiolated Poly (Ethylene Glycol)-B Lock-Poly (L-Lysine): A Potential Carrier for Systemic Delivery of Antisense DNA. *Biomacromolecules* **2001,** 2, 491-497.
282. Christie, R. J.; Matsumoto, Y.; Miyata, K.; Nomoto, T.; Fukushima, S.; Osada, K.; Halnaut, J.; Pittella, F.; Kim, H. J.; Nishiyama, N.; Kataoka, K. Targeted Polymeric Micelles for Sirna Treatment of Experimental Cancer by Intravenous Injection. *ACS Nano* **2012,** 6, 5174-5189.
283. Kim, S. H.; Jeong, J. H.; Lee, S. H.; Kim, S. W.; Park, T. G. Local and Systemic Delivery of Vegf Sirna Using Polyelectrolyte Complex Micelles for Effective Treatment of Cancer. *J. Control. Release* **2008,** 129, 107-116.
284. Christensen, L. V.; Chang, C. W.; Kim, W. J.; Kim, S. W.; Zhong, Z. Y.; Lin, C.; Engbersen, J. F. J.; Feijen, J. Reducible Poly(Amido Ethylenimine)S Designed for Triggered Intracellular Gene Delivery. *Bioconjugate Chem.* **2006,** 17, 1233-1240.
285. Vader, P.; van der Aa, L. J.; Engbersen, J. F. J.; Storm, G.; Schiffelers, R. M. Physicochemical and Biological Evaluation of Sirna Polyplexes Based on Pegylated Poly (Amido Amine) S. *Pharmaceut. Res.* **2012,** 29, 352-361.
286. Bernstein, E.; Caudy, A. A.; Hammond, S. M.; Hannon, G. J. Role for a Bidentate Ribonuclease in the Initiation Step of Rna Interference. *Nature* **2001,** 409, 363-366.
287. Vandenbroucke, R. E.; De Geest, B. G.; Bonne, S.; Vinken, M.; Van Haecke, T.; Heimberg, H.; Wagner, E.; Rogiers, V.; De Smedt, S. C.; Demeester, J.; Sanders, N. N. Prolonged Gene Silencing in Hepatoma Cells and Primary Hepatocytes after Small Interfering Rna Delivery with Biodegradable Poly(Beta-Amino Esters). *J. Gene. Med.* **2008,** 10, 783-794.
288. Kozielski, K. L.; Tzeng, S. Y.; Green, J. J. A Bioreducible Linear Poly(Beta-Amino Ester) for Sirna Delivery. *Chem. Commun.* **2013**.

289. Woodrow, K. A.; Cu, Y.; Booth, C. J.; Saucier-Sawyer, J. K.; Wood, M. J.; Saltzman, W. M. Intravaginal Gene Silencing Using Biodegradable Polymer Nanoparticles Densely Loaded with Small-Interfering Rna. *Nature Mater.* **2009,** 8, 526-533.
290. Yuan, X. D.; Shah, B. A.; Kotadia, N. K.; Li, J. A.; Gu, H.; Wu, Z. Q. The Development and Mechanism Studies of Cationic Chitosan-Modified Biodegradable Plga Nanoparticles for Efficient Sirna Drug Delivery. *Pharmaceut. Res.* **2010,** 27, 1285-1295.
291. Zhou, J.; Patel, T. R.; Fu, M.; Bertram, J. P.; Saltzman, W. M. Octa-Functional Plga Nanoparticles for Targeted and Efficient Sirna Delivery to Tumors. *Biomaterials* **2012,** 33, 583-591.
292. Tzeng, S. Y.; Lavik, E. B. Photopolymerizable Nanoarray Hydrogels Deliver Cntf and Promote Differentiation of Neural Stem Cells. *Soft Matter* **2010,** 6, 2208-2215.
293. Bertram, J. P.; Williams, C. A.; Robinson, R.; Segal, S. S.; Flynn, N. T.; Lavik, E. B. Intravenous Hemostat: Nanotechnology to Halt Bleeding. *Sci. Transl. Med.* **2009,** 1.
294. Davis, M. E. The First Targeted Delivery of Sirna in Humans Via a Self-Assembling, Cyclodextrin Polymer-Based Nanoparticle: From Concept to Clinic. *Mol. Pharm.* **2009,** 6, 659-668.
295. Kakizawa, Y.; Furukawa, S.; Ishii, A.; Kataoka, K. Organic-Inorganic Hybrid-Nanocarrier of Sirna Constructing through the Self-Assembly of Calcium Phosphate and Peg-Based Block Aniomer. *J. Control. Release* **2006,** 111, 368-370.
296. Zhang, M.; Ishii, A.; Nishiyama, N.; Matsumoto, S.; Ishii, T.; Yamasaki, Y.; Kataoka, K. Pegylated Calcium Phosphate Nanocomposites as Smart Environment-Sensitive Carriers for Sirna Delivery. *Adv. Mater.* **2009,** 21, 3520-3525.
297. Love, J. C.; Estroff, L. A.; Kriebel, J. K.; Nuzzo, R. G.; Whitesides, G. M. Self-Assembled Monolayers of Thiolates on Metals as a Form of Nanotechnology. *Chemical Reviews-Columbus* **2005,** 105, 1103-1170.
298. Decher, G.; Hong, J. D. In *Buildup of Ultrathin Multilayer Films by a Self-Assembly Process, 1 Consecutive Adsorption of Anionic and Cationic Bipolar Amphiphiles on Charged Surfaces*, Makromolekulare Chemie. Macromolecular Symposia, Wiley Online Library: 1991; pp 321-327.
299. Giljohann, D. A.; Seferos, D. S.; Prigodich, A. E.; Patel, P. C.; Mirkin, C. A. Gene Regulation with Polyvalent Sirna-Nanoparticle Conjugates. *J. Am. Chem. Soc.* **2009,** 131, 2072-2073.
300. Zheng, D.; Giljohann, D. A.; Chen, D. L.; Massich, M. D.; Wang, X. Q.; Iordanov, H.; Mirkin, C. A.; Paller, A. S. Topical Delivery of Sirna-Based Spherical Nucleic Acid Nanoparticle Conjugates for Gene Regulation. *Proc. Natl. Acad. Sci.* **2012,** 109, 11975-11980.
301. Tanaka, T.; Mangala, L. S.; Vivas-Mejia, P. E.; Nieves-Alicea, R.; Mann, A. P.; Mora, E.; Han, H. D.; Shahzad, M. M.; Liu, X.; Bhavane, R.; Gu, J.; Fakhoury, J. R.; Chiappini, C.; Lu, C.; Matsuo, K.; Godin, B.; Stone, R. L.; Nick, A. M.; Lopez-Berestein, G.; Sood, A. K.; Ferrari, M. Sustained Small Interfering Rna Delivery by Mesoporous Silicon Particles. *Cancer Res.* **2010,** 70, 3687-3696.
302. Meng, H.; Liong, M.; Xia, T.; Li, Z.; Ji, Z.; Zink, J. I.; Nel, A. E. Engineered Design of Mesoporous Silica Nanoparticles to Deliver Doxorubicin and P-Glycoprotein Sirna to Overcome Drug Resistance in a Cancer Cell Line. *ACS Nano* **2010,** 4, 4539-4550.
303. Wu, X.; Liu, H.; Liu, J.; Haley, K. N.; Treadway, J. A.; Larson, J. P.; Ge, N.; Peale, F.; Bruchez, M. P. Immunofluorescent Labeling of Cancer Marker Her2 and Other Cellular Targets with Semiconductor Quantum Dots. *Nat. Biotechnol.* **2002,** 21, 41-46.

304. Derfus, A. M.; Chan, W. C. W.; Bhatia, S. N. Probing the Cytotoxicity of Semiconductor Quantum Dots. *Nano Lett.* **2004,** 4, 11-18.
305. Mattheakis, L. C.; Dias, J. M.; Choi, Y. J.; Gong, J.; Bruchez, M. P.; Liu, J.; Wang, E. Optical Coding of Mammalian Cells Using Semiconductor Quantum Dots. *Anal. Biochem.* **2004,** 327, 200-208.
306. Chen, A. A.; Derfus, A. M.; Khetani, S. R.; Bhatia, S. N. Quantum Dots to Monitor Rnai Delivery and Improve Gene Silencing. *Nucleic Acids Res.* **2005,** 33, e190-e190.
307. Ameres, S. L.; Martinez, J.; Schroeder, R. Molecular Basis for Target Rna Recognition and Cleavage by Human Risc. *Cell* **2007,** 130, 101-112.
308. Singh, N.; Agrawal, A.; Leung, A. K. L.; Sharp, P. A.; Bhatia, S. N. Effect of Nanoparticle Conjugation on Gene Silencing by Rna Interference. *J. Am. Chem. Soc.* **2010,** 132, 8241-8243.
309. Medarova, Z.; Pham, W.; Farrar, C.; Petkova, V.; Moore, A. In Vivo Imaging of Sirna Delivery and Silencing in Tumors. *Nat. Med.* **2007,** 13, 372-377.
310. Kim, S. H.; Jeong, J. H.; Lee, S. H.; Kim, S. W.; Park, T. G. Peg Conjugated Vegf Sirna for Anti-Angiogenic Gene Therapy. *J. Control. Release* **2006,** 116, 123-129.
311. Soutschek, J.; Akinc, A.; Bramlage, B.; Charisse, K.; Constien, R.; Donoghue, M.; Elbashir, S.; Geick, A.; Hadwiger, P.; Harborth, J.; John, M.; Kesavan, V.; Lavine, G.; Pandey, R. K.; Racie, T.; Rajeev, K. G.; Rohl, I.; Toudjarska, I.; Wang, G.; Wuschko, S.; Bumcrot, D.; Koteliansky, V.; Limmer, S.; Manoharan, M.; Vornlocher, H. P. Therapeutic Silencing of an Endogenous Gene by Systemic Administration of Modified Sirnas. *Nature* **2004,** 432, 173-178.
312. Wolfrum, C.; Shi, S.; Jayaprakash, K. N.; Jayaraman, M.; Wang, G.; Pandey, R. K.; Rajeev, K. G.; Nakayama, T.; Charrise, K.; Ndungo, E. M.; Zimmermann, T.; Koteliansky, V.; Manoharan, M.; Stoffel, M. Mechanisms and Optimization of in Vivo Delivery of Lipophilic Sirnas. *Nat. Biotechnol.* **2007,** 25, 1149-1157.
313. Bolcato-Bellemin, A. L.; Bonnet, M. E.; Creusat, G.; Erbacher, P.; Behr, J. P. Sticky Overhangs Enhance Sirna-Mediated Gene Silencing. *Proc. Natl. Acad. Sci.* **2007,** 104, 16050-16055.
314. Mok, H.; Lee, S. H.; Park, J. W.; Park, T. G. Multimeric Small Interfering Ribonucleic Acid for Highly Efficient Sequence-Specific Gene Silencing. *Nature Mater.* **2010,** 9, 272-278.
315. Lee, J. B.; Hong, J.; Bonner, D. K.; Poon, Z.; Hammond, P. T. Self-Assembled Rna Interference Microsponges for Efficient Sirna Delivery. *Nature Mater.* **2012**.
316. Diegelman, A. M.; Kool, E. T. Generation of Circular Rnas and Trans-Cleaving Catalytic Rnas by Rolling Transcription of Circular DNA Oligonucleotides Encoding Hairpin Ribozymes. *Nucleic Acids Res.* **1998,** 26, 3235-3241.
317. Cutler, J. I.; Zhang, K.; Zheng, D.; Auyeung, E.; Prigodich, A. E.; Mirkin, C. A. Polyvalent Nucleic Acid Nanostructures. *J. Am. Chem. Soc.* **2011,** 133, 9254-9257.
318. Semple, S. C.; Akinc, A.; Chen, J.; Sandhu, A. P.; Mui, B. L.; Cho, C. K.; Sah, D. W.; Stebbing, D.; Crosley, E. J.; Yaworski, E.; Hafez, I. M.; Dorkin, J. R.; Qin, J.; Lam, K.; Rajeev, K. G.; Wong, K. F.; Jeffs, L. B.; Nechev, L.; Eisenhardt, M. L.; Jayaraman, M.; Kazem, M.; Maier, M. A.; Srinivasulu, M.; Weinstein, M. J.; Chen, Q.; Alvarez, R.; Barros, S. A.; De, S.; Klimuk, S. K.; Borland, T.; Kosovrasti, V.; Cantley, W. L.; Tam, Y. K.; Manoharan, M.; Ciufolini, M. A.; Tracy, M. A.; de Fougerolles, A.; MacLachlan, I.; Cullis, P. R.; Madden, T. D.; Hope, M. J. Rational Design of Cationic Lipids for Sirna Delivery. *Nat. Biotechnol.* **2010,** 28, 172-176.

319. van der Aa, L.; Vader, P.; Storm, G.; Schiffelers, R.; Engbersen, J. Optimization of Poly (Amido Amine) S as Vectors for Sirna Delivery. *J. Control. Release* **2011,** 150, 177-186.

Chapter 3

Nanoparticle mediated delivery of a cancer-killing gene to glioblastoma as a cancer therapeutic

3.1. Introduction

Glioblastoma (GB) remains one of the most lethal cancers in humans with a median survival after maximal therapy of less than 2 years after first diagnosis.[1-3] Despite improvements in the past few decades with intraoperative surgical techniques, chemotherapy, and radiation therapy, predictable curative treatment for GB does not exist yet. New insights into specific gene mutations and dysregulated signaling pathways of the pathogenesis of brain tumors[4, 5] have highlighted gene therapy as a potential approach for the treatment of GB. This approach is based on the local delivery of a vector or nanoparticle carrying genetic material to cause overexpression of a gene or replace a gene that is missing or under-expressed in order to kill cancer cells.[6]

Approaches to gene therapy for GB include: (1) delivery of suicide genes, which convert pro-drugs *in situ* and cause tumor cell death;[7] (2) delivery of cytokine genes, which mobilize immune cells to fight the tumor;[8, 9] (3) delivery of tumor-suppressor genes, which induce apoptosis in tumor cells;[10, 11] and (4) delivery of conditionally-replicating viruses to specifically lyse tumor cells while sparing normal tissue.[12, 13] Gene therapy has most often been performed using viral carriers. However, viruses pose significant safety risks due to their inherent toxicity, immunogenicity, and tumorigenicity.[14]

This chapter contains material modified from the following article, previously published as: Mangraviti, A.;***** Tzeng, S.Y.;***** **Kozielski, K.L.**;***** Wang, Y.;***** Pedone, M.; Buaron, N.; Liu, A.; Wilson, D.R.; Hansen, S.K.; Rodriguez, F.J.; Gao, G.; DiMeco, F.; Brem, H.; Olivi, A.; Tyler, B.; Green, J.J.: Polymeric nanoparticles for non-viral gene therapy extend brain tumor survival *in vivo*. *ACS Nano* **2015,** *9,* 1236-1249. (*These authors contributed equally)

Non-viral gene delivery vectors have traditionally been unable to match the efficacy of viral gene delivery;[15] however, they can be engineered to avoid the risks that viruses pose. Non-viral methods of gene delivery have recently expanded and several effective nanomaterials exist including lipid-based,[16, 17] polymeric,[18-20] and inorganic[21-23] nanoparticles, some of which have reached clinical trials.[24] Successful DNA delivery can be achieved by designing materials that can overcome extra- and intracellular barriers.[25-28] Cationic, primary amine-containing polymers such as poly(*L*-lysine) (PLL) can bind anionic DNA and compact it into positively charged nanoparticles. This protects the DNA and promotes cellular uptake via the electrostatic interaction between the cationic nanoparticle and anionic cell surface.[28, 29] Tertiary amine-containing polymers with high buffering capacities, such as poly(ethyleneimine) (PEI), enable endocytosis and are then able to escape the endosome via the proton sponge mechanism.[29] DNA release can be achieved by hydrolytic polymer degradation in the cytoplasm of the cell following escape from the endosome. Poly(β-amino ester)s (PBAEs) are a class of polymers that can be engineered to contain primary, secondary, and tertiary amines and hydrolytically cleavable ester bonds.[30] These chemical properties enable effective DNA binding, endocytosis, endosomal escape, and intracellular DNA release within minutes to hours, all of which are prerequisite to nuclear uptake of the DNA[31-33] PBAEs have previously been shown to be safe and effective DNA delivery vectors *in vitro* to several cell types and *in vivo* to retinal and brain tumor tissue.[32-34]

In previous studies, we have also shown that these polymers degrade quickly under physiological conditions, with a half-life of only a few hours.[35] We believe that this is important both to minimize potential nanoparticle cytotoxicity as well as to ensure successful release of the DNA cargo.[35] Interestingly, PBAEs can also be engineered to exhibit cell-type specificity and to

selectively transfect tumor tissue while avoiding surrounding healthy tissue.[34, 36] These advantages make this class of polymers a promising option to use for the fabrication of polymeric gene delivery nanoparticles for the treatment of brain tumors. Convection-enhanced delivery (CED) has recently been shown to be effective for the delivery of polymeric nanoparticles encapsulating small molecule drugs, such as dithiazanine iodide, Doxil, and O6-benzylguanine , to brain tumors.[37-39] Moreover, CED and gene therapy have been suggested as a promising combination for the treatment of glioma.[40] Specifically, CED leads to better volume of distribution by maintaining a pressure gradient which enhances diffusion throughout the tumor mass.[41] We hypothesized that intratumoral infusion via CED may represent an effective approach for the delivery of PBAE/DNA nanoparticles, as they are "soft" nanocomplexes which can be deformed and may more easily be convected though small spaces while encapsulating large DNA molecules.

The present study investigates the efficacy of PBAE nanoparticles for the intracellular delivery of the herpes simplex virus (HSV)-derived enzyme thymidine kinase (HSVtk), which acts as a suicide gene in an aggressive gliosarcoma model. Suicide therapy is based on the systemic delivery of an inactive prodrug with tumor-specific expression of a drug-activating enzyme (the *suicide gene*)[42] in order to avoid toxicity in normal cells. The HSVtk-ganciclovir system has been previously used for gene therapy in several viral approaches such as with non-replicating herpes virus or adenovirus.[43-45] HSVtk catalyzes the phosphorylation of the cytotoxic nucleoside analogue ganciclovir (GCV) that can be incorporated into the DNA of actively proliferating cells, which disrupts DNA replication and halts cell division.[46, 47] Since the prodrug nucleosides are poor substrates for mammalian thymidine kinase, the toxic effect is initially restricted to cancer cells, as active GCV kills proliferating cells only.[48] An attractive aspect of

the *HSVtk*/*GCV* enzyme/prodrug system is that this therapy benefits from the phenomenon known as "bystander effect", whereby even cancer cells that do not express HSVtk become sensitive to GCV due to the activation of GCV in neighboring transfected cancer cells.[49, 50]

This work presents a biodegradable nanomedicine capable of effectively and selectively delivering DNA to malignant glioma *in vivo*. A library of PBAE nanoparticles was evaluated *in vitro* to optimize DNA delivery while minimizing toxicity. The optimal nanoparticle formulation was then physically characterized. We demonstrate that these nanoparticles can deliver an HSVtk transgene *in vitro* and initiate glioma cell killing via the local activation of GCV. We also demonstrate transfection of malignant gliomas *in vivo*. Using this nanoparticle-based therapy, we were able to statistically improve survival of rats with malignant glioma (**Scheme 1**). This work presents an exciting frontier in nanomedicine with significant potential to treat malignant gliomas.

3.2. Materials and methods

3.2.1. Polymer materials

Monomers used for polymer synthesis were purchased as follows: 1,4-butanediol diacrylate (B4; Alfa Aesar, Ward Hill, MA); 1,5-pentanediol diacrylate (B5; Monomer-Polymer and Dajac Laboratories, Trevose, PA); 3-amino-1-propanol (S3; Alfa Aesar); 4-amino-1-butanol (S4; Alfa Aesar); 5-amino-1-pentanol (S5; Alfa Aesar); pentane-1,3-diamine (E3; TCI America); 2-(3-aminopropylamino)ethanol (E6; Sigma-Aldrich); 1-(3-aminopropyl)-4-methylpiperazine (E7; Alfa Aesar). Lipofectamine® 2000 was purchased from Invitrogen (Carlsbad, CA) and used according to manufacturer's instructions. The pEGFP-N1 plasmid (GFP) was purchased from Elim Biopharmaceuticals and amplified by Aldevron (Fargo, ND). Herpes simplex virus type 1-

derived thymidine kinase (HSVtk) gene was cloned into the pcDNA3.1 vector (Life Technologies) according to the manufacturer's protocols. *Label* IT® Tracker Cy5 Kit was purchased from Mirus Bio (Madison, WI). For staining, 2-(4-amidinophenyl)-1H -indole-6-carboxamidine (DAPI) was purchased from Life Technologies™, propidium iodide (PI) was purchased from Invitrogen (Carlsbad, CA), the conjugated antibody anti-Ki67 Alexa Fluor® 647 (rabbit anti-rat 1:50) was purchased from Cell Signaling Technology (Beverly, MA). CellTiter 96® AQ_{ueous} One MTS assay was purchased from Promega (Fitchburg, WI). Ganciclovir was purchased from both Invivogen (San Diego, CA) and Euroasian Chemicals PVT LTD (Lower Parel, Mumbai, India).

3.2.2. Polymer synthesis

PBAEs were synthesized using a two-step reaction (**Figure 1**) in a manner similar to Bhise *et al*.[51] Base monomers B4, B5, or B6 were each polymerized by Michael Addition of one of the side chain monomers S3, S4, or S5 at ratios following **Table S1**, for 24 h at 90°C in the absence of solvent. Monomer acrylate-to-amine molar ratios used for synthesis ranged from 1.2:1 to 1.05:1. For the second step of synthesis, the diacrylate-terminated base polymers (B-S) were dissolved in anhydrous tetrahydrofuran (THF, Sigma) at 100 mg/mL and combined with 0.2 M amine-containing small molecules (E3, E6, or E7) as polymer endcapping groups. The reaction was conducted for 1 h at room temperature while shaking. Polymers were then purified to remove excess monomer via precipitation in diethyl ether. The ether was decanted to collect polymer, the polymer was washed again with ether, the ether was decanted, and then the polymer was allowed to dry under vacuum for 48 h. The neat polymers were then dissolved in dimethyl sulfoxide (DMSO) at 100 mg/mL and stored at -20°C in small aliquots to limit freeze-thaw cycles. The molecular weight and polydispersities of the polymers were determined by gel

permeation chromatography (GPC; Waters, Milford, MA) in BHT-stabilized tetrahydrofuran with 5% DMSO and 1% piperidine. Number-averaged and weight-averaged molecular weights (M_n and M_w, respectively) were measured using polystyrene standards (**Table S1**). Purity of the leading polymer, 1-(3-aminopropyl)-4-methylpiperazine end-modified poly(1,4-butanediol diacrylate-co-4-amino-1-butanol) (447), was confirmed by ^{1}H NMR spectra (**Figure S1**).

3.2.3. Preparation of Cy5-labeled DNA

GFP DNA was labeled with Cy5 using the *Label* IT® Tracker Cy5 Kit following manufacturer instructions. The amount of Cy5 labeling was measured to be approximately one dye molecule per 205 base pairs.

3.2.4. Cell culture

F98 glioma cells were provided from R. Barth (Ohio State University, Columbus, OH) and the 9L gliosarcoma line was obtained from the Brain Tumor Research Center (University of California, San Francisco, CA). Cells were grown in high glucose Dulbecco's modified Eagle's medium (DMEM; Gibco® Life Technologies, Carlsbad, CA) supplemented with 10% fetal bovine serum (FBS; Sigma-Aldrich), 0.8 mM *L*-glutamine, and 1% penicillin-streptomycin (Gibco® Life Technologies, Carlsbad, CA). Cells were cultured at 37°C in a humidified incubator with 5% CO_2.

3.2.5 *In vitro* DNA delivery to rat glioma cells

In vitro DNA delivery to glioma cells utilizing PBAE nanoparticles

One day prior to transfection, 9L and F98 cells were plated in 96-well cell culture plates at a cell density of 10,000 cells/well in 100 μL of complete medium, and allowed to adhere at 37 °C overnight. For nanoparticle preparation, following previously reported protocols,[34, 51] GFP DNA was diluted to 60 μg/mL in 25 mM sodium acetate pH 5 buffer (NaAc). PBAEs were

diluted from their stock solutions in DMSO in 25 mM NaAc and added to DNA solutions at PBAE/DNA mass ratios (w/w) of 30, 60, or 90. Polymers were added to DNA 1:1 (v/v), mixed via pipetting, and incubated at room temperature for 10 min to allow for self-assembly, which has previously been shown to be sufficient time for DNA binding to the polymer.[52] Nanoparticles (20 μL) in NaAc were added directly to the cells that were in 100 μL/well of cell culture medium in 96-well plates (final DNA concentration of 600 ng/well). Nanoparticles were incubated with the cells for 2 h at 37 °C, after which the media was removed and replaced with fresh, complete media. Four replicates were evaluated for each transfection condition. For lyophilized nanoparticle formation and evaluation (**Figure 4**), nanoparticles were initially formed as described above, including allowing 10 min for self-assembly. Subsequently, D-sucrose was added as a cyroprotectant to a final concentration of 30 mg/mL sucrose, the nanoparticles were frozen at -80 °C, and they were lyophilized as we have recently described.[53] Lyophilized nanoparticles were stored at −20 °C until use and were then reconstituted in sterile water and used at the same concentration as freshly prepared nanoparticles.

Evaluation of transfection by flow cytometry and fluorescence microscopy

Transfection efficacy was evaluated by measuring the percentage of cells expressing the exogenously delivered GFP DNA. Fluorescence microscopy images were obtained using a Zeiss Axio observer A1 microscope with a Zeiss Axiocam MRm camera using AxioVision Release 4.8.2 software. Transfection efficacy was evaluated by microscopy after 48 hrs at 5X magnification.

Flow cytometry was completed 48 h following transfection using an Intellicyt high-throughput autosampler attached to an BD Accuri™ C6 flow cytometer (emission filter: 530/30 nm). Hypercyt software was used to assign events to each well and FlowJo 7 software (Treestar)

was used to analyze the flow cytometry results. Plates were prepared for flow cytometry by trypsinization using 30 μL of 0.05% Trypsin-EDTA, followed by addition of 170 μL of a solution of 2% FBS in PBS. Samples were transferred to round bottom 96-well plates, centrifuged, and 170 μL of volume was removed. Cells were then resusupended via pipetting and loaded onto the Hypercyt autosampler.

Measurement of cytotoxicity

Non-specific cell toxicity was defined as the loss of metabolic activity in each well following transfection. Cell toxicity was determined at 24 h post-transfection using a CellTiter 96® AQ_{ueous} One MTS assay following manufacturer's instructions. A BioTek® Synergy™ 2 Microplate Reader was used to read absorbance at 490 nm, and cell toxicity was determined by normalizing the metabolic activity values of treated wells to untreated wells.

3.2.5. Evaluation of HSVtk/GCV-induced cytotoxicity in 9L and F98 glioma cell lines

Cells were transfected as described above using polymer 447 at 30 w/w, using either HSVtk or GFP DNA (n=4). GCV was added to the cell culture medium at 24 h post-transfection at concentrations from 0 to 50 μg/mL and replenished every two days. At five days post-transfection, cells were stained with PI, fixed, and then stained with DAPI. Each well was photographed at 5X magnification to capture PI and DAPI fluorescence as well as a brightfield image using a Zeiss Axio observer A1 microscope with a Zeiss Axiocam MRm camera using AxioVision Release 4.8.2 software. Cells positive for PI and/or DAPI were counted using ImageJ v1.47 software. PI cell counts were subtracted from DAPI cell counts to remove dead cells from the total cell count, and then the total cell count of each well was normalized to that of untreated wells.

3.2.6. Nanoparticle Physical Characterization

The hydrodynamic radius and zeta-potential of the leading nanoparticle formulation, 447 30 w/w, was determined via dynamic light scattering (DLS) using a Malvern Zetasizer NanoZS (Malvern Instruments, Malvern, U.K). Fresh and lyophilized nanoparticles were formed as previously described for transfection, and then diluted into PBS at a 1:6 v/v dilution in order to better approximate the physiological salt concentration and pH that particles would experience in cell culture or in an organism. To measure particle size, the intensity-weighted Z-average of the particle diameter is reported in nm. Zeta potentials were analyzed using the Smoluchowski model and average electrophoretic mobilities were measured at 25 °C at pH 7.4.

Transmission electron microscopy (TEM) was used to image 447 30 w/w nanoparticles using a Philips/FEI BioTwin CM120 transmission electron microscope. Nanoparticles were formed as described for transfection, and 5 μL of the nanoparticle solution was loaded onto a carbon-coated copper TEM grid and allowed to dry completely prior to imaging.

3.2.7. *In vivo* modeling of rat glioma

Animals

Female F344 rats, weighing 125-175 g each (Harlan Bioproducts, Indiana, IN), were housed in standard facilities and were provided with ad libitum access to food and water. The policies and guidelines of the Johns Hopkins University Animal Care and Use Committee were strictly followed throughout the study.

Tumor implantation

F344 rats were intracranially implanted with 9L gliosarcoma, which was maintained and passaged every 2-3 weeks. For surgical intracranial implantation, the tumor was removed from the carrier animal, cut into 2-mm^3 pieces, and placed in sterile 0.9% saline on ice as previously described.[54] Rats were anesthetized with an intraperitoneal injection of 3-5 mL/kg of a stock

solution containing ketamine HCl (75 mg/kg; 100 mg/ml), xylazine (7.5 mg/kg; 100 mg/ml), and ethanol (14.25%) in sterile 0.9% NaCl. For the orthotopic tumor inoculation, the head was shaved and prepared with alcohol and Prepodyne solution (DeLaval, Inc.). In order to expose the sagittal and coronal sutures, a midline scalp incision was made. A small hole was made using an electric drill in the skull centered 3 mm lateral to the sagittal suture and 5 mm posterior to the coronal suture. The superior sagittal sinus was carefully avoided. Under microscopic magnification, a dural opening and then a cortical opening were made. A small area of cortex and white matter was resected. Once hemostasis was achieved, a single tumor piece (2 mm^3) was placed into the resection cavity. The skin was then closed with surgical staples. All surgical procedures were performed using standard sterile surgical technique.

3.2.8. *In vivo* delivery of cancer-killing therapy via nanoparticles

In vivo nanoparticle administration

Under full anesthesia, six days after tumor inoculation, the original incision was opened and the original burr hole was located. For Convection-Enhanced Delivery (CED), a 25-gauge needle was stereotactically placed at a depth of 3 mm into the rat striatum. The infusion was performed using an UltraMicroPump (UMP3) with SYS-Micro4 Controller (World Precision Instruments, Inc., Sarasota, FL, USA) at a rate of 1 μL/min for 25 min. After the injection the needle was maintained in the cortex for another 5 min to avoid backflow. Following needle removal the incision was stapled and the animal was allowed to awaken and recover. Bolus administration delivered the same volume of nanoparticles by manual injection as previously described.[54] Throughout the study three types of DNA were complexed with 447 30 w/w to form nanoparticles and used *in vivo* in lyophilized form: (1) GFP, (2) Cy5-labeled GFP, and (3) HSVtk. The nanoparticles were stored in -20°C and were resuspended in water prior to injection.

The particles were injected both by bolus (manual injection) or infused by CED. The two methods of nanoparticle administration were compared using 12 tumor-bearing rats infused with PBAE/GFPs 6 days after tumor implantation. The animals were euthanized at 24 h post-infusion and the brains were fixed in formalin for imaging. The efficacy study was performed using CED

In vivo safety studies

The safety of intracranial injection of PBAEs was evaluated. PBAE 447/GFP DNA nanoparticles (26 μg DNA/780 μg polymer) were infused in a volume of 25 μL using CED in six wild type healthy rats and three 9L tumor-bearing rats for a total number of 9 rats. All rats were observed daily for any signs of neurotoxicity. Three animals from each group were euthanized 3 days after nanoparticle infusion, while the remaining non-tumor-bearing animals were observed for 60 days after nanoparticle infusion and then euthanized. Subsequently, their brains were harvested and placed in formalin for histopathological analysis. Specifically, the brains were cut in 3 slices of 2 mm: one centered on the site of the injection and the other two centered 2 mm anteriorly and posteriorly from it.

The safety of systemically injected ganciclovir was assessed in 6 rats for 10 days: 3 rats were treated with intraperitoneal administration of 50 mg/kg once a day and the other 3 with 50 mg/kg twice a day for 10 days. Rats were evaluated daily for signs of pain and distress, including ruffled fur, dehydration, hunched position, weakness, lethargy, immobility, lack of coordination, labored respiration, or cyanosis according to the Johns Hopkins Animal Care and Use Guidelines. At the end of the study the brains were fixed, sectioned and processed for light microscopic analysis to determine histopathology and to evaluate tissue damage.

Efficacy studies

For intracranial implantation, 48 F344 rats (24 rats for the first study and 24 for the second) were anesthetized and received tumor as described above. Six days after tumor implantation, when tumor area was approximately 2×3 mm, the rats were randomized into the following groups: Control group, which received an intracranial infusion of 25 μL of saline by CED (n=16); GCV group which received intraperitoneal administration of 50 mg/kg of GCV twice a day (n=8); NP-GFP + GCV group, which received intracranial infusion of PBAE/GFP nanoparticles plus intraperitoneal administration of GCV (n=8); DNA + GCV group, which received intracranial infusion of HSVtk DNA plus intraperitoneal administration of GCV (n= 8); and the NP-HSVtk + GCV group, which received intracranial infusion of PBAE/HSVtk nanoparticles plus intraperitoneal administration of GCV (n= 8).

GCV was administered for 10 days, from Day 4 to Day 13, i.e. starting 4 days after tumor implantation and 2 days before PBAE/HSVtk infusion due to the aggressive nature of the 9L glioma, as described previously.[48] The animals were monitored daily and assessed for neurological impairment. The animals were perfused as they became moribund and brains were placed in formalin for histological analysis.

3.2.9. Histological analysis of therapeutic efficacy of nanoparticle drug delivery

Brain imaging

Immunofluorescence staining of the *in vivo* transfection was assessed. A total of 6 rats were used for imaging *in vivo* transfection 24 hr post-infusion via CED. Animals were infused at 6 days after tumor implantation with Cy5-labeled GFP DNA using the DNA/polymer ratio used for the efficacy study. A comparison of nanoparticle delivery via bolus injection and CED infusion was subsequently conducted. The image analysis was performed with ImageJ as previously described[55] and the whole tumor was considered as the region of interest (ROI). The boundaries

of the tumor area were determined by a neuropathologist via blind analysis of H&E and DAPI stained slides. The corrected total cell fluorescence (CTCF) intensity of the whole tumor area, both after CED infusion and after bolus injection was compared and calculated as follows: integrated density - (area of selected cell × mean fluorescence of background readings), normalized by the number of pixels in the tumor area. To evaluate PBAE distribution between the two administration methods and how this might affect transfection efficacy, 12 9L tumor-bearing rats were divided into two groups: a CED group (n=6) and an intracranial bolus injection group (n=6). Cy5 labeled GFP-nanoparticles were infused via CED infusion or bolus injection on Day 6 and the rats were sacrificed 24 hr later. The animals were anesthetized and perfused with 0.1 M phosphate-buffered saline (PBS), followed by 4% paraformaldehyde in 0.1 M PBS solution. The brain was immediately removed from the skull and transferred to 4% paraformaldehyde at 4°C for 24 hours.

Immunohistochemistry

The brains, fixed in 4% paraformaldehyde at 4°C for at least 24 hr, were cryoprotected by sinking in 30% sucrose in 0.1 M PBS for 3 days and then embedded in Optimal Cutting Temperature compound (OCT) compound. Cryosection slides were prepared at 10 μm using a Leica CM1905 cryostat. The slices were imaged to assess transfection by confocal laser scanning microscope (Leica TCS SP5 Microsystems) and captured with Axiovision software (Axiovision Rel 4.9).

3.2.10. Data analysis and statistical methods

Transfection efficacy of PBAE nanoparticles was compared to Lipofectamine® 2000 using One-way ANOVA and Dunnett posttests (GraphPad Prism 5.0). Comparisons of fresh and lyophilized nanoparticles were conducted using two-tailed t-tests (GraphPad Prism 5.0). The

statistical analysis for survival was completed using Kaplan-Meier survival plots (GraphPad Prism 5.0), and the survival curves were compared using the Log-rank (Mantel-Cox) test. $p<0.05$ was considered statistically significant in all cases.

3.3 Results and Discussion

3.3.1. PBAE-Based Nanoparticles Show High in Vitro Gene Delivery to Glioma Cells

A library of poly(β-amino ester)s (PBAEs) was synthesized following methods that we have previously described.[31] Briefly, base monomers 1,4-butanediol diacrylate (B4) or 1,5-pentanediol diacrylate (B5) were polymerized via a Michael Addition reaction with side chain monomers 3-amino-1-propanol (S3), 4-amino-1-butanol (S4), or 5-amino-1-pentanol (S5) at ratios of either 1.05:1, 1.1:1, or 1.2:1 following **Table 3.1**, yielding acrylate-terminated polymers. These polymers were then endcapped with endcapping monomers pentane-1,3-diamine (E3), 2-((3-aminopropyl)amino)ethan-1-ol (E6), or 1-(3-aminopropyl)-4-methylpiperazine (E7). As an example, the polymer made from base monomer B4, side chain S4, and endcap E7 is 1-(3-aminopropyl)-4-methylpiperazine end-modified poly(1,4-butanediol diacrylate-co-4-amino-1-butanol) and will be referred to as 447 for the duration of the manuscript. **Figure 3.1** shows the monomer structures and the polymerization and endcapping reaction schemes. Gel permeation chromatography (GPC) was used to determine polymer size and polydispersity (**Table 3.1**). The M_n of the polymers varied from 3 kDa – 16 kDa, with the average being 10 kDa. The PDI of the polymers varied from 1.74-8.07 among the polymer types, with average PDI being 3.28. The lead polymer, 447, had a M_n of 11,345 Da, a M_w of 36,814 Da, and a PI of 3.25. It was chosen as the lead polymer based on its high gene delivery efficacy. It is possible that the small proportion of polymer chains in the batch that are of

relatively high molecular weight help in increasing the transfection. Some of our previous work has shown that increased PBAE polymer molecular weight can increase the binding affinity of the polymer with DNA and this can improve gene delivery efficacy.[56] Polymer structure of polymer 447 was characterized via ^{1}H-NMR, and was shown to match previously described structures (**Figure 3.2**).[53, 57]

The *in vitro* DNA delivery efficacy of the PBAE library was assessed in 9L rat gliosarcoma (9L) and F98 rat glioma (F98) cell lines using plasmid DNA coding for green fluorescent protein (GFP). Cytotoxicity was measured using an MTS assay, and transfection was assessed using high-throughput flow cytometry and fluorescence microscopy. Nanoparticles were formed by mixing polymer and DNA at mass ratios of 30, 60, or 90 polymer-to-DNA (w/w) in aqueous conditions and delivering to the cells at a final DNA concentration of 5 ng/μL (**Figure 3.3**). Of the nanoparticle formulations tested on 9L cells, ten nanoparticle formulations enabled greater than 50% transfection with less than 20% toxicity (**Figure 3.3a,c**). In F98 cells eight nanoparticle formulations enabled GFP expression in greater than 50% of cells while maintaining less than 20% toxicity (**Figure 3.3b,d**). Compared to Lipofectamine® 2000, a leading commercially available non-viral transfection reagent, we found that three PBAE nanoparticle formulations had superior performance in 9L cells and fifteen had superior performance in F98 cells. Interestingly, the polymer structures that were found to lead to the highest efficacy in one glioma cell type were not necessarily the optimal structures for the other glioma cell type. For example, 453 30 w/w transfected 68 ± 3% of F98s, but only 9 ± 1% of 9Ls. In contrast, 457 90 w/w shows some signs of potential cytotoxicity in F98, but has higher transfection (64 ± 4%) and no cytotoxicity in 9Ls. This potential cell-type specificity based on polymer structure is something that we have observed with other PBAE structures and other cell

types, such as human endothelial cells.[58, 59] In considering polymer structure that makes up the nanoparticles, the E7 endcapping group 1-(3-aminopropyl)-4-methylpiperazine generally led to improved transfection compared to the E3 or E6 endcapping groups across the base polymers and glioma cell types evaluated. This is consistent with prior work done in other cell types, showing that the E7 endcap is generally one of the most effective in our library.[34, 52, 57] Among the non-E7 polymers, 536 60 w/w and 536 90 w/w nanoparticles had the most robust gene expression (respectively, 59 ± 5% and 65 ± 2 % in 9L cells, and 73 ± 3% and 71 ± 5% in F98 cells).

Critically, certain polymeric nanoparticle formulations, such as 447 30 w/w, transfected both glioma cells lines at similarly high levels and without any cytotoxicity, also in keeping with prior investigation of the differential activity of PBAEs,[52] in which we found that polymers of moderate hydrophobicity led to high transfection rates without overly compromising cell viability. Based on the results of this study, we chose polymer 447 at 30 w/w as the optimal nanoparticle formulation for both 9L and F98 cells (77 ± 3% and 68 ± 1% transfection, respectively). Polymer 447 formed nanoparticles with GFP DNA through self-assembly that were 131 ± 3 nm in size and 15 ± 0.4 mV in zeta potential and with HSVtk DNA that were 138 ± 4 nm in size and 13 ± 1 mV in zeta potential (neither particle size nor zeta potential is statistically different between these two formulations). Even though the plasmid sizes were different, the total nucleic acid mass that was used to form the nanoparticles was the same and this led to nanoparticles with the same biophysical properties. This finding also matches our lab's previous finding that DNA plasmid sequence and length does not affect the nanoparticle size or charge of these PBAE-based nanoparticles within the plasmid DNA size range of 2-26 kilobases.[52] These nanoparticles also compared favorably to transfection with a leading

commercially available non-viral transfection reagent, Lipofectamine® 2000, which led to 52 ± 1% and 37 ± 4% transfection in 9L and F98 cells, respectively (see **Table 3.2** for full statistical analysis on transfection efficacy).

The polymer that makes up these nanoparticles, 447, has also recently shown robust transfection of other cancer types, including human brain cancer cells.[34] Although the physicochemical properties that govern the efficacy and activity of PBAE-based nanoparticles currently under investigation and likely include the chemical structure and molecular weight of the polymer, the polymer-DNA binding strength, and the cellular uptake pathway of the nanoparticles,[52, 56, 60] the exact mechanisms have not yet been fully elucidated. For example, although cellular uptake is certainly an important first step in transfection, previous work in our group has shown that PBAE-DNA nanoparticles often have very high overall uptake by cells without necessarily leading to successful gene expression.[34, 61] Similarly, we have seen that two cell types with very different transgene expression rates can show statistically similar nanoparticle uptake rates.[31] Early work in our group also suggests that the particular cell uptake pathway can affect successful transfection rates with PBAE nanoparticles.[60] Nonetheless, we have consistently observed certain trends across various cell types and culture systems. For instance, the polymers used here were synthesized using monomer ratios that yielded products with relatively high molecular weight, which we and others have shown to have a generally positive correlation with transfection efficacy,[52, 56, 62] and the small molecules used for polymer library synthesis were chosen based on their transfection efficacy in other work.[52, 56, 60]

3.3.2. PBAE/HSVtk Nanoparticles and a Ganciclovir Prodrug Kill Glioma Cells in Vitro

We sought to examine the anti-tumor efficacy of the PBAE/HSVtk nanoparticles *in vitro*. Using the optimal nanoparticle formulation 447 at 30 w/w, we delivered plasmid DNA encoding

either GFP or HSVtk, and treated the cells with GCV at 0, 5, and 50 μg/mL. Viability was assessed quantitatively via cell counting in 9L and F98 cells (**Figure 3.4b,d**). We found that cancer cell death was dependent on the presence of both HSVtk and GCV, as HSVtk-transfected cells were viable when no GCV was present, while GFP-transfected cells were viable in spite of the presence of GCV. Specifically, we observed that the nanoparticle-mediated HSVtk/GCV-induced cytotoxicity was powerful, resulting in 106 ± 3% cell death of 9Ls and 96 ± 7% cell death of F98s at 5 μg/mL GCV when the cells were transfected with HSVtk versus GFP. At 50 μg/mL GCV, 104 ± 5% of 9L cells and 101 ± 2% of F98 cells were dead. These measurements of approximately 100% cell death are consistent with the complete cell death that was observed by microscopy (**Figure 3.4a,c**).

Although the two plasmids used, GFP and HSVtk, are of different size and may result in slightly different transfection rates, the lack of difference in the physicochemical properties of nanoparticles formed with different types of DNA allows the use of the GFP plasmid as a non-functional control for the HSVtk plasmid. As both these types of nanoparticles are formed with the same total mass of polymer and nucleic acid and have the same physicochemical properties, there is not expected to be a difference in polymer- or nanoparticle-induced toxicity between the two plasmids or their particle distribution. While the percent of cells transfected with GFP cannot be assumed to be exactly the same as the percent of cells positive for HSVtk, the strong cytotoxic effect of GCV in HSVtk-transfected cells shows that this transfection, like the GFP transfection, is sufficient for a significant biological effect. These data suggest that nanoparticle-based delivery of the HSVtk gene enables local activation of GCV into a cell-killing drug, which is known to cause cell death in malignant glioma lines via activation of apoptosis.[47, 63] Moreover, the proportion of cells killed (approximately 100%) was greater than the transfection efficiency

of the glioma cells (<80%), illustrating the strong bystander effect of the HSVtk/GCV therapeutic strategy. This is particularly important in the treatment of a tumor, as even if <100% of the cancer cells are transfected *in vivo*, the fraction of cancer cells that positively express HSVtk can lead to the apoptosis of neighboring untransfected tumor cells. This nanoparticle-mediated suicide gene therapy finding is consistent with studies done in other laboratories with an analogous HSVtk/GCV viral gene therapy strategy.[64, 65] Few previous studies have been conducted using non-viral HSVtk gene delivery in cancer models. Two examples in the literature include Neurotensin (NTS)-polyplex nanoparticles[66] used to transfect triple negative breast cancer cells (MDA-MB-231), and poly(ethylene glycol)-poly(gamma-benzyl-L-glutamate) (PEG-PBLG)[67] nanoparticles used to transfect oral squamous cell carcinoma (Tca8113). The transfection efficacy with these non-viral nanoparticle systems was lower than in our present study, with only 18% and 30% transfected, respectively. In those cases, the efficacy of GCV treatment was shown to increase cancer cell death to 50% and 80% through the bystander mechanism. In contrast, our approach with PBAE nanoparticles led to 70% transfection efficacy with 100% cell death. To our knowledge, this is the first demonstration of significant efficacy and anti-cancer effects of PBAE/DNA delivery to treat brain cancer.

3.3.3. PBAE/DNA Nanoparticles Can be Lyophilized with no Change in Properties or Efficacy

Lyophilization of nanoparticles prior to *in vivo* administration has several benefits. Drying the nanoparticles enables subsequent reconstitution at a higher concentration, which was particularly beneficial for intracranial injections, in which volumes were limited due to size and pressure constraints within the brain. Lyophilized PBAE nanoparticles can also be stored for years without losing efficacy[34, 53] and are easier to administer, as the user simply needs to add

water and inject. The amount of solutes added to the particles during formulation is easily adjustable to ensure that the resulting aqueous suspension is isotonic after adding water. To ensure that the 447 30 w/w nanoparticles did not lose efficacy after lyophilization, lyophilized particles were compared to freshly prepared particles. We compared the size and zeta potential of 447 30 w/w nanoparticles and found no significant difference between freshly prepared and lyophilized nanoparticles (**Figure 3.5a**). We also compared *in vitro* transfection of fresh versus lyophilized nanoparticles and found that measurements of transfection efficacy, percent of GFP-positive cells, and geometric mean fluorescence showed no statistical difference ($p > 0.05$) (**Figure 3.5b**). Finally, we imaged fresh and lyophilized nanoparticles via transmission electron microscopy (TEM), and found that nanoparticles from each batch were morphologically similar (**Figure 3.5c,d**).

3.3.4. PBAE Nanoparticles are Safe to Deliver to the Brain

We assessed the safety of delivering PBAE/DNA nanoparticles to the brain *in vivo* in both wild type healthy rats (at day 3 and at day 60 post-nanoparticle infusion) and 9L tumor-bearing rats (at day 3 post-nanoparticle infusion). We used 25 μL as the infusion volume, which was previously shown to be safe.[68] PBAE/GFP 447 30 w/w nanoparticles were injected in 10% (w/v) sucrose and were tested at 26 μg DNA with 780 μg PBAE. This dose was found to be safe and was used for subsequent *in vivo* studies. 50 mg/kg GCV injected twice a day was well tolerated and was therefore chosen for all efficacy studies.

With the exception of animals euthanized at the early time point (day 3 post-nanoparticle infusion) for histopathological analysis, all non-tumor-bearing animals survived until the end of the study (60 days post-nanoparticle infusion). No signs of neurotoxicity or paralysis were observed. The histopathology from day 3 (healthy wild type rats and 9L tumor-bearing rats) and

day 60 (healthy wild type rats) showed no discernable signs of early or late tissue damage and did not include cytological changes, edema, gliosis, neuroinflammation, or necrosis (**Figure 3.6**). These data provide *in vivo* confirmation of one of the strengths of biodegradable PBAEs, a strong safety profile, even when used at high concentration.

3.3.5. Intratumoral Infusion of PBAE/GFP Nanoparticles Leads to Wide Distribution and Transfection in the Brain

The intratumoral distribution and transfection of PBAEs nanoparticles after local brain delivery was assessed. To evaluate the nanoparticle distribution and transfection through the tumor *in vivo*, we used nanoparticles containing Cy5-labeled GFP DNA and examined the distribution of $Cy5^+$ and GFP^+ cells (**Figure 3.7a-d**). On Day 7, 24 h post-nanoparticle infusion, the tumor mass was approximately 2x3 mm, extending from the cortex towards the ipsilateral caudate/putamen area and invading the left lateral ventricle (**Figure 3.7a**). Immunofluorescence staining showed high GFP signal in the corresponding area of the tumor. Specifically, 24 h after CED infusion of Cy5-labeled GFP DNA-containing nanoparticles, the nanoparticles transfected the tumor mass, while the normal brain remained GFP-negative (**Figure 3.7b**). Importantly, the nanoparticles transfected cells fairly homogeneously throughout the entire tumor mass, even distant from the site of infusion (**Figure 3.7d-f**).

Limited tumor penetration and low transfection rates are major obstacles in non-viral gene therapy for the treatment of brain tumors.[37] Transport depends on physio-anatomic barriers[69] and the physicochemical characteristics of the particle, including its size, shape, and surface charge. In this study we show that CED positively affects the biodistribution of the PBAE nanoparticles compared to bolus injection (**Figure 3.8**). This is due to the creation of a positive pressure gradient, which creates bulk fluid movement in the brain interstitium. Tumor-

bearing rats treated with a bolus injection of an equal amount of PBAE/DNA nanoparticles underwent brain analysis via immunofluorescence staining as well. Analysis showed that bolus injection led to transfection in the areas around the needle-path at the bottom of the tumor, with much of the core and margins without nanoparticle-mediated gene transfer. After CED infusion, on the other hand, the nanoparticle-mediated exogenous gene expression led to positive GFP signal across the whole tumor mass, from the core to the top, bottom, and margins. Moreover, the normalized GFP fluorescence per pixel of the tumor area (using Image J software) showed a 36% increase by CED infusion compared to bolus injection (15.8 ± 0.1 RFU vs. 11.6 ± 0.2 RFU, $p<0.0001$) These findings show for the first time that PBAE nanoparticles can penetrate the entirety of the tumor volume and therefore are promising for gene delivery when combined with CED.

3.3.6. PBAE/HSVtk Nanoparticle/GCV Treatment Leads to Prolonged Survival of 9L Gliosarcoma-Bearing Rats

After demonstrating the *in vitro* efficacy of PBAE/HSVtk nanoparticles in F98 and 9L glioma cells and the *in vivo* safety of PBAE nanoparticles for intratumoral transfection, we proceeded to test their *in vivo* therapeutic efficacy in 9L tumor-bearing rats (**Figure 3.9**). 9L gliosarcoma is a highly aggressive syngeneic glioma model [70, 71] and is well known as a challenging survival model due to its fast rate of growth. This model, although rodent-based, has achieved undisputed clinical relevance as it has been used as a preclinical model for multiple clinical trials in the investigation of novel chemo and immunotherapies, drug delivery strategies, and gene therapies.[72-77] Animal survival after treatment with PBAE/HSVtk nanoparticles in combination with GCV was significantly longer compared to the untreated control group ($p = 0.0012$) (**Figure 3.10**). PBAE/HSVtk nanoparticles were also found to provide survival benefits

compared to all the other control groups: GCV only ($p = 0.0102$), PBAE/GFP +GCV ($p = 0.027$), and HSVtk DNA+ GCV ($p = 0.027$).

Considering that 9L is characterized by an exponential-Gompertzian curve of growth after 6 days,[70, 71, 78] such a statistically significant benefit in survival in the group treated with PBAE/HSVtk plus GCV is promising. The efficacy of the HSVtk/GCV paradigm has previously been shown in the 9L model using other strategies[79, 80] and the bystander effect and a resulting immune response can both contribute to the overall cytotoxicity of the PBAE/HSVtk GCV treatment.[81, 82] Due to the positive relationship between the bystander effect and the percent of HSVtk transfected cells,[50] the improvement in survival observed here is highly indicative of strong PBAE transfection efficacy *in vivo* matching what was also observed *in vitro*. PBAE-based gene delivery has a potential role as alternative strategy to virus mediated gene therapy for glioblastoma.

HSVtk/GCV therapy has previously been used in brain tumor treatment clinical trials with retroviral[83-85] and adenoviral[86] vectors with limited success in progression-free and overall survival. This has been attributed to poor distribution of the carrier and limited delivery of HSVtk into the tumor. The HSVtk/GCV system has also been used to investigate the efficacy of non-viral vectors in Phase I-II studies conducted with cationic liposomal vectors, which showed, via positron emission tomography with a ^{124}I-labeled specific substrate for HSV-1, presence of thymidine kinase in one out of five patients.[87] A subsequent study using liposomes had encouraging results by showing reduction of the tumor volume mass in two out of eight patients.[88] Yet, non-viral gene therapy is generally considered less efficient than viral gene therapy.[89] While siRNA delivery nanomedicine approaches have been progressing rapidly, including approaches such as spherical nucleic acids for the treatment of glioblastoma,[90] DNA

delivery has been more challenging. This is likely due to in large part to the much larger size of DNA as a nanomedicine drug cargo and the need for it to be delivered into nucleus rather than just into the cytoplasm.[87] Due to the wide tumor penetration, high exogenous gene expression, and bystander effect capabilities, the PBAE/HSVtk nanoparticles may be able to overcome the previously encountered limitations and be a promising new nanomedicine for brain cancer.

3.4. Conclusion

In this work, we have developed a new gene transfer nanomedicine that causes the expression of suicide gene herpes simplex virus type I thymidine kinase (HSVtk) within brain tumor cells *in vitro* and *in vivo*. Biodegradable nanoparticles were synthesized, characterized, and utilized to treat malignant glioma using convection-enhanced delivery (CED). The lead polymer structure, poly(beta-amino ester) 1-(3-aminopropyl)-4-methylpiperazine end-modified poly(1,4-butanediol diacrylate-co-4-amino-1-butanol), formed DNA nanoparticles with suitable biophysical properties for intracellular delivery and a wide biodistribution when injected intracranially. CED led to improved levels of tumor transfection. These PBAE/HSVtk nanoparticles combined with systemic administration of ganciclovir as a prodrug led to a significant increase in survival in a 9L glioma model ($p=0.0012$ vs. control). Our results provide the first demonstration of a successful non-viral nanomedicine method for HSVtk/GCV treatment of brain cancer.

Acknowledgements

This work was supported in part by the NIH (1R01EB016721). KLK also thanks the NIH Cancer Nanotechnology Training Center (R25CA153952) at the JHU Institute for

Nanobiotechnology for fellowship support and SYT thanks the NSF for fellowship support. Laboratory support from Joshua and Genine Fidler is also gratefully acknowledged. The authors would also like to thank Dr. Tara L. Deans for her assistance with the molecular biology components of this work.

3.5. Tables

Table 3.1. Gel permeation chromatography (GPC) results of all polymers indicating the number average (MN) and weight average (MW) molecular weight and polydispersity (PDI) of each polymer. (Reproduced from Mangraviti *et al*. 2015)

Polymer	B:S ratio	M_N	M_W	PDI
446	1.1:1	3342	6398	1.91
447	1.1:1	11345	36814	3.25
453	1.2:1	13719	110715	8.07
456	1.2:1	4208	7411	1.76
457	1.1:1	16005	62522	3.91
536	1.1:1	4876	8468	1.74
537	1.05:1	14899	35287	2.37

Table 3.2. Results of one-way ANOVA with Dunnett's post-test in 9L and F98 cells versus Lipofectamine® 2000 delivering either 0.6 or 0.3 µg GFP DNA per well. (ns = not significant, * = $p < 0.05$, ** = $p < 0.01$, *** = $p < 0.001$) (Reproduced from Mangraviti *et al*. 2015)

	9L Gliosarcoma		F98 Glioma	
	Lipo 0.6 µg	Lipo 0.3 µg	Lipo 0.6 µg	Lipo 0.3 µg
446 30 w/w	***	***	***	***
446 60 w/w	***	***	**	ns
446 90 w/w	***	***	ns	ns
447 30 w/w	***	***	***	***
447 60 w/w	ns	ns	***	***
447 90 w/w	**	ns	***	***
453 30 w/w	***	***	***	***
453 60 w/w	*	***	***	***
453 90 w/w	ns	***	ns	*
456 30 w/w	***	***	ns	ns
456 60 w/w	ns	*	***	***
456 90 w/w	ns	ns	***	***
457 30 w/w	***	***	***	***
457 60 w/w	ns	ns	***	***
457 90 w/w	ns	ns	***	***
536 30 w/w	***	***	ns	ns
536 60 w/w	ns	ns	***	***
536 90 w/w	*	ns	***	***
537 30 w/w	***	***	***	***
537 60 w/w	ns	ns	***	***
537 90 w/w	ns	ns	*	**

3.6. Figures

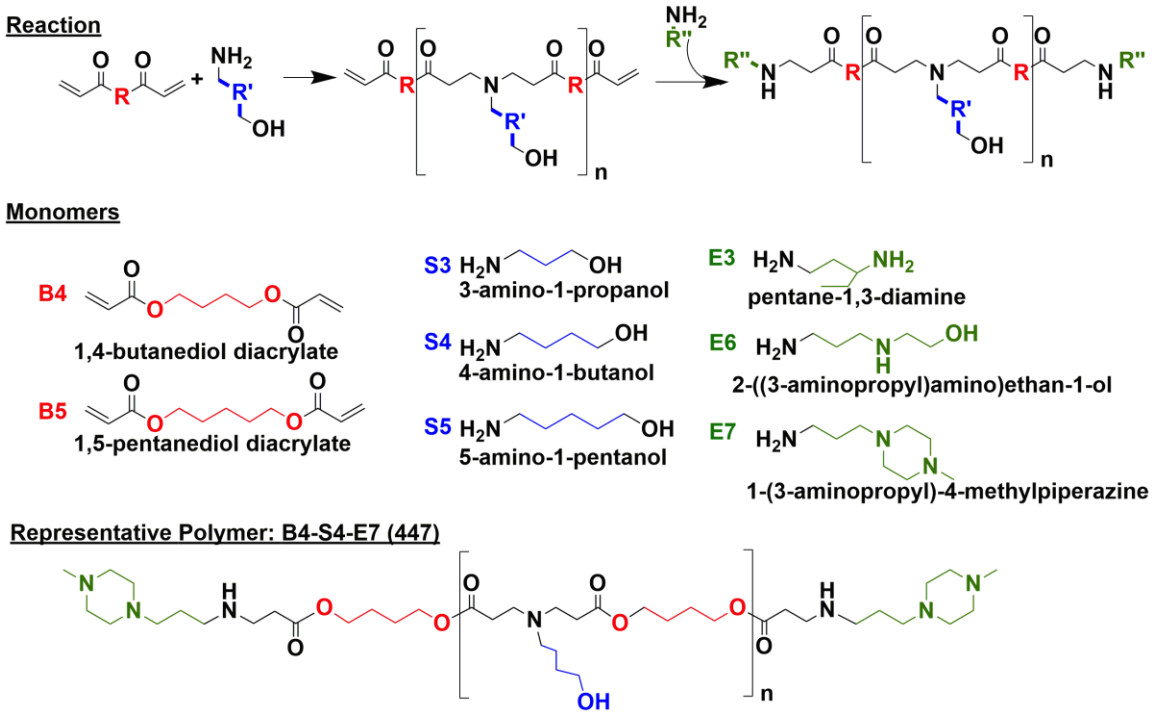

Figure 3.1. Polymer synthesis scheme and monomer chemical structures. Base monomers (B) and side chain monomers (S) are polymerized, and polymers are then endcapped with endcapping monomers (E). (Reproduced from Mangraviti *et al*. 2015)

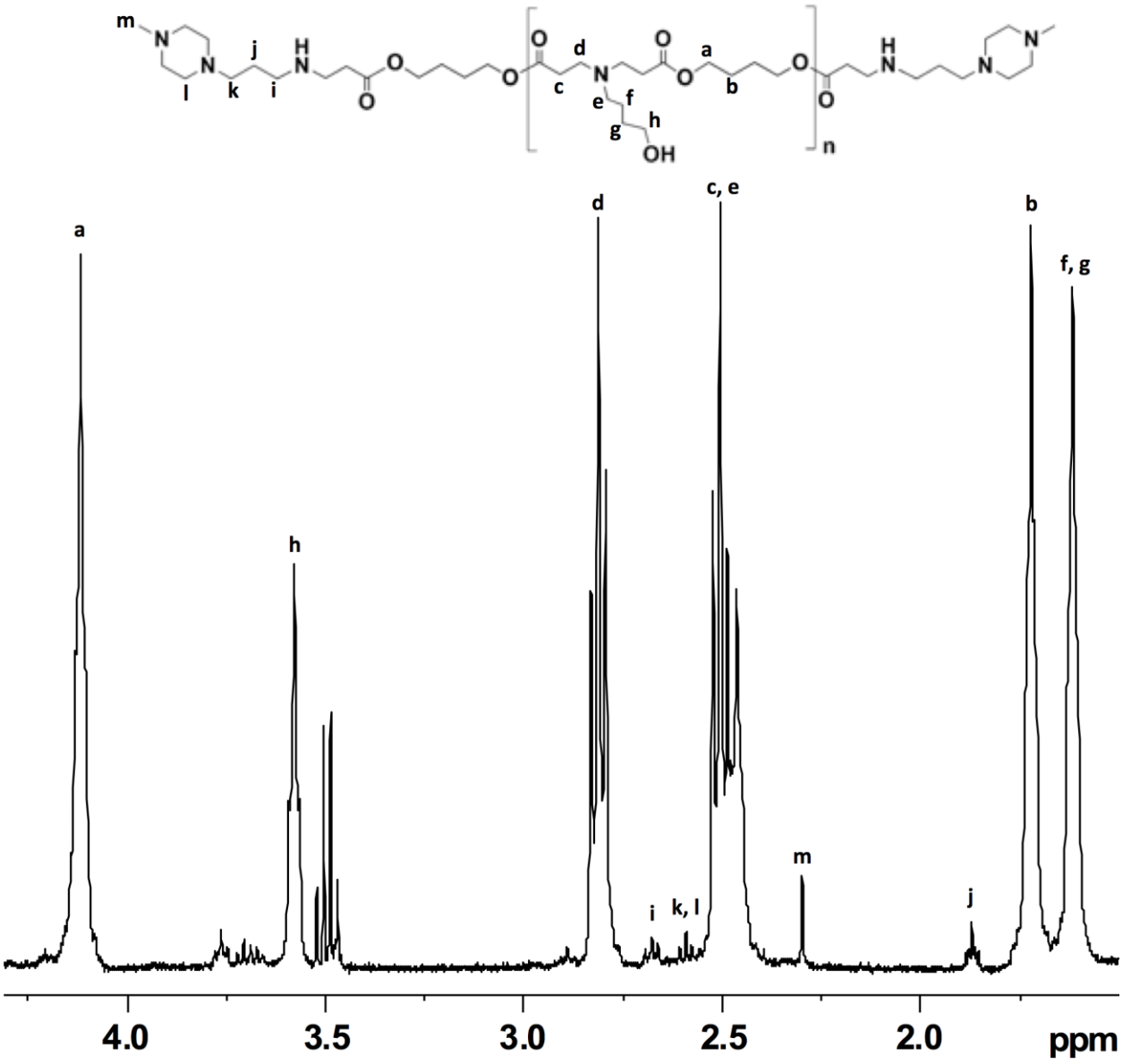

Figure 3.2. H^1-NMR spectrum of polymer 447 (CDCl3, 400 Hz). Protons peaks are labeled with letters corresponding to protons along the structure of 447. (Reproduced from Mangraviti *et al*. 2015)

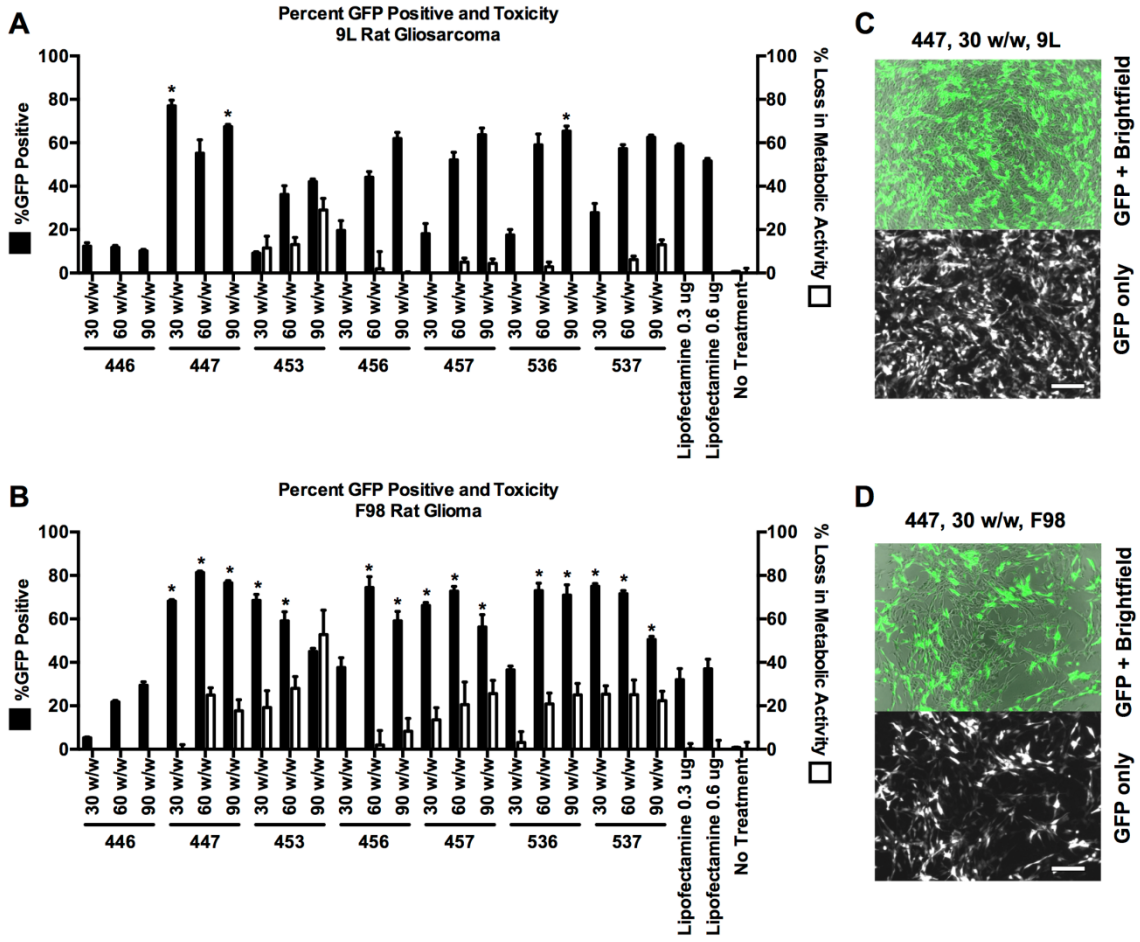

Figure 3.3. PBAE nanoparticles effectively transfect 9L and F98 malignant glioma cells *in vitro*. All polymers were screened at 30, 60, and 90 w/w delivering 0.6 μg of GFP DNA (**A, B**). Of the nanoparticles tested on 9L and F98 cells, three and fifteen formulations, respectively, were found to deliver GFP DNA more effectively than commercially available transfection reagent Lipofectamine® 2000 (* = $p < 0.05$ versus Lipofectamine with 0.6 μg DNA via one-way ANOVA with Dunnett's post-test). Fluorescence microscopy shows cells transfected with GFP using PBAE nanoparticles (**C, D**). Transfection efficacy was quantified using flow cytometry. Loss in metabolic activity was quantified using an MTS assay with colorimetric readout, measured by a multiplate reader. (Reproduced from Mangraviti *et al*. 2015)

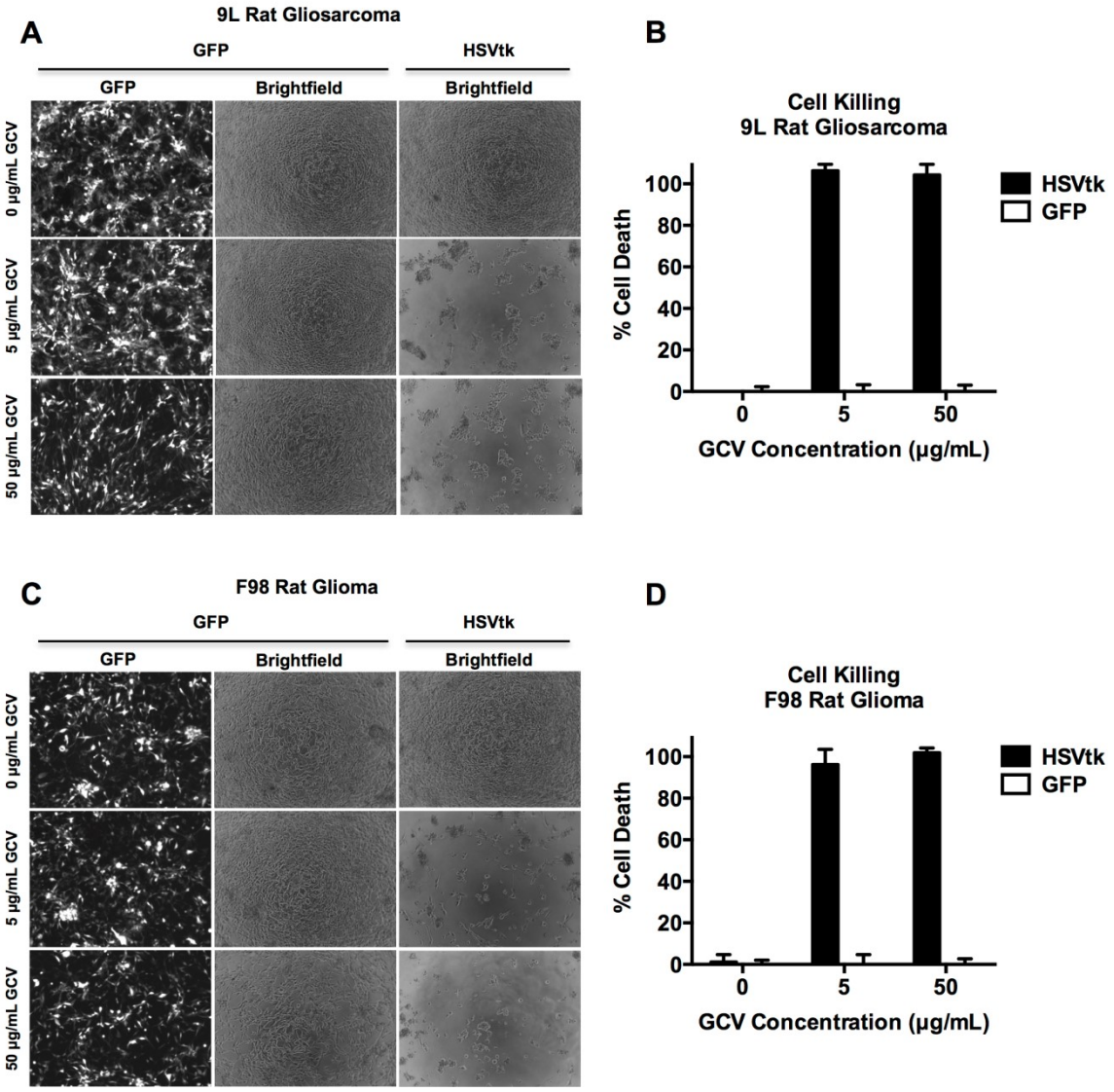

Figure 3.4. PBAE delivery of HSVtk plasmid enables GCV-mediated killing of malignant glioma cells *in vitro*. 9L and F98 cells were transfected with plasmids encoding either GFP or HSVtk and then treated with 0, 5, or 50 µg/mL GCV prodrug. Cells treated with both HSVtk and GCV exhibit 100% cancer cell killing, measured by cell counting, versus GFP-transfected cells treated with GCV, showing that GCV-induced cell killing is dependent on the presence of HSVtk. Additionally, HSVtk without GCV does not kill cells. (Reproduced from Mangraviti *et al*. 2015)

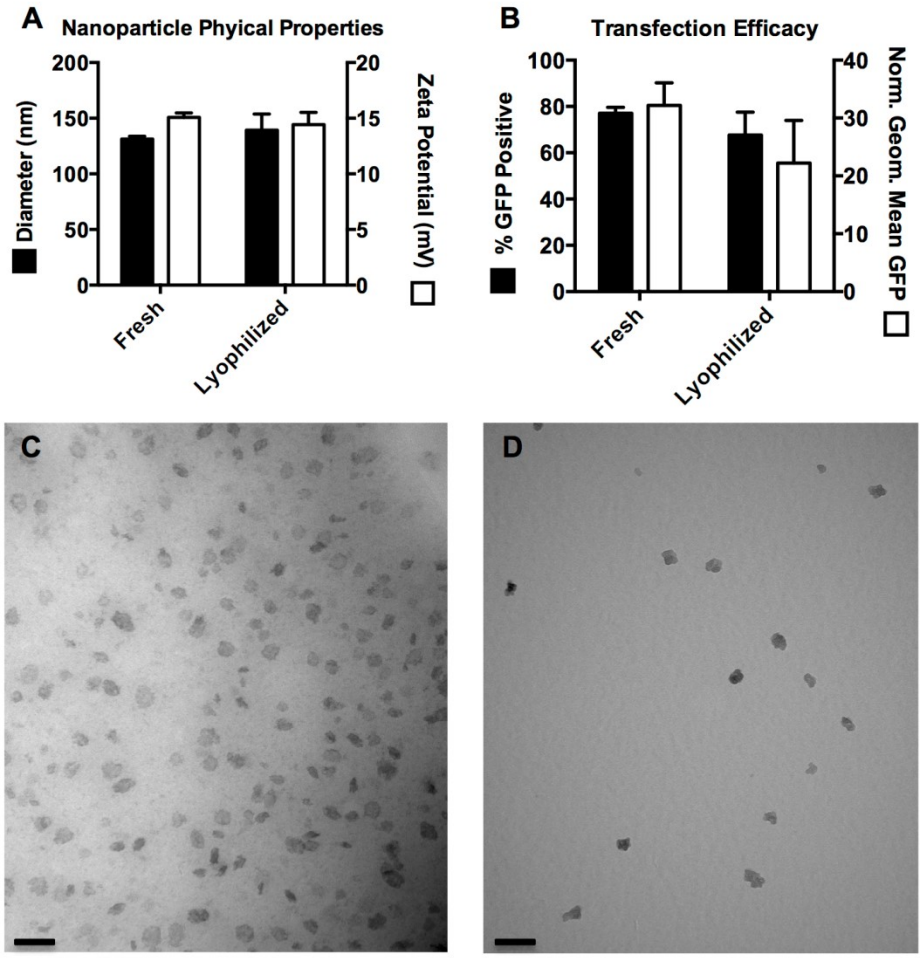

Figure 3.5. Nanoparticles maintain their physical characteristics and transfection capability following lyophilization. Fresh and lyophilized nanoparticles showed no statistical difference ($p > 0.05$) in their sizes and zeta-potentials (**A**) and showed no statistical difference in percent transfection and geometric mean GFP in 9L cells (**B**). TEM imaging of fresh (**C**) and lyophilized (**D**) nanoparticles shows nanoparticles of the same size and morphology (scale bar = 100 nm). (Reproduced from Mangraviti *et al*. 2015)

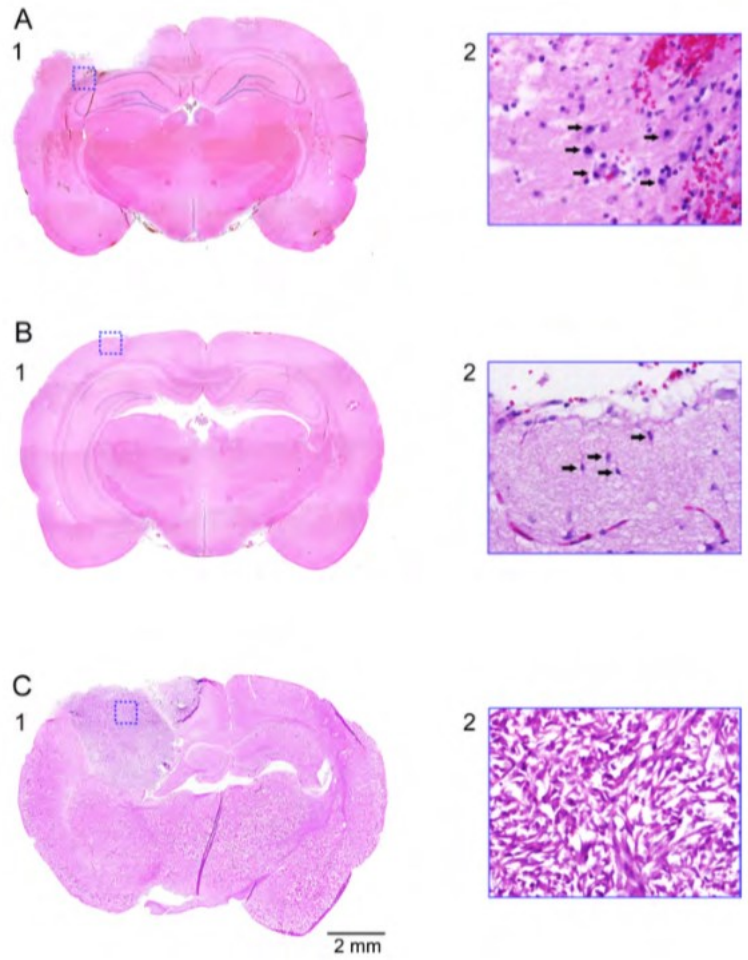

Figure 3.6. Safety of local brain delivery of PBAE nanoparticles. Representative coronal sections of rat brains from wild type and 9L tumor-bearing animals infused with PBAE/GFP nanoparticles. The H&E images taken within 1 mm around the site of the infusion show no sign of neuropathological damage. (A1) Wild type animal euthanized 3 days post-nanoparticle infusion. The image shows indentation into the cortex with inflammation, consistent with acute injury at the injection site. No sign of neurotoxicity. Under microscopic view: presence of neutrophils with a few macrophages within the injection site (black arrows) (A2). (B) Wild type animal euthanized 60 days post-nanoparticle infusion. The figure shows a very small indentation with tissue shrinkage. Under microscopic view: astrocytes are present (black arrows), and the tissue shows no sign of inflammation (B2). (C) 9L tumor-bearing animal euthanized 3 days post-PBAE/GFP nanoparticle infusion. The image shows a tumor mass causing contralateral brain midline shift and robust mass effect on the surrounding structures. There is a distinguishable sign of needle entrance within the tumor mass. Under microscopic view: characteristic cellular density of tumor tissue and no inflammation or tissue damage referable to any cause of damage other than tumor (C2). (A2,B2,C2, X 600 magnification) (Reproduced from Mangraviti *et al*. 2015)

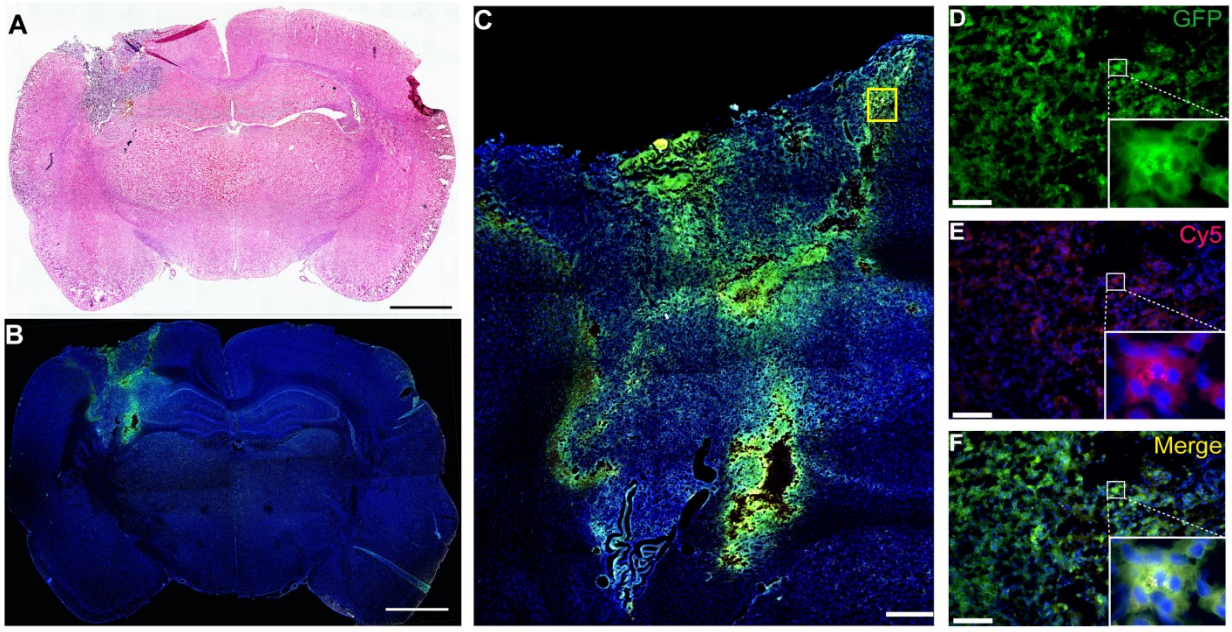

Figure 3.7. Local brain delivery of PBAE/GFP Nanoparticle via CED leads to effective tumor transfection in vivo. Coronal section of a 9L tumor bearing rat brain at 7 days post PBAE/GFP infusion showing the tumor region (A, scale bar=2 mm). Fluorescence microscopy images show GFP+ transfected cells in the tumor area (B, scale bar=2 mm). Enlarged area shows a wide distribution of GFP+cells within the entire tumor area including the periphery (C, scale bar=500 μm). The co-localization of GFP and Cy5 shows that the nanoparticles penetrate into the cells and successfully transfect them (D-F, scale bar: 50 μm). Red: Cy5, green: GFP, blue: DAPI (Reproduced from Mangraviti *et al*. 2015)

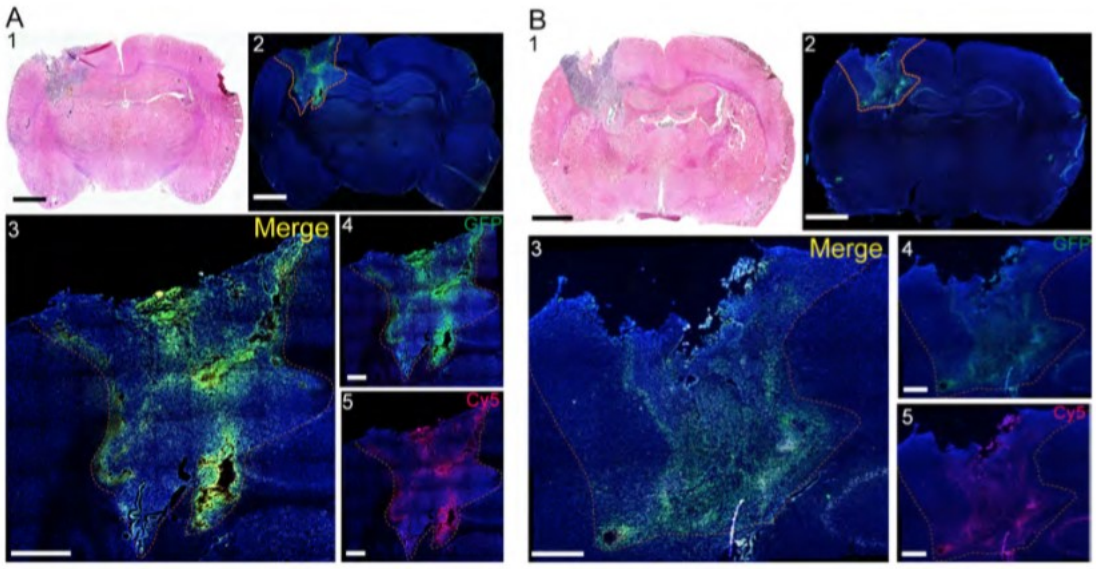

Figure 3.8. Convection-enhanced delivery of PBAE/GFP nanoparticles improves the level of intratumoral transfection. Coronal section of 9L-bearing rats infused via CED (A) and injected with bolus administration (B). Fluorescence microscopy of both brains show higher intratumoral transfection efficacy after CED infusion (A2, B2, scale bar=2mm). The images focused on the tumor area show a distribution of Cy5 and GFP signal that is favorable in CED compared to bolus (A3-5, B3-5 scale bar=1 mm). Red: Cy5, green: GFP, blue: DAPI. (Reproduced from Mangraviti *et al*. 2015)

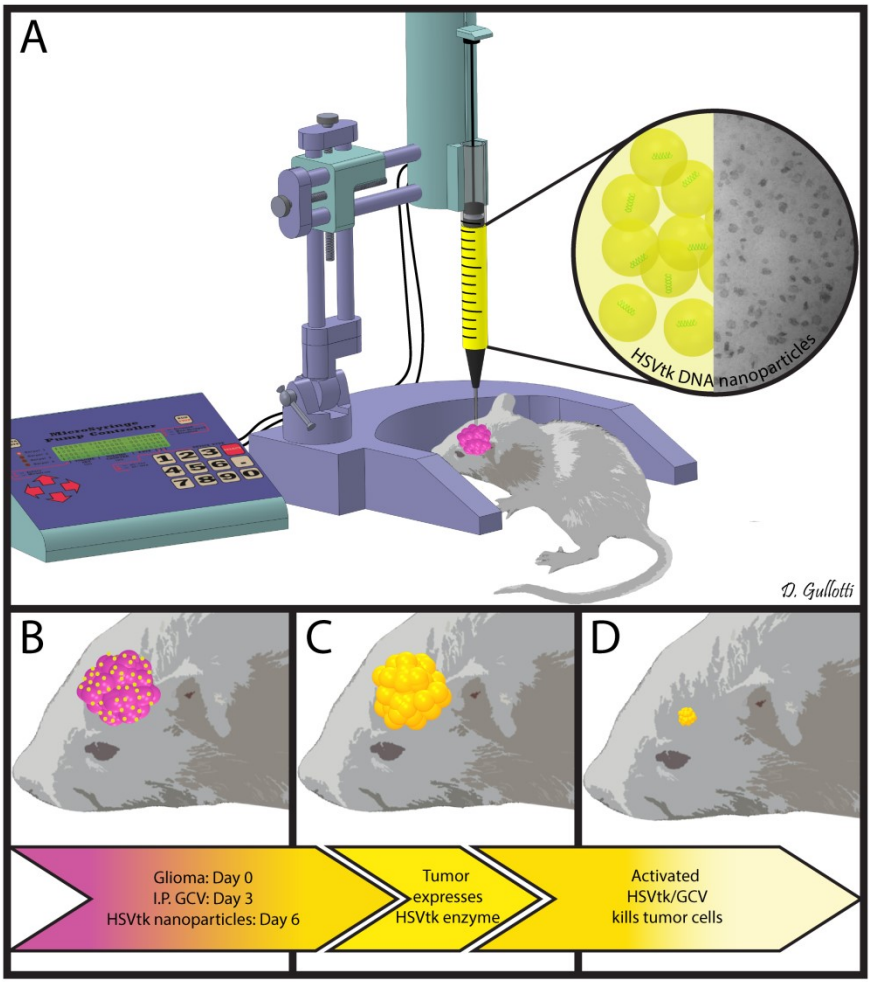

Figure 3.9. Schematic representation of the *in vivo* study. The 9L bearing rats were treated with intraperitoneal administration of ganciclovir twice a day beginning on day 4 and then treated with a single CED infusion of PBAE/HSV-tk nanoparticles on day 6 (**A)**. These treated animals showed a significant benefit in survival (p=.0012 vs. control) (**B-D).** (Reproduced from Mangraviti *et al*. 2015)

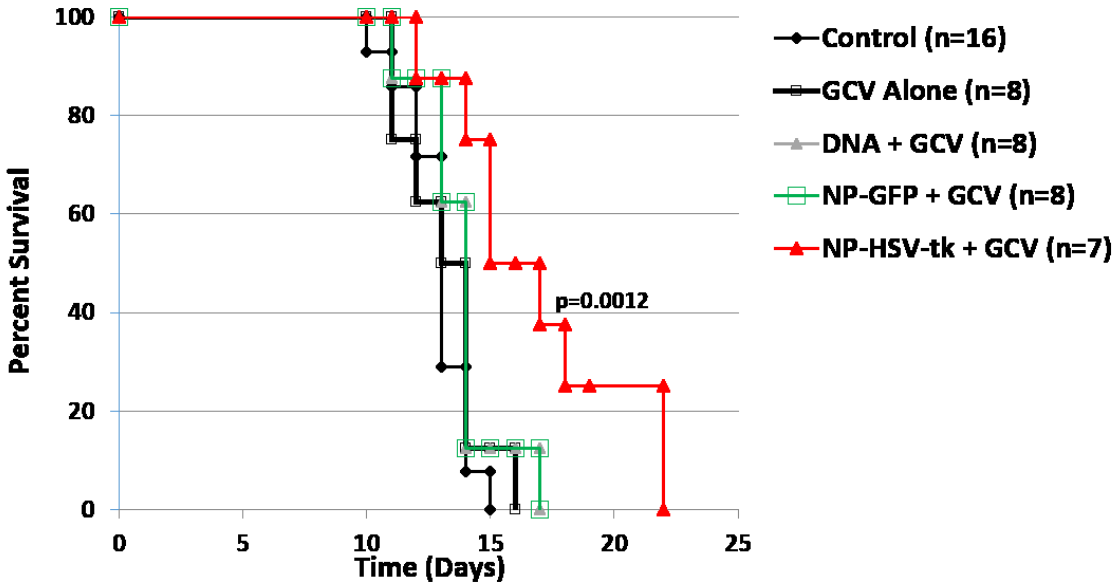

Figure 3.10. PBAE/HSVtk nanoparticles and ganciclovir (GCV) extend survival in a 9L glioasarcoma model. Kaplan-Meier plots of F344 rats that were implanted with 9L and either given no treatment (9L Control, n=16); 50mg/kg/ twice a day of systemic administration of GCV on days 4-10 (GCV Alone, n=8); intracranial infusion of PBAE/GFP nanoparticles plus systemic administration of GCV (NP-GFP + GCV, n=8); intracranial infusion of HSVtk DNA plus systemic administration of GCV (DNA + GCV n=8); or intracranial infusion of PBAE/HSVtk nanoparticles plus systemic administration of GCV (NP-HSVtk + GCV, n=8). The median survival of the group receiving PBAE/HSVtk nanoparticles in combination with GCV is significantly longer compared to that of the untreated control group ($p = 0.0012$). (Reproduced from Mangraviti *et al*. 2015)

3.7. References

1. Chaichana, K. L.; Zadnik, P.; Weingart, J. D.; Olivi, A.; Gallia, G. L.; Blakeley, J.; Lim, M.; Brem, H.; Quinones-Hinojosa, A. Multiple Resections for Patients with Glioblastoma: Prolonging Survival. *J Neurosurg* **2013,** 118, 812-820.
2. McGirt, M. J.; Chaichana, K. L.; Gathinji, M.; Attenello, F. J.; Than, K.; Olivi, A.; Weingart, J. D.; Brem, H.; Quinones-Hinojosa, A. R. Independent Association of Extent of Resection with Survival in Patients with Malignant Brain Astrocytoma. *Journal of Neurosurgery* **2009,** 110, 156-162.
3. Stupp, R.; Mason, W. P.; van den Bent, M. J.; Weller, M.; Fisher, B.; Taphoorn, M. J. B.; Belanger, K.; Brandes, A. A.; Marosi, C.; Bogdahn, U.; Curschmann, J.; Janzer, R. C.; Ludwin, S. K.; Gorlia, T.; Allgeier, A.; Lacombe, D.; Cairncross, J. G.; Eisenhauer, E.; Mirimanoff, R. O. Radiotherapy Plus Concomitant and Adjuvant Temozolomide for Glioblastoma. *New England Journal of Medicine* **2005,** 352, 987-996.
4. Mao, H.; LeBrun, D. G.; Yang, J.; Zhu, V. F.; Li, M. Deregulated Signaling Pathways in Glioblastoma Multiforme: Molecular Mechanisms and Therapeutic Targets. *Cancer investigation* **2012,** 30, 48-56.
5. Ohgaki, H.; Kleihues, P. Genetic Pathways to Primary and Secondary Glioblastoma. *The American journal of pathology* **2007,** 170, 1445-1453.
6. Kwiatkowska, A.; Nandhu, M. S.; Behera, P.; Chiocca, E. A.; Viapiano, M. S. Strategies in Gene Therapy for Glioblastoma. *Cancers* **2013,** 5, 1271-1305.
7. Zarogoulidis, P.; Darwiche, K.; Sakkas, A.; Yarmus, L.; Huang, H.; Li, Q.; Freitag, L.; Zarogoulidis, K.; Malecki, M. Suicide Gene Therapy for Cancer - Current Strategies. *J Genet Syndr Gene Ther* **2013,** 9, 16849.
8. Okada, H.; Villa, L.; Attanucci, J.; Erff, M.; Fellows, W. K.; Lotze, M. T.; Pollack, I. F.; Chambers, W. H. Cytokine Gene Therapy of Gliomas: Effective Induction of Therapeutic Immunity to Intracranial Tumors by Peripheral Immunization with Interleukin-4 Transduced Glioma Cells. *Gene Ther.* **2001,** 8, 1157-1166.
9. Okada, H.; Pollack, I. F. Cytokine Gene Therapy for Malignant Glioma. *Expert Opin Biol Ther* **2004,** 4, 1609-1620.
10. Lang, F. F.; Bruner, J. M.; Fuller, G. N.; Aldape, K.; Prados, M. D.; Chang, S.; Berger, M. S.; McDermott, M. W.; Kunwar, S. M.; Junck, L. R.; Chandler, W.; Zwiebel, J. A.; Kaplan, R. S.; Yung, W. K. A. Phase I Trial of Adenovirus-Mediated P53 Gene Therapy for Recurrent Glioma: Biological and Clinical Results. *Journal of Clinical Oncology* **2003,** 21, 2508-2518.
11. Wang, T. J.; Huang, M. S.; Hong, C. Y.; Tse, V.; Silverberg, G. D.; Hsiao, M. Comparisons of Tumor Suppressor P53, P21, and P16 Gene Therapy Effects on Glioblastoma Tumorigenicity in Situ. *Biochem. Biophys. Res. Commun.* **2001,** 287, 173-180.
12. Ning, J.; Wakimoto, H. Oncolytic Herpes Simplex Virus-Based Strategies: Toward a Breakthrough in Glioblastoma Therapy. *Front Microbiol* **2014,** 5.
13. Markert, J. M.; Medlock, M. D.; Rabkin, S. D.; Gillespie, G. Y.; Todo, T.; Hunter, W. D.; Palmer, C. A.; Feigenbaum, F.; Tornatore, C.; Tufaro, F.; Martuza, R. L. Conditionally Replicating Herpes Simplex Virus Mutant, G207 for the Treatment of Malignant Glioma: Results of a Phase I Trial. *Gene Ther.* **2000,** 7, 867-874.
14. Thomas, C. E.; Ehrhardt, A.; Kay, M. A. Progress and Problems with the Use of Viral Vectors for Gene Therapy. *Nat. Rev. Genet.* **2003,** 4, 346-358.

15. Pack, D. W.; Hoffman, A. S.; Pun, S.; Stayton, P. S. Design and Development of Polymers for Gene Delivery. *Nat. Rev. Drug Discov.* **2005,** 4, 581-593.
16. Akinc, A.; Zumbuehl, A.; Goldberg, M.; Leshchiner, E. S.; Busini, V.; Hossain, N.; Bacallado, S. A.; Nguyen, D. N.; Fuller, J.; Alvarez, R.; Borodovsky, A.; Borland, T.; Constien, R.; de Fougerolles, A.; Dorkin, J. R.; Jayaprakash, K. N.; Jayaraman, M.; John, M.; Koteliansky, V.; Manoharan, M.; Nechev, L.; Qin, J.; Racie, T.; Raitcheva, D.; Rajeev, K. G.; Sah, D. W. Y.; Soutschek, J.; Toudjarska, I.; Vornlocher, H. P.; Zimmermann, T. S.; Langer, R.; Anderson, D. G. A Combinatorial Library of Lipid-Like Materials for Delivery of Rnai Therapeutics. *Nat. Biotechnol.* **2008,** 26, 561-569.
17. Semple, S. C.; Akinc, A.; Chen, J.; Sandhu, A. P.; Mui, B. L.; Cho, C. K.; Sah, D. W.; Stebbing, D.; Crosley, E. J.; Yaworski, E.; Hafez, I. M.; Dorkin, J. R.; Qin, J.; Lam, K.; Rajeev, K. G.; Wong, K. F.; Jeffs, L. B.; Nechev, L.; Eisenhardt, M. L.; Jayaraman, M.; Kazem, M.; Maier, M. A.; Srinivasulu, M.; Weinstein, M. J.; Chen, Q.; Alvarez, R.; Barros, S. A.; De, S.; Klimuk, S. K.; Borland, T.; Kosovrasti, V.; Cantley, W. L.; Tam, Y. K.; Manoharan, M.; Ciufolini, M. A.; Tracy, M. A.; de Fougerolles, A.; MacLachlan, I.; Cullis, P. R.; Madden, T. D.; Hope, M. J. Rational Design of Cationic Lipids for Sirna Delivery. *Nat. Biotechnol.* **2010,** 28, 172-176.
18. Breunig, M.; Hozsa, C.; Lungwitz, U.; Watanabe, K.; Umeda, I.; Kato, H.; Goepferich, A. Mechanistic Investigation of Poly (Ethylene Imine)-Based Sirna Delivery: Disulfide Bonds Boost Intracellular Release of the Cargo. *J. Control. Release* **2008,** 130, 57-63.
19. Matsumoto, S.; Christie, R. J.; Nishiyama, N.; Miyata, K.; Ishii, A.; Oba, M.; Koyama, H.; Yamasaki, Y.; Kataoka, K. Environment-Responsive Block Copolymer Micelles with a Disulfide Cross-Linked Core for Enhanced Sirna Delivery. *Biomacromolecules* **2009,** 10, 119-127.
20. van der Aa, L. J.; Vader, P.; Storm, G.; Schiffelers, R. M.; Engbersen, J. F. J. Optimization of Poly(Amido Amine)S as Vectors for Sirna Delivery. *J. Control. Release* **2011,** 150, 177-186.
21. Derfus, A. M.; Chen, A. A.; Min, D. H.; Ruoslahti, E.; Bhatia, S. N. Targeted Quantum Dot Conjugates for Sirna Delivery. *Bioconjugate Chem.* **2007,** 18, 1391-1396.
22. Elbakry, A.; Zaky, A.; Liebl, R.; Rachel, R.; Goepferich, A.; Breunig, M. Layer-by-Layer Assembled Gold Nanoparticles for Sirna Delivery. *Nano Lett.* **2009,** 9, 2059-2064.
23. Kakizawa, Y.; Furukawa, S.; Ishii, A.; Kataoka, K. Organic-Inorganic Hybrid-Nanocarrier of Sirna Constructing through the Self-Assembly of Calcium Phosphate and Peg-Based Block Aniomer. *J. Control. Release* **2006,** 111, 368-370.
24. Forbes, D. C.; Peppas, N. A. Oral Delivery of Small Rna and DNA. *J. Control. Release* **2012,** 162, 438-435.
25. Curiel, D. T.; Agarwal, S.; Wagner, E.; Cotten, M. Adenovirus Enhancement of Transferrin Polylysine-Mediated Gene Delivery. *Proc. Natl. Acad. Sci.* **1991,** 88, 8850-8854.
26. Midoux, P.; Monsigny, M. Efficient Gene Transfer by Histidylated Polylysine/Pdna Complexes. *Bioconjugate Chem.* **1999,** 10, 406-411.
27. Gary, D. J.; Puri, N.; Won, Y. Y. Polymer-Based Sirna Delivery: Perspectives on the Fundamental and Phenomenological Distinctions from Polymer-Based DNA Delivery. *J. Control. Release* **2007,** 121, 64-73.
28. Luo, D.; Saltzman, W. M. Synthetic DNA Delivery Systems. *Nat. Biotechnol.* **2000,** 18, 33-37.

29. Boussif, O.; Lezoualc'h, F.; Zanta, M. A.; Mergny, M. D.; Scherman, D.; Demeneix, B.; Behr, J.-P. A Versatile Vector for Gene and Oligonucleotide Transfer into Cells in Culture and in Vivo: Polyethylenimine. *Proc. Natl. Acad. Sci.* **1995,** 92, 7297-7301.
30. Lynn, D. M.; Langer, R. Degradable Poly(B-Amino Esters): Synthesis, Characterization, and Self-Assembly with Plasmid DNA. *J. Am. Chem. Soc.* **2000,** 122, 10761-10768.
31. Green, J. J.; Langer, R.; Anderson, D. G. A Combinatorial Polymer Library Approach Yields Insight into Nonviral Gene Delivery. *Accounts of chemical research* **2008,** 41, 749-759.
32. Sunshine, J.; Green, J. J.; Mahon, K. P.; Yang, F.; Eltoukhy, A. A.; Nguyen, D. N.; Langer, R.; Anderson, D. G. Small-Molecule End-Groups of Linear Polymer Determine Cell-Type Gene-Delivery Efficacy. *Adv. Mater.* **2009,** 21, 4947-4951.
33. Sunshine, J. C.; Sunshine, S. B.; Bhutto, I.; Handa, J. T.; Green, J. J. Poly(B-Amino Ester)-Nanoparticle Mediated Transfection of Retinal Pigment Epithelial Cells in Vitro and in Vivo. *PLoS ONE* **2012,** 7, e37543.
34. Guerrero-Cázares, H.; Tzeng, S. Y.; Young, N. P.; Abutaleb, A. O.; Quiñones-Hinojosa, A.; Green, J. J. Biodegradable Polymeric Nanoparticles Show High Efficacy and Specificity at DNA Delivery to Human Glioblastoma in Vitro and in Vivo. *ACS Nano* **2014,** 8, 5141-5153.
35. Sunshine, J. C.; Peng, D. Y.; Green, J. J. Uptake and Transfection with Polymeric Nanoparticles Are Dependent on Polymer End-Group Structure, but Largely Independent of Nanoparticle Physical and Chemical Properties. *Mol. Pharm.* **2012,** 9, 3375 - 3383.
36. Kozielski, K. L.; Tzeng, S. Y.; Mendoza, B. A. H. d.; Green, J. J. Bioreducible Cationic Polymer-Based Nanoparticles for Efficient and Environmentally Triggered Cytoplasmic Sirna Delivery to Primary Human Brain Cancer Cells. *ACS Nano* **2014,** 8, 3232-3241.
37. Zhou, J.; Patel, T. R.; Sirianni, R. W.; Strohbehn, G.; Zheng, M. Q.; Duong, N.; Schafbauer, T.; Huttner, A. J.; Huang, Y.; Carson, R. E.; Zhang, Y.; Sullivan, D. J., Jr.; Piepmeier, J. M.; Saltzman, W. M. Highly Penetrative, Drug-Loaded Nanocarriers Improve Treatment of Glioblastoma. *Proc Natl Acad Sci U S A* **2013,** 110, 11751-11756.
38. Saito, R.; Bringas, J. R.; McKnight, T. R.; Wendland, M. F.; Mamot, C.; Drummond, D. C.; Kirpotin, D. B.; Park, J. W.; Berger, M. S.; Bankiewicz, K. S. Distribution of Liposomes into Brain and Rat Brain Tumor Models by Convection-Enhanced Delivery Monitored with Magnetic Resonance Imaging. *Cancer Res.* **2004,** 64, 2572-2579.
39. Stephen, Z. R.; Kievit, F. M.; Veiseh, O.; Chiarelli, P. A.; Fang, C.; Wang, K.; Hatzinger, S. J.; Ellenbogen, R. G.; Silber, J. R.; Zhang, M. Redox-Responsive Magnetic Nanoparticle for Targeted Convection-Enhanced Delivery of O 6-Benzylguanine to Brain Tumors. *ACS nano* **2014,** 8, 10383-10395.
40. Juratli, T. A.; Schackert, G.; Krex, D. Current Status of Local Therapy in Malignant Gliomas—a Clinical Review of Three Selected Approaches. *Pharmacology & therapeutics* **2013,** 139, 341-358.
41. Allard, E.; Passirani, C.; Benoit, J.-P. Convection-Enhanced Delivery of Nanocarriers for the Treatment of Brain Tumors. *Biomaterials* **2009,** 30, 2302-2318.
42. Freeman, S. M.; Abboud, C. N.; Whartenby, K. A.; Packman, C. H.; Koeplin, D. S.; Moolten, F. L.; Abraham, G. N. The "Bystander Effect": Tumor Regression When a Fraction of the Tumor Mass Is Genetically Modified. *Cancer Res.* **1993,** 53, 5274-5283.
43. Boucher, P. D.; Ruch, R. J.; Shewach, D. S. Differential Ganciclovir-Mediated Cytotoxicity and Bystander Killing in Human Colon Carcinoma Cell Lines Expressing Herpes Simplex Virus Thymidine Kinase. *Hum Gene Ther* **1998,** 9, 801-814.

44. DiMaio, J. M.; Clary, B. M.; Via, D. F.; Coveney, E.; Pappas, T. N.; Lyerly, H. K. Directed Enzyme Pro-Drug Gene Therapy for Pancreatic Cancer in Vivo. *Surgery* **1994,** 116, 205-213.
45. Martuza, R. L.; Malick, A.; Markert, J. M.; Ruffner, K. L.; Coen, D. M. Experimental Therapy of Human Glioma by Means of a Genetically Engineered Virus Mutant. *Science* **1991,** 252, 854-856.
46. Rubsam, L. Z.; Boucher, P. D.; Murphy, P. J.; KuKuruga, M.; Shewach, D. S. Cytotoxicity and Accumulation of Ganciclovir Triphosphate in Bystander Cells Cocultured with Herpes Simplex Virus Type 1 Thymidine Kinase-Expressing Human Glioblastoma Cells. *Cancer Res.* **1999,** 59, 669-675.
47. Tomicic, M. T.; Thust, R.; Kaina, B. Ganciclovir-Induced Apoptosis in Hsv-1 Thymidine Kinase Expressing Cells: Critical Role of DNA Breaks, Bcl-2 Decline and Caspase-9 Activation. *Oncogene* **2002,** 21, 2141-2153.
48. Amano, S.; Gu, C.; Koizumi, S.; Tokuyama, T.; Namba, H. Timing of Ganciclovir Administration in Glioma Gene Therapy Using Hsvtk Gene-Transduced Mesenchymal Stem Cells. *Cancer Genomics Proteomics* **2011,** 8, 245-250.
49. Denning, C.; Pitts, J. D. Bystander Effects of Different Enzyme-Prodrug Systems for Cancer Gene Therapy Depend on Different Pathways for Intercellular Transfer of Toxic Metabolites, a Factor That Will Govern Clinical Choice of Appropriate Regimes. *Hum Gene Ther* **1997,** 8, 1825-1835.
50. Mesnil, M.; Yamasaki, H. Bystander Effect in Herpes Simplex Virus-Thymidine Kinase/Ganciclovir Cancer Gene Therapy: Role of Gap-Junctional Intercellular Communication1. *Cancer Res.* **2000,** 60, 3989-3999.
51. Bhise, N. S.; Gray, R. S.; Sunshine, J. C.; Htet, S.; Ewald, A. J.; Green, J. J. The Relationship between Terminal Functionalization and Molecular Weight of a Gene Delivery Polymer and Transfection Efficacy in Mammary Epithelial 2-D Cultures and 3-D Organotypic Cultures. *Biomaterials* **2010,** 31, 8088-8096.
52. Tzeng, S. Y.; Green, J. J. Subtle Changes to Polymer Structure and Degradation Mechanism Enable Highly Effective Nanoparticles for Sirna and DNA Delivery to Human Brain Cancer. *Adv. Healthcare Mater.* **2013,** 2, 468-480.
53. Tzeng, S. Y.; Guerrero-Cázares, H.; Martinez, E. E.; Sunshine, J. C.; Quiñones-Hinojosa, A.; Green, J. J. Non-Viral Gene Delivery Nanoparticles Based on Poly(B-Amino Esters) for Treatment of Glioblastoma. *Biomaterials* **2011,** 32, 5402-5410.
54. Tyler, B.; Wadsworth, S.; Recinos, V.; Mehta, V.; Vellimana, A.; Li, K.; Rosenblatt, J.; Do, H.; Gallia, G. L.; Siu, I. M.; Wicks, R. T.; Rudek, M. A.; Zhao, M.; Brem, H. Local Delivery of Rapamycin: A Toxicity and Efficacy Study in an Experimental Malignant Glioma Model in Rats. *Neuro Oncol* **2011,** 13, 700-709.
55. Burgess, A.; Vigneron, S.; Brioudes, E.; Labbe, J. C.; Lorca, T.; Castro, A. Loss of Human Greatwall Results in G2 Arrest and Multiple Mitotic Defects Due to Deregulation of the Cyclin B-Cdc2/Pp2a Balance. *Proc Natl Acad Sci U S A* **2010,** 107, 12564-12569.
56. Bishop, C. J.; Ketola, T.-M.; Tzeng, S. Y.; Sunshine, J. C.; Urtti, A.; Lemmetyinen, H.; Vuorimaa-Laukkanen, E.; Yliperttula, M.; Green, J. J. The Effect and Role of Carbon Atoms in Poly(B-Amino Ester)S for DNA Binding and Gene Delivery. *J. Am. Chem. Soc.* **2013,** 135, 6951-6957.

57. Sunshine, J. C.; Akanda, M. I.; Li, D.; Kozielski, K. L.; Green, J. J. Effects of Base Polymer Hydrophobicity and End-Group Modification on Polymeric Gene Delivery. *Biomacromolecules* **2011,** 12, 3592-3600.
58. Green, J. J. 2011 Rita Schaffer Lecture: Nanoparticles for Intracellular Nucleic Acid Delivery. *Annals of Biomedical Engineering* **2012,** 40, 1408-1418.
59. Shmueli, R. B.; Sunshine, J. C.; Xu, Z.; Duh, E. J.; Green, J. J. Gene Delivery Nanoparticles Specific for Human Microvasculature and Macrovasculature. *Nanomedicine* **2012,** 8, 1200-1207.
60. Kim, J.; Sunshine, J. C.; Green, J. J. Differential Polymer Structure Tunes Mechanism of Cellular Uptake and Transfection Routes of Poly(Beta-Amino Ester) Polyplexes in Human Breast Cancer Cells. *Bioconjugate Chem.* **2014,** 25, 43-51.
61. Tzeng, S. Y.; Higgins, L. J.; Pomper, M. G.; Green, J. J. Student Award Winner in the Ph.D. Category for the 2013 Society for Biomaterials Annual Meeting and Exposition, April 10-13, 2013, Boston, Massachusetts : Biomaterial-Mediated Cancer-Specific DNA Delivery to Liver Cell Cultures Using Synthetic Poly(Beta-Amino Ester)S. *Journal of biomedical materials research. Part A* **2013,** 101, 1837-1845.
62. Eltoukhy, A. A.; Siegwart, D. J.; Alabi, C. A.; Rajan, J. S.; Langer, R.; Anderson, D. G. Effect of Molecular Weight of Amine End-Modified Poly(Beta-Amino Ester)S on Gene Delivery Efficiency and Toxicity. *Biomaterials* **2012,** 33, 3594-3603.
63. Zhang, Z.; Lin, J.; Chu, J.; Ma, Y.; Zeng, S.; Luo, Q. Activation of Caspase-3 Noninvolved in the Bystander Effect of the Herpes Simplex Virus Thymidine Kinase Gene/Ganciclovir (Hsv-Tk/Gcv) System. *J Biomed Opt* **2008,** 13, 031209.
64. Immonen, A.; Vapalahti, M.; Tyynela, K.; Hurskainen, H.; Sandmair, A.; Vanninen, R.; Langford, G.; Murray, N.; Yla-Herttuala, S. Advhsv-Tk Gene Therapy with Intravenous Ganciclovir Improves Survival in Human Malignant Glioma: A Randomised, Controlled Study. *Mol. Ther.* **2004,** 10, 967-972.
65. Moolten, F. L. Drug-Sensitivity (Suicide) Genes for Selective Cancer-Chemotherapy. *Cancer Gene Therapy* **1994,** 1, 279-287.
66. Castillo-Rodriguez, R. A.; Arango-Rodriguez, M. L.; Escobedo, L.; Hernandez-Baltazar, D.; Gompel, A.; Forgez, P.; Martinez-Fong, D. Suicide Hsvtk Gene Delivery by Neurotensin-Polyplex Nanoparticles Via the Bloodstream and Gcv Treatment Specifically Inhibit the Growth of Human Mda-Mb-231 Triple Negative Breast Cancer Tumors Xenografted in Athymic Mice. *PLoS One* **2014,** 9, e97151.
67. Yu, D.; Wang, A.; Huang, H.; Chen, Y. Peg-Pblg Nanoparticle-Mediated Hsv-Tk/Gcv Gene Therapy for Oral Squamous Cell Carcinoma. *Nanomedicine (Lond)* **2008,** 3, 813-821.
68. Bernal, G. M.; LaRiviere, M. J.; Mansour, N.; Pytel, P.; Cahill, K. E.; Voce, D. J.; Kang, S.; Spretz, R.; Welp, U.; Noriega, S. E. Convection-Enhanced Delivery and in Vivo Imaging of Polymeric Nanoparticles for the Treatment of Malignant Glioma. *Nanomedicine: Nanotechnology, Biology and Medicine* **2014,** 10, 149-157.
69. Woodworth, G. F.; Dunn, G. P.; Nance, E. A.; Hanes, J.; Brem, H. Emerging Insights into Barriers to Effective Brain Tumor Therapeutics. *Front Oncol* **2014,** 4.
70. Salhotra, A.; Lal, B.; Laterra, J.; Sun, P. Z.; van Zijl, P. C.; Zhou, J. Amide Proton Transfer Imaging of 9l Gliosarcoma and Human Glioblastoma Xenografts. *NMR Biomed* **2008,** 21, 489-497.
71. Zhou, J.; Tryggestad, E.; Wen, Z.; Lal, B.; Zhou, T.; Grossman, R.; Wang, S.; Yan, K.; Fu, D. X.; Ford, E.; Tyler, B.; Blakeley, J.; Laterra, J.; van Zijl, P. C. Differentiation between

Glioma and Radiation Necrosis Using Molecular Magnetic Resonance Imaging of Endogenous Proteins and Peptides. *Nat. Med.* **2011,** 17, 130-134.
72. Dimeco, F.; Rhines, L. D.; Hanes, J.; Tyler, B. M.; Brat, D.; Torchiana, E.; Guarnieri, M.; Colombo, M. P.; Pardoll, D. M.; Finocchiaro, G. Paracrine Delivery of Il-12 against Intracranial 9l Gliosarcoma in Rats. *Journal of neurosurgery* **2000,** 92, 419-427.
73. Recinos, V. R.; Tyler, B. M.; Bekelis, K.; Sarah Brem Sunshine, B.; Vellimana, A.; Li, K. W.; Brem, H. Combination of Intracranial Temozolomide with Intracranial Carmustine Improves Survival When Compared with Either Treatment Alone in a Rodent Glioma Model. *Neurosurgery* **2010,** 66, 530-537.
74. Rhines, L. D.; Sampath, P.; DiMeco, F.; Lawson, H. C.; Tyler, B. M.; Hanes, J.; Olivi, A.; Brem, H. Local Immunotherapy with Interleukin-2 Delivered from Biodegradable Polymer Microspheres Combined with Interstitial Chemotherapy: A Novel Treatment for Experimental Malignant Glioma. *Neurosurgery* **2003,** 52, 872-880.
75. Tamargo, R. J.; Myseros, J. S.; Epstein, J. I.; Yang, M. B.; Chasin, M.; Brem, H. Interstitial Chemotherapy of the 9l Gliosarcoma: Controlled Release Polymers for Drug Delivery in the Brain. *Cancer Res.* **1993,** 53, 329-333.
76. Walter, K. A.; Cahan, M. A.; Gur, A.; Tyler, B.; Hilton, J.; Colvin, O. M.; Burger, P. C.; Domb, A.; Brem, H. Interstitial Taxol Delivered from a Biodegradable Polymer Implant against Experimental Malignant Glioma. *Cancer Res.* **1994,** 54, 2207-2212.
77. Weingart, J. D.; Sipos, E. P.; Brem, H. The Role of Minocycline in the Treatment of Intracranial 9l Glioma. *Journal of neurosurgery* **1995,** 82, 635-640.
78. Stojiljkovic, M.; Piperski, V.; Dacevic, M.; Rakic, L.; Ruzdijic, S.; Kanazir, S. Characterization of 9l Glioma Model of the Wistar Rat. *Journal of neuro-oncology* **2003,** 63, 1-7.
79. Barba, D.; Hardin, J.; Ray, J.; Gage, F. H. Thymidine Kinase-Mediated Killing of Rat Brain Tumors. *Journal of neurosurgery* **1993,** 79, 729-735.
80. Miletic, H.; Fischer, Y.; Litwak, S.; Giroglou, T.; Waerzeggers, Y.; Winkeler, A.; Li, H.; Himmelreich, U.; Lange, C.; Stenzel, W. Bystander Killing of Malignant Glioma by Bone Marrow–Derived Tumor-Infiltrating Progenitor Cells Expressing a Suicide Gene. *Mol. Ther.* **2007,** 15, 1373-1381.
81. Sandmair, A.-M.; Turunen, M.; Tyynelä, K.; Loimas, S.; Vainio, P.; Vanninen, R.; Vapalahti, M.; Bjerkvig, R.; Jänne, J.; Ylä-Herttuala, S. Herpes Simplex Virus Thymidine Kinase Gene Therapy in Experimental Rat Bt4c Glioma Model: Effect of the Percentage of Thymidine Kinase-Positive Glioma Cells on Treatment Effect, Survival Time, and Tissue Reactions. *Cancer gene therapy* **2000,** 7, 413-421.
82. Sanson, M.; Marcaud, V.; Robin, E.; Valéry, C.; Sturtz, F.; Zalc, B. Connexin 43–Mediated Bystander Effect in Two Rat Glioma Cell Models. *Cancer gene therapy* **2002,** 9, 149-155.
83. Rainov, N. G. A Phase Iii Clinical Evaluation of Herpes Simplex Virus Type 1 Thymidine Kinase and Ganciclovir Gene Therapy as an Adjuvant to Surgical Resection and Radiation in Adults with Previously Untreated Glioblastoma Multiforme. *Hum Gene Ther* **2000,** 11, 2389-2401.
84. Shand, N.; Weber, F.; Mariani, L.; Bernstein, M.; Gianella-Borradori, A.; Long, Z.; Sorensen, A. G.; Barbier, N. A Phase 1-2 Clinical Trial of Gene Therapy for Recurrent Glioblastoma Multiforme by Tumor Transduction with the Herpes Simplex Thymidine Kinase Gene Followed by Ganciclovir. Gli328 European-Canadian Study Group. *Hum Gene Ther* **1999,** 10, 2325-2335.

85. Harsh, G. R.; Deisboeck, T. S.; Louis, D. N.; Hilton, J.; Colvin, M.; Silver, J. S.; Qureshi, N. H.; Kracher, J.; Finkelstein, D.; Chiocca, E. A.; Hochberg, F. H. Thymidine Kinase Activation of Ganciclovir in Recurrent Malignant Gliomas: A Gene-Marking and Neuropathological Study. *J Neurosurg* **2000,** 92, 804-811.
86. Trask, T. W.; Trask, R. P.; Aguilar-Cordova, E.; Shine, H. D.; Wyde, P. R.; Goodman, J. C.; Hamilton, W. J.; Rojas-Martinez, A.; Chen, S. H.; Woo, S. L.; Grossman, R. G. Phase I Study of Adenoviral Delivery of the Hsv-Tk Gene and Ganciclovir Administration in Patients with Current Malignant Brain Tumors. *Mol. Ther.* **2000,** 1, 195-203.
87. Jacobs, A.; Voges, J.; Reszka, R.; Lercher, M.; Gossmann, A.; Kracht, L.; Kaestle, C.; Wagner, R.; Wienhard, K.; Heiss, W. D. Positron-Emission Tomography of Vector-Mediated Gene Expression in Gene Therapy for Gliomas. *Lancet* **2001,** 358, 727-729.
88. Reszka, R. C.; Jacobs, A.; Voges, J. Liposome-Mediated Suicide Gene Therapy in Humans. *Methods Enzymol* **2005,** 391, 200-208.
89. Pulkkanen, K. J.; Yla-Herttuala, S. Gene Therapy for Malignant Glioma: Current Clinical Status. *Mol. Ther.* **2005,** 12, 585-598.
90. Jensen, S. A.; Day, E. S.; Ko, C. H.; Hurley, L. A.; Luciano, J. P.; Kouri, F. M.; Merkel, T. J.; Luthi, A. J.; Patel, P. C.; Cutler, J. I.; Daniel, W. L.; Scott, A. W.; Rotz, M. W.; Meade, T. J.; Giljohann, D. A.; Mirkin, C. A.; Stegh, A. H. Spherical Nucleic Acid Nanoparticle Conjugates as an Rnai-Based Therapy for Glioblastoma. *Sci. Transl. Med.* **2013,** 5, 209ra152.

Chapter 4

Synthesis, characterization, and optimization of a novel polymeric nanoparticle for the delivery of siRNA to human GBM

4.1. Introduction

RNA interference (RNAi) is a naturally occurring cellular mechanism that ultimately results in sequence-specific gene knockdown and can be externally induced by intracellular delivery of short interfering RNA (siRNA).[1] Targeted gene knockdown *via* siRNA delivery has exciting potential for the treatment of diseases caused by aberrant gene expression.[2, 3] However, safe and efficient intracellular siRNA delivery remains a challenging obstacle.

Promising siRNA delivery strategies have been suggested that employ lipid-based,[4, 5] inorganic,[6-8] or polymeric materials[9-11] similar to those designed for DNA delivery. Certain siRNA delivery material design parameters can be addressed using the same materials found to effectively deliver DNA. Cationic polymers with high buffering capacities, such as poly(ethyleneimine) (PEI), promote nucleic acid compaction and protection, cellular internalization, and endosomal escape.[12] Polymer degradability such as that afforded by hydrolytically cleavable poly(β-amino ester)s (PBAE)s results in cargo release far superior to nondegradable PEI.[13]

Two key delivery obstacles specific to siRNA are unstable particle formation and cytoplasmic targeting. The former concern results from the relatively small size and rigidity of siRNA, which is ~200 times smaller than most plasmids used for DNA delivery and is stiffer than

---

This chapter contains material modified from the following articles, previously published as:
Kozielski, K.L.; Tzeng, S. Y.; Green, J. J.: A bioreducible linear poly(beta-amino ester) for siRNA delivery. *Chemical Communications* **2013**, *49,* 5319-5321.
Kozielski, K.L.; Tzeng, S. Y.; Hurtado de Mendoza, B. A.; Green, J.J: Bioreducible cationic polymer-based nanoparticles for efficient and environmentally triggered cytoplasmic siRNA delivery to primary human brain cancer cells. *ACS Nano* **2014**, *8,* 3232-3241.

DNA.[14, 15] Shorter length results in reduced mutivalency of electrostatic interactions between a cationic polymer and anionic siRNA molecule, while rigidity may prevent siRNA from conforming into shapes favorable for binding and nanoparticle (NP) self-assembly. In addition, cytoplasmic targeting of siRNA is required for optimal gene knockdown, as the cytosol is the site of RNAi-induced mRNA degradation.[16] Polymer bioreduction by glutathione (GSH) in the reducing cytoplasmic environment is a simple and specific method to engineer triggered cytoplasmic siRNA release.[17] This can be achieved by the inclusion of bioreducible disulfide linkages as a crosslinking agent,[18] adjacent to cationic groups on polymer end-caps[19, 20] or along the polymer backbone.[21]

The use of bioreducible moieties in other siRNA delivery vehicles has met with success in the past. Linear, low-molecular weight PEI segments linked with disulfide bonds were shown to be as effective as commercially-available, branched 25 kDa PEI (bPEI) while being less cytotoxic. In particular, this material was capable of roughly 50% knockdown of a fluorescent marker gene during *in vitro*, serum-free siRNA delivery to Chinese hamster ovary cells (CHO-K1) using 100 nM siRNA.[9] Disulfide-containing poly(amido amine)s have shown successful *in vitro* siRNA delivery in human head and neck carcinoma cells (UM-SCC-14C),[22] non-small cell lung carcinoma (H1299),[11] and human prostate cancer cells in which ~80% knockdown was achieved with 30 nM siRNA.[23] The KALA peptide (a 30-residue peptide containing 3 Lys-Ala-Leu-Ala repeats)[24] modified with cysteine residues and crosslinked to form a bioreducible polymer was electrostatically complexed with PEGylated siRNA.[25] This delivery system achieved nearly 50% gene knockdown *in vitro* in 10% serum-containing media to MDA-MB-435 melanoma cells using ~60 nM siRNA. PBAEs containing disulfides in the polymer end-caps achieved ~70% knockdown

in human umbilical vein cells in an *in vitro* study in which 60 nM siRNA was delivered in the presence of 2% serum.[26]

PBAE-nucleic acid nanoparticles allow nucleic acid release by hydrolytic degradation of esters along the polymer backbone on the time scale of several hours to a few days.[13, 27] However, this release mechanism limits control over where release will occur. In order to specifically target release to the cytoplasm, we have synthesized a novel linear PBAE polymer with disulfide bonds along the polymer backbone.

We sought to create a new bioreducible nanobiotechnology that could be highly effective for siRNA delivery to human cells. As the literature shows that lipid-based transfection reagents, such as the leading commercially available reagent Lipofectamine™ 2000, are generally superior for siRNA delivery compared to polymers such as PEI, we used Lipofectamine™ 2000 as the benchmark positive control. Recently, other disulfide-containing PBAE nucleic acid delivery vehicles for RNAi have been investigated. Yin *et. al.* formed disulfide-containing PBAEs for plasmid delivery of short hairpin RNA (shRNA), but as diamines and diacrylates were used for polymerization, degree of branching was not user-controlled, which could compromise the reproducibility of the material properties.[28, 29] Additionally, while this method was effective for delivery of plasmid DNA, reports have shown standard linear PBAEs are generally ineffective for siRNA delivery without the use of additional components.[30] This is not unexpected as siRNA is a molecule ~200-times smaller than DNA and its delivery may require different biomaterials. Our group recently described linear PBAEs containing disulfide bonds only in the polymer end-cap groups, not in the main base polymer, and used them for siRNA delivery to promote siRNA triggered released into the cytosol.[20] These polymers were effective and presented an interesting

initial step for creating PBAE-based siRNA delivery polymers, and motivated the work presented herein.

We hypothesized that a new reducible, disulfide-containing analog of a previously established non-reducible PBAE polymer would promote enhanced siRNA-mediated gene knockdown. Our goal was to create reducible nanoparticles that would be as physically identical as possible to their non-reducible analogs when in an extracellular environment, but would then efficiently release siRNA when in a reducing cytoplasmic environment.

We synthesized a new reducible form of a monomer that we have previously used, hexane-1,6-diyl diacrylate (B6) to form "reducible B6," 2,2'-disulfanediylbis(ethane-2,1-diyl) diacrylate (BR6), in order to form polymers with similar structure and the same charge density as B6 polymers.[21] In more recent work, we sought to improve siRNA delivery with bioreducible PBAE-based nanoparticles by specifically addressing the instability of siRNA nanoparticles and the need for cytoplasmic targeting. We wanted to engineer a class of polymers for siRNA nanoparticle formation and efficient siRNA delivery by balancing polymer bioreducibility and hydrophobicity, as PBAE hydrophobicity may enhance particle stability and has been shown to promote enhanced delivery of both DNA and siRNA.[19, 31] Polymer bioreducibility was used to reduce potential cytotoxicity and to impart cytoplasmic targeting of siRNA release. To further elucidate ideal siRNA delivery criteria, we also examined the effects of changing nanoparticle formulation parameters and physical properties on gene knockdown and cytotoxicity. The results presented herein show that bioreducible PBAE chemical properties and nanoparticle physical properties can be engineered for simple, safe, and effective siRNA delivery.

4.2. Materials and methods

4.2.1. Materials

All chemicals used for the synthesis of monomer BR6 were purchased from Sigma-Aldrich Chemical Co. (St. Louis, MO) and used without further purification. All other monomers were purchased from Alfa Aesar (Ward Hill, MA). YO-PRO®-1 Iodide was purchased from Life Technologies™ (Carlsbad, CA). Lipofectamine™ 2000 and Opti-MEM™ I were purchased from Invitrogen (Carlsbad, CA) and used according to manufacturer's instructions. Ambion® *Silencer*® eGFP and Ambion® *Silencer*® Negative Control #1 siRNA were purchased from Life Technologies™. CellTiter 96® AQ_{ueous} One MTS assay was purchased from Promega (Fitchburg, WI) and used according to manufacturer's instructions. Cells were grown in 89% GIBCO® DMEM-F12, 1% GIBCO® Antibiotic-Antimycotic (Invitrogen), and 10% Corning Cellgro® Heat-Inactivated FBS.

4.2.2. Bioreducible monomer synthesis

Bis(2-hydroxyethyl) disulfide (15.4 g, 10 mmol) and triethylamine (TEA, 37.5 mL, 300 mmol) were dissolved in 450 mL of tetrahydrofuran (THF) (previously dried with Na_2SO_4) in a 1 L round bottom flask; the contents were then flushed with N_2 for 10 min and maintained under a N_2 environment for the remainder of the reaction time. Acryloyl chloride (24.4 mL, 300 mmol) was dissolved in 50 mL of dried tetrahydrofuran, added to the flask dropwise over 2 hrs while stirring, and the reaction was allowed to continue at room temperature for 24 h. Following reaction, TEA HCl precipitate was removed by filtration, and THF was removed by rotary evaporation. The product was dissolved in 200 mL dichloromethane (DCM) and washed five times with 200 mL of aqueous 0.2 M Na_2CO_3 and three times with distilled water. The solution was dried with Na_2SO_4 and DCM was removed by rotary evaporation. The product 2,2'-disulfanediylbis(ethane-2,1-diyl) (BR6) was confirmed *via* ^{1}H NMR: ($CDCl_3$, 400Hz), δ2.95 (2H, *t*, $CH_2CHCOOCH_2CH_2S$), δ3.95

(2H, *t*, $CH_2CHCOOCH_2CH_2S$), δ5.8-5.9 (1H, *d*, $CH_2CHCOOCH_2CH_2S$), δ6.1-6.2 (1H, *dd*, $CH_2CHCOOCH_2CH_2S$), δ6.4-6.5 (1H, *d*, $CH_2CHCOOCH_2CH_2S$).

4.2.3. Bioreducible polymer synthesis

Polymer synthesis was carried out in a method similar to Bhise *et al.*[32] The diacrylate base monomers used for polymerization were BR6 (see above) or hexane-1,6-diyl diacrylate (B6). Backbone monomers BR6 and hexane-1,6-diyl diacrylate (B6) were mixed at a molar ratio of either 1:0, 3:1, 1:1, 1:3, or 0:1 prior to polymerization. Side chain monomers used were 3-amino-1-propanol (S3), 4-amino-1-butanol (S4), or 5-amino-1-pentanol (S5). The end-caps used were 2-(3-(aminopropyl)amino)ethanol (E6) and 1-(3-aminopropyl)-4-methylpiperazine (E7). For all polymers, polymerization was completed using a base monomer to side chain ratio of 1.01:1 at 500 mg/mL in dimethyl sulfoxide (DMSO) at 90ºC for 24 hrs while stirring. The polymers were end-capped in DMSO at 100 mg/mL with 0.2 M E7 for 1 h at room temperature while shaking. Excess E7 monomer was not removed from the polymer solution, however examining E7 monomer cytotoxicity showed that free E7 was not significantly cytotoxic to GBM 319 cells (**Figure 4.1**). As we have found with our prior work with this class of polymers,[32] the step growth polymerization of the bifunctional monomers leads to short linear polymers without any byproducts or side reactions. Purity of polymers and the identity of copolymers is confirmed by ^{1}H NMR spectra. The ^{1}H NMR spectra for representative polymers R647, 1:1 R647, and 647 are shown in **Figure 4.2**. The integration of the peaks of the copolymers validate that base monomers B6 and BR6 incorporate into a copolymer at the same molar ratio as is used during polymer synthesis.

4.2.4. *In vitro* siRNA Delivery to human GBM cells and cell viability

GFP$^+$ GBM 319 glioblastoma cells were plated at a cell density of 15,000 cells/well in 96-well tissue culture plates in 89% GIBCO® DMEM-F12, 1% GIBCO® Antibiotic-Antimycotic (Invitrogen), and 10% Corning Cellgro® Heat-Inactivated FBS and allowed to adhere overnight. fNPC 34 cells were utilized to compare siRNA delivery between primary human glioblastoma cells and healthy human primary cells found in the brain. fNPC 34 cells are primary fetal neural progenitor cells obtained as described previously following procedures approved by the Johns Hopkins University Institutional Review Board.[33] fNPC 34 cells were plated at a density of 15,000 cells/well in 96-well tissue culture plates in 97% GIBCO® DMEM-F12, 1% GIBCO® Antibiotic-Antimycotic (Invitrogen), 2% B-27® Serum-Free Supplement, and 20 μg/mL each of basic fibroblast growth factor (Roche Applied Science) and epidermal growth factor (Sigma) and allowed to adhere overnight prior to transfection. The siRNAs used were either siRNA targeting eGFP with sequence 5'-CAAGCUGACCCUGAAGUUCTT (sense) and 3'-GAACUUCAGGGUCAGCUUGCC (antisense), or a scrambled control siRNA (scRNA) with sequence 5'-AGUACUGCUUACGAUACGGTT (sense) and 3'-CCGUAUCGUAAGCAGUACUTT (anti-sense). AllStars Human Cell Death siRNA was purchased from Qiagen. For all transfections, siRNA and polymers were diluted in 25 mM NaAc at twelve times the final concentration listed for each group, and siRNA and polymers were combined in a 1:1 v/v ratio and allowed to form cells for 10 min at room temperature. As an example, nanoparticles listed at final concentrations of "180 μg/mL and 20 nM siRNA" were formed by mixing a 2.16 mg/mL solution of polymer with a 240 nM solution of siRNA. The cell culture media was removed and replaced with serum-free media prior to adding nanoparticles. Nanoparticle formulations were diluted in each well in quadruplicates in a 1:6 v/v ratio to yield the final siRNA and polymer concentrations listed for each group. Cells were incubated with

nanoparticles for 4 h for siGFP experiments and 2 h for death siRNA experiments, after which the nanoparticle solutions were removed and fresh, serum-containing media was added. Cytoxicity for siGFP transfections was assessed 24 h after transfection CellTiter 96® AQ_{ueous} One MTS assay following manufacturer's instructions and read using a BioTek® Synergy™ 2 Microplate Reader.

Cell death in death siRNA experments was assessed by staining cells with propidium iodide (PI) in DMEM-F12 at 1:200 (v/v) PI prior to fixation and 750 nM 2-(4-amidinophenyl)-1H -indole-6-carboxamidine (DAPI) following fixation in 10% formalin. Cell images were taken at 5X magnification using a Zeiss Axio observer A1 microscope with a Zeiss Axiocam MRm camera using AxioVision Release 4.8.2 software. Fluorescence was provided by an Exfo X-Cite® series 120Q. Live and dead cells were quantified using ImageJ v1.47 software, and dead cells were subtracted from the live cell count to yield the total cell count for each well.

4.2.5. Flow cytometry

All flow cytometry was completed at 9 d post-transfection using an Intellicyt high-throughput loader attached to an BD Accuri™ C6 flow cytometer (emission filter: 530/30 nm). Hypercyt software was used to discriminate events between each well and FlowJo 7 software was used to analyze the flow cytometry results. Cells were prepared for flow cytometry by 5 min of trypsinization with 30 μL of 0.05% trypsin-EDTA, followed by the addition of 170 μL of a buffer of PBS containing 1:50 (v/v) FBS and 1:200 (v/v) propidium iodide (PI). Cell suspensions were moved to round-bottom 96-well plates and centrifuged for 5 min at 1000 rpm. 170 μL of supernatant was removed and cells were resuspended in the remaining buffer. PI signal was used to distinguish dead or dying cells from live cells so that the unhealthy cells could be removed from analysis. GFP knockdown was determined by finding the geometric mean FL1 fluorescence signal for each sample. Percent knockdown was calculated by normalizing the GFP expression of siRNA-

treated cells to scRNA-treated cells. All the transfections were carried out using the same cell line, siRNAs, controls, and data collection protocols, and all formulations that caused >60% loss in metabolic activity were considered non-viable and excluded from further analysis.

4.2.6. Gel retention assay

Nanoparticles were formed using 0.01 mg/mL scrambled control RNA (scRNA) in 25 mM sodium acetate (NaAc) and polymer at weight ratios to scRNA ranging from 600 wt/wt to 0 wt/wt (siRNA) alone. Polymer to siRNA ratios are also described as N:P ratios. These were incubated for 10 min at room temperature to allow for particle formation. To compare the effects of a nonreducing and reducing environment on the particles, either PBS or PBS containing L-glutathione (GSH) to yield a final GSH concentration of 0 mM or 5 mM, respectively, were added and allowed to incubate at room temperature for 15 min. A solution of 30% glycerol was added to the particles in a 1:5 v/v ratio. The particles were loaded into a 1% agarose gel containing 1 μg/mL ethidium bromide and electrophoresed at 100 mV for 20 min. Gels were visualized using UV light exposure.

4.2.7. Nanoparticle characterization

Particle Size and Concentration Determination: Nanoparticle Tracking Analysis

All nanoparticles were made in the same manner that they were for transfection and then diluted so that their sizes and concentrations could be accurately determined using Nanoparticle Tracking Analysis (NTA). NTA was performed using a NanoSight NS500 and analyzed using NanoSight NTA 2.4 software. As an example, particles for transfection groups labeled “180 μg/mL polymer with 20 nM siRNA” were synthesized by forming particles at a polymer concentration of 1.08 mg/mL and scRNA at 120 nM in NaAc, as these particles would be diluted in a 1:6 v/v ratio in media during transfection. For NTA, however, these particles were diluted in PBS following

the protocol recommended by Bhise *et al.*[34] All measurements were repeated with three separate formulations for each condition. The NTA analysis reported the number-average hydrodynamic radius of the particles. All particle concentrations were reported as the number of particles per volume that would be present in the transfection wells.

siRNA loading was calculated by dividing the total amount of siRNA per transfection well by the number of particles per well. This calculation was only completed for particle formulations with wt/wt ratios high enough to completely bind all siRNA as determined by the gel retention assay. For this reason, any particle formulations with wt/wt ratios at or below 75 wt/wt were excluded from siRNA loading calculations.

Particle Zeta-Potential Determination: Dynamic Light Scattering

Particles were formed at the same concentrations and in the same manner as described for particle sizing. Particles were diluted 1:650 v/v in PBS and loaded into a disposable cuvette cell. Particle surface charge was determined *via* dynamic light scattering (DLS) using a Malvern Zetasizer NanoZS.

Transmission Electron Microscopy

Nanoparticles formed using 1:1 R647 at 180 μg/mL and 20 nM siRNA were imaged using transmission electron microscopy (TEM). 1:1 R647 was diluted to 2.16 μg/mL in 25 mM NaAc, scRNA was diluted to 240 nM in NaAc, and the two solutions were combined in a 1:1 v/v ratio and allowed to form particles for 10 min at room temperature. Following particle formation, 5 μL of the nanoparticle solution was placed onto a carbon-coated copper TEM grid and allowed to dry. Particles were imaged using a Philips/FEI BioTwin CM120 transmission electron microscope.

YO-PRO®-1 Iodide Competition Binding Assay

siRNA was diluted to 1.33 μM in 25 mM NaAc and combined in a 1:1 v/v ratio with 1.33 μM YO-PRO®-1 Iodide in 25mM NaAc in all wells of a black-bottom 96-well plate. Polymers were diluted at concentrations ranging from 512 to 0.5 times these concentrations and combined in quadruplicates in a 1:2 v/v ratio with the siRNA/YO-PRO solution, and allowed to incubate for 15 min at room temperature. 25 mM NaAc without polymer was also added in a 1:2 v/v ratio to four siRNA/YO-PRO solutions to supply background fluorescence values. Fluorescence was measured at 15 min using a BioTek Synergy 2 fluorescence plate reader at 490/510 nm (ex/em).

4.2.8. Polymer characterization

Gel Permeation Chromatography

GPC was performed using a Waters GPC system with three Waters Styragel columns in a series (HR 1, HR 3 and HR4) and a Waters 2414 refractive index detector, both maintained at 40ºC throughout all samples, which were loaded using a Waters 717plus autosampler (Waters Corp., Milford, MA). All samples were loaded at 5 mg/mL using 94% THF, 5% DMSO, and 1% piperidine (v/v) as the eluent at a flow rate of 1.0 mL/min for 40 min. Polymer molecular weights were calculated relative to polystyrene standards (Shodex, Japan).

To assess polymer degradation in various conditions, each polymer R647 or 647 was either diluted in PBS or in a solution of 5 mM GSH in PBS to a final polymer concentration of 7 mg/mL. Each was allowed to incubate for 5 min at room temperature and was then frozen at -80°C and lyophilized. GPC was performed on these samples following the GPC protocol above. Excess salts were precipitated out of the GPC solvent and removed by filtration prior to performing GPC.

4.2.9. Statistical analysis

All results are presented as mean ± standard error of the mean. Statistical significance results for all % GFP knockdown and % loss in metabolic activity were determined using a one-

way ANOVA with Dunnett's post-tests using Lipofectamine™ 2000 as the control. All particle formulations that caused > 60% toxicity were considered non-viable and excluded from statistical testing. A two-way ANOVA with Tukey's multiple comparisons post-test was also used to compare changes in loss in metabolic activities of cells treated with different polymers using side chain and base monomer as the parameters. Statistical significance of results for nanoparticle size and ζ-potential were determined using a one-way ANOVA with Tukey's Multiple Comparison post tests. R squared correlation values were calculated compared to either linear or nonlinear regressions as labeled in each figure caption. All significance tests with $p < 0.05$ were considered significant.

4.3. Results and Discussion

4.3.1. Bioreducible polymer synthesis

We synthesized a new reducible form of a monomer that we have previously used, hexane-1,6-diyl diacrylate (B6) to form "reducible B6," 2,2'-disulfanediylbis(ethane-2,1-diyl) diacrylate (BR6), in order to form polymers with similar structure and the same charge density as B6 polymers. Synthesis of BR6 was carried out in a method similar to Chen et. al.[35] Briefly, bis(2-hydroxyethyl) disulfide was acrylated with acryloyl chloride in the presence of triethylamine (TEA). Following reaction, TEA HCl precipitate was removed by filtration, and the product was purified with aqueous Na_2CO_3 washes followed by rotary evaporation (**Figure 4.3**). The product was confirmed by proton nuclear magnetic resonance (H^1-NMR).

The two-step polymer synthesis was carried out in a similar manner as in Bhise *et. al.*[32] Either diacrylate monomer, BR6 or B6, was polymerized with 4-amino-1-butanol (S4) in a 1.01:1 molar ratio, yielding acrylate terminated base polymers. The B6-S4 or BR6-S4 base polymers were

then end-capped with 1-(3-aminopropyl)-4-methylpiperazine (E7) to yield either B6-S4-E7 (647) or BR6-S4-E7 (R647). End-cap E7 was chosen as it has been shown to work well for PBAE delivery of siRNA in our preliminary studies with non-reducible polymers.[36] Polymer size and structure were confirmed using gel permeation chromatography (GPC) and H^1-NMR, respectively.† GPC results of R647 yielded M_N of 3745 Da, M_W of 7368 Da, and a PDI of 1.967. GPC results of 647 yielded a comparable size profile (M_N 4037 Da, M_W 6221 Da, PDI 1.597).

4.3.2. Assessment of polymer-siRNA binding and nanoparticle formation and biodegradation

The siRNA binding capability of each polymer was evaluated by a YO-PRO®-1 Iodide competition binding assay (**Figure 4.4**), in which YO-PRO®-1 Iodide fluoresces upon binding siRNA and is quenched as it is displaced by increasing concentrations of polymer. Over the polymer concentrations tested, R647 showed comparable to slightly higher siRNA binding affinity compared to 647 as measured by YO-PRO®-1 Iodide quenching.

Polymer-siRNA binding was further characterized using a gel retention assay (**Figure 4.5**), in which nanoparticles are added to the wells of an agarose gel, and tightly bound siRNA is unable to migrate under electric field (100 V). In order to repeat this assay in conditions mimicking the reducing cytoplasmic environment, GSH was added to the particles (final concentration 5 mM) immediately prior to electrophoresis. Without GSH, both R647 and 647 showed complete siRNA complexation with polymer:siRNA weight ratios (wt/wts) as low as 75:1. In the presence of cytoplasmic levels of GSH, R647 completely released siRNA, even at the highest wt/wt examined, while 647 binding was unaffected. GPC results of each polymer show that incubation with 5 mM GSH for 5 min is capable of degrading R647 but not 647 (**Figure 4.6**). These results combined with the competition binding data show that R647 can not only condense and protect siRNA as

well as or slightly better than 647 when in extracellular conditions but is also able to completely release siRNA within minutes of exposure to cytoplasmic GSH levels.

Nanoparticles formed from R647 and 647 were characterized by size via nanoparticle tracking analysis (NTA) using a NanoSight NS500 and surface charge (ζ-potential) via dynamic light scattering (DLS) using a Malvern Zetasizer NanoZS (**Figure 4.7**). For each polymer, nanoparticles were formed at either 450 wt/wt or 112.5 wt/wt. For all four formulations tested, nanoparticle diameter remained between 111 nm and 118 nm, which falls in the appropriate size range for efficient cellular uptake.[37] For particles formed at 112.5 wt/wt with either R647 or 647, ζ-potential was neutral (between -10 and +10 mV), while particles formed at 450 wt/wt with R647 or 647 had a ζ-potential of 19.0 ± 1 mV and 20.6 ± 1 mV, respectively.

4.3.3. *In vitro* assessment of siRNA delivery to human GBM using novel bioreducible PBAE

Gene knockdown and cellular loss in metabolic activity were evaluated in glioblastoma GBM 319 cells expressing constitutive GFP,[38] using siRNA targeted at GFP with sequence 5'-CAAGCUGACCCUGAAGUUCTT (sense) and 3'-GAACUUCAGGGUCAGCUUGCC (antisense), or a scrambled control siRNA (scRNA) with sequence 5'-AGUACUGCUUACGAUACGGTT (sense) and 3'-CCGUAUCGUAAGCAGUACUTT (anti-sense) (**Figure 4.8**). Loss in metabolic activity was measured 24 h post transfection using a CellTiter 96® AQueous One Solution cell proliferation assay and read using a BioTek® Synergy™ 2 Microplate Reader. GFP expression was measured 9 d post-transfection using a BD Accuri™ C6 flow cytometer (emission filter: 530/30 nm). Transfections were performed with 26.7 nM siRNA using R647 or 647 at either 450 wt/wt or 112.5 wt/wt. The 450 wt/wt formulation of 647 achieved 75 ± 12% GFP knockdown but with 94 ± 1% loss in metabolic activity, indicating that this treatment was very toxic. The 112.5 wt/wt formulations of R647 and 647 did not exhibit

marked loss in metabolic activity, but were unable to achieve substantial GFP knockdown at 2 ± 4% and 4 ± 4% knockdown, respectively. This result is not surprising as polymer hydrophobicity has been shown to promote better siRNA delivery; however, there is no concentration at which 647 is both safe and effective.[19] Incredibly, R647 at 450 wt/wt achieved 92 ± 1% GFP knockdown, with no measurable loss in metabolic activity. This demonstrates that addition of a bioreducible moiety to the PBAE backbone not only improved siRNA delivery but also attenuated toxicity. Compared to the leading commercially available reagent Lipofectamine™ 2000, R647 achieved more than double the % knockdown and prevented typically observed cytotoxicity.

4.3.4. Synthesis and characterization of bioreducible/hydrophobic PBAEs

We were able to successfully synthesize and characterize bioreducible and hydrophobic PBAEs. Bioreducible monomer 2,2'-disulfanediylbis(ethane-2,1-diyl) diacrylate BR6 was synthesized in a method similar to Chen *et al.*[35] Synthesis of bioreducible and hydrophobic polymers was achieved by mixing backbone monomers 2,2'-disulfanediylbis(ethane-2,1-diyl) (BR6) and hexane-1,6-diyl diacrylate (B6) at ratios of either 1:0, 3:1, 1:1, 1:3, or 0:1 prior to polymerization with side chain monomers 3-amino-1-propanol (S3), 4-amino-1-butanol (S4), or 5-amino-1-pentanol (S5). Polymers were then endcapped with small molecule 1-(3-aminopropyl)-4-methylpiperazine (E7) (**Figure 4.9**). As an example, a polymer synthesized with a 3:1 BR6:B6 ratio, side chain S3, and end-capped with E7 will be referred to as "3:1 R637", while the same polymer with a 0:1 BR6:B6 ratio will be referred to as "637." BR6 has almost the same structure as B6, except that it contains a disulfide linkage. As the ratio of BR6:B6 increases, so does the bioreducibility of the combined polymer. Proton nuclear magnetic resonance (^{1}H NMR) was used to confirm the identity and purity of the polymers (**Figure 4.10**), while gel permeation

chromatography (GPC) was used to confirm the size and polydispersities of the polymers (**Table 4.1**).

4.3.5. Trends in *in vitro* delivery of bioreducible/hydrophobic PBAEs

The *in vitro* siRNA delivery efficacy and cytotoxicity of each of these fifteen polymers was evaluated in primary human glioblastoma (GBM 319) cells expressing constitutive GFP,[38] using GFP-targeting or a scrambled control siRNA (scRNA). Lipofectamine™ 2000 and siRNA alone were used as controls with 20 nM siRNA. To evaluate the effect of polymer structure, nanoparticles were formed with all fifteen polymers to yield final *in vitro* concentrations of 180 μg/mL polymer and 20 nM siRNA. These results, which are presented in **Figure 4.11**, show interesting trends with regard to polymer bioreducibility and hydrophobicity. First, the results show that as the polymer side chain becomes more hydrophobic, toxicity increases, a conclusion supported by the statistical results shown in **Table 4.2**. An example is polymer 1:1 R647 that formed nanoparticles that caused -9 ± 11% (essentially zero) loss in metabolic activity *versus* polymer 1:1 R657, which has a side chain longer by only one hydrocarbon but formed nanoparticles that caused 77 ± 13% loss in metabolic activity. Second, the results show that polymer bioreducibility significantly reduces cytotoxicity. For example, polymers based on 1:1 BR6:B6, in which ~50% of repeat units are bioreducible, have dramatically less cytotoxicity than polymers based on 1:3 BR6:B6, in which only ~25% of repeat units are bioreducible (**Table 4.2**). A particular example of this extreme toxicity change with a small change to polymer structure is 1:1 R647, which formed nanoparticles that caused no significant loss in metabolic activity, *versus* 1:3 R647-based nanoparticles, which caused a loss in metabolic activity of 83 ± 1%.

The tuneable toxicities of these polymers is interesting, as polymer hydrophobicity has been shown to promote enhanced nucleic acid delivery[19, 31]; therefore, hydrophobic polymers, such

as 647, may be effective for siRNA delivery but are too toxic to have an effective therapeutic window. By combining hydrophobic monomers with bioreducible ones, we have been able to harness the useful properties of hydrophobicity while reducing cytotoxicity and promoting cytoplasmic cargo release. Polymer R647, for example, formed nanoparticles that achieved 81 ± 3% GFP knockdown *versus* 3:1 R647, which achieved 91 ± 1%, a significant increase ($p < 0.05$ by Student's T test), resulting only from making 25% of repeat units more hydrophobic. Another interesting result from these studies was that eight of the polymeric nanoparticles tested achieved significantly higher GFP knockdown than Lipofectamine™ 2000 without causing significantly higher loss of metabolic activity. An example fluorescence image of 1:1 R647 nanoparticle treated cells demonstrating safety and efficacy is shown in **Figure 4.12e**.

In order to further elucidate the nanoparticle properties favorable for safe and effective siRNA delivery, we sought to examine the effects of changing nanoparticle formulation and the resulting physical properties associated with these changes. First, siRNA dose-dependency was examined by delivering siRNA at final *in vitro* doses ranging from 1-160 nM using polymer 1:1 R647 at a fixed concentration of 180 μg/mL (**Figure 4.12a,c**). An intriguing result from this experiment is that we were able to achieve significantly higher GFP knockdown using only 5 nM siRNA (76 ± 14%) compared to leading commercially-available Lipofectamine™ 2000 with 20 nM siRNA (40 ± 7%). Importantly, none of the formulations tested was significantly more toxic to the cells than Lipofectamine™ 2000. Additionally, we achieved 63 ± 16% GFP knockdown with as little as 1 nM siRNA, demonstrating the efficiency of these bioreducible siRNA-containing nanoparticles. Interestingly, we did not see a particularly strong siRNA dose-dependent trend of GFP knockdown within the range of nanoparticle formulations tested, as almost all siRNA doses evaluated caused uniformly high knockdown. Of the nine polymer/siRNA doses tested, seven

achieved more than 75% knockdown and were significantly more effective than Lipofectamine™ 2000. For these samples, knockdown correlated semilogarithmically with siRNA dose (R^2 = 0.8649).

Polymer concentration dependency was examined by carrying out transfections with 20 nM siRNA and varying 1:1 R647 concentrations from 11.25-360 μg/mL (**Figure 4.12b,d**). Interestingly, GFP knockdown correlated linearly with polymer concentration with R^2 = 0.9440. In order to elucidate the mechanisms behind these surprising results, we analyzed the nanoparticle physical properties associated with each delivery method to determine the size, zeta potential, nanoparticle concentration, and siRNA loading of each formulation. siRNA loading was calculated from the nanoparticle concentration, total siRNA dose, and siRNA molecular weight. Nanoparticle concentration measurements were quantified in a manner consistent with the protocol described by Bhise *et al.*[34]

4.3.6. Trends in bioreducible/hydrophobic PBAE nanoparticle physical properties

In order to evaluate the ability of the polymers to complex with siRNA to form nanoparticles, we determined the polymer/siRNA weight ratios (wt/wts) at which siRNA became completely complexed. We performed a gel retention assay using 1:1 R647 with wt/wts ranging from 37.5-600 wt/wt (**Figure 4.13**). We found that siRNA is completely bound to 1:1 R647 at wt/wts as low as 150 wt/wt, but not at 75 or 37.5 wt/wt. This study also enabled us to validate that siRNA loading could not be accurately calculated for nanoparticle formulations at these lower wt/wts. In order to demonstrate the siRNA release efficacy of this polymer in a reducing environment comparable to the cytosol,[17] particles were incubated in a solution of 5 mM glutathione for 15 min prior to electrophoresis. All formulations tested showed complete siRNA release, showing that siRNA unloading can occur within minutes of reaching the cytosol, in an

environmentally triggered manner, due to the disulfide linkages in the polymer. While there are also ester linkages in these bioreducible PBAEs, the half-life for hydrolysis of the ester bonds in this class of materials is on the order of hours,[39] while the half-life for bioreduction of the disulfide bonds is on the order of minutes in the presence of glutathione.[21] While **Figure 4.13** shows that intracellular siRNA release is likely driven by disulfide degradation, the hydrolytic degradability of the polymers may afford an additional reduction in potential toxicity.

Nanoparticle properties were measured using the same formulations shown in **Figure 4.12a**, in which siRNA dose was varied from 1-160 nM and 1:1 R647 concentration remained the same at 180 μg/mL. Nanoparticle diameter was shown to correlate with siRNA dose on a semilogarithmic scale (R^2 = 0.9077), while zeta potential remained consistently between 18-22 mV (**Figure 4.14a**). Size measurements were also completed using 0 nM siRNA, which showed smaller polymeric particles, 78 ± 4 nm in size. Nanoparticle concentration remained nearly constant with changing siRNA dose, even with 0 nM siRNA, staying between 1.29-1.66 x 10^{11} particles/mL (R^2 = 0.0013). siRNA loading was calculated and demonstrated a linear correlation with siRNA dose (R^2 = 0.9980).

We repeated the same experiments, this time using the nanoparticle formulations shown in **Figure 4.12b**, where siRNA dose remained constant at 20 nM and 1:1 R647 concentration was varied from 11.25-360 μg/mL. Polymer concentration did not correlate well with either nanoparticle diameter (R^2 = 0.3012) or zeta potential (R^2 = 0.4280) (**Figure 4.14b**). Nanoparticle concentration, however, fit a linear regression *versus* polymer concentration (R^2 = 0.9496). This resulted in siRNA loading values that exponentially decayed with increasing polymer concentration (R^2 = 0.9989), meaning that the most effective siRNA delivery formulations in this

group consisted of the highest nanoparticle concentrations but with the lowest siRNA loading values.

When calculating siRNA loading, we were calculating average siRNA loading across a nanoparticle batch. We believe that siRNA loading within these batches is also roughly uniform based on the presence of a constant nanoparticle concentration across all siRNA doses as well as linearly increasing nanoparticle diameters with increasing siRNA dose. To further characterize nanoparticle size and siRNA loading, we performed transmission electron microscopy (TEM) on 1:1 R647 at 180 μg/mL with 20 nM siRNA and compared the size histogram results from NTA of this nanoparticle formulation to the corresponding nanoparticle formulation without siRNA (**Figure 4.15**). TEM shows a roughly uniform size distribution, with the presence of a few larger particles/aggregates (**Figure 4.15a**). This matches the NTA analysis as well (**Figure 4.15b**). The NTA histogram of the nanoparticles containing 20 nM siRNA (113 ± 2 nm) were distinct from the smaller nanoparticles containing 0 nM siRNA (78 ± 4 nm). Due to this greater size and monodisperse distribution, it is most likely that as siRNA dose is increased, each nanoparticle contains more siRNA per particle, rather than a significant fraction of nanoparticles remaining empty, which would have resulted in a bimodal particle distribution.

We envision that these bioreducible siRNA nanoparticles could potentially be used for local intracranial delivery of siRNA for the treatment of glioblastoma. In this approach, they would applied in a manner analogous to the GLIADEL® Wafer following surgical resection of glioblastoma. Although we intend for this potential therapeutic to be used for local delivery, rather than systemic delivery, we also looked at transfection in the presence of serum proteins, which are known to reduce the efficacy of many gene delivery systems. We found that

bioreducible PBAE polymers can enable high (80 ± 4%) GFP knockdown in the presence of 10% serum-containing media and knockdown can persist for at least two weeks (**Figure 4.16**).

4.4. Conclusions

We have synthesized and characterized a novel bioreducible PBAE for siRNA delivery to primary human glioblastoma that is both efficacious and non-cytotoxic. The reducible polymer R647 was shown to bind siRNA as well as or slightly better than its non-reducible analog 647. It was determined that this new polymer is capable of condensing siRNA in nanoparticles with the same physical properties as the previously established 647 particles. It was also shown that siRNA release from R647 occurs within minutes of entering a reducing environment comparable to cytosol. We finally demonstrated that R647 nanoparticles that differed from 647 only in reducibility were able to achieve near-complete gene knockdown with no toxicity in human brain cancer cells, while analogous 647 nanoparticles were either extremely toxic or ineffective. This new class of polymer has exciting therapeutic potential as a safe and effective siRNA delivery vehicle.

We were able to show that combining polymer hydrophobicity, a property known to promote enhanced siRNA and DNA delivery,[19, 31] with bioreducibility decreased the cytotoxic effects typical of hydrophobic polymers while optimizing environmentally triggered cytoplasmic cargo release to enhance siRNA delivery. These nanoparticles are safe and effective even at very low siRNA doses. We examined the effects of changing nanoparticle formulation and were able to show that, with this class of materials, nanoparticle concentration is largely determined by polymer concentration and that higher polymer concentrations promote enhanced siRNA delivery. Gene knockdown was shown to be very effective (91 ± 1%) with moderate doses of siRNA (20 nM), and effective (63 ± 16%) even at very low doses of siRNA (1 nM). Bioreducible PBAEs with

tuneable hydrophobicities have exciting potential as safe and efficient siRNA delivery vehicles for nanomedicine applications.

Acknowledgments

This work was supported in part by the NIH (1R01EB016721 and R21CA152473). K.L.K. thanks the NIH Cancer Nanotechnology Training Center (R25CA153952) at the JHU Institute for Nanobiotechnology for fellowship support and S.Y.T. thanks the National Science Foundation for fellowship support. The authors thank the Microscopy and Imaging Core Module of the Wilmer Core Grant, EY001765 for flow cytometry studies. The authors thank Alfredo Quiñones-Hinojosa for the use of GBM 319 and fNPC 34 cells for these experiments.

4.5. Tables

Table 4.1. Gel permeation chromatography results of all polymers

Polymer	M_n	M_w	PDI
R637	2344	3899	1.66
3:1 R637	2623	4548	1.73
1:1 R637	2882	5046	1.75
1:3 R637	3416	5711	1,67
637	2369	3244	1.37
R647	2474	4001	1.62
3:1 R647	2843	4900	1.72
1:1 R647	3211	5597	1.74
1:3 R647	3483	6347	1.82
647	3962	6193	1.56
R657	2628	4102	1.56
3:1 R657	3233	4198	1.30
1:1 R657	2779	4683	1.69
1:3 R657	3560	6038	1.70
657	2357	4158	1.76
R646	2984	5360	1.67
R65Ac	3233	3460	1.07

Table 4.2. Two-way ANOVA of loss in metabolic activity of all polymers

Two-way ANOVA results of loss in metabolic activity	P value	Significance
Side chains		
S3 vs. S4	0.5877	ns
S3 vs. S5	< 0.0001	****
S4 vs. S5	0.0006	***
Base monomers		
R6 vs. 3:1	0.721	ns
R6 vs. 1:1	0.2547	ns
R6 vs. 1:3	< 0.0001	****
R6 vs. B6	< 0.0001	****
3:1 vs. 1:1	0.9266	ns
3:1 vs. 1:3	< 0.0001	****
3:1 vs. B6	< 0.0001	****
1:1 vs. 1:3	< 0.0001	****
1:1 vs. B6	< 0.0001	****
1:3 vs. B6	0.7468	ns

4.6. Figures

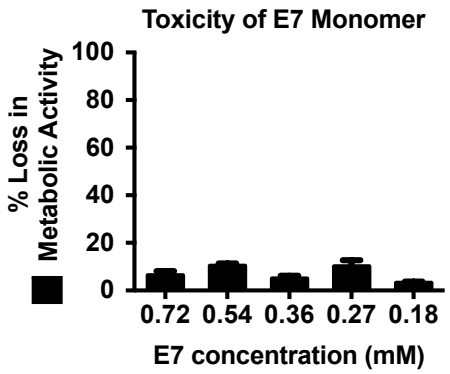

Figure 4.1. Cytotoxicity of monomer E7 to glioblastoma cells at 24 h post-transfection.

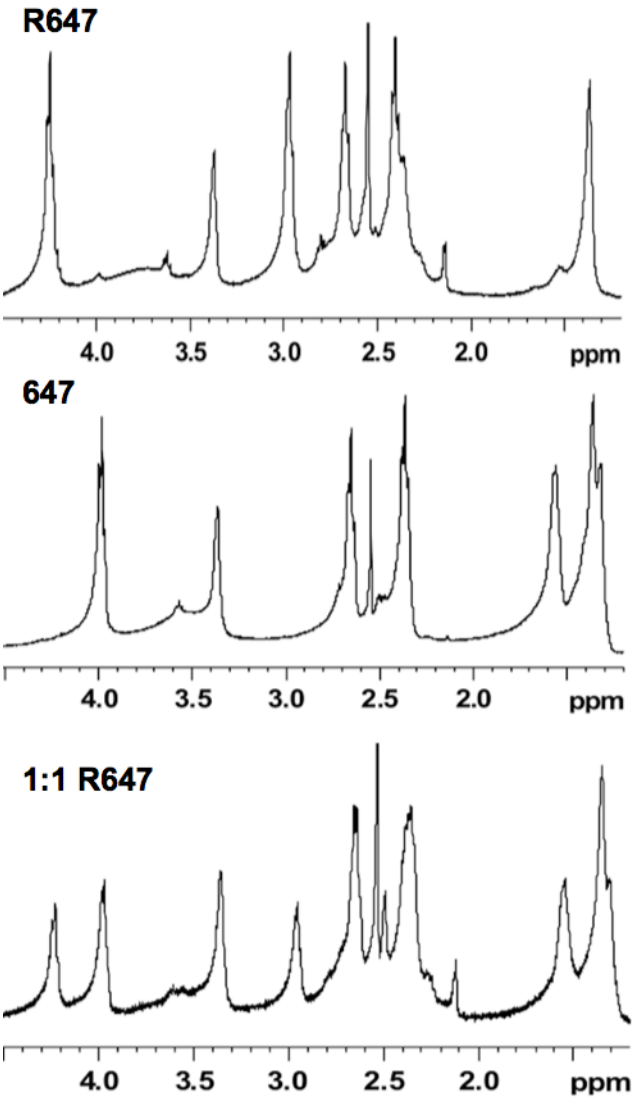

Figure 4.2. NMR spectra of polymers R647, 647, and 1:1 R647. The ratio of BR6:B6 incorporated into polymer 1:1 R647 was calculated by comparing the integrals of the peaks found at δ4.2-4.4 *versus* δ3.9-4.1 (1.00 vs. 1.04). R647 base polymer: (d_6-DMSO, 400Hz), δ1.25-1.5 (4H, *br*, $NCH_2CH_2CH_2CH_2OH$), δ2.3-2.5 (6H, *br,* $OOCCH_2CH_2N$ and $NCH_2CH_2CH_2CH_2OH$), δ2.6-2.7 (4H, *t*, $OOCCH_2CH_2N$), δ2.9-3.1 (4H, *t*, $COOCH_2CH_2S$), δ3.3-3.4 (2H, br, obsc, $NCH_2CH_2CH_2CH_2OH$), δ4.2-4.4 (4H, *t*, $COOCH_2CH_2S$). H^1-NMR of 647 base polymer: (d_6-DMSO, 400Hz), δ1.25-1.5 (8H, br, $NCH_2CH_2CH_2CH_2OH$ and $COOCH_2CH_2CH_2$), δ1.5-1.65 (4H, br, $COOCH_2CH_2CH_2$), δ2.3-2.5 (6H, br, $NCH_2CH_2CH_2CH_2OH$ and $OOCCH_2CH_2N$), δ2.6-2.7 (4H, br, $OOCCH_2CH_2N$), δ3.3-3.4 (2H, br, obsc, $NCH_2CH_2CH_2CH_2OH$), δ3.9-4.1 (4H, br t, $COOCH_2CH_2CH_2$). H^1-NMR of 1:1 R647 base polymer: (d_6-DMSO, 400Hz), δ1.25-1.5 (8H, br, $NCH_2CH_2CH_2CH_2OH$ and $COOCH_2CH_2CH_2$), δ1.5-1.65 (4H, *br*, $COOCH_2CH_2CH_2$), δ2.3-2.5 (6H, *br*, $NCH_2CH_2CH_2CH_2OH$ and $OOCCH_2CH_2N$), δ2.6-2.7 (4H, *t*, $OOCCH_2C$ δ3.9-4.1 (4H, br t, $COOCH_2CH_2CH_2$), H_2N), δ2.9-3.1 (4H, *t*, $COOCH_2CH_2S$), δ3.3-3.4 (2H, br, obsc, $NCH_2CH_2CH_2CH_2OH$), δ3.9-4.1 (4H, br t, $COOCH_2CH_2CH_2$), δ4.2-4.4 (4H, *t*, $COOCH_2CH_2S$). H^1-NMR of E7 endcap: (d_6-DMSO,

400Hz), δ1.50, (2H, quint, $NHCH_2C\mathit{H_2}CH_2N<(CH_2CH_2)>NCH_3$), δ2.13 (3H, s, $NHCH_2CH_2CH_2N<(CH_2CH_2)>NC\mathit{H_3}$), δ2.3-2.4 (10H, br, obsc, $NHCH_2CH_2C\mathit{H_2}N<(C\mathit{H_2}C\mathit{H_2})>NCH_3$), δ2.47 (2H, t, $NHC\mathit{H_2}CH_2CH_2N<(CH_2CH_2)>NCH_3$).

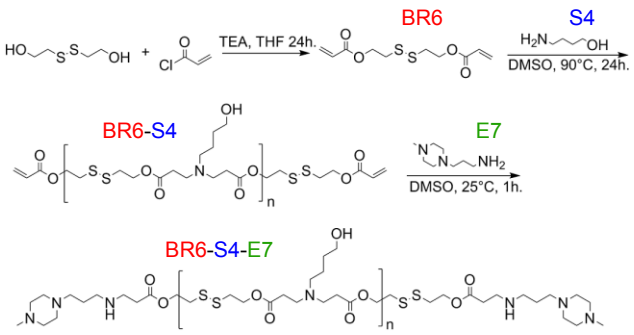

Figure 4.3. Synthesis of bioreducible monomer BR6 and polymer R647.

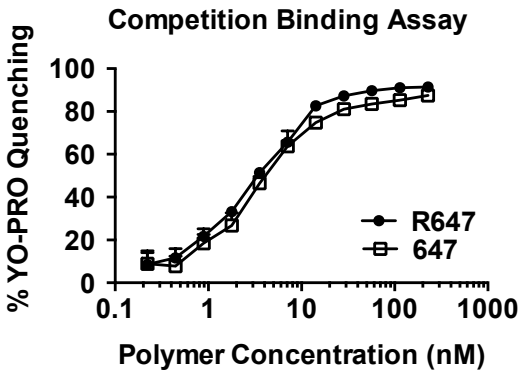

Figure 4.4. Polymer/siRNA competitive binding assay for R647 and 647. Polymer to siRNA binding strength is assessed by quenching of YO-PRO®-1 Iodide fluorescence over increasing polymer concentrations.

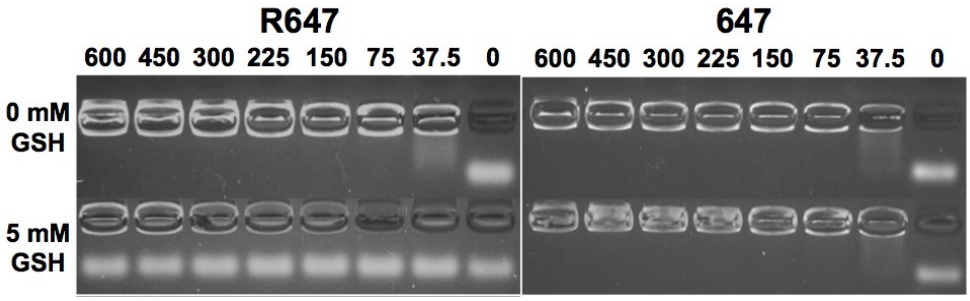

Figure 4.5. Gel retention assay. Gel electrophoresis image of siRNA complexed with R647 (left) or 647 (right) in the absence (0 mM) or presence (5 mM) of GSH. Numbers above each well indicate the polymer to siRNA weight ratio.

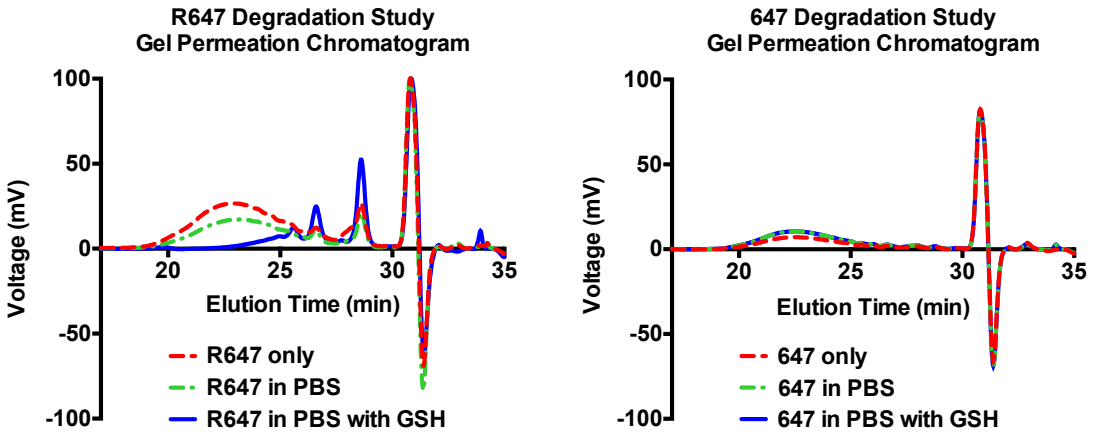

Figure 4.6. GPC results of R647 (left) and 647 (right) following degradation study. Red dashed lines show GPC chromatogram of untreated polymers, green dashed lines show each polymer following a 5 min incubation in PBS, solid blue lines show each polymer following a 5 min incubation in PBS containing 5 mM GSH. The results demonstrate that a reducing environment comparable to the cytosol is capable of degrading R647 and not 647 within 5 min.

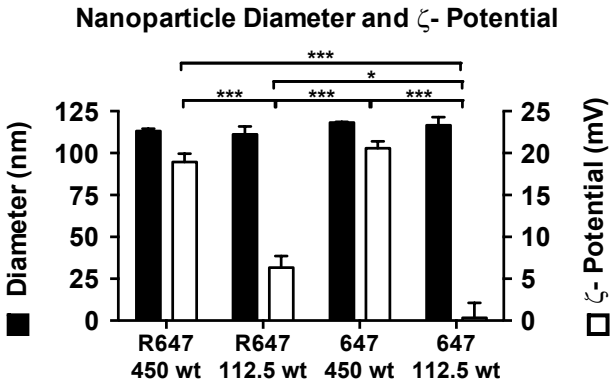

Figure 4.7. Nanoparticle size and surface charge. Nanoparticle diameter and ζ-potential of particles formed using either R647 or 647 at either 450 wt/wt or 112.5 wt/wt. Nanoparticle diameter was measured using NTA. ζ-potential was measured using DLS. Statistical significance was calculated by one-way ANOVA with Tukey's Multiple Comparison post-tests. Nanoparticle diameters of all samples were not significantly different ($p > 0.05$). Nanoparticle zeta potentials that are statistically significant are indicated (* = $p<0.05$, *** = $p<0.001$).

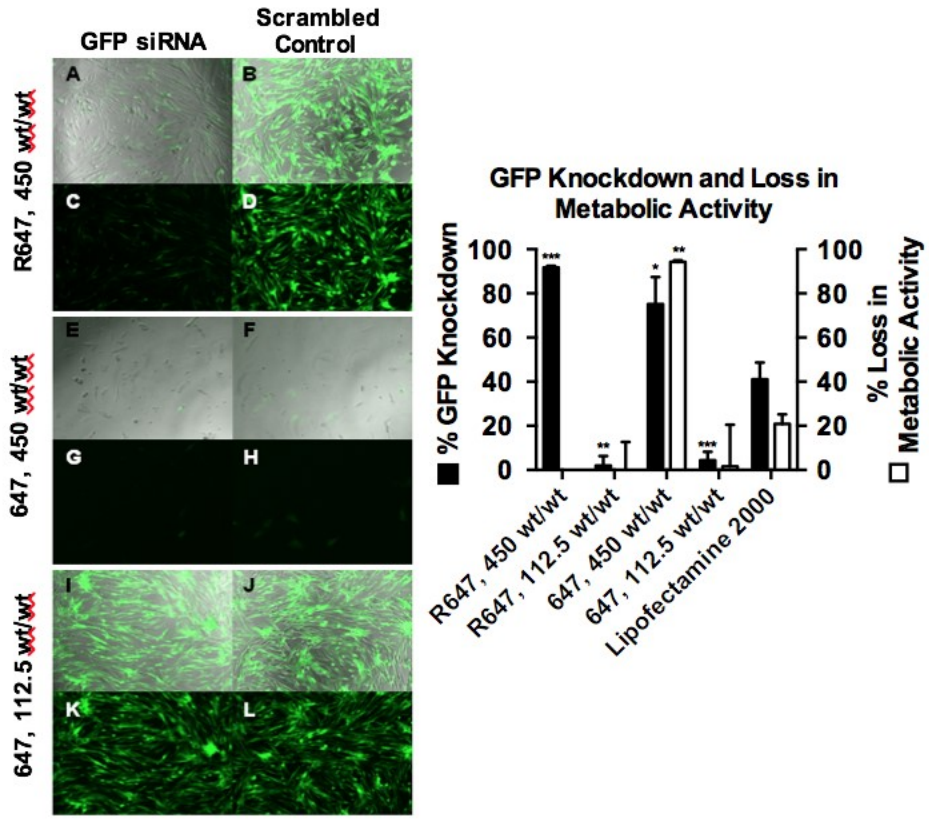

Figure 4.8. Day 9 gene knockdown of GFP$^+$ GBM 319 cells transfected with R647 and 647 at either 450 or 112.5 wt/wt with 26.7 nM siRNA targeted against GFP. Left panel: Brightfield images of R647, 450 wt/wt treated cells (A,B) and 647, 112.5 wt/wt treated cells (I,J) show viable cells while 647, 450 wt/wt treated cells (E,F) show significant toxicity. Fluorescence images of R647, 450 wt/wt treated cells show significantly less GFP expression when formulations contain GFP siRNA (C) versus scrambled control siRNA (D). Fluorescence images of 647, 112.5 wt/wt treated cells show comparable GFP expression in both GFP siRNA (K) and scrambled control treated cells (L). Right panel: Graphical representation of knockdown and loss in metabolic activity results. Lipofectamine™ 2000 positive control with 26.7 nM siRNA is used as the control for statistical comparisons by one-way ANOVA with Dunnett's post-tests (* = $p<0.05$, ** = $p<0.01$, *** = $p<0.001$).

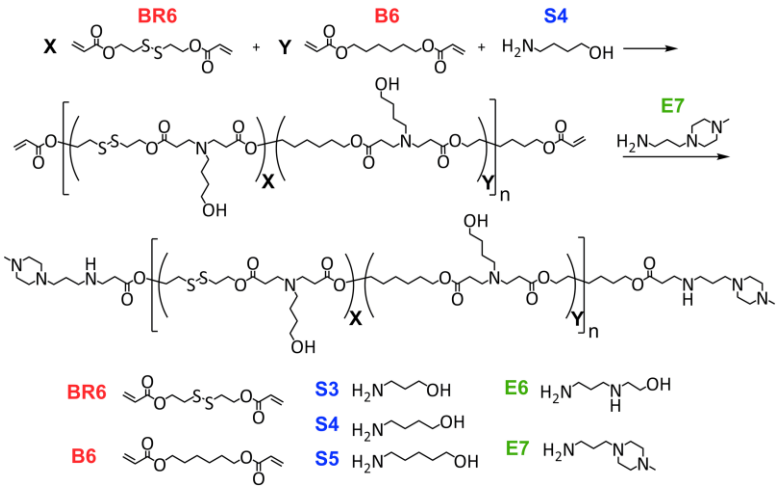

Figure 4.9. Polymer synthesis scheme. Diacrylate backbone monomers BR6 and B6 were randomly copolymerized at a ratio of X:Y with side chain S3, S4, or S5, (demonstrated with S4 above). The resulting acrylate-terminated base polymers were then endcapped with small molecules E6 or E7. The representative polymer shown above would be referred to as "X:Y R647."

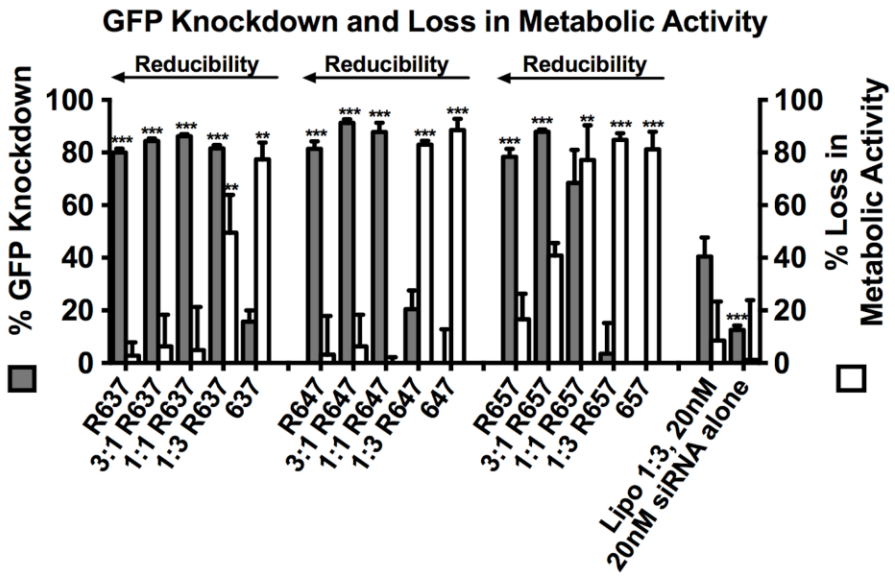

Figure 4.10. Gene knockdown and loss in metabolic activity of polymers with varying bioreducibility and hydrophobicity. Results shown include day 1 loss in metabolic activity and day 9 gene knockdown of GFP^+ GBM 319 cells transfected with all polymers using 180 μg/mL polymer and 20 nM siRNA targeting GFP, normalized to cells treated with the same nanoparticle formulation using scrambled control RNA. Lipofectamine™ 2000 is used as the control for statistical comparisons by one-way ANOVA with Dunnett's post-tests (* = $p<0.05$, ** = $p< 0.01$, *** = $p<0.001$).

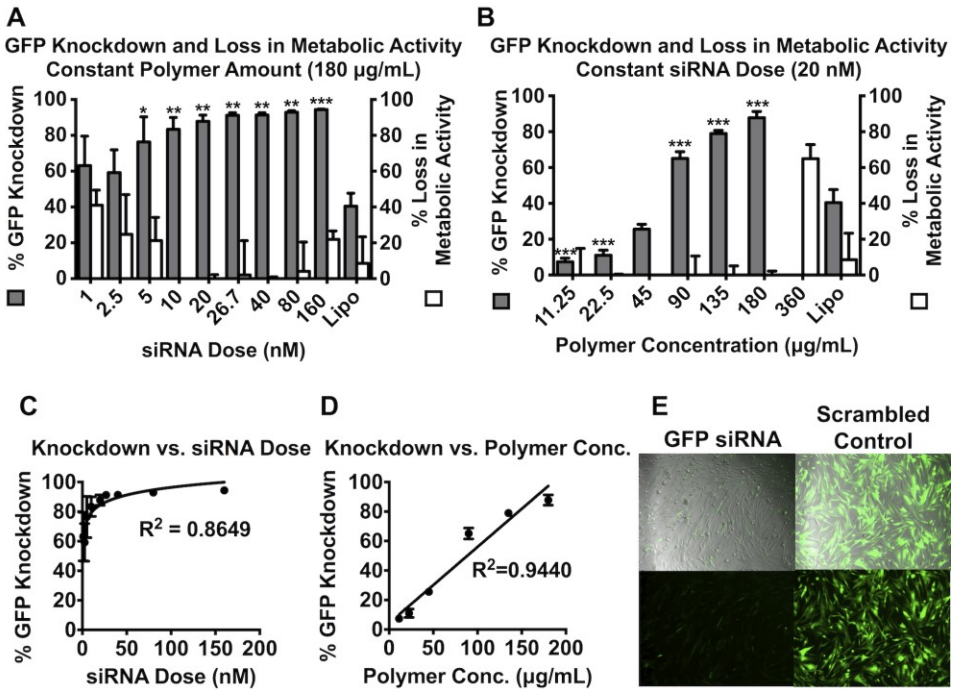

Figure 4.11. GFP knockdown and loss of metabolic activity in GFP$^+$ GBM 319 cells transfected with various formulations of 1:1 R647 siRNA nanoparticles. All knockdown values are normalized to scrambled control RNA. (A) Transfection results using 180 µg/mL polymer with siRNA doses ranging from 1-160 nM. The Lipofectamine™ 2000 control shown used 20 nM siRNA. (B) Transfection results using 20 nM siRNA with polymer concentrations ranging from 11.25-360 µg/mL. (C) Correlation of knockdown efficiency and varying siRNA doses with polymer concentration fixed at 180 µg/mL fitted to a semilogarithmic line. (D) Correlation of knockdown efficiency and varying polymer concentrations with siRNA concentration fixed at 20 nM fitted to a linear regression. (E) Phase contrast (top) and fluorescence (bottom) images of GFP$^+$ GBM cells treated with 1:1 R647 at 180 µg/mL and 20 nM of either siRNA targeting GFP (left) or scrambled control RNA (right) nanoparticles. Lipofectamine™ 2000 is used as the control for statistical comparisons by one-way ANOVA with Dunnett's post-tests (* = $p<0.05$, ** = $p< 0.01$, *** = $p<0.001$).

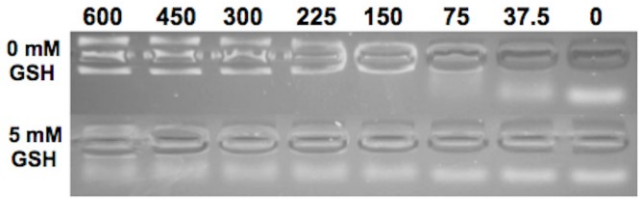

Figure 4.12. Gel retention assay of 1:1 R647 particles formed at varying wt/wts and incubated for 15 min at room temperature in the absence (top) or presence (bottom) of 5 mM GSH. Columns above each well indicate polymer to siRNA weight ratio (wt/wt).

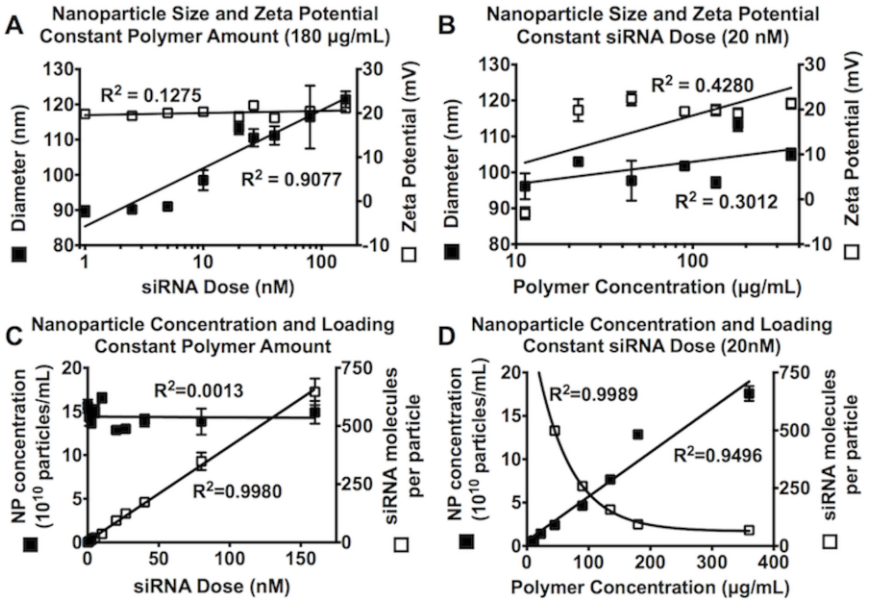

Figure 4.13. Characterization of nanoparticle size, zeta potential, concentration, and loading of nanoparticles synthesized with 180 µg/mL 1:1 R647 and varying siRNA doses (A, C) or with 20 nM siRNA and varying polymer concentrations (B, D). Size and concentration were measured by NTA, zeta potential was measured using DLS, and siRNA loading was calculated from concentration. (A) Nanoparticle size positively correlates with siRNA dose on a semilogarthimic scale, while zeta potential does not change. (B) Nanoparticle size and zeta potential do not strongly correlate with polymer concentration. (C) Nanoparticle concentration remains consistent despite changing siRNA dose, while siRNA loading increases linearly. (D) Nanoparticle concentration linearly increases with polymer concentration resulting in exponential decay of siRNA loading with increasing polymer concentration.

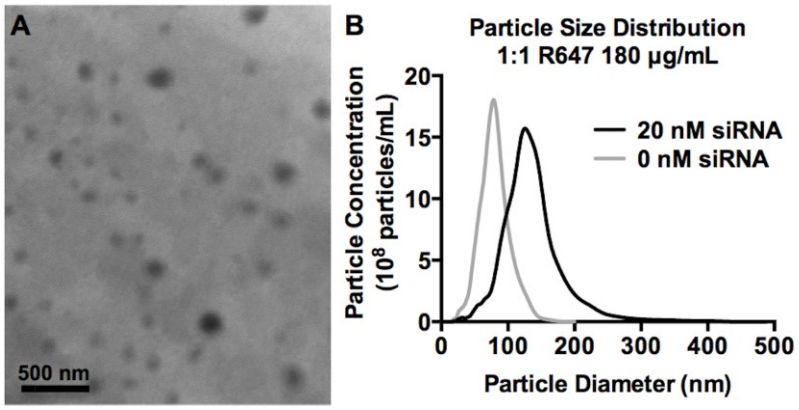

Figure 4.14. Characterization of nanoparticle size distribution. (A) TEM image of nanoparticles made with 1:1 R647 at 180 µg/mL and 20 nM siRNA. (B) Nanoparticle size distribution of 1:1 R647 at 180 µg/mL and either 20 nM siRNA or 0 nM siRNA as measured by NTA.

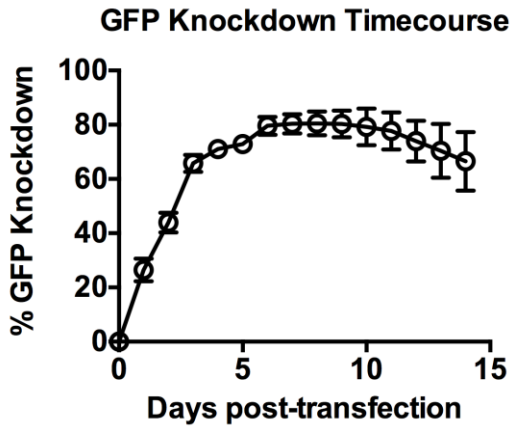

Figure 4.15. Gene knockdown in serum-containing media. Results show timecourse of GFP knockdown in GFP^+ glioblastoma cells following transfection in media containing 10% serum. Polymer R65Ac was used at a 600 wt/wt ratio with 45 nM siRNA.

4.7. References

1. Fire, A.; Xu, S. Q.; Montgomery, M. K.; Kostas, S. A.; Driver, S. E.; Mello, C. C. Potent and Specific Genetic Interference by Double-Stranded Rna in Caenorhabditis Elegans. *Nature* **1998,** 391, 806-811.
2. Wu, W.; Sun, M.; Zou, G. M.; Chen, J. Microrna and Cancer: Current Status and Prospective. *Int. J. Cancer* **2007,** 120, 953-960.
3. Yadav, S.; van Vlerken, L. E.; Little, S. R.; Amiji, M. M. Evaluations of Combination Mdr-1 Gene Silencing and Paclitaxel Administration in Biodegradable Polymeric Nanoparticle Formulations to Overcome Multidrug Resistance in Cancer Cells. *Cancer Chemother. Pharmacol.* **2009,** 63, 711-722.
4. Akinc, A.; Zumbuehl, A.; Goldberg, M.; Leshchiner, E. S.; Busini, V.; Hossain, N.; Bacallado, S. A.; Nguyen, D. N.; Fuller, J.; Alvarez, R.; Borodovsky, A.; Borland, T.; Constien, R.; de Fougerolles, A.; Dorkin, J. R.; Jayaprakash, K. N.; Jayaraman, M.; John, M.; Koteliansky, V.; Manoharan, M.; Nechev, L.; Qin, J.; Racie, T.; Raitcheva, D.; Rajeev, K. G.; Sah, D. W. Y.; Soutschek, J.; Toudjarska, I.; Vornlocher, H. P.; Zimmermann, T. S.; Langer, R.; Anderson, D. G. A Combinatorial Library of Lipid-Like Materials for Delivery of Rnai Therapeutics. *Nat. Biotechnol.* **2008,** 26, 561-569.
5. Semple, S. C.; Akinc, A.; Chen, J.; Sandhu, A. P.; Mui, B. L.; Cho, C. K.; Sah, D. W.; Stebbing, D.; Crosley, E. J.; Yaworski, E.; Hafez, I. M.; Dorkin, J. R.; Qin, J.; Lam, K.; Rajeev, K. G.; Wong, K. F.; Jeffs, L. B.; Nechev, L.; Eisenhardt, M. L.; Jayaraman, M.; Kazem, M.; Maier, M. A.; Srinivasulu, M.; Weinstein, M. J.; Chen, Q.; Alvarez, R.; Barros, S. A.; De, S.; Klimuk, S. K.; Borland, T.; Kosovrasti, V.; Cantley, W. L.; Tam, Y. K.; Manoharan, M.; Ciufolini, M. A.; Tracy, M. A.; de Fougerolles, A.; MacLachlan, I.; Cullis, P. R.; Madden, T. D.; Hope, M. J. Rational Design of Cationic Lipids for Sirna Delivery. *Nat. Biotechnol.* **2010,** 28, 172-176.
6. Derfus, A. M.; Chen, A. A.; Min, D. H.; Ruoslahti, E.; Bhatia, S. N. Targeted Quantum Dot Conjugates for Sirna Delivery. *Bioconjugate Chem.* **2007,** 18, 1391-1396.
7. Elbakry, A.; Zaky, A.; Liebl, R.; Rachel, R.; Goepferich, A.; Breunig, M. Layer-by-Layer Assembled Gold Nanoparticles for Sirna Delivery. *Nano Lett.* **2009,** 9, 2059-2064.
8. Kakizawa, Y.; Furukawa, S.; Ishii, A.; Kataoka, K. Organic-Inorganic Hybrid-Nanocarrier of Sirna Constructing through the Self-Assembly of Calcium Phosphate and Peg-Based Block Aniomer. *J. Control. Release* **2006,** 111, 368-370.
9. Breunig, M.; Hozsa, C.; Lungwitz, U.; Watanabe, K.; Umeda, I.; Kato, H.; Goepferich, A. Mechanistic Investigation of Poly (Ethylene Imine)-Based Sirna Delivery: Disulfide Bonds Boost Intracellular Release of the Cargo. *J. Control. Release* **2008,** 130, 57-63.
10. Matsumoto, S.; Christie, R. J.; Nishiyama, N.; Miyata, K.; Ishii, A.; Oba, M.; Koyama, H.; Yamasaki, Y.; Kataoka, K. Environment-Responsive Block Copolymer Micelles with a Disulfide Cross-Linked Core for Enhanced Sirna Delivery. *Biomacromolecules* **2009,** 10, 119-127.
11. van der Aa, L. J.; Vader, P.; Storm, G.; Schiffelers, R. M.; Engbersen, J. F. J. Optimization of Poly(Amido Amine)S as Vectors for Sirna Delivery. *J. Control. Release* **2011,** 150, 177-186.
12. Boussif, O.; Lezoualch, F.; Zanta, M. A.; Mergny, M. D.; Scherman, D.; Demeneix, B.; Behr, J. P. A Versatile Vector for Gene and Oligonucleotide Transfer into Cells in Culture and in-Vivo - Polyethylenimine. *P Natl Acad Sci USA* **1995,** 92, 7297-7301.

13. Lynn, D. M.; Langer, R. Degradable Poly (Beta-Amino Esters): Synthesis, Characterization, and Self-Assembly with Plasmid DNA. *Journal of the American Chemical Society* **2000,** 122, 10761-10768.
14. Hagerman, P. J. Flexibility of Rna. *Annu. Rev. Biophys. Biomol. Struct.* **1997,** 26, 139-156.
15. Kebbekus, P.; Draper, D. E.; Hagerman, P. Persistence Length of Rna. *Biochemistry* **1995,** 34, 4354-4357.
16. Kawasaki, H.; Taira, K. Short Hairpin Type of Dsrnas That Are Controlled by Trnaval Promoter Significantly Induce Rnai-Mediated Gene Silencing in the Cytoplasm of Human Cells. *Nucleic Acids Res.* **2003,** 31, 700-707.
17. Griffith, O. W. Biologic and Pharmacologic Regulation of Mammalian Glutathione Synthesis. *Free Radical Bio. Med.* **1999,** 27, 922-935.
18. Miyata, K.; Kakizawa, Y.; Nishiyama, N.; Harada, A.; Yamasaki, Y.; Koyama, H.; Kataoka, K. Block Catiomer Polyplexes with Regulated Densities of Charge and Disulfide Cross-Linking Directed to Enhance Gene Expression. *J. Am. Chem. Soc.* **2004,** 126, 2355-2361.
19. Tzeng, S. Y.; Green, J. J. Subtle Changes to Polymer Structure and Degradation Mechanism Enable Highly Effective Nanoparticles for Sirna and DNA Delivery to Human Brain Cancer. *Advanced Healthcare Materials* **2013,** 2, 468-480.
20. Tzeng, S. Y.; Hung, B. P.; Grayson, W. L.; Green, J. J. Cystamine-Terminated Poly(Beta-Amino Ester)S for Sirna Delivery to Human Mesenchymal Stem Cells and Enhancement of Osteogenic Differentiation. *Biomaterials* **2012,** 33, 8142-8151.
21. Kozielski, K. L.; Tzeng, S. Y.; Green, J. J. A Bioreducible Linear Poly(Beta-Amino Ester) for Sirna Delivery. *Chem. Commun.* **2013,** 49, 5319 - 5321.
22. Vader, P.; van der Aa, L. J.; Engbersen, J. F. J.; Storm, G.; Schiffelers, R. M. Disulfide-Based Poly(Amido Amine)S for Sirna Delivery: Effects of Structure on Sirna Complexation, Cellular Uptake, Gene Silencing and Toxicity. *Pharmaceut. Res.* **2011,** 28, 1013-1022.
23. Jeong, J. H.; Christensen, L. V.; Yockman, J. W.; Zhong, Z. Y.; Engbersen, J. F. J.; Kim, W. J.; Feijen, J.; Kim, S. W. Reducible Poly(Amido Ethylenimine) Directed to Enhance Rna Interference. *Biomaterials* **2007,** 28, 1912-1917.
24. Wyman, T. B.; Nicol, F.; Zelphati, O.; Scaria, P.; Plank, C.; Szoka Jr, F. C. Design, Synthesis, and Characterization of a Cationic Peptide That Binds to Nucleic Acids and Permeabilizes Bilayers. *Biochemistry-Us* **1997,** 36, 3008-3017.
25. Mok, H.; Park, T. G. Self-Crosslinked and Reducible Fusogenic Peptides for Intracellular Delivery of Sirna. *Biopolymers* **2008,** 89, 881-888.
26. Tzeng, S. Y.; Yang, P. H.; Grayson, W. L.; Green, J. J. Synthetic Poly(Ester Amine) and Poly(Amido Amine) Nanoparticles for Efficient DNA and Sirna Delivery to Human Endothelial Cells. *Int. J. Nanomedicine* **2012,** 6, 3309-3322.
27. Sunshine, J. C.; Peng, D. Y.; Green, J. J. Uptake and Transfection with Polymeric Nanoparticles Are Dependent on Polymer End-Group Structure, but Largely Independent of Nanoparticle Physical and Chemical Properties. *Mol. Pharm.* **2012,** 9, 3375 - 3383.
28. Yin, Q.; Gao, Y.; Zhang, Z.; Zhang, P.; Li, Y. Bioreducible Poly (Beta-Amino Esters)/Shrna Complex Nanoparticles for Efficient Rna Delivery. *J. Control. Release* **2011,** 151, 35-44.
29. Yin, Q.; Shen, J.; Chen, L.; Zhang, Z.; Gu, W.; Li, Y. Overcoming Multidrug Resistance by Co-Delivery of Mdr-1 and Survivin-Targeting Rna with Reduction-Responsible Cationic Poly (Beta-Amino Esters). *Biomaterials* **2012,** 33.

30. Lee, J. S.; Green, J. J.; Love, K. T.; Sunshine, J.; Langer, R.; Anderson, D. G. Gold, Poly(Beta-Amino Ester) Nanoparticles for Small Interfering Rna Delivery. *Nano Letters* **2009,** 9, 2402-2406.
31. Sunshine, J. C.; Akanda, M. I.; Li, D.; Kozielski, K. L.; Green, J. J. Effects of Base Polymer Hydrophobicity and End-Group Modification on Polymeric Gene Delivery. *Biomacromolecules* **2011,** 12, 3592-3600.
32. Bhise, N. S.; Gray, R. S.; Sunshine, J. C.; Htet, S.; Ewald, A. J.; Green, J. J. The Relationship between Terminal Functionalization and Molecular Weight of a Gene Delivery Polymer and Transfection Efficacy in Mammary Epithelial 2-D Cultures and 3-D Organotypic Cultures. *Biomaterials* **2010,** 31, 8088-8096.
33. Ravin, R.; Blank, P. S.; Steinkamp, A.; Rappaport, S. M.; Ravin, N.; Bezrukov, L.; Guerrero-Cazares, H.; Quinones-Hinojosa, A.; Bezrukov, S. M.; Zimmerberg, J. Shear Forces During Blast, Not Abrupt Changes in Pressure Alone, Generate Calcium Activity in Human Brain Cells. *PLoS One* **2012,** 7, e39421.
34. Bhise, N. S.; Shmueli, R. B.; Gonzalez, J.; Green, J. J. A Novel Assay for Quantifying the Number of Plasmids Encapsulated by Polymer Nanoparticles. *Small* **2012,** 8, 367-373.
35. Chen, J.; Qiu, X.; Ouyang, J.; Kong, J.; Zhong, W.; Xing, M. M. Ph and Reduction Dual-Sensitive Copolymeric Micelles for Intracellular Doxorubicin Delivery. *Biomacromolecules* **2011,** 12, 3601-3611.
36. Tzeng, S. Y.; Yang, P. H.; Grayson, W. L.; Green, J. J. Synthetic Poly (Ester Amine) and Poly (Amido Amine) Nanoparticles for Efficient DNA and Sirna Delivery to Human Endothelial Cells. *International journal of nanomedicine* **2011,** 6, 3309-3322.
37. Green, J. J.; Langer, R.; Anderson, D. G. A Combinatorial Polymer Library Approach Yields Insight into Nonviral Gene Delivery. *Accounts of chemical research* **2008,** 41, 749-759.
38. Tzeng, S. Y.; Guerrero-Cazares, H.; Martinez, E. E.; Sunshine, J. C.; Quiñones-Hinojosa, A.; Green, J. J. Non-Viral Gene Delivery Nanoparticles Based on Poly (Beta-Amino Esters) for Treatment of Glioblastoma. *Biomaterials* **2011,** 32, 5402-5410.
39. Sunshine, J. C.; Peng, D. Y.; Green, J. J. Uptake and Transfection with Polymeric Nanoparticles Are Dependent on Polymer End-Group Structure, but Largely Independent of Nanoparticle Physical and Chemical Properties. *Mol Pharm* **2012,** 9, 3375-3383.

Chapter 5

Cancer-selective nanoparticles for combinatorial siRNA delivery to primary human GBM *in vitro* and *in vivo*

5.1. Introduction

The goal of this work was to create a novel siRNA delivery nanotechnology capable of treating and preventing the recurrence of glioblastoma, the most malignant primary human brain cancer.[1-3] There is increasing evidence that brain tumor recurrence is due to the presence of a subset of cancer cells that are stem-like and tumor-propagating. These cells are believed to be able to survive conventional treatments and to be able to migrate away from the primary tumor site and form new tumors.[4, 5] RNA interference (RNAi), a natural cellular process that can prevent the expression of genes in a sequence-specific manner, can be induced by the introduction of short interfering RNA (siRNA) into the cells.[6] Using siRNA to turn off the genes that allow GBM cells to survive treatment, to migrate, and to form new tumors has the potential to prevent tumor recurrence following treatment. However, siRNA delivery is challenging. Viral siRNA delivery has many potential problems such as tumorigenicity and immunogenicity, and is generally limited to carrying one type of siRNA, as multiple doses could increase the risks of using them in patients.[7]

In **Chapter 4**, we showed that we have been able to synthesize a novel, bioreducible poly(beta-amino ester) (PBAE)-based nanoparticle capable of safe and effective delivery of siRNA to primary human glioblastoma cells.[8] We have also shown that we can achieve near complete gene knockdown of a fluorescent marker gene using only a fraction of the siRNA that

---

This chapter contains material modified from the following article, previously published as:
Kozielski, K.L.; Tzeng, S. Y.; Hurtado de Mendoza, B. A.; Green, J.J: Bioreducible cationic polymer-based nanoparticles for efficient and environmentally triggered cytoplasmic siRNA delivery to primary human brain cancer cells. *ACS Nano* **2014**, *8,* 3232-3241.

we can load into the nanoparticles.[9] This work led us to hypothesize that since only a fraction of the loaded siRNA was needed for gene knockdown, perhaps we could load several different siRNAs into each particle and still achieve simultaneous knockdown of all targeted genes. Herein we will discuss the ability of bioreducible PBAEs to simultaneously and robustly knockdown the expression of multiple genes that promote tumor survival and enable recurrence.

We will also show *in vitro* work that demonstrates that these nanoparticles preferentially induce RNAi in GBM cells and not in healthy human brain cells. Synthesizing nanoparticles capable of selectively delivering siRNA to tumor cells would allow us to target any gene necessary to tumor survival without worrying about delivering a potentially harmful siRNA to surrounding healthy cells. Targeting genes that allow tumor cells to survive, migrate, and form new tumors will allow us to create a technology capable of reducing GBM cells' proliferative and regenerative capacity. Moreover, delivering multiple siRNAs will allow us to shut down parallel biological pathways simultaneously so that compensatory mechanisms cannot restore the cell's malignant phenotype. Generating a tumor-targeting therapy capable of simultaneously shutting down multiple pathways that enable tumor behavior has the potential to be a selective and robust GBM therapy.

5.2. Materials and Methods

5.2.1. Materials

All chemicals used to synthesize bioreducible PBAE monomer BR6 were purchased from Sigma-Aldrich Chemical Company (St. Louis, MO) and used without further purification. PBAE monomers were purchased from Alfa Aesar (Ward Hill, MA). All siRNA oligos were purchased from Origene Technologies (Rockville, MD), with the exception of AllStars Human Cell Death

siRNA (siDeath), which was purchased from Qiagen. Western blotting antibodies for Yes-associated protein 1 (YAP1), Sodium-potassium-chloride cotransporter 1 (NKCC1), Survivin, Roundabout homolog 1 (Robo1), Endothelial growth factor receptor (EGFR), and β-Actin were purchased from vendors listed in **Table 5.1**. Cannulas for orthotopic tumor implantation and nanoparticle administration were purchased from Plastics One Inc. (Roanoke, VA).

5.2.2. Bioreducible polymer synthesis

Monomer BR6 was synthesized as previously described in **Chapter 4**. Briefly, bis(2-hydroxyethyl) disulfide was acrylated with acryloyl chloride in anhydrous conditions in the presence of triethylamine (TEA). TEA HCl precipitate was removed via filtration, and other impurities were removed via aqueous washes of Na_2CO_3, followed by water. The final product was purified from organic solvents using rotary evaporation. Polymer synthesis of polymer R646 was carried out in a method similar to as described in **Chapter 4**, although tetrahydrofuran (THF) was used as the polymerization solvent and the polymerization reaction temperature was 60ºC. Following polymerization and end-capping, unreacted monomer was removed via ether purification, in which the polymer solution was mixed in a 1:5 v/v ratio with diethyl ether, centrifuged at 3220 RCF, and excess ether removed via decantation. This was repeated, and remaining ether was allowed to evaporate from the polymer under vacuum. The polymer was resuspended in DMSO at 100 mg/mL, and polymers were stored under desiccant at -20ºC.

5.2.3. Cell Culture

fNPC 34 cells were utilized to compare siRNA delivery between primary human glioblastoma cells and healthy human primary cells found in the brain. fNPC 34 cells are primary fetal neural progenitor cells obtained as described previously following procedures approved by the Johns Hopkins University Institutional Review Board.[10] fNPCs cells were

grown in 65% GIBCO® DMEM, 32% GIBCO® DMEM-F12, 2% B-27® Serum-Free Supplement, 1% Antibiotic-Antimycotic (Invitrogen), 10 μg/mL each of basic fibroblast growth factor (Roche Applied Science), epidermal growth factor (Sigma), Leukemia inhibitory factor (Millipore), and 5 mg/mL Heparin (Sigma). Primary human GBM cells were isolated from intraoperative samples by the Quinones laboratory.[10] GBM cells were grown in in 97% GIBCO® DMEM-F12, 1% GIBCO® Antibiotic-Antimycotic (Invitrogen), 2% B-27® Serum-Free Supplement, and 20 μg/mL each of basic fibroblast growth factor (Roche Applied Science) and epidermal growth factor (Sigma) for all experiments. Tissue culture plates were coated in 5 μg/mL laminin (Sigma) for to allow GBM and fNPC cells to adhere for all experiments. Primary human neurospheres (GBM1A, used for orthotopic tumors) were grown in the same media and conditions as all other GBM, but cells were grown in suspension for culture and only plated onto laminin-coated plates for *in vitro* experiments. For all *in vitro* experiments, cells were plated at a density of 47 x 10^3 cells/cm^2 and allowed to adhere overnight.

5.2.4. *In vitro delivery of siRNA*

For all transfections, polymer R646 and siRNA were separately diluted in 25 mM NaAc, and mixed in a 1:1 v/v ratio and allowed to self-assemble into nanoparticles for 10 min prior to being added to cells. Nanoparticles were incubated with cells for 2 h, and then the media were removed and replaced with fresh media. For all transfections following **Figure 5.1** the total concentrations of R646 and siRNA were 270 μg/mL and 120 nM, respectively. For experiments in which more than one siRNA was used in a nanoparticle formulation, siRNA oligos were blended in 25 mM NaAc prior to exposure to polymer.

For cellular uptake experiments, scrambled control RNA (scRNA) was first labeled with a Cy5 fluorophore using the MirusBio Label IT® Nucleic Acid labeling kit following

manufacturer's instructions. Nanoparticles stuck to the surface of cells were removed by washing with heparin sulfate prior to flow cytometry. Flow cytometry and cell preparation was otherwise carried out as described in **Chapter 4**, in which a BD Accuri™ C6 flow cytometer equipped with a Hypercyt autosampler was used to collect data, and FlowJo 7 software was used for data analysis.

5.2.6. Quantification of siRNA-induced cell killing

Five days following transfection with either siDeath or scRNA, cells were stained with 1:200 propidium iodide (PI), fixed with 10% formalin containing methanol (for membrane permeabilization), and stained with 1:200 4',6-diamidino-2-phenylindole (DAPI). Microscopic images were captured at 5X magnification using a Zeiss Axio observer A1 microscope with a Zeiss Axiocam MRm camera and AxioVision software. Fluorescence was provided by an Exfo X-Cite® series 120Q. Live and dead cells were quantified using ImageJ v1.47 software, and dead cells were subtracted from the live cell count to yield the total cell count for each well.

5.2.7. Western Blotting

Except where noted otherwise, *in vitro* cell harvests were conducted 3 days post-transfection. *In vitro* protein lysates were isolated using 5.2 $\mu L/cm^2$ of radioimmunoprecipitatoin assay (RIPA) buffer in tissue culture flasks. Cells were dissociated via cell scraping, lysates were kept on ice for 30 min with vortexing at 5 min intervals. Cell debris was removed by centrifugation at 19.2 x 10^3 RCF, and the supernatant was collected and stored at -80°C. For *in vivo* protein isolation, animals were sacrificed at 3 days following nanoparticle administration, and subcutaneous tumors were cut from surrounding tissue. Tumor tissue was homogenized in RIPA buffer, and debris removed via centrifugation as described above.

All protein electrophoresis was carried out using 4-12% NuPAGE Noves Bis-Tris gels (ThermoFisher Scientific) in 10% 3-(N-morpholino)propanesulfonic acid (MOPS) buffer (ThermoFisher Scientific) at 135V for 90 min. Proteins were transferred to a polyvinylidene fluoride (PVDF) membrane using a Pierce G2 Fast Blotter (ThermoFisher Scientific) following manufacturer's instructions. All blocking and antibody solutions contained 5% milk in 1X Tris-buffered saline with Tween 20 (TBST). Primary antibody incubations were completed overnight at 4°C, and secondary antibody incubations for 1 hr at room temperature. Antibody dilutions and specifications are found in **Table 5.1**.

5.2.8. Subcutaneous human GBM model and nanoparticle administration

Subcutaneous human GBM tumors were created in the flank of 4 week-old athymic nu/nu mice by injecting 2 million GBM 612 cells into the subcutaneous space. Isofluorane was used to anesthetize the mice. Tumors were allowed to form for 1 month to allow the tumors to reach approximately 1 cm^3 in size. Nanoparticles were injected directly into the tumor space with a total siRNA dose of 27 ug per tumor. Tumors were harvested for Western blotting analysis as described above.

5.2.9. Orthotopic human GBM model and nanoparticle administration

All experiments were conducted using 4 week-old athymic nu/nu mice. Transcranial cannulas (Plastics One Inc., Roanoke, VA) were implanted using a stereotactic frame to implant the tip of the cannula within the right striatum of the brain. Cyanoacrylate glue was used to attach the cannula to the skull, and suturing was used to close the surrounding skin. Ketamine/xylazine was used as an anesthetic.

Animals were inoculated with 500,000 luciferase-positive GBM1A cells using an internal cannula inserted within the transcranial cannula. A total of 4 μL of cell suspension was injected

at 1 μL/min. Lyophilized nanoparticles were prepared as previously described[11] and 4 μL of nanoparticle solution was injected at 1 μL/min through the cannulas. The total dose of siRNA per mouse was 0.6 μg. Nanoparticle injections began 14 d following tumor inoculation, and were repeated twice weekly for two weeks.

5.2.10. *In Vivo* Imaging System (IVIS) analysis of tumor growth

Luciferase-positive GBM tumors were imaged using an IVIS Spectrum (Caliper Life Sciences) and analyzed using Living Image® software (PerkinElmer). Animals were injected intraperitoneally with 4.5 mg D-Luciferin potassium salt (GoldBio) in 1X PBS 10 min prior to imaging. Mice (n=3) were imaged at 14, 17, and 21 days post tumor inoculation.

5.2.11. Brain tissue harvest, histological preparation and analysis

Four weeks following tumor inoculation, animals were anesthetized using ketamine/xylazine and their brains perfused using 10% formalin via intracardiac administration. The skulls were removed and brains stored in 10% formalin overnight. Brains were transferred to a solution of 30% sucrose for two days, then Optimal Cutting Temperature (OCT) compound (Fisher Scientific) overnight. Brains were frozen in OCT, and cut into 14 μm slices using a Leica CM1905 cryostat. Histological slices (3 animals per group, 6 sections per animal) were stained with hematoxylin and eosin (H&E), and slides were photographed using a Zeiss Axio observer A1 microscope with a Zeiss Axiocam MRm camera at 2.5X magnification. Tumor growth inhibition was determined by computer-assisted morphometric quantification of tumor area in H&E-stained histologic sections using AxioVision 4.8 software.

5.2.12. Statistical Analysis

All data is presented as the mean ± the standard error of the mean. Transfection efficacy and cellular uptake of siRNA nanoparticles in GBM versus fNPC cells, and tumor burden were

analyzed using a two-tailed *t*-test. P-values < 0.05 were considered statistically significant in all cases.

5.3 Results and Discussion

To evaluate the therapeutic potential of the bioreducible nanoparticles *in vitro*, primary human glioblastoma and primary human non-cancer neural progenitor cells were both transfected with the same bioreducible nanoparticles containing siRNA that could cause cell death to successfully transfected cells. We evaluated the brain cancer killing potential of these nanoparticles, their potential off-target cytotoxicity to non-cancer human primary cells, and the potential for the nanoparticles to effectively target siRNA delivery to brain cancer cells over healthy brain cells.

To accomplish this goal, we optimized siRNA delivery to human fetal neural progenitor cells (fNPC 34s) and GBM 319 cells over a range of polymer and siRNA concentrations. We found R646 to be optimal for siRNA delivery to the fNPC 34 cells, which included minimizing cytotoxicity, and was therefore utilized for subsequent functional siRNA delivery studies. Functional delivery efficacy was detected using a positive control cell death-inducing siRNA, with which successfully delivered siRNA would result in cell death. Cell death was measured using DAPI and propidium iodide (PI) to stain healthy and dying cells, respectively, and cell death was calculated using fluorescence microscopy followed by quantification with ImageJ software. Nanoparticle toxicity was calculated by normalizing scrambled RNA (scRNA)-treated cell counts to untreated cell counts, while siRNA delivery efficacy was calculated by normalizing death siRNA-treated cell counts to scRNA-treated cell counts.

For all R646 nanoparticle formulations tested, the GBM 319 cells showed near-complete siRNA-mediated cell death (79 – 97%) while the fNPC 34 cells had 0 - 27% siRNA-mediated cell death under the same conditions (**Figure 5.1**). For certain nanoparticle formulations, high knockdown leading to specific cell death of human glioblastoma cells was achieved (>90%) while non-specific cytotoxicity to both human glioblastoma and healthy human neural cells was kept low (< 20%). As the siRNA itself was not specific to GBM 319 cells over fNPC 34 cells and the same particle and siRNA doses were utilized, this finding suggests that bioreducible PBAE-based nanoparticles themselves preferentially transfect cancer cells over non-cancer cells.

In order to determine if this knockdown was robust in siRNA delivery to GBM from multiple patients, we repeated the cell-killing experiment in GBM cells from four patient intraoperative samples, as well as cells from three different fNPC tissue samples. Despite the heterogeneity between patient GBM tissue, we found that the nanoparticles preferentially transfected and killed the GBM cells (72 ± 9%) while avoiding the healthy cells (6 ± 12%) (**Figure 5.2**).[9] This result was exciting in that we found that our nanoparticles are tumor selective, meaning that we could potentially prevent harmful side effects in healthy brain tissue when delivering them *in vivo*.

In order to elucidate the mechanism by which cancer-selective delivery was achieved, we tested to see if nanoparticle uptake was different in the two cell types. We used Cy5 fluorphore-labeled siRNAs in the R646 nanoparticles, repeated the transfections, and used flow cytometry to measure the percent of cells positive for Cy5. Interestingly we found no significant difference between the percent of cells positive for siRNA in either cell type (94 ± 2% in GBM vs. 94 ± 1% in fNPC) (**Figure 5.3a**). We also used the geometric mean Cy5 intensity measurement to indirectly measure the amount of nanoparticles taken up by each cell, and also found no significant difference

between the two cell types (121 ± 23 normalized fluorescence units (NFU) in GBM vs. 169 ± 58 NFU in fNPC) (**Figure 5.3b**). This result is interesting in that it shows that the bulk uptake of nanoparticles into each cell does not seem to be the obstacle preventing successful fNPC transfection.

In order to assess the therapeutic potential of bioreducible PBAE nanoparticles, we then wanted to see if we were able to knockdown genes important to GBM behavior. We began with Roundabout homolog 1 (Robo1), a protein identified as key to GBM migration.[12] In order to first determine what the timeline of our knockdown would be, we delivered siRobo1 to GBM *in vitro* and harvested cells each day for 4 days. We began with a cocktail of 3 siRobo1 oligos blended within each particle, as we purchased them from OriGene Technologies, which guarantees that at least 2 of their oligos will achieve successful knockdown upon transfection. This would allow us to have at least two thirds of the encapsulated siRNA be functional. We found that nanoparticle delivery of siRobo1 was able to successfully knockdown Robo1 expression from days 1 – 4 post-transfection (**Figure 5.4a**). In similar experiments conducted knocking down Yes-associated protein 1 (YAP1) and Sodium-potassium-chloride cotransporter (NKCC1) we were able to maintain gene knockdown for at least 7 days post-transfection (**Figure 5.4b,c**). For all future *in vitro* siRNA delivery experiments we harvested at 3 days post-transfection, as this seemed to be universally appropriate timing for all proteins tested.

For each gene, we then wanted to select one of the three siRNA oligo options. We transfected GBM cells *in vitro* using each oligo (labeled A, B, or C) using a blend of all three as a positive control and untreated cells and scRNA-treated cells as negative controls. For five proteins (Robo1, YAP1, NKCC1, Survivin, and endothelial growth factor receptor (EGFR)) we were able to find sequences capable of successful knockdown (**Figure 5.5**). (See **Table 5.2** for full list of

oligos). For all further experiments, we used only one oligo targeting each gene as indicated in **Table 5.2**.

We then wanted to assess the potential to codeliver each siRNA while maintaining knockdown of each individual gene. We formed nanoparticles maintaining the total siRNA dose at 120 nM, but we blended in various concentrations of siRobo1 with scRNA, varying from 100% siRobo1 to 1 %. We were able to show that even with as little as 5%, or 6 nM siRobo1, we were still able to achieve near-complete gene knockdown (**Figure 5.6a**). This indicates that in a Robo1 knockdown study in which we attempt to use siRNAs targeting multiple genes, it would be possible to use as little as 6 nM siRobo1 and leave the remaining 114 nM to knockdown other genes. We have also been able to see similar knockdown strength in experiments done targeting YAP1 and NKCC1 (**Figure 5.6b,c**).

Finally, we wanted to show that this combination knockdown was possible as we hypothesized. We formed nanoparticles loaded with 24 nM each of Robo1, YAP1, NKCC1, Survivn, and EGFR (this will be referred to as "siRNA-5") for a total dose of 120 nM. We found that we were able to successfully knockdown each gene using a single nanoparticle formulation (**Figure 5.7**). We attempted a similar experiment in a subcutaneous model of human GBM in athymic mice, and were able to show knockdown of Survivin, EGFR, and NKCC1 (**Figure 5.8**).

As our ultimate goal was to change the malignant, proliferative phenotype of GBM, we then tested the effect of siRNA-5 knockdown on tumor growth in an orthotopic model of GBM. We inoculated athymic mice with luciferase-expressing primary human GBM (GBM1A) into the right striatum, allowed tumors to grow for 14 d, and then used intracranial cannulas to deliver siRNA-5 nanoparticles intratumorally twice weekly for two weeks. Using the *In Vivo* Imaging System® (IVIS) Spectrum system and intraperitoneal delivery of D-Luciferin, we indirectly

tracked tumor size using bioluminescence at 0, 7, and 14 days following the start of nanoparticle treatment (**Figure 5.9c**). At day 14 following the start of treatment, we found tumor bioluminescent flux for scRNA treated tumors to be 17.3 ± 5.4 x 10^7 photons/sec, higher than siRNA treated tumors, which had a flux of 6.9 ± 2.5 x 10^7 photons/sec.

Animals were sacrificed for histological analysis of the tumors at 14 d following the start of nanoparticle treatment. Histological sections were stained with hematoxylin and eosin (H&E) in order to visualize tumors and calculate tumor burden (**Figure 5.9a,b,d**). We found that tumor burden in mice treated with siRNA-5 nanoparticles was significantly lower (3.5 ± 0.6 mm^2) than those treated with scRNA nanoparticles (6.9 ± 0.4 mm^2).

5.4. Conclusions

We have demonstrated that bioreducible PBAEs selectively deliver siRNA and enable gene knockdown in primary human brain cancer while avoiding gene knockdown in healthy brain tissue cells. This effect is efficient and robust, in that we have shown this in four different patient GBM cells. This presents an interesting opportunity in siRNA-based nanomedicine as future siRNA targets and siRNA combinations may not need to be limited to proteins that would specifically effect cancer cell viability without harming the surrounding tissue, but instead could enable effective targeting and knockdown of any protein necessary to tumor survival as the material itself could provide cancer specificity. We have also expanded upon work shown in **Chapter 4**, in which we demonstrated knockdown with low siRNA doses, and shown that we can effectively knockdown five genes simultaneously in both *in vitro* and *in vivo* human GBM models. We have also shown the potential to eventually increase this to ten or twenty genes. Bioreducible PBAE codelivery of five genes to *in vivo* human GBM tumor models showed gene knockdown and a

reduction in tumor growth following treatment. This shows the potential of bioreducible PBAEs as a potent, combinatorial, and cancer-specific siRNA delivery vehicle.

5.5. Tables

Table 5.1. List of antibodies uses for Western blotting and their specifications.

Protein	Vendor	Vendor Product Number	Primary Antibody Dilution	Host Species	Secondary Antibody Dilution
Robo1	Abcam	ab85312	1:400	Rabbit	1:5000
YAP1	Cell Signaling	4912	1:1000	Rabbit	1:5000
NKCC1	Cell Signaling	8351	1:2000	Rabbit	1:5000
EGFR	Millipore	6847	1:1000	Rabbit	1:5000
Survivin	Cell Signaling	2803	1:1000	Rabbit	1:5000
Beta-actin	Abcam	ab8226	1:10000	Mouse	1:5000

Table 5.2. siRNA oligos used, their sequences, and the assessment of their ability to knockdown their respective target protein in the human GBM cells tested. Sequences marked with an asterisk indicate those that were chosen to use following isoform selection studies.

Target Protein	Product Number	NCBI Reference	Isoform	Sequence	Function in GBM?
NKCC1	SR304439	NM_001046.2	A	rArGrGrUrUrUrCrArUrArGrArGrArArCrArArArGrGrUrGAT	Yes
			B	rGrGrUrArGrUrArArGrUrGrUrGrGrArArUrArUrArGrUrAAA	Yes*
			C	rGrCrArArCrUrArArUrGrGrArUrUrUrGrUrArArGrArGrGAG	Yes
YAP1	SR307060	NM_001130145.2	A	rArGrUrArCrArGrArCrArGrUrGrGrArCrUrArArGrCrArUGA	Yes*
			B	rGrCrCrArCrCrArArGrCrUrArGrArUrArArArGrArArArGCT	No
			C	rGrGrUrUrGrArUrCrArCrUrCrArUrArArUrArArUrUrGrACT	Yes
Robo1	SR304090	NM_133631	A	rGrCrArGrUrArCrUrArArGrGrGrArArCrArArUrCrCrArUGT	Yes*
			B	rArCrCrArArUrUrGrArGrUrArArGrArArCrArUrCrCrCrUGT	No
			C	rArGrGrGrCrUrCrUrCrArArArGrUrArUrArArUrCrUrUrUCT	Yes
Survivin	SR300234	NM_001012270	A	rArGrArArUrArGrArGrUrGrArUrArGrGrArArGrCrGrUrCTG	Yes
			B	rGrGrArArArGrArGrUrArArCrUrCrArCrArArUrUrGrCrCAA	No
			C	rCrUrCrCrUrCrUrArCrUrGrUrUrUrArArCrArArCrArUrGGC	Yes*
EGFR	SR301357	NM_005228	A	rGrGrArArArUrUrArCrCrUrArUrGrUrGrCrArGrArGrGrAAT	Yes*
			B	rArGrCrUrArUrGrArGrArUrGrGrArGrGrArArGrArCrGrGCG	No
			C	rCrGrArGrGrGrCrArArArUrArCrArGrCrUrUrUrGrGrUrGCC	No

5.6. Figures

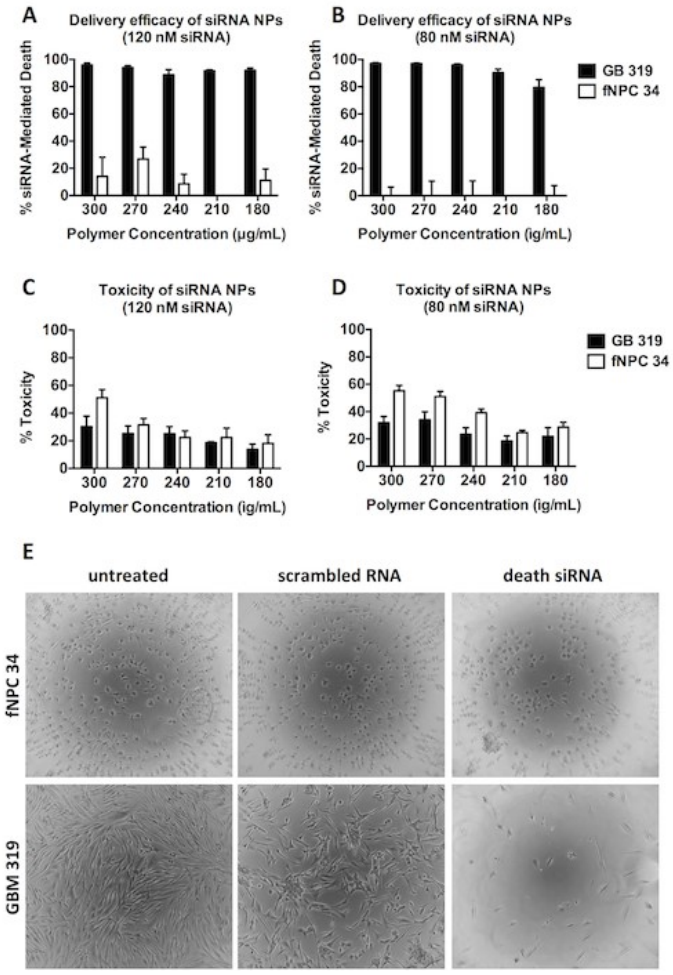

Figure 5.1. Delivery of death siRNA to cancer and non-cancer brain cells using polymer R646. (A-B) Delivery efficacy of death positive control siRNA to cancer (GBM 319) and non-cancer (fNPC 34) cells using a range of bioreducible PBAE nanoparticle formulations. All % siRNA-mediated death values are calculated versus cell counts of scrambled control RNA-treated cells. (C-D) Toxicity of nanoparticle treatments to GBM 319 and fNPC 34 cells. (E) Phase contrast images of fNPC 34 (top) and GBM 319 (bottom) cells following treatment with nanoparticles containing 120 nM of either scrambled RNA or death positive control siRNA.

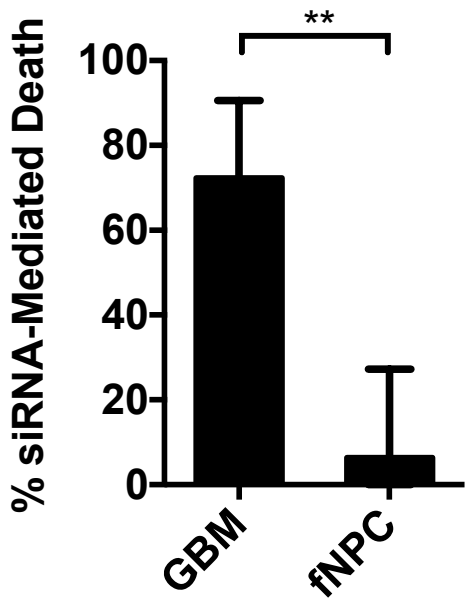

Figure 5.2. Bioreducible PBAE nanoparticles selectively transfect primary human GBM cells versus primary human neural progenitor cells (fNPCs). siRNA-mediated death following transfection using a death positive control siRNA shows significantly more cell killing in the four GBM cell samples tested versus three fNPC cell samples tested.

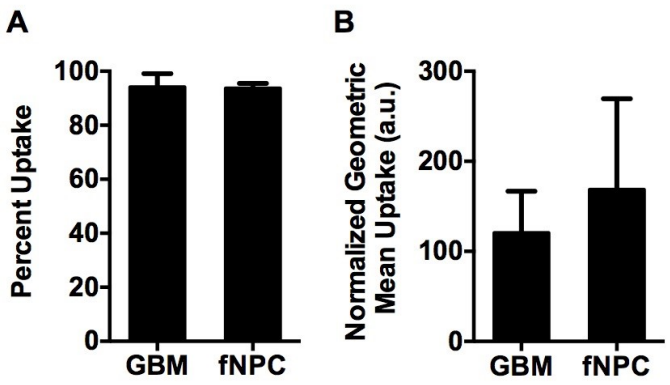

Figure 5.3. Nanoparticle uptake is not statistically different between GBM and fNPC cells. (A) The percent of cell positive for fluorophore-labeled siRNA is not statistically different. (B) The geometric mean fluorescence of fluorophore-labeled siRNA within each cell, and indirect measure of nanoparticles per cell, is not statistically different between GBM and fNPC cells.

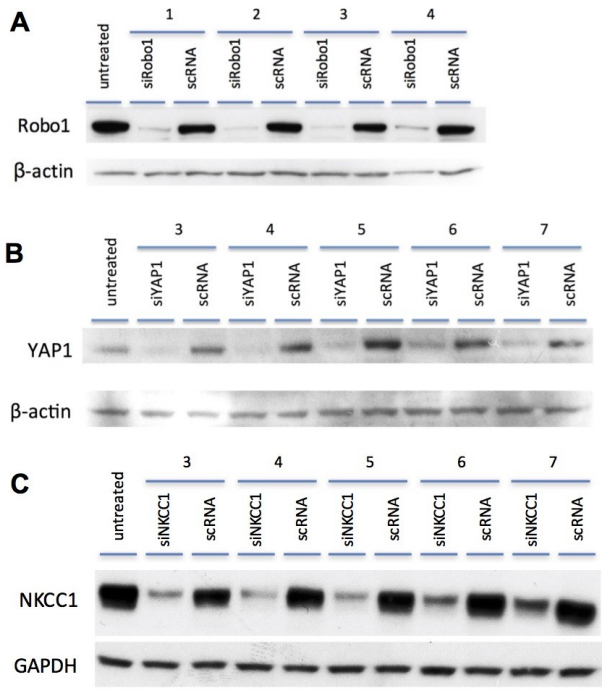

Figure 5.4. Timecourse of knockdown of Robo1 (A), YAP1 (B), and NKCC1 (C) in primary human GBM.

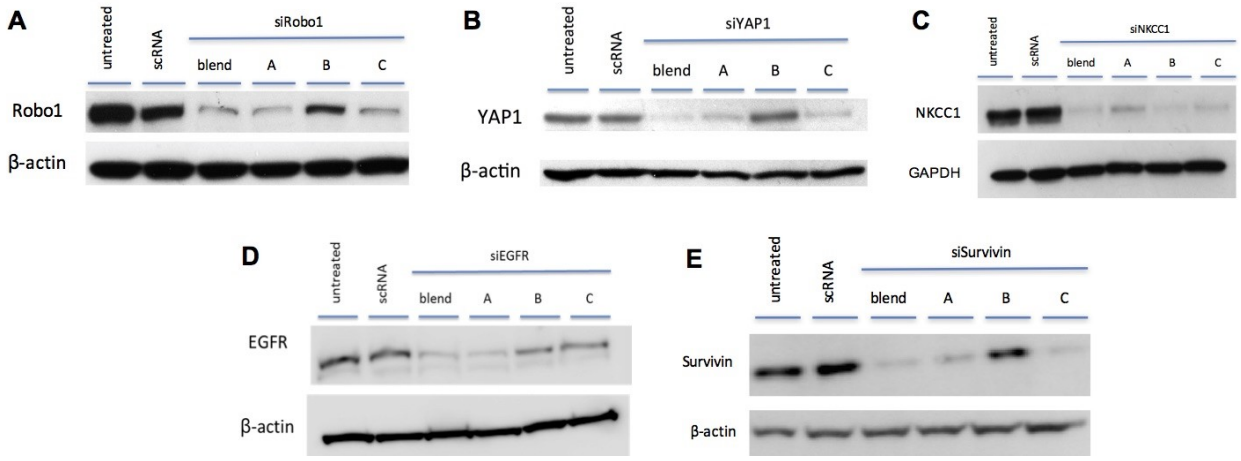

Figure 5.5. Western blotting images showing the selection of the most effective siRNA oligos for knockdown of each of five genes in primary human GBM.

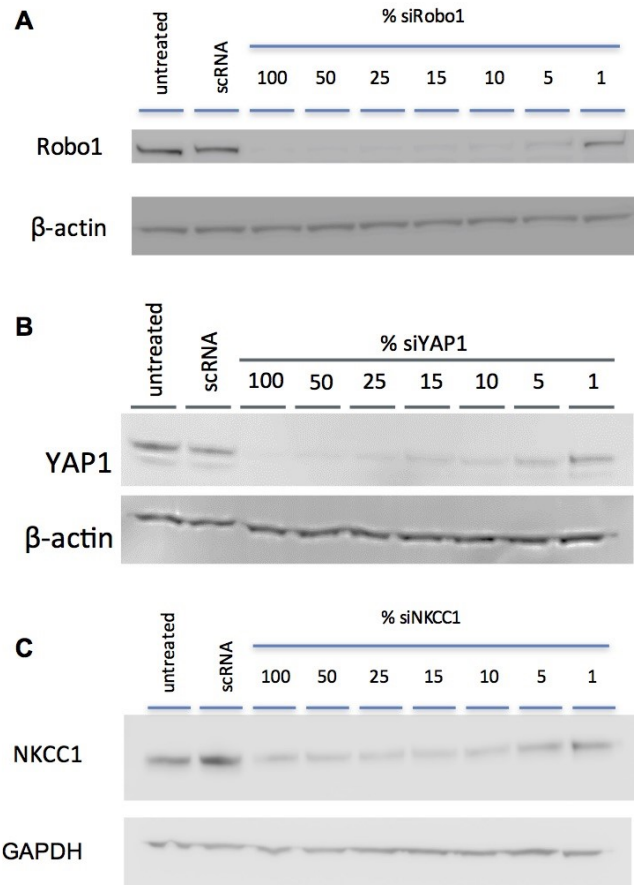

Figure 5.6. Dose response of gene knockdown in primary human GBM of genes Robo1 (A), YAP1 (B), and NKCC1 (C).

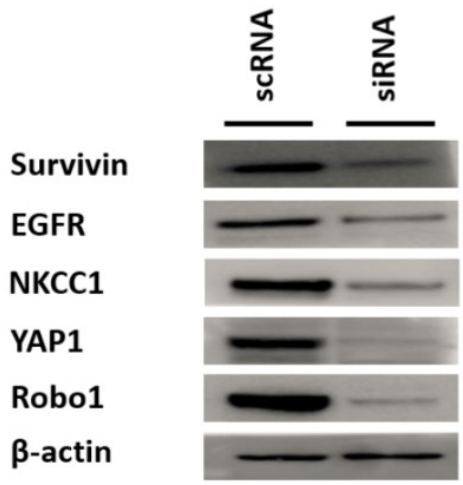

Figure 5.7. Simultaneous knockdown of 5 genes following *in vitro* transfection of primary human GBM with a single formulation of bioreducible PBAE nanoparticles.

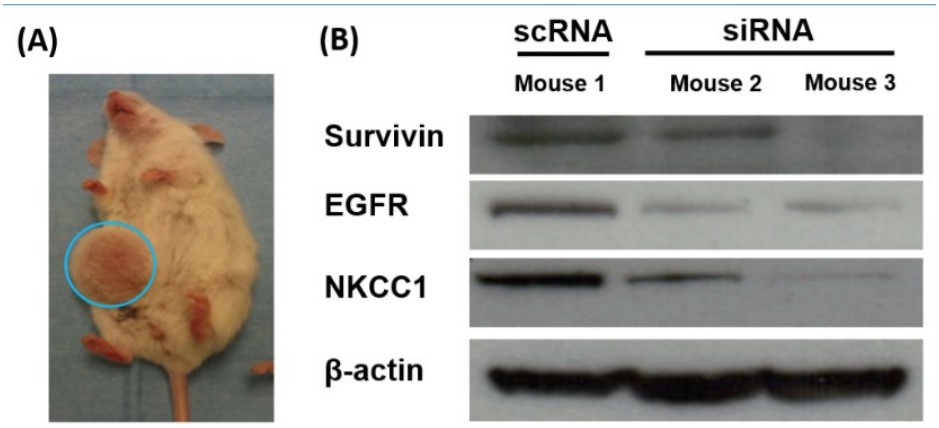

Figure 5.8. Simultaneous knockdown of 3 genes following *in vivo* transfection of primary human GBM in a subcutaneous tumor model with a single formulation of bioreducible PBAE nanoparticles.

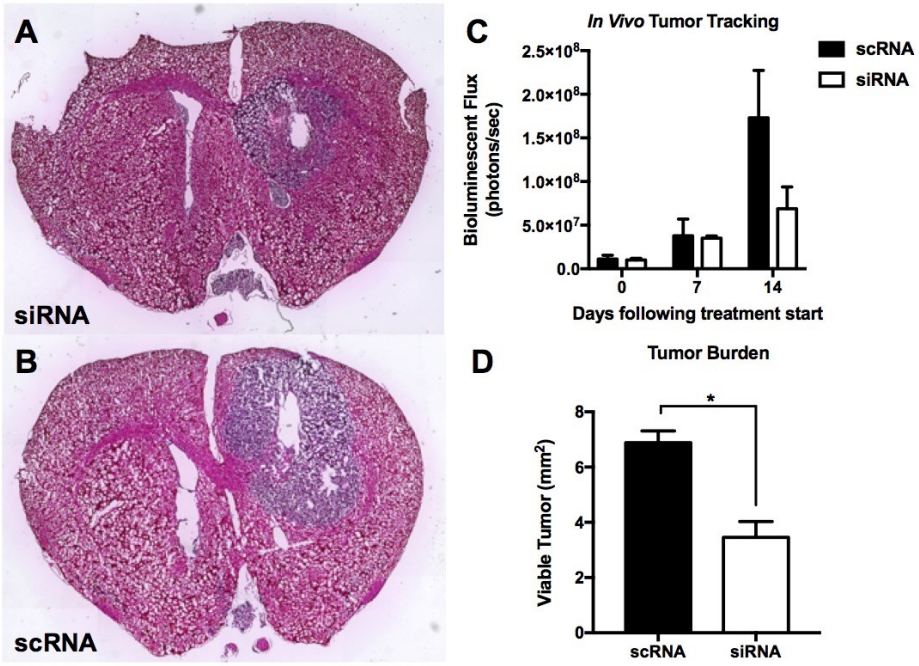

Figure 5.9. PBAE nanoparticle codelivery of 5 siRNAs reduced tumor growth in an orthotopic model of human GBM. Hemotoxylin and eosin-stained histological slides of siRNA-5 treated tumors (A) show reduced tumor burden versus scRNA treated tumors (B, quantification in D). IVIS tracking of luciferase-positive GBM tumors shows tumor growth slowing in siRNA-5 treated tumors (C).

5.7. References

1. Chaichana, K. L.; Zadnik, P.; Weingart, J. D.; Olivi, A.; Gallia, G. L.; Blakeley, J.; Lim, M.; Brem, H.; Quinones-Hinojosa, A. Multiple Resections for Patients with Glioblastoma: Prolonging Survival. *J Neurosurg* **2013,** 118, 812-820.
2. McGirt, M. J.; Chaichana, K. L.; Gathinji, M.; Attenello, F. J.; Than, K.; Olivi, A.; Weingart, J. D.; Brem, H.; Quinones-Hinojosa, A. R. Independent Association of Extent of Resection with Survival in Patients with Malignant Brain Astrocytoma. *Journal of Neurosurgery* **2009,** 110, 156-162.
3. Stupp, R.; Mason, W. P.; van den Bent, M. J.; Weller, M.; Fisher, B.; Taphoorn, M. J. B.; Belanger, K.; Brandes, A. A.; Marosi, C.; Bogdahn, U.; Curschmann, J.; Janzer, R. C.; Ludwin, S. K.; Gorlia, T.; Allgeier, A.; Lacombe, D.; Cairncross, J. G.; Eisenhauer, E.; Mirimanoff, R. O. Radiotherapy Plus Concomitant and Adjuvant Temozolomide for Glioblastoma. *New England Journal of Medicine* **2005,** 352, 987-996.
4. Woolard, K.; Fine, H. A. Glioma Stem Cells: Better Flat Than Round. *Cell Stem Cell* **2009,** 4, 466-467.
5. Zaidi, H., A; DiMeco, F.; Quinones-Hinojosa, A. Brain Tumor Stem Cells. In *Youman's Neurological Surgery*, 2009.
6. Fire, A.; Xu, S. Q.; Montgomery, M. K.; Kostas, S. A.; Driver, S. E.; Mello, C. C. Potent and Specific Genetic Interference by Double-Stranded Rna in Caenorhabditis Elegans. *Nature* **1998,** 391, 806-811.
7. Thomas, C. E.; Ehrhardt, A.; Kay, M. A. Progress and Problems with the Use of Viral Vectors for Gene Therapy. *Nat. Rev. Genet.* **2003,** 4, 346-358.
8. Kozielski, K. L.; Tzeng, S. Y.; Green, J. J. A Bioreducible Linear Poly(Beta-Amino Ester) for Sirna Delivery. *Chem. Commun.* **2013,** 49, 5319 - 5321.
9. Kozielski, K. L.; Tzeng, S. Y.; Mendoza, B. A. H. d.; Green, J. J. Bioreducible Cationic Polymer-Based Nanoparticles for Efficient and Environmentally Triggered Cytoplasmic Sirna Delivery to Primary Human Brain Cancer Cells. *ACS Nano* **2014,** 8, 3232-3241.
10. Ravin, R.; Blank, P. S.; Steinkamp, A.; Rappaport, S. M.; Ravin, N.; Bezrukov, L.; Guerrero-Cazares, H.; Quinones-Hinojosa, A.; Bezrukov, S. M.; Zimmerberg, J. Shear Forces During Blast, Not Abrupt Changes in Pressure Alone, Generate Calcium Activity in Human Brain Cells. *PLoS One* **2012,** 7, e39421.
11. Tzeng, S. Y.; Guerrero-Cazares, H.; Martinez, E. E.; Sunshine, J. C.; Quinones-Hinojosa, A.; Green, J. J. Non-Viral Gene Delivery Nanoparticles Based on Poly(Beta-Amino Esters) for Treatment of Glioblastoma. *Biomaterials* **2011,** 32, 5402-5410.
12. Mertsch, S.; Schmitz, N.; Jeibmann, A.; Geng, J. G.; Paulus, W.; Senner, V. Slit2 Involvement in Glioma Cell Migration Is Mediated by Robo1 Receptor. *Journal of Neuro-Oncology* **2008,** 87, 1-7.

Chapter 6

Delivery of microRNA to human glioblastoma for the reduction of tumor stem-like properties and tumor sensitization to conventional therapy

6.1. Introduction

More than 78,000 new cases of brain cancer are diagnosed in the U.S. each year with glioblastoma (GBM) being the most common and deadly form[1]. Despite aggressive treatment consisting of surgical resection and radiotherapy/chemotherapy, the median life expectancy for GBM patients remains only between 14 and 20 months, highlighting the need for new therapeutic approaches[2]. Treatment options for GBM remain limited in part due to the difficulty in delivery of drugs through the blood-brain barrier (BBB) and resistance of tumor cells to chemotherapy drugs[3, 4]. These tumors are heterogeneous at the cellular level and contain cells that vary in their capacity to propagate tumor growth[5]. Among these different cell subpopulations are multi-potent stem-like cells (also referred to as cancer stem cells or CSCs) that are critical determinants of tumor propagation, therapeutic resistance, and recurrence following treatment. Substantial evidence indicates that cancer cells are highly plastic and dynamically transition bi-directionally between stem-like/tumor propagating cells (CSC state) and more differentiated/non-tumor propagating states (non-CSC state) in response to contextual epigenetic events[6]. The mechanisms driving these phenotypic transitions represent a vulnerability amenable to therapeutic targeting[7].

Epigenetic modifications, involving alterations in chromatin structure and function such as histone modification, DNA modification, and deregulation of non-coding RNAs, are important determinants of gene expression and essential drivers of neoplastic phenotypes[8, 9]. Non-coding RNAs, in particular miRNAs, are emerging as critical epigenetic regulators of cell fate and oncogenesis. MiRNAs act by selectively inhibiting gene expression primarily by targeting mRNA for degradation usually via complementary 3'-UTR seed sequences. Numerous miRNAs have

been found to regulate tumorigenesis and cancer cell stemness by virtue of their capacity to target tumor-suppressing or tumor promoting transcripts[10]. We recently showed that the coordinated actions of Oct4 and Sox2 induce a tumor-propagating stem-like state in GBM cells through a mechanism that involves the induction of DNMTs and down-regulation of a network of miRNAs through promoter DNA methylation. We further showed that two of the miRNAs repressed by Oct4/Sox2, miR-148a and miR-296-5p, efficiently inhibit the GBM stem-like phenotype and their repression is required for the induction of GBM tumor propagating capacity by Oct4/Sox2, making their reconstitution an excellent strategy for therapeutic intervention[11, 12].

Despite the improved understanding of the molecular determinants of GBM stem cells and tumor propagating capacity, translating these advances remains a challenge[13]. Viral methods to introduce nucleic acid cargo to cells, while effective, have to potential to cause tumorigenic and immunogenic responses[14]. Viral gene delivery is also limited in its clinical translation due to factors such as scalability and limited cargo size[15]. The latter concern is particularly critical for codelivery of multiple nucleic acid cargoes, as viral delivery of two miRNA constructs would likely require exposure to viral vectors twice, increasing the chance of insertional mutagenesis or an inflammatory response with each exposure. Nonviral vectors are not limited in their scalability, and can be designed to avoid immunogenic and tumorigenic activities. Additionally, nonviral delivery vehicles can carry hundreds of DNA plasmids[16], or RNA oligos[17] within a single nanoparticle.

Nonviral nucleic acid delivery can be carried out using lipid-based[18], inorganic[19], or polymeric[20] nanoparticle systems. Cationic polymers such as poly(*L*-lysine) (PLL) and polyethyleneimine (PEI) are capable of encapsulating nucleic acid cargoes into nanoparticles and facilitating endosomal cellular uptake due to the charge interaction between the cationic polymers

and anionic cell surface[21]. While PLL-based nanoparticles often remain sequestered within endosomal compartments, PEI nanoparticles have a high buffering capacity which enables them to escape the endosome[20]. Poly(beta-amino ester) (PBAE) nanoparticles are cationic and have a high buffering capacity, but promote superior gene delivery versus PEI as they contain hydrolytically-cleavable ester bonds. This reduces cytotoxicity as well as enhances cargo release, a necessary step in successful transfection[22].

Like most gene delivery vehicles, PBAEs were first optimized for DNA delivery, and although DNA and RNA oligos such as miRNA share some physicochemical similarities, the materials that are effective for DNA delivery often vary from those that are effective for RNA delivery[23]. We recently developed a novel, bioreducible PBAE analog, designed to encapsulate short interfering RNA (siRNA) into nanoparticles and release it upon entering the reducing environment in the cytosol[24]. We were able to show that bioreducibility imparted reduced cytotoxicity, promoted cytoplasmically-targeted release and effective gene knockdown in primary human GBM *in vitro*. We were also able to demonstrate selective delivery of siRNA to GBM versus healthy neural progenitor cells, and the ability to deliver more than 600 siRNA molecules per nanoparticle[17]. It is due to these results that we chose to use these bioreducible PBAEs for miRNA delivery in the work presented herein. MiRNA and siRNA are both short (21-28nt), double stranded RNA oligos who block mRNA translation via RNA interference (RNAi) in the cytosol[25]. We therefore hypothesized that the materials that are effective for siRNA delivery would also be effective miRNA delivery vehicles.

In this report we combine this cutting-edge nanoparticle technology with our newly discovered stem cell inhibiting miRNAs to develop miRNA nanoparticles to treat gliomas. We developed and characterized novel PBAE polymers that can effectively deliver miRNA mimics

and inhibit the stem cell phenotype of GBM neurosphere cells *in vitro*. For the first time, we show these miRNA nanoparticles distribute throughout an established tumor *in vivo*, and more importantly, that delivering these tumor-suppressing miRNAs using these biomaterials inhibits the growth of established GBM tumor in mouse models. Our findings demonstrate that identifying and validating stem cell-inhibitory miRNAs in combination with current advances in nanomedicine will undoubtedly impact the development of novel therapies for targeting the CSC population and treating GBM.

6.2. Materials and Methods

6.2.1. GBM Neurosphere Culture

GBM-derived neurosphere lines (GBM1A and GBM1B) were originally derived and characterized by Vescovi and colleagues[26] and the A172-iGSC line was developed by us[11]. Neurospheres were cultured in serum-free medium containing DMEM/F-12 (Invitrogen, Carlsbad, CA, USA), supplemented with 1% BSA, 20 ng/ml epidermal growth factor (EGF) and 10 ng/ml fibroblast growth factor (FGF).

6.2.2. Materials

All chemicals used to synthesize bioreducible monomer 2,2'-disulfanediylbis(ethane-2,1-diyl) (BR6) were purchased from Sigma-Aldrich (St. Louis, MO) and used without further purification. All other monomers used for polymer synthesis were purchased from Alfa Aesar (Ward Hill, MA). AllStars Human Cell Death siRNA was purchased from Qiagen. The following mature miRNA mimics used in the study were purchased from Dharmacon (GE Healthcare): hsa-miR-148a-3p (C-300540-05-0005), hsa-miR-296-5p (C-300659-03-0005), and microRNA Hairpin Inhibitor Transfection Control with Dy547 (IP-004500-01-05).

6.2.3. Bioreducible polymer synthesis

Bioreducible monomer BR6 was synthesized as previously described.[24] Briefly, the acrylation of bis(2-hydroxyethyl) disulfide was carried out in tetrahydrofuran (THF) anhydrous conditions with acryloyl chloride as the acrylation reagent and in the presence of triethylamine (TEA). Following overnight reaction at room temperature, the TEA HCl precipitate was removed via filtration, THF was removed via rotary evaporation, and the impure product was dissolved in dichloromethane (DCM). The product was purified using aqueous washes of Na_2CO_3, followed by water, after which DCM was removed via rotary evaporation.

Polymers were synthesized in a method similar to Kozielski *et al*.[17] in which monomer BR6 was polymerized at a 1.01:1 molar ratio with monomer 4-amino-1-butanol (S4) at 500 mg/mL in THF at 60°C for 24 h. Polymers were endcapped in THF at 100 mg/mL with 0.2 M -(3-(aminopropyl)amino)methanol (E6) at room temperature for 1 h while stirring. Unreacted monomers were removed by precipitating out polymer using diethyl ether, centrifuging at 3220 RCF, and decanting off ether. This was repeated, and the polymer was stored under vacuum to allow ether to evaporate. The final polymer product was dissolved in dimethyl sulfoxide (DMSO) at 100 mg/mL and stored at -20°C under dessicant.

6.2.4. Bioreducible PBAE nanoparticle formulation and screening in GBM neurospheres

Nanoparticle formulations were screened using a AllStars Human Death Control siRNA (siDeath), a blend of siRNAs that target genes necessary for human cell survival. GBM1A and GBM1B cells were plated on poly-L-lysine (PLL) coated tissue culture flasks and allowed to adhere overnight. R646 polymer was complexed with either siDeath or a scrambled control RNA (scRNA) in 25 mM sodium acetate (NaAc); the solution was mixed, and nanoparticles were allowed to self-assemble for 10 min. Nanoparticles were added directly to the cell culture media,

and each RNA was at a final concentration of 120 or 80 nM, with final polymer concentrations of 330, 270, or 310 μg/mL. Nanoparticles were incubated with cells for 2 h, after which they were removed and replaced with fresh media. Nanoparticles were allowed to release from the tissue culture flask and form neurospheres for 5 d, after which cells were imaged to assess cell death.

All further *in vitro* work was carried out in the same manner, using a final RNA concentration of 120 nM, and a final R646 concentration of 270 μg/mL. For all groups, the total dose of each functional miRNA was kept at 60 nM, while the total miRNA dose was 120 nM. As an example, "miR-148a + miR-296-5p" nanoparticles contained 60 nM miR-148a and 60 nM miR-296-5p, while "miR-148a" nanoparticles contained 60 nM miR-148a and 60 nM miR-Ctrl. This enables us to keep the nanoparticle physical properties consistent while maintaining the same dose of functional miRNA the same if it being used alone or in combination.

6.2.5. Bioreducible PBAE nanoparticle characterization

Transmission Electron Microscopy

Nanoparticles were synthesized as described above and the solution was placed onto a carbon-coated copper TEM grid and allowed to dry. Particles were imaged using a Philips/FEI BioTwin CM120 transmission electron microscope. Image J software was used to analyze particle size as captured via TEM images.

Nanoparticle Tracking Analysis

Nanoparticles were synthesized as described above and diluted in PBS at a 1:400, 600, or 800 v/v ratio prior to loading particles into a NanoSight NS500. Particles were tracked and their size and concentration determined using NanoSight NTA 2.4 software. All measurements were repeated with three formulations of nanoparticles to allow us to determine batch-to-batch variability. All particle concentrations represented are scaled so that they report the number of

particles per volume that would be present in the *in vitro* transfection wells. The loading of siRNA molecules per particle was calculated by dividing the dose of siRNA in each transfection by the number of particles per well.

Dynamic Light Scattering

Nanoparticles were synthesized as described above and diluted in PBS at a 1:6 v/v ratio prior to loading into a disposable cuvette cell. Nanoparticle size and surface charge (ζ-potential) were measured using Dynamic Light Scattering (DLS) via a Malvern Zetasizer NanoZS. Nanoparticles were measured from three separate formulations to account for synthesis variability. Nanoparticle hydrodynamic diameter is reported as the mean and SEM of the Z-average diameter.

Gel retention analysis of nanoparticles in extracellular and cytosolic reducing conditions

Nanoparticles were formed as previously described, and diluted at a 1:100 v/v ratio in either artificial cerebrospinal fluid (aCSF) or PBS containing 5 mM glutathione (GSH). aCSF is a solution of ions that mimics the ionic composition of human CSF.[27] Glutathione is present in human cells' cytosol in concentrations ranging from 1 – 8 mM, while extracellular concentrations range from 5 – 50 μM.[28] Nanoparticles were incubated in either solution at 37°C while shaking, and samples of each solution were removed at 0 min, 5 min, 15 min, 30 min, 1 h, 2 h, 4 h, 6 h, and 8h. Upon removal of the nanoparticles, 30 mg/mL sucrose was added as a cryoprotectant, samples were frozen at -80°C, and lyophilized. Particles were resuspended to their original concentration using deionized water and a 30% solution of glycerol was added to the particle solution in a 1:5 v/v ratio. Particles were loaded into a 1% w/v agarose gel containing 1 μg/mL ethidium bromide and electrophoresed at 100 mV for 15 min, after which gels were visualized using UV light exposure.

6.2.6. QRT-PCR and miRNA expression

Total RNA was extracted from cells using RNeasy Mini Kit (Qiagen). cDNA was made by reverse-transcribing 1 μg of total RNA using MuLV Reverse Transcriptase and Oligo (dT) primers (Applied Biosystems). qRT-PCR was performed with a Bio-Rad CFX detection System (Bio-Rad) and expression of target genes was measured using Power SYBR green PCR kit (Applied Biosystems). Samples were amplified in triplicate and relative gene expression was analyzed using Bio-Rad CFX manager software and normalized to 18S RNA. Primer sequences used were previously described[11, 12].

For miRNA analysis, total RNA including small RNA was extracted using miRNeasy kit and 1 μg of total RNA was used as template to generate cDNA using miScript II RT kit according to manufacturer's protocol. Mature miRNA expression was detected using miScript SYBR green PCR kit using probes for RNU6 (Cat.# MS00033740), miR-148a (MS00003556), and miR-296-5p (Cat. # MS00016401). All kits and probes used to detect mature miRNAs were purchased from Qiagen.

6.2.7. Tumor formation *in vivo*

A transcranial cannula was placed so that the tip is in the right caudate/putamen of female athymic nude NCR Nu/Nu mice (8-week old). One week after cannula placement, animals received either GBM1A or A172-iGSC neurospheres cells via the cannula and assigned into different treatment groups in a non-blinded, non-randomize manner[29, 30]. Using the same cannula, control cohort received nanoparticles loaded with a non-targeting control miRNA labeled with Dy547 and the experimental group received nanoparticles loaded with the indicated miRNAs.

For *in* vivo delivery, nanoparticles were synthesized using the same polymer to miRNA w/w ratio as in all earlier studies (150 w/w), but the total polymer concentration was 5 mg/mL so that we could synthesize particles at a higher concentration. Particles were cryoprotected using 30 mg/mL

sucrose prior to freezing and lyophilization following previously established protocols.[31] For use *in vivo*, nanoparticles were resuspended using deionized water to a final polymer concentration of 16.7 mg/mL and a final sucrose solution of 100 mg/mL.

Number of animals used for each experiment is indicated in the corresponding figure legend. Tumor growth inhibition was determined by computer-assisted morphometric quantification of tumor area in H&E-stained histologic sections as previously described[30]. Data for all *in vivo* experiments are shown as the mean tumor area distribution of all animals used in the study. All animal procedures were approved by the Johns Hopkins Institutional Animal Care and Use Committee (Protocol# MO14M307), and were in accordance with the NIH Guide for the Care and Use of Laboratory Animals.

6.2.8. Statistical Analysis

All experiments were performed in triplicates and repeated at least twice in each cell model. All values are represented as mean ± the standard error of the mean. Statistical significance results for miRNA overexpression, neurosphere formation, stem marker knockdown were determined using a one-way ANOVA with Dunnett's post-tests using miR-Ctrl as the control. All other statistical significance was determined using a one-way ANOVA with Tukey's post-tests. All significance tests with $p < 0.05$ were considered significant.

6.3. Results and Discussion

6.3.1. PBAE nanoparticles deliver miRNAs to human GBM *in vitro.*

To determine the optimal Polymer:RNA ratio and dosing required to transfect GBM neurospheres, PBAE/siRNA conjugates were prepared by mixing increasing amounts of PBAE polymer (**Figure 6.1**) with a scrambled siRNA or a cell-killing positive control siRNA (siDeath).

These PBAE/siRNA formulations were then used to transfect GBM1A and GBM1B neurospheres and siRNA-induced cell death was measured qualitatively versus scrambled control RNA (siCtrl)-treated cells. Combining 270 μg/ml of PBAE polymer with either 80nM or 120nM of siDeath strongly enhanced neurosphere cell killing compared to cells transfected with the siCtrl. (**Figure 6.2**). As 270 μg/mL PBAE with either 120 nM or 80 nM siCtrl both showed no nanoparticle-mediated toxicity, we chose to use 270 μg/mL PBAE with 120 nM RNA for a polymer:RNA weight ratio (wt/wt) of 150 for all remaining experiments. As previously demonstrated, this higher RNA dose with a lower polymer wt/wt would allow us to load more RNA molecules into each nanoparticle[17] and therefore increase the number of nanoparticles that can carry several different miRNAs within a single particle.

6.3.2. PBAE nanoparticles encapsulate miRNA into nanoparticles and effectively release miRNA in a cytosolic redox environment.

The physical and chemical properties of gene delivery nanoparticles often play a major role in their success as gene delivery vehicles. We physically characterized the nanoparticles formed by incubating bioreducible PBAE polymers with miRNA, as this has previously never been demonstrated and we were unsure of what nanostructure, if any, would form. In order to determine if bioreducible PBAEs could encapsulate miRNA into nanoparticles, we physically characterized nanoparticle formation and miRNA binding. We formed nanoparticles at a polymer to miRNA weight ratio (wt/wt) of 150 wt/ wt and measured nanoparticle hydrodynamic diameter and zeta potential using dynamic light scattering (DLS), hydrodynamic diameter and concentration via nanoparticle tracking analysis (NTA), and nanoparticle dried size via transmission electron microscopy (TEM). We were able to show via TEM that we were able to form miRNA nanoparticles with a round morphology (**Figure 6.3a.**) Zeta-potential was

measured to be 18 ± 0.4 mV (**Figure 6.3c**). Via DLS, the nanoparticle hydrodynamic diameter was 159 ± 4 nm, and via NTA, the hydrodynamic diameter was 138 ± 3 nm (**Figure 6.3a,b**). The disparity between nanoparticle size as measured via DLS versus NTA is anticipated as DLS yields an intensity-weighted measurement, which weighs larger particles more than smaller ones when calculating an average, while NTA yields a number-average measurement, explaining why the average size via NTA is smaller. Via TEM, nanoparticle size was measured to be 56 ± 2 nm. This difference in these modes of measurement is important in that TEM measures the dried size of the nanoparticles, while DLS and NTA measure the hydrodynamic diameter. Nanoparticle concentration upon *in vitro* delivery was measured to be 1.3 ± .12 x 10^{10} particles/mL (**Figure 6.3d**).

In order to determine if these nanoparticles are able to completely encapsulate miRNA, we performed a gel retention assay, in which nanoparticles are loaded into an agarose gel, and tightly bound RNA is unable to electrophorese under an applied voltage. We first incubated miRNA nanoparticles in artificial cerebrospinal fluid (aCSF) to mimic the redox and ionic environment in the brain extracellular space[32]. We found that all miRNA was bound by PBAE polymer. Given that all miRNA is bound into nanoparticles at this formulation, the nanoparticle concentration, and our known *in vitro* dose of 120 nM miRNA, this indicates that the average miRNA loading within each nanoparticle is 5456 ± 512 miRNA molecules per particle (**Figure 6.2e**). This was an important finding, as a major advantage of using nanoparticle delivery versus a viral vector is facile codelivery. However, previous work showing codelivery of plasmid DNA demonstrated that having two plasmids within the same batch of particles is not sufficient, that the plasmids must be blended within the particles themselves in order to successfully deliver both plasmids to each cell[33]. Having thousands of miRNAs within a single nanoparticle would be

beneficial, as both miR-148a and miR-296-5p need to be codelivered to successfully reduce tumor cell stemness.

We continued to incubate the nanoparticles in aCSF and found that miRNA remained completely bound within the first hour of aCSF incubation, began to release at 2 hr and completely released by 8 hr. To assess miRNA binding in an environment mimicking the reducing cytosolic space, we incubated miRNA nanoparticles in 5 mM glutathione (GSH), the primary reducing agent in the cytosol[28]. In the presence of GSH, miRNA began to release within 5 min of incubation, and was completely released within 30 min (**Figure 6.2f**). The quick release of miRNA is dually important, as polymer degradability reduces cytotoxicity[34] and because dissociation of nucleic acid cargo from its carrier is a necessary step for transfection[35, 36].

6.3.3. PBAE nano/miRs inhibit the GBM stem cell phenotype *in vitro.*

miRNAs and siRNAs share chemical, physical, biological, and biochemical properties[37] prompting us to hypothesize that the polymer formulations we developed to deliver siRNAs will also efficiently deliver miRNAs. To test this hypothesis mature miRNA mimics labeled with Dy547 were complexed with PBAE polymers to generate PBAE nano/miRs used to transfect GBM neurospheres. Nanoparticle assembly and payload delivery was monitored using fluorescent microscopy. We detected fluorescence from the Dy547-labeled control miRNA starting 3 days after the transfection and the signal persisted for at least 12 days (**Figure 6.4a, 6.5**). These results show that we can stably and efficiently deliver miRNAs using this PBAE formulation.

One major advantage of nonviral gene delivery via cationic polymers is that particles can be easily loaded with individual miRNAs or combinations by simply incubating polymer with RNA to allow electrostatically-induced self-assembly[13, 38]. We recently identified two miRNAs, *i.e.* miR-148a and miR-296-5p, that are down-regulated during GBM stemness induction by

Oct4/Sox2 and whose reintroduction inhibits the stem cell phenotype and tumor-propagating potential of these cells [11, 12]. To measure the ability of these PBAE polymers to deliver these bio-active miRNAs, nano/miRs consisting of control miRNA (miCtrl), miR-148a mimic, miR-296-5p mimic, or miR-148a+miR-296-5p (comb.) were prepared and used to transfect GBM neurospheres. The total RNA concentration was kept at 120 nM, and miR-148a or miR-296-5p were either blended with miCtrl or one another, so that the total dose of each functional miRNA remained at 60 nM in all conditions. Expression of mature miRNAs was measured using qRT-PCR 3 days after transfection. Transfecting GBM neurospheres using miR-148a nano/miRs increased levels by 24-fold and using this approach to deliver miR-296-5p increased levels by 27-fold. The combination nano/miR increased levels of miR-148a and miR-296-5p by 16- and 30-fold respectively (**Figure 6.4b**). To directly test the effects of these nano/miRs on the GBM stem cell phenotype, two distinct neurosphere lines were transfected using the formulations mentioned above and the sphere formation capacity of these cells was measured 12 days after transfection. MiRNA delivery using this approach significantly inhibited sphere forming capacity (**Figure 6.4c**) concurrent with the decreased expression of stem cell drivers and markers Sox2, Nanog, and Olig2 (**Figure 6.4d**). These data recapitulate our previous results using lenti-viral systems for miRNA reconstitution[11, 12] and suggests that PBAE polymers are an excellent vehicle to deliver bio-active miRNAs *in vitro.*

6.3.4. PBAE nanoparticles penetrate an orthotopic model of human GBM, deliver miRNA to human GBM, and reduce the GBM stem cell phenotype *in vivo.*

A major obstacle that prevents drug delivery to the brain is the blood brain barrier, which limits the accessibility of highly charged molecules such as miRNAs or PBAE polymers, making systemic delivery of nano/miRs very challenging[39]. To circumvent this obstacle we used a

technique that closely resembles the clinically translatable convection enhanced delivery (CED) to test the biological effects of our nano/miRs *in vivo*[30]. A trans-cranial cannula was placed so that the tip is inside the right caudate/putamen of mice. One week after cannula placement, animals received A172-iGSCs[11] cells via the cannula and 3 weeks after cell implantation, we started the PBAE nano/miR delivery. Twice per week animals received slow infusions of control miRNA mimics labeled with Dy547 or miR-148a via the cannula to optimally localize delivery to tumor site. Brains were collected and sections were visualized using fluorescent microscopy and compared to the adjacent H&E stained counterparts. The expression of fluorescently labeled control miRNA was detectable in ~70% of the tumor volume (**Figure 6.6a**), demonstrating we can efficiently deliver miRNAs to an established tumor using our PBAE formulation. To test if the miRNAs delivered using this protocol retained their biological function, we measured the expression of Dnmt1 and Dnmt3b, two well described miR-148a targets[11], in tumor sections using immunohistochemistry (**Figure 6.6b**). Tumor treated with miR-148a nano/miRs had significantly lower expression levels of both Dnmt1 and Dnmt3b compared to control treated animals, indicating the miRNAs retain their biological activity.

6.3.5. miRNA codelivery via PBAE nanoparticles reduces GBM growth and promotes tumor killing in an orthotopic model of human GBM.

It is well accepted that stem-like cells drive the tumor-initiation and that loss of self-renewal capacity or differentiation of these cell population results in loss of tumor-propagating capacity[4, 6]. To test if reconstituting these stem cell inhibitory miRNAs prevents the growth of an established tumor, GBM1A neurospheres, which closely recapitulate the tumor pathology of GBM patients[26], were implanted in animals using the same experimental paradigm as before (**Figure 6.6c**). Tumors were then treated with control miRNA, miR-148a, miR-296-5p, or the combination.

Consistent with the stem cell inhibitory properties of miR-14a and miR-296-5p, we observed decreased tumor burden in all three treated groups, with the combination having the most profound effect (**Figure 6.6d,e**). This decrease in tumor size coincided with an increase in tissue necrosis (**Figure 6.6f**) and activation of apoptosis (**Figure 6.6g),** as measured by histopathology and cleaved Caspase 3 immunohistochemistry respectively. These findings demonstrate that PBAE nano/miRs inhibit the growth of an established GBM tumor in an orthotopic xenograft model and suggest this approach can be successfully developed into new ways to treat brain tumors.

6.3.6. miR-148a delivery sensitizes GBM to killing via radiation therapy.

We then assessed the ability of miR-148a delivery via nanoparticles to sensitize GBM tumors to radiation therapy (**Figure 6.7**). We used immunohistochemical analysis to assess tumor progression in each group by assessing vascularization, apoptosis, and miR-148a activity (**Figure 6.8a**). Laminin staining allowed us to visualize blood vessels, and we found that miR-148a treated tumors, both with and without IR showed significantly less vessels per field of view than control tumors (miR-Ctrl and no IR) (**Figure 6.8b**). We stained for cleaved caspase-3 to assess tumor apoptosis and found that miR-148a, with and without IR, showed significantly higher expression of the apoptotic marker than control mice (**Figure 6.8c**). We also measured expression of DNA methyl transferase-3b (DNMT3b), a target of miR-148a, and showed that both miR-148a treated groups showed a significant reduction in DNMT3b expression (**Figure 6.8d**).

Finally, we used hemotoxylin and eosin (H&E) staining to visualize tumors and calculate tumor burden. We showed that miR-148a nanoparticle treatment combined with IR therapy significantly reduced tumor volume to 12 ± 4 mm^2, versus miR-Ctrl treated mice without IR (79 ± 11 mm^2) and with IR (75 ± 13 mm^2) (**Figure 6.9**). Radiation had no significant effect on tumor volume versus control. This suggests that nanoparticles carrying miR-148a to tumor cells

sensitized the tumor to radiation therapy. As our *in vitro* data showed that we could use miR-148a delivery to reduce the tumor-propagating and stem-like phenotype of GBM cells, we believe that this caused the radiation sensitization.

6.4. Conclusion

Herein, we have described the synthesis of a novel, bioreducible PBAE capable of encapsulating miRNA into nanoparticles and delivering it intracellularly. We have demonstrated that imparting bioreducibility enables near-immediate cargo release when nanoparticles reach their subcellular target location in the cytosol. We have demonstrated that this property enables the nanoparticles to successfully carry RNA into human GBM cells, and that their fast degradation profile significantly reduces cytotoxicity. We have shown that we can load miR-148a and miR-296-5p, either alone or in combination, into these nanoparticles and deliver it to human brain cancer *in vitro*, and that this significantly reduces the stem-like and tumor propagating phenotype of GBM. When delivered intratumorally, miR-148a or miR-296-5p nanoparticles significantly reduce tumor vacularization, increase tumor apoptosis, and decrease the expression of a target of miR-148a. In combination, these effects are strengthened. We have shown that delivery of miR-148a or miR-296-5p reduces tumor size and increases tumor killing, and that combination miR-148/296-5p delivery enhances this effect. Finally, we have shown that miR-148a nanoparticle treatment sensitizes GBM to radiation therapy and reduces tumor burden. The results presented herein show that bioreducible PBAE nanoparticles have the potential to be a safe, effective, and tumor-specific delivery vehicle for intratumoral delivery of RNA cargos. They also suggest that bioreducible PBAE nanoparticles carrying miR-148a have the potential to sensitize brain tumors to radiation therapy and thereby treat brain cancer.

6.5. Figures

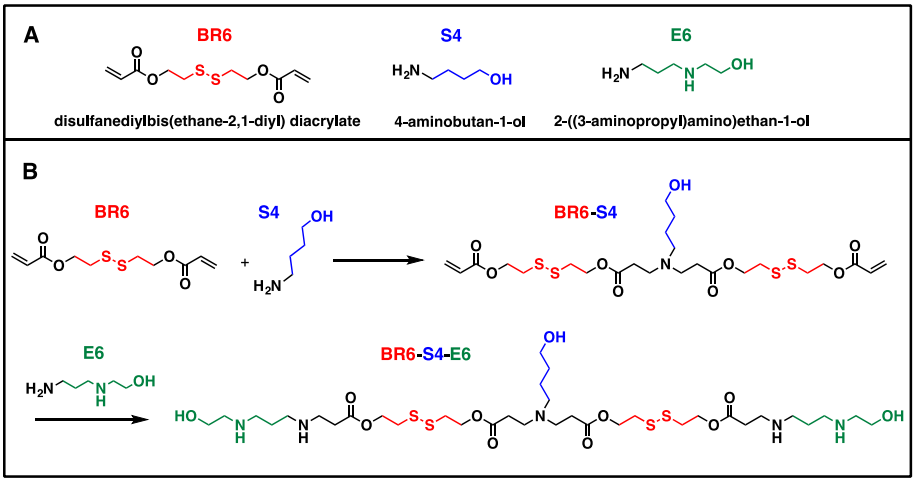

Figure 6.1. Bioreducible PBAE polymer synthesis. (A) PBAE monomer structures are shown, including bioreducible monomer BR6. (B) Bioreducible PBAE synthesis is carried out via Michael Addition of diacrylate monomer BR6 and amine-containing monomer S4 at a 1.1:1 BR6:S4 ratio to yield acrylate-terminated polymer BR6-S4. This polymer is endcapped with amine-containing monomer E6 to yield BR6-S4-E6 (R646), a polymer that has redox-responsive disulfide moieties as well as hydrolytically cleavable ester linkages.

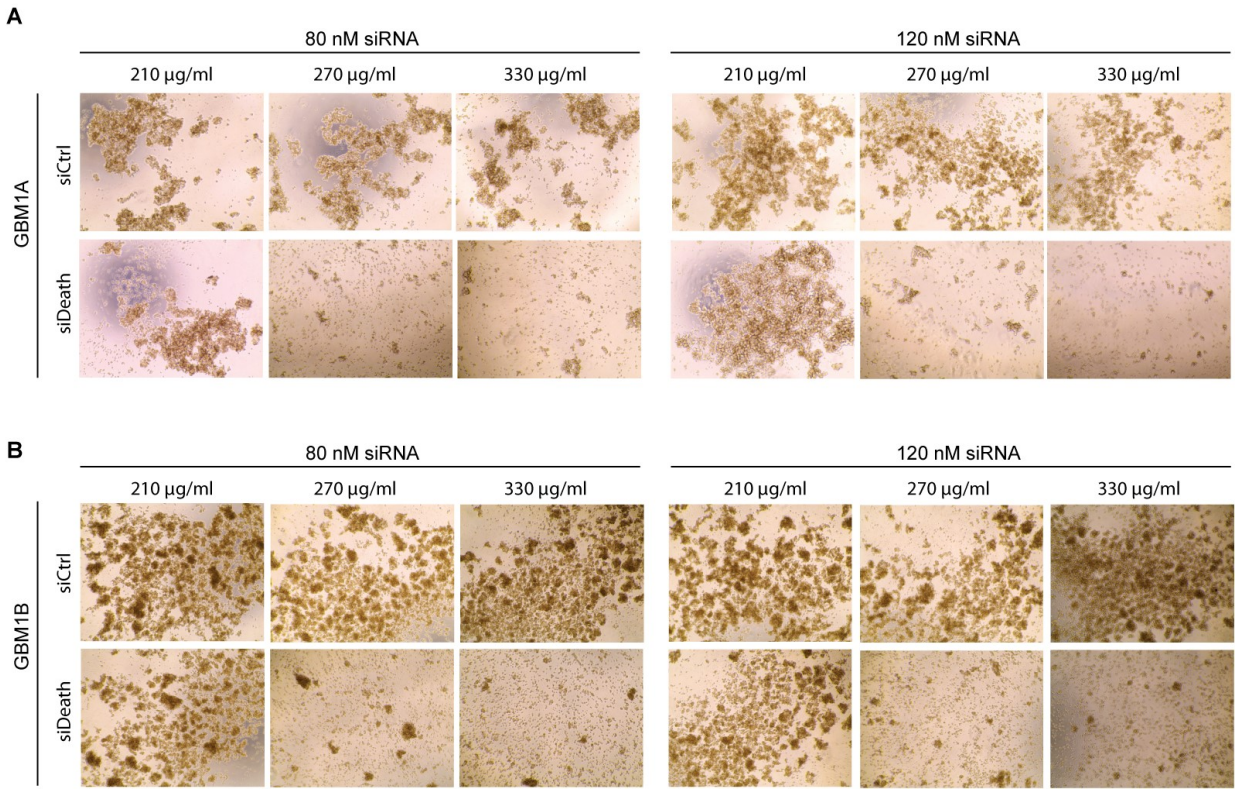

Figure 6.2. PBAE Polymers can efficiently deliver siRNAs to GBM neurospheres. GBM1A (A) and GBM1B (B) neurospheres were dissociated into single cell, seeded onto 96-well plates pre-treated with Poly-L-Lysine ($1.0x10^4$ cells/well) and transfected with increasing amounts of PBAE polymers loaded with either 80nM or 120nM of a control siRNA (siCtrl.) or a toxic siRNA (siDeath). Representative pictures were taken 12 days after siRNA delivery.

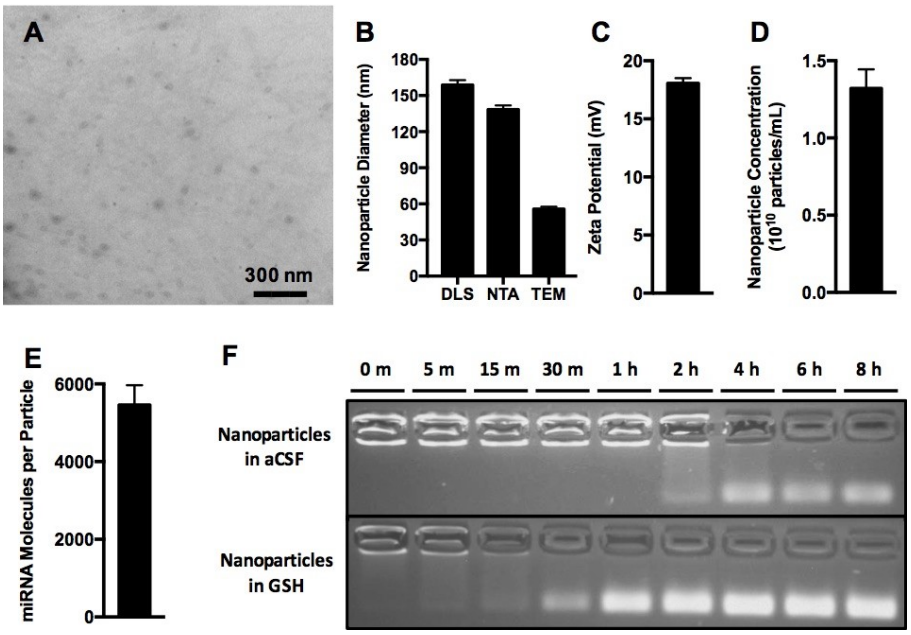

Figure 6.3. PBAEs form nanoparticles with miRNA and effectively release it in a reducing environment. PBAE polymers were used to form nanoparticles with miRNA and their physical properties in varying conditions were characterized. (A) TEM imaging of PBAE/miRNA nanoparticles showing dried particle size a morphology. (B) Nanoparticle hydrodynamic diameter as measured using either intensity-weighted (DLS) or number-average (NTA) measurement, and dried nanoparticle diameter as measured by TEM. (C) Nanoparticle surface charge (ζ-potential) is reported as measured via DLS. (D,E) Nanoparticle concentration as measured by NTA is reported to show the concentration delivered *in vitro*, and the calculated miRNA loading in each nanoparticle. (F) A gel retention assay was performed to assess miRNA binding in artificial CSF (aCSF) versus in 5 mM glutathione (GSH), to mimic the extracellular versus intracellular space within the brain. miRNA that is tightly bound within PBAE nanoparticles is unable to run along the gel.

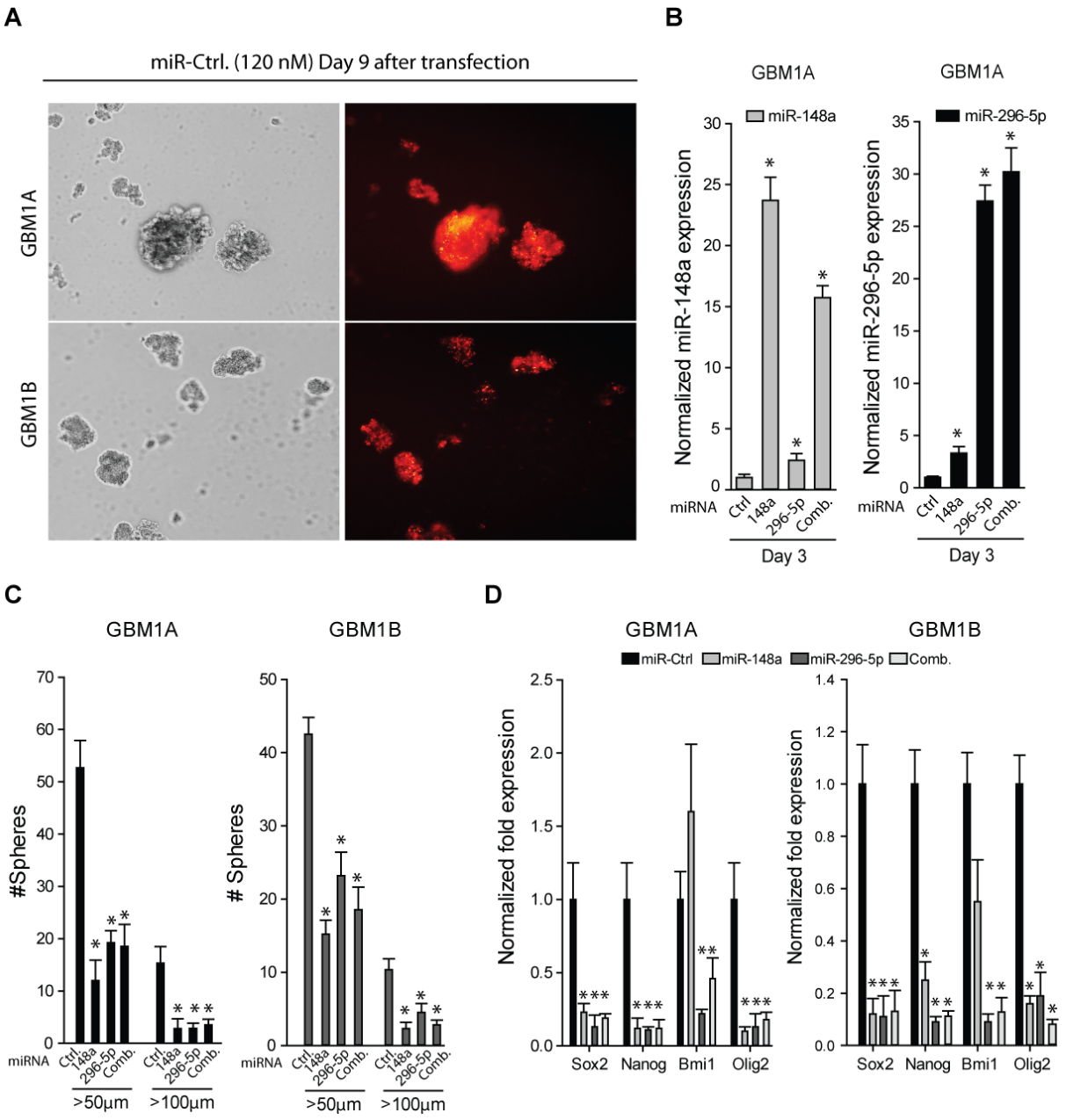

Figure 6.4. PBAE nano/miRs inhibit the GBM stem cell phenotype. GBM1A and GBM1B neurospheres were dissociated into single cell, seeded onto plates pre-treated with Poly-L-Lysine ($1.5x10^5$ cells/ml) and transfected with either miR-Ctrl., miR-148a, miR-296-5p, or the combination (120nM) using PBAE polymers (270mg/ml). (A) miR-Ctrl labeled with Dy547 was visualized 9 days after transfection using fluorescent microscopy. (B) Expression of mature miR-148a and miR-296-5p was measured by qRT-PCR 3 days after transfection. (C) Equal numbers of GBM1A or GBM1B cells transfected with nano/miRNA conjugates were cultured in neurosphere medium containing EGF/FGF for 12 days and neurosphere numbers (>100µm diameter) were quantified by computer-assisted image analysis. (D) qRT-PCR analysis to measure expression of stem cell markers in GBM1A or GBM1B neurospheres transfected with nano/miRNA conjugates. *$p< 0.05$

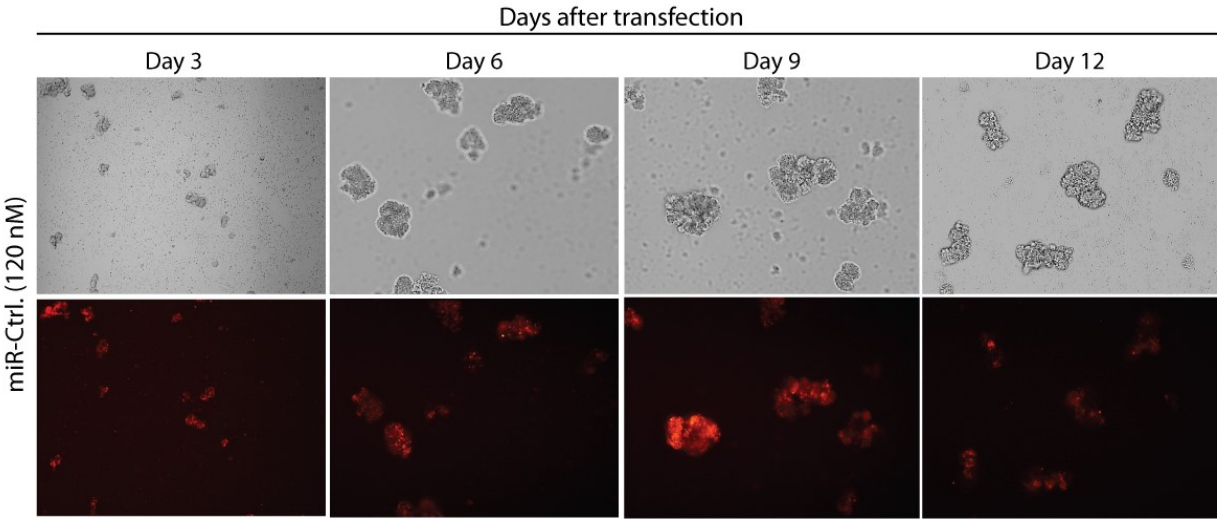

Figure 6.5. PBAE nanoparticle delivery of Dy547-labeled miRNA successfully penetrates GBM cells and persists for 12 d post-transfection.

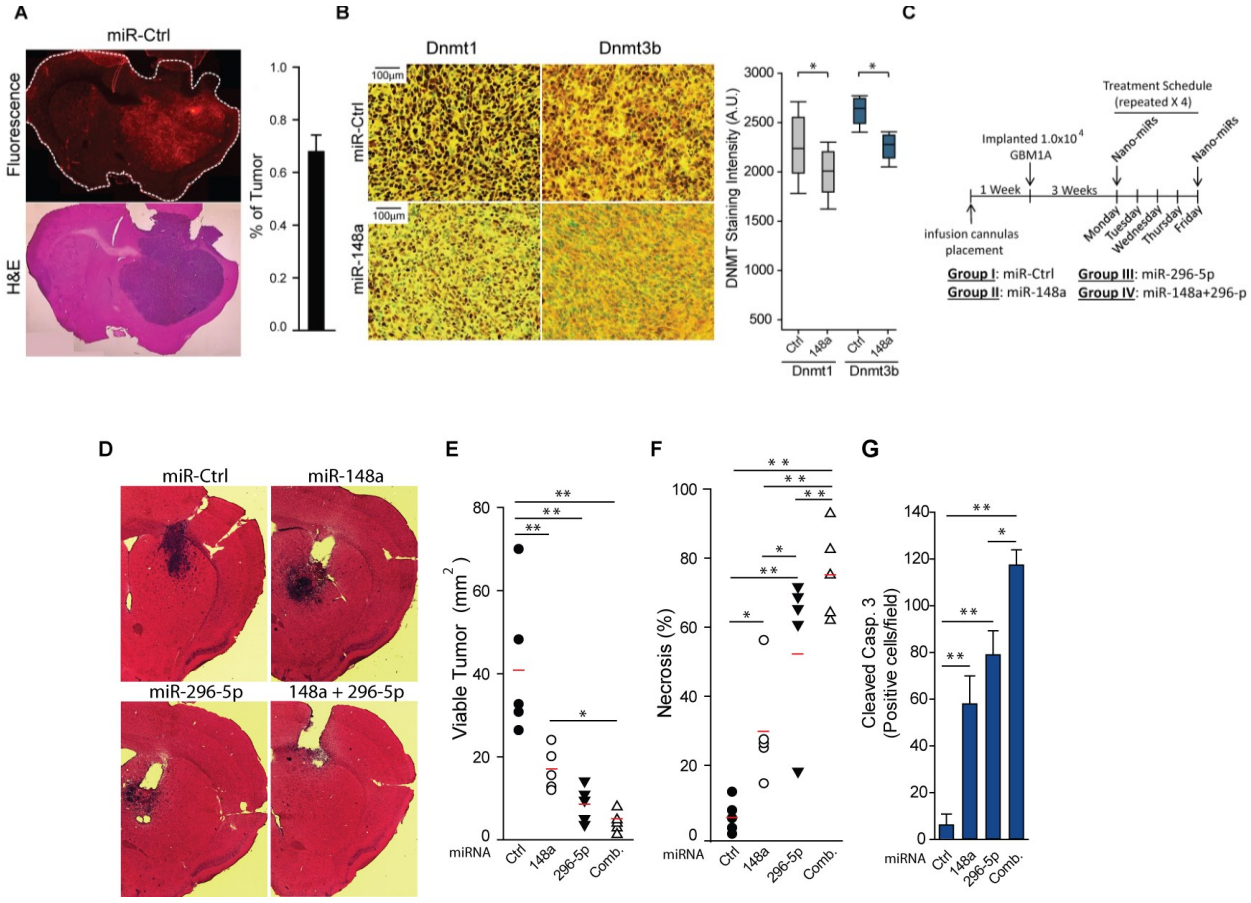

Figure 6.6. miR-148a and miR-296-5p co-delivery using PBAE polymers inhibits GBM tumor growth *in vivo*. $3.0x10^4$ A172-iGSCs cells were injected into the right striatum of Nod SCID mice. 3 weeks after injection, 5 μL of PBAE/miRNA conjugates were convected into the brains twice a week for 3 weeks. Brains were collected, fixed and 20 μm sections were cut. (A) miR-Ctrl labeled with Dy547 was visualized using fluorescent microscopy (top, left panel) and compared to adjacent H&E stained sections (bottom, left panel). The intra-tumoral distribution of the nanomiR conjugates was calculated as the ratio of fluorescence area divided by tumor area X 100 (N=3, right panel). (B) Immunohistochemical analysis of DNMT1 and DNMT3b in tumor sections treated with miR-Ctrl or miR-148a (left panel). Quantification of DNMT1 and DNMT3b expression in tumor sections treated with miR-Ctrl. or miR-148a using computer-assisted densitometry analysis (right panel) (C) Schematic summarizing treatment schedule for *in vivo* delivery of nano/miR conjugates. (D) Representative H&E stained brain sections from mice implanted with GBM1A neurosphere cells treated with the indicated Nano/miR conjugates. Maximum tumor X-sectional areas following treatment with Nano/miR conjugates representing viable tumor tissue (E) and necrotic tumor tissue (F) were quantified from H&E stained sections using ImageJ software. (G) Apoptotic index was measured in tumor sections by immunohistochemical analysis using cleaved Caspase 3. (**p<0.01, *p< 0.05).

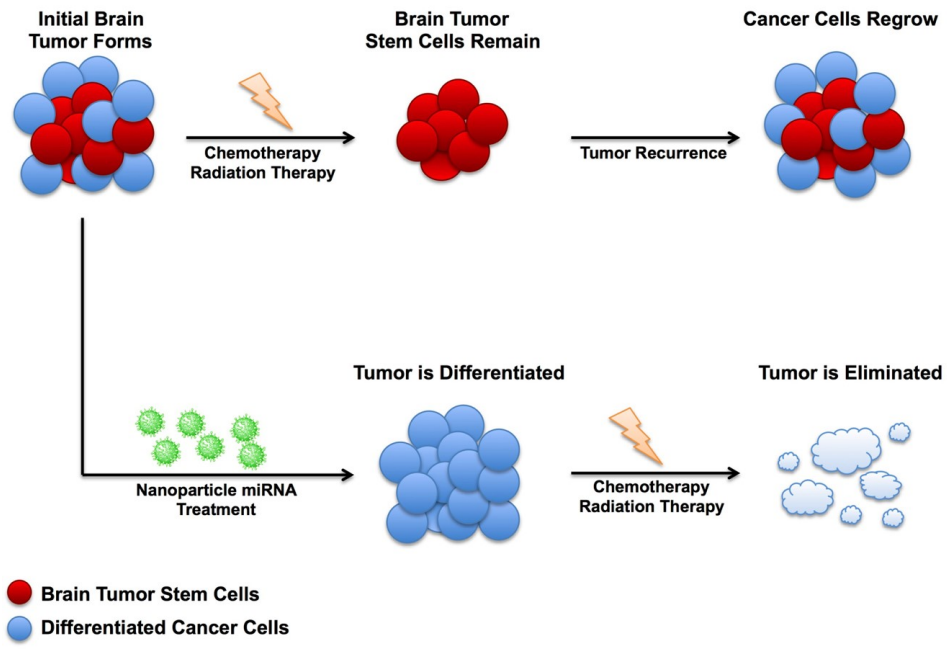

Figure 6.7. Nanoparticles carrying miRNA convert brain tumor stem cells to cancer cells, thereby sensitizing them to killing via conventional cancer therapies.

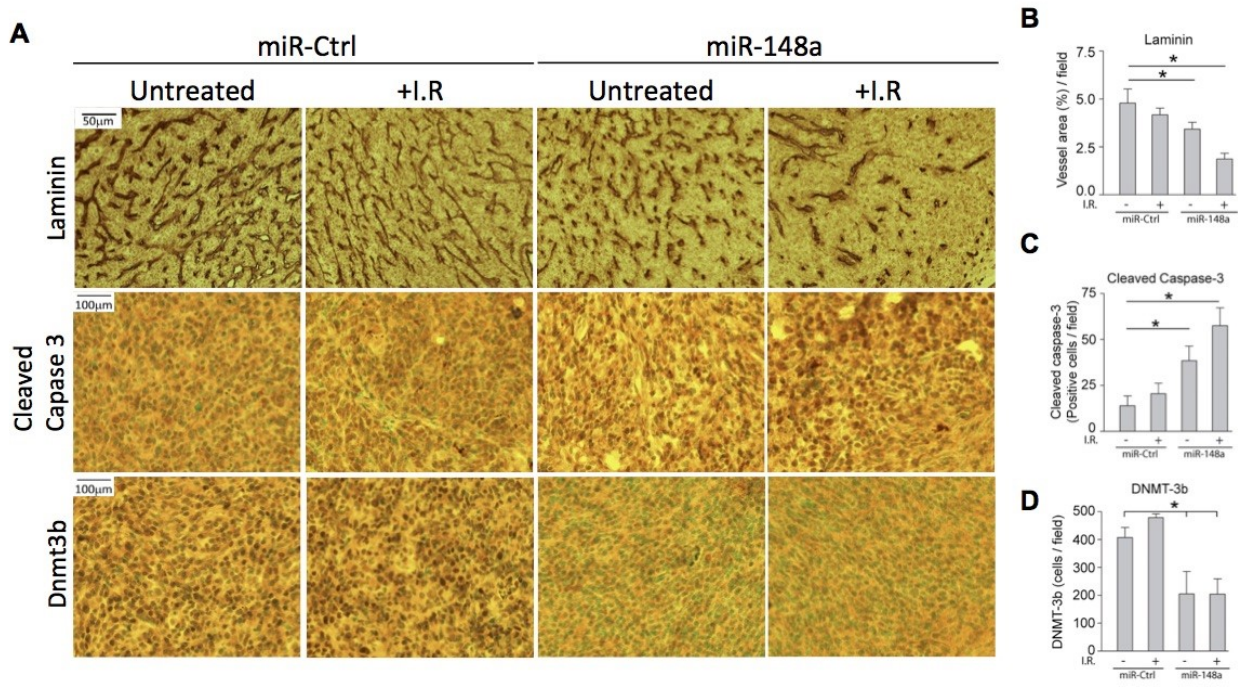

Figure 6.8. Immunohistochemical analysis of tumor tissue. Laminin staining shows reduced vessel area per field of view in tumors treated with miR-148a nanoparticles with and without radiation, indicating reduced tumor vascularization, a marker of aggression (B). Cleaved Caspase-3 staining shows increased tumor cell apoptosis in tumors treated with miR-148a nanoparticles both with and without radiation (C) DNMT-3b staining shows miR-148a nanoparticles reduce the expression of DNMT-3b, a direct target of miR-148a (D). Radiation alone shows no significant change in vascularization, apoptosis, or DNMT-3b activity.

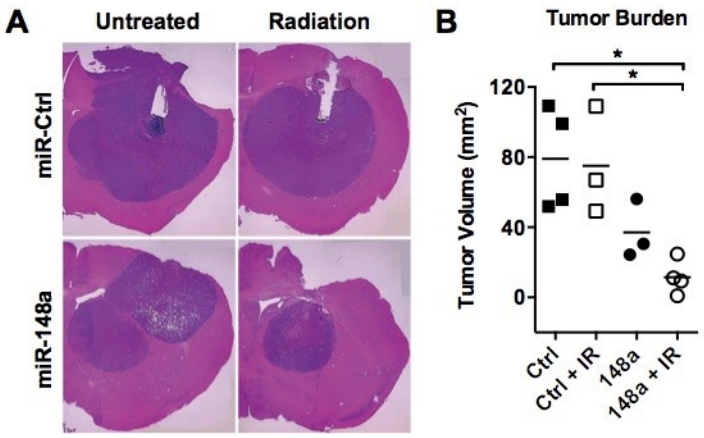

Figure 6.9. *In vivo* delivery of miR-148a nanoparticles with combined with ionizing radiation (IR) reduces tumor burden in mice versus miR-Ctrl-treated mice with IR, suggesting that miR-148a nanoparticles sensitized the tumor to radiation therapy. Radiation alone shows no significant reduction in tumor burden. Tumors treated with miR-148a alone show some decrease in tumor burden, but this is not significant. This highlights the importance of using miR-148a nanoparticles and radiation in combination.

6.6. References

1. Ostrom, Q. T.; Gittleman, H.; de Blank, P. M.; Finlay, J. L.; Gurney, J. G.; McKean-Cowdin, R.; Stearns, D. S.; Wolff, J. E.; Liu, M.; Wolinsky, Y.; Kruchko, C.; Barnholtz-Sloan, J. S. American Brain Tumor Association Adolescent and Young Adult Primary Brain and Central Nervous System Tumors Diagnosed in the United States in 2008-2012. *Neuro-oncology* **2016,** 18 Suppl 1, i1-i50.
2. Seystahl, K.; Wick, W.; Weller, M. Therapeutic Options in Recurrent Glioblastoma-an Update. *Critical reviews in oncology/hematology* **2016,** 99, 389-408.
3. Tamai, I.; Tsuji, A. Transporter-Mediated Permeation of Drugs across the Blood-Brain Barrier. *Journal of pharmaceutical sciences* **2000,** 89, 1371-1388.
4. Lopez-Bertoni, H.; Li, Y.; Laterra, J. Cancer Stem Cells: Dynamic Entities in an Ever-Evolving Paradigm. *Biol Med (Aligarh)* **2015,** 7.
5. Hernando Lopez-Bertoni, Y. L. a. J. L. Cancer Stem Cells: Dynamic Entities in an Ever-Evolving Paradigm. *Biology and Medicine* **2014,** S2.
6. Li, Y.; Laterra, J. Cancer Stem Cells: Distinct Entities or Dynamically Regulated Phenotypes? *Cancer research* **2012,** 72, 576-580.
7. Mack, S. C.; Hubert, C. G.; Miller, T. E.; Taylor, M. D.; Rich, J. N. An Epigenetic Gateway to Brain Tumor Cell Identity. *Nature neuroscience* **2016,** 19, 10-19.
8. Choi, J. D.; Lee, J. S. Interplay between Epigenetics and Genetics in Cancer. *Genomics & informatics* **2013,** 11, 164-173.
9. Easwaran, H.; Tsai, H. C.; Baylin, S. B. Cancer Epigenetics: Tumor Heterogeneity, Plasticity of Stem-Like States, and Drug Resistance. *Molecular cell* **2014,** 54, 716-727.
10. Sato, F.; Tsuchiya, S.; Meltzer, S. J.; Shimizu, K. Micrornas and Epigenetics. *FEBS J* **2011,** 278, 1598-1609.
11. Lopez-Bertoni, H.; Lal, B.; Li, A.; Caplan, M.; Guerrero-Cazares, H.; Eberhart, C. G.; Quinones-Hinojosa, A.; Glas, M.; Scheffler, B.; Laterra, J.; Li, Y. Dnmt-Dependent Suppression of Microrna Regulates the Induction of Gbm Tumor-Propagating Phenotype by Oct4 and Sox2. *Oncogene* **2014**.
12. Lopez-Bertoni, H.; Lal, B.; Michelson, N.; Guerrero-Cazares, H.; Quinones-Hinojosa, A.; Li, Y.; Laterra, J. Epigenetic Modulation of a Mir-296-5p:Hmga1 Axis Regulates Sox2 Expression and Glioblastoma Stem Cells. *Oncogene* **2016**.
13. Tzeng, S. Y.; Green, J. J. Therapeutic Nanomedicine for Brain Cancer. *Ther Deliv* **2013,** 4, 687-704.
14. Thomas, C. E.; Ehrhardt, A.; Kay, M. A. Progress and Problems with the Use of Viral Vectors for Gene Therapy. *Nat. Rev. Genet.* **2003,** 4, 346-358.
15. Verma, I. M.; Somia, N. Gene Therapy-Promises, Problems and Prospects. *Nature* **1997,** 389, 239-242.
16. Bhise, N. S.; Shmueli, R. B.; Gonzalez, J.; Green, J. J. A Novel Assay for Quantifying the Number of Plasmids Encapsulated by Polymer Nanoparticles. *Small* **2012,** 8, 367-373.
17. Kozielski, K. L.; Tzeng, S. Y.; Mendoza, B. A. H. d.; Green, J. J. Bioreducible Cationic Polymer-Based Nanoparticles for Efficient and Environmentally Triggered Cytoplasmic Sirna Delivery to Primary Human Brain Cancer Cells. *ACS Nano* **2014,** 8, 3232-3241.
18. Akinc, A.; Zumbuehl, A.; Goldberg, M.; Leshchiner, E. S.; Busini, V.; Hossain, N.; Bacallado, S. A.; Nguyen, D. N.; Fuller, J.; Alvarez, R.; Borodovsky, A.; Borland, T.; Constien, R.; de Fougerolles, A.; Dorkin, J. R.; Jayaprakash, K. N.; Jayaraman, M.; John, M.; Koteliansky,

V.; Manoharan, M.; Nechev, L.; Qin, J.; Racie, T.; Raitcheva, D.; Rajeev, K. G.; Sah, D. W. Y.; Soutschek, J.; Toudjarska, I.; Vornlocher, H. P.; Zimmermann, T. S.; Langer, R.; Anderson, D. G. A Combinatorial Library of Lipid-Like Materials for Delivery of Rnai Therapeutics. *Nat. Biotechnol.* **2008,** 26, 561-569.
19. Kakizawa, Y.; Furukawa, S.; Ishii, A.; Kataoka, K. Organic-Inorganic Hybrid-Nanocarrier of Sirna Constructing through the Self-Assembly of Calcium Phosphate and Peg-Based Block Aniomer. *J. Control. Release* **2006,** 111, 368-370.
20. Boussif, O.; Lezoualc'h, F.; Zanta, M. A.; Mergny, M. D.; Scherman, D.; Demeneix, B.; Behr, J.-P. A Versatile Vector for Gene and Oligonucleotide Transfer into Cells in Culture and in Vivo: Polyethylenimine. *Proc. Natl. Acad. Sci.* **1995,** 92, 7297-7301.
21. Wu, G. Y.; Wu, C. H. Receptor-Mediated in Vitro Gene Transformation by a Soluble DNA Carrier System. *J. Biol. Chem.* **1987,** 262, 4429-4432.
22. Lynn, D. M.; Langer, R. Degradable Poly(B-Amino Esters): Synthesis, Characterization, and Self-Assembly with Plasmid DNA. *J. Am. Chem. Soc.* **2000,** 122, 10761-10768.
23. Tzeng, S. Y.; Green, J. J. Subtle Changes to Polymer Structure and Degradation Mechanism Enable Highly Effective Nanoparticles for Sirna and DNA Delivery to Human Brain Cancer. *Adv. Healthcare Mater.* **2013,** 2, 468-480.
24. Kozielski, K. L.; Tzeng, S. Y.; Green, J. J. A Bioreducible Linear Poly(Beta-Amino Ester) for Sirna Delivery. *Chem. Commun.* **2013,** 49, 5319 - 5321.
25. Fire, A.; Xu, S. Q.; Montgomery, M. K.; Kostas, S. A.; Driver, S. E.; Mello, C. C. Potent and Specific Genetic Interference by Double-Stranded Rna in Caenorhabditis Elegans. *Nature* **1998,** 391, 806-811.
26. Galli, R.; Binda, E.; Orfanelli, U.; Cipelletti, B.; Gritti, A.; De Vitis, S.; Fiocco, R.; Foroni, C.; Dimeco, F.; Vescovi, A. Isolation and Characterization of Tumorigenic, Stem-Like Neural Precursors from Human Glioblastoma. *Cancer research* **2004,** 64, 7011-7021.
27. Davson, H. *Physiology of the Cerebrospinal Fluid*. J. & A. Churchill, Ltd.: London, 1967.
28. Griffith, O. W. Biologic and Pharmacologic Regulation of Mammalian Glutathione Synthesis. *Free Radical Bio. Med.* **1999,** 27, 922-935.
29. Moreno-Estelles, M.; Diaz-Moreno, M.; Gonzalez-Gomez, P.; Andreu, Z.; Mira, H. Single and Dual Birthdating Procedures for Assessing the Response of Adult Neural Stem Cells to the Infusion of a Soluble Factor Using Halogenated Thymidine Analogs. *Current protocols in stem cell biology* **2012,** Chapter 2, Unit 2D 10.
30. Lal, B.; Xia, S.; Abounader, R.; Laterra, J. Targeting the C-Met Pathway Potentiates Glioblastoma Responses to Gamma-Radiation. *Clinical cancer research : an official journal of the American Association for Cancer Research* **2005,** 11, 4479-4486.
31. Tzeng, S. Y.; Guerrero-Cázares, H.; Martinez, E. E.; Sunshine, J. C.; Quiñones-Hinojosa, A.; Green, J. J. Non-Viral Gene Delivery Nanoparticles Based on Poly(B-Amino Esters) for Treatment of Glioblastoma. *Biomaterials* **2011,** 32, 5402-5410.
32. Davson, H. Physiology of the Cerebrospinal Fluid. **1970**.
33. Bhise, N. S.; Wahlin, K.; Zack, D.; Green, J. J. Evaluating the Potential of Poly(Beta-Amino Ester) Nanoparticles for Reprogramming Human Fibroblasts to Become Induced Pluripotent Stem Cells. *International Journal of Nanomedicine* **2013,** 8, 4641-4658.
34. Hill, I. R.; Garnett, M. C.; Bignotti, F.; Davis, S. S. In Vitro Cytotoxicity of Poly(Amidoamine)S: Relevance to DNA Delivery. *Biochim. Biophys. Acta* **1999,** 1427, 161-174.

35. Elbakry, A.; Zaky, A.; Liebl, R.; Rachel, R.; Goepferich, A.; Breunig, M. Layer-by-Layer Assembled Gold Nanoparticles for Sirna Delivery. *Nano Lett.* **2009,** 9, 2059-2064.
36. Gary, D. J.; Puri, N.; Won, Y. Y. Polymer-Based Sirna Delivery: Perspectives on the Fundamental and Phenomenological Distinctions from Polymer-Based DNA Delivery. *J. Control. Release* **2007,** 121, 64-73.
37. Muthiah, M.; Park, I. K.; Cho, C. S. Nanoparticle-Mediated Delivery of Therapeutic Genes: Focus on Mirna Therapeutics. *Expert opinion on drug delivery* **2013,** 10, 1259-1273.
38. Kozielski, K. L.; Tzeng, S. Y.; Green, J. J. Bioengineered Nanoparticles for Sirna Delivery. *Wiley interdisciplinary reviews. Nanomedicine and nanobiotechnology* **2013,** 5, 449-468.
39. Banks, W. A. From Blood-Brain Barrier to Blood-Brain Interface: New Opportunities for Cns Drug Delivery. *Nature reviews. Drug discovery* **2016,** 15, 275-292.

Vita

Kristen Kozielski
Biomedical Engineering Ph.D. candidate
kkoziel1@jhu.edu
410-627-4649

Education

Johns Hopkins University School of Medicine (JHUSOM): 2011 - 2016

- Ph.D. in Biomedical Engineering, expected graduation 2016
- Ruth L. Kirchstein F31 NIH National Research Service Award Fellowship, National Cancer Institute (2015-present)
- ARCS Foundation Scholarship (2015 – present)
- NIH Cancer Nanobiotechnology Training Center Fellowship (2012 - 2014)

Johns Hopkins University (2006 - 2010)

- B.S. in Biomedical Engineering
- General and Departmental Honors
- Dean's list (2006 - 2010)

Peer-reviewed Publications

1. **Kozielski, K.L.**;* Lopez-Bertoni, H.;* Lal. B.; Vaughan, H.; Michelson, N.; Eberhart, C.; Laterra, J.; Green. J.J. Nanoparticle delivery of stem cell-inhibitory miRNAs hinders GBM growth and prolongs animal survival. *Manuscript in preparation*.
2. Huang, Y.; Schiapparelli, P.; **Kozielski, K.L.**; Green, J.J.; Lavell, E.; Guerrero-Cazares, H.; Quinones-Hinojosa, A.; Searson, P. Electrophoresis of Cell Membrane Heparan Sulfate Regulates Galvanotaxis in Glial Cells. *Nature Communications*. **2016**, *Submitted.*
3. **Kozielski, K.L.**;* Rui, Y.;* Green, J.J.: Non-viral methods of intracelllular DNA and siRNA delivery. *Expert Opinion on Drug Delivery*. **2016**, *ePub ahead of print.*
4. Mangraviti, A.;* Tzeng, S.Y.;* Gullotti, D.; **Kozielski, K.L.**; Kim, J.E.; Seng, M.; Abbadi, S.; Schiapparelli, P.; Sarabia-Estrada, R.; Brem, H.; Vescovi, A.; Olivi, A.; Tyler, B.; Green, J.J.; Quinones-Hinojosa, A. Human adipose mesenchymal stem cells engineered via non-viral gene therapy produce BMP4, target brain tumors, and extend survival *in vivo*. *Biomaterials*. **2016,** *100*, 53-66.
5. Li, X.; **Kozielski, K.L.**; Cheng, Y.; Liu, H.; Zamboni, C.; Green, J.J.; Mao, H. Nanoparticle-mediated conversion of primary human astrocytes into neuronal cells and oligodendrocyte progenitors. *Biomaterials Science*. **2016**, *4*, 1100-1112.
6. **Kozielski, K.L.**; Green, J.J.: Bioreducible poly(beta-amino ester)s for intracellular delivery of siRNA. *Methods in Molecular Biology.* **2016**, *1364*, 79-87.
7. Bishop, C.J.;***** **Kozielski, K.L.**;***** Green, J.J.: Exploring the role of polymer structure on intracellular nucleic acid delivery via polymeric nanoparticles. *Journal of Controlled Release*. **2015**, *213*, 488-499.
8. Mangraviti, A.;***** Tzeng, S.Y.;***** **Kozielski, K.L.**;***** Wang, Y.;***** Pedone, M.; Buaron, N.; Liu, A.; Wilson, D.R.; Hansen, S.K.; Rodriguez, F.J.; Gao, G.; DiMeco, F.; Brem, H.; Olivi, A.; Tyler, B.; Green, J.J.: Polymeric nanoparticles for non-viral gene therapy extend brain tumor survival *in vivo*. *ACS Nano* **2015,** *9,* 1236-1249.
    - Highlighted as the *ACS Nano* most read / most downloaded article from the past 12 months (#1 March 2015, Top 10: March 2015-present)

- Editor's Choice: Stephan, M.; Nanocarriers deliver DNA to brain tumors. *Science Translational Medicine*. **2015**, *7,* 276ec34.
- Highlighted by the NIH NIBIB "New Nanoparticle Gene Therapy Treats Brain Cancer in Rats." April 10, 2015

9. Hung, B.P.; Hutton, D.L.; **Kozielski, K.L.**; Bishop, C.J.; Naved, B.; Green, J.J.; Caplan, A.I.; Gimble, J.M.; Dorafshar, A.H.; Grayson, W.L.: Platelet-derived growth factor BB enhances osteogenesis of adipose-derived but not bone marrow-derived mesenchymal stromal/stem cells. *Stem Cells* **2015,** *33*, 2773-2784.
10. **Kozielski, K.L.**; Tzeng, S. Y.; Hurtado de Mendoza, B. A.; Green, J.J: Bioreducible cationic polymer-based nanoparticles for efficient and environmentally triggered cytoplasmic siRNA delivery to primary human brain cancer cells. *ACS Nano* **2014**, *8,* 3232-3241.
11. **Kozielski, K.L.;** Tzeng, S. Y.; Green, J. J.: A bioreducible linear poly(beta-amino ester) for siRNA delivery. *Chemical Communications* **2013**, *49,* 5319-5321.
12. **Kozielski, K.L.**;***** Tzeng, S.Y;***** Green, J.J.: Bioengineered nanoparticles for siRNA delivery. *WIREs Nanomedicine and Nanobiotechnology* **2013**, *5,* 449-468.
13. **Kozielski, K.L.**;***** Tzeng, S. Y.;***** Green, J. J.: siRNA nanomedicine: the promise of bioreducible materials. *Expert Review of Medical Devices* **2013**, *10*, 7-10.
14. Sunshine, J. C.; Akanda, M. I.; Li, D.; **Kozielski, K.L.**; Green, J. J.: Effects of base polymer hydrophobicity and end-group modification on polymeric gene delivery. *Biomacromolecules* **2011**, *12*, 3592-3600.
15. Reid, B.; Tzeng, S.; Warren, A.; **Kozielski, K.L.**; Elisseeff, J.: Development of a PEG Derivative Containing Hydrolytically Degradable Hemiacetals. *Macromolecules* **2010**, *43*, 9588-9590.
16. Saliaris, A. P.; Amado, L. C.; Minhas, K. M.; Schuleri, K. H.; Lehrke, S.; John, M. S.; Fitton, T.; Barreiro, C.; Berry, C.; Zheng, M.; **Kozielski, K.L.;** Eneboe, V.; Brawn, J.; Hare, J. M.: Chronic allopurinol administration ameliorates maladaptive alterations in Ca2+ cycling proteins and beta-adrenergic hyporesponsiveness in heart failure. *American Journal of Physiology-Heart and Circulatory Physiology* **2007**, *292*, H1328-H1335.

****These authors contributed equally***

Patents

1. Green, J.J.; **Kozielski, K.L.**; Tzeng, S.Y.; "Bioreducible Poly(beta-amino ester)s for siRNA Delivery" U.S. Patent Application PCT/US2013/066901 Filed: Oct 25, 2013. U.S. Prov. Patents 61/718.536 and 61/860,638.
2. Green, J.J.; Popel, A.S.; Sunshine, J.C.; Shmueli, R.B.; Tzeng, S.Y.; **Kozielski, K.L**.; "Polymeric Systems for Delivery of Peptides and Other Biological Agents" U.S. Prov. Patents 61/542,995 and 61/543,046. Filed: October 4, 2011.
3. Green, J.J.; Popel, A.S.; Sunshine, J.C.; Shmueli, R.B.; Tzeng, S.Y.; **Kozielski, K.L.;** "Peptide/particle delivery systems" U.S. Patent Application No. 13/272,042. Filed: October 12, 2011. U.S. Prov. Patent. 61/392,224. Optioned/Licensed.

Textbook Chapters

1. Kim, J.J.;***** **Kozielski, K.L.**;***** Wilson, D.R.;***** Green, J.J.: Biodegradable polymeric nanoparticles for gene delivery. In *Perspectives in Micro and Nanotechnology for Biomedical Applications*. Xu, C. and Chan, J.M. eds.; Imperial College Press: London, UK, 2015, *In press*.

Awards and Recognition

- Whitaker International Program Post-Doctoral Scholarship (2016)

- Johns Hopkins University Institute for Nanobiotechnology Annual Symposium Poster Competition Third Place Award (2016)
- Ruth L. Kirchstein F31 NIH National Research Service Award Fellowship, National Cancer Institute (2015-present)
- ARCS Foundation Scholarship recipient (2015-present)
- Founding Member of the JHU Graduate Women's Empowerment Network (2013-present)
- Founding Member, Vice President (2013-2015), and Academic Chair (2011-2013) of the Translational Tissue Engineering Center Student Association
- NSF Fellowship recipient to attend the International Summer School on Biocomplexity and Biodesign (2013)
- NIH Cancer Nanobiotechnology Training Center Fellowship recipient (2012)
- NSF GRFP Honorable Mention (2011 and 2012)
- Dean's list (2006-2010)
- Centennial Athletic Conference Honor Roll for volleyball (2009 and 2010)
- Vice President (2008-2010) and Treasurer (2007-2008) of Johns Hopkins Society of Women Engineers

Invited Talks and Oral Conference Sessions

1. **Kozielski, K.L.**; Lopez-Bertoni, H.; Lal, B.; Vaughan, H.; Laterra, J.; Green, J.J. MicroRNA delivery via poly(beta-amino ester) nanoparticles as a treatment for human glioblastoma. *Presentation*. (2016) 10th World Biomaterials Congress, Montreal, QC Canada.
2. **Kozielski, K.L.**; Lopez-Bertoni, H.; Lal, B.; Vaughan, H.; Laterra, J.; Green, J.J. Environmentally triggered miRNA nanoparticles as a treatment for human glioblastoma. *Presentation*. (2015) US-Japan Symposium on Drug Delivery Systems, Lahaina, HI.
3. **Kozielski, K.L.**; Lange, R.; Green, J.J. Cutting Edge Treatment of Brain Tumors. *Presentation*. (2015) Johns Hopkins University School of Medicine Partnering Toward Discovery Seminar Series, Baltimore, MD.
4. **Kozielski, K.L.**; Green, J.J. Environmentally-triggered nanoparticles for selective and combinatorial delivery of siRNA and DNA for the treatment of brain cancer. *Presentation*. (2015) Johns Hopkins University Department of Biomedical Engineering Seminar Series, Baltimore, MD.
5. **Kozielski, K.L.**; Lopez-Bertoni, H.; Lal, B.; Vaughan, H.; Laterra, J.; Green, J.J. Nanoparticles for miRNA Delivery as a Potent and Combinatorial Treatment for Glioblastoma. *Presentation.* (2015) Biomedical Engineering Society Annual Meeting, Tampa, FL.
6. **Kozielski, K.L.**; Vaughan, H.; Kim, B.H.; Tzeng, S.Y.; Magraviti, A.M.; Wang, Y.; Guerrero-Cazares, H.; Quinones-Hinojosa, A.; Brem, H.; Tyler, B.; Green, J.J.: Poly(beta-amino ester) nanoparticles for selective and combinatorial delivery of siRNA and DNA to brain cancer. *Presentation*. (2015) 6th Annual Advanced Study Institute on Global Healthcare Challenges, Izmir, Turkey.
7. **Kozielski, K.L.**; Vaughan, H.; Kim, B.H.; Tzeng, S.Y.; Guerrero-Cazares, H.; Quinones-Hinojosa, A.; Green, J.J.: Poly(beta-amino ester) nanoparticles for selective and combinatorial delivery of siRNA to brain cancer. *Presentation*. (2015) Society for Biomaterials, Charlotte, NC.
8. **Kozielski, K.L.**; Vaughan, H.; Kim, B.H.; Tzeng, S.Y.; Guerrero-Cazares, H.; Quinones-Hinojosa, A.; Green, J.J.: Environmentally triggered nanoparticles for efficient and cancer-specific DNA and siRNA delivery to glioblastoma. *Presentation*. (2015) Johns Hopkins School of Medicine Neurooncology Monthly Research Meeting, Baltimore, MD.
9. **Kozielski, K.L.**; Vaughan, H.; Kim, B.; Tzeng, S.Y.; Guerrero-Cazares, H.; Quinones-Hinojosa, A.; Green, J.J.: Bioreducible nanoparticles for efficient and combinatorial siRNA delivery to primary human glioblastoma. *Presentation*. (2014) Johns Hopkins University Institute for Nanobiotechnology Mini Symposium, Baltimore, MD.
10. **Kozielski, K.L.**; Tzeng, S.Y. Hurtado de Mendoza, B.A.; Green, J.J. Environmentally triggered nanoparticles for efficient and cancer-specific siRNA delivery to primary human glioblastoma.

Presentation. (2014) 5th Annual Advanced Study Institute on Global Healthcare Challenges, Antalya, Turkey.

11. **Kozielski, K.L.**; Tzeng, S.Y.; Green, J.J. Crosslinked and bioreducible poly(beta-amino ester)-based nanoparticles for enhanced siRNA delivery. *Presentation.* (2013) BMES Annual Meeting, Seattle, WA.
12. **Kozielski, K.L.**; Tzeng, S.Y.; Green, J.J. Bioreducible, crosslinked nanoparticles for efficient and environmentally triggered siRNA delivery to human glioblastoma cells. *Presentation.* (2013) 12th Annual Summer School for Biocomplexity and Biodesign, Istanbul, Turkey.
13. **Kozielski, K.L.;** Green, J.J.: Bioreducible poly(beta-amino ester)s for siRNA delivery. *Presentation*. (2012) BMES Annual Meeting, Atlanta, GA.

Conference Abstracts and Poster Presentations

1. Bishop, C.J.; Tzeng, S.Y.; **Kozielski, K.L.**; Quinones-Hinojosa, A.; Green, J.J. Polymeric nanoparticle systems for non-viral gene delivery. *Presentation*. (2016) 10th World Biomaterials Congress, Montreal, QC Canada. Johns Hopkins University Institute for Nanobiotechnology Annual Symposium, Baltimore, MD.
2. Zamboni, C.; **Kozielski, K.L.**; Radant, N.; Higgins, L.J.; Pomper, M.G.; Green, J.J. Effective and cancer-specific siRNA delivery to human hepatocellular carcinoma cells mediated by poly(beta-amino ester) nanoparticles. *Presentation*. (2016) 10th World Biomaterials Congress, Montreal, QC Canada.
3. **Kozielski, K.L.**; Lopez-Bertoni, H.; Lal, B.; Vaughan, H.; Laterra, J.; Green, J.J. Environmentally triggered miRNA nanoparticles as a treatment for human glioblastoma. *Poster.* (2016)
4. Mangraviti, A.; Tzeng, S.Y.; Gullotti, D.; **Kozielski, K.L.**; Sarabia-Estrada, R.; Brem, H.; Tyler, B.; Olivi, A.; Green, J.J.; Quinones-Hinojosa, A. Brain Tumor Gene Delivery via Non-Viral Engineered Adipose Mesenchymal Stem Cells Extend Survival In Vivo. *Poster*. (2016) 84th AANS Annual Scientific Meeting, Chicago, IL.
5. Mangraviti, A.; Tzeng, S.Y.; Gullotti, D.; **Kozielski, K.L**.; Seng, M.; Abbadi, S.; Schiapparelli, P.; Sarabia-Estrada, R.; Brem, H.; Tyler, B.; Olivi, A.; Green, J.J.; Quinones-Hinojosa, A. Non-viral Genetically Engineered Adipose Mesenchymal Stem Cells for Brain Tumor Therapy. *Presentation.* (2015) Biomedical Engineering Society Annual Meeting, Tampa, FL.
6. Li, X.; **Kozielski, K.L.**; Cheng, Yu-Hao; Green, J.J.; Mao, H. Nanoparticle-mediated Transdifferentiation of Astrocytes into Non-glial Cells. *Presentation.* (2015) Biomedical Engineering Society Annual Meeting, Tampa, FL.
7. Mangraviti, A; Tzeng, S.Y.; **Kozielski, K.L.**; Wang, Y.; Jin, Y.; Gullotti, D.; Pedone, M.; Buaron, N.; Liu, A.; Wilson, D.; Hansen, S.; Rodriquez, F.; Gao, G.; DiMeco, F.; Brem, H.; Olivi, A.; Tyler, B.; Green, J.J. Polymeric Nanoparticles for Non-Viral Gene Therapy Extend Brain Tumor Survival *In Vivo. Poster*. (2015) Biomedical Engineering Society Annual Meeting, Tampa, FL.
8. Li, X.; Cheng, Y.; **Kozielski, K.L.**; Liu, H.; Green, J.J.; Mao, H.(2015) Tissue Engineering and Regenerative Medicine Society World Congress, Boston, MA.
9. **Kozielski, K.L.**; Vaughan, H.; Kim, B.H.; Tzeng, S.Y.; Mangraviti, A.; Wang, Y.; Guerrero-Cazares, H.; Quinones-Hinojosa, A.; Brem, H.; Tyler, B.; Green, J.J. Poly(β-amino ester) nanoparticles for selective and combinatorial delivery of siRNA and DNA to brain cancer. *Poster*. (2015) Johns Hopkins University Institute for Nanobiotechnology Annual Symposium, Baltimore, MD.
10. Zamboni, C.G.; Higgins, L.J.; **Kozielski, K.L.**; Minn, I.; Pomper, M.G.; Green, J.J.; Cancer-specific nanoparticles mediated DNA delivery to human hepatocellular carcinoma using synthetic poly(beta-amino ester) vectors. *Presentation*. (2015) Society for Interventional Radiology, Atlanta, GA.
11. Mangraviti A.M; Tzeng S.Y.; **Kozielski, K.L**.; Wang Y.; Jin Y.; Gullotti D.; Pedone M.; Buaron N.; Liu A.; Wilson D.R.; Hansen S.; Rodriguez F.; Gao G.D.; DiMeco F.; Brem H.; Olivi A.; Tyler B.; Green J.J.; Brain tumor non-viral gene therapy via polymeric nanoparticle extends survival in vivo. *Presentation.* (2015) AANS/CNS Section on Tumors, 11th Biennial Satellite Symposium, Washington D.C.
12. Hung, B.P.; Hutton, D.L.; **Kozielski, K.L**.; Bishop, C.J.; Naved, B.; Green, J.J.; Dorafshar, A.H.; Grayson, W.L. PDGF-BB enhances osteogenesis in adipose-derived but not marrow-derived

mesenchymal stem cells. *Poster*. (2014) Tissue Engineering and Regenerative Medicine International Society Annual Meeting, Washington, D.C.

13. **Kozielski, K.L.;** Vaughan, H.; Kim, B.; Tzeng, S.Y.; Green, J.J.; Environmentally triggered nanoparticles for efficient and cancer-specific siRNA delivery to primary human glioblastoma. *Poster*. (2014) Tissue Engineering and Regenerative Medicine International Society Annual Meeting, Washington, D.C.
14. Mangraviti, A.; Tzeng, S.Y.; Seng, M.; Abbadi, S.; **Kozielski, K.L.**; Schiapparelli, P.; Wijesekera, O.; Sarabia-Estrada, R.; Brem, H.; Tyler, B.; Olivi, A.; Green, J.J.; Quinones-Hinojosa, A.: BMP4-secreting hAdMSCs engineered with nanoparticles: A non-viral MSC-based therapy for glioblastoma. *Presentation*. (2014) 19th Annual Scientific Meeting of the Society for Neuro-Oncology, Miami, FL.
15. **Kozielski, K.L.**; Tzeng, S.Y.; Hurtado de Mendoza, B.A.; Green, J.J. Environmentally triggered, bioreducible nanoparticles for efficient and cancer-specific siRNA delivery to primary human glioblastoma cells. *Poster*. (2014) Johns Hopkins University Institute for Nanobiotechnology Annual Symposium, Baltimore, MD.
16. **Kozielski, K.L.;** Tzeng, S.Y.; Green, J.J. Bioreducible poly(beta-amino ester)s for siRNA delivery. *Poster.* (2013). Johns Hopkins University Institute for Nanobiotechnology Annual Symposium, Baltimore, MD.
17. Reid, B; **Kozielski, K.**; Elisseeff, J.H.: Modifying polyethylene glycol hydrogel degradation rate post-fabrication. *Poster.* (2009). BMES Annual Meeting, Pittsburgh, PA.

Research Experience

Johns Hopkins University Biomedical Engineering, Advisor: Dr. Jordan Green (2011-present)

- Creating a method to engineer stem cells isolated from patient adipose tissue to migrate to brain tumors and secrete tumor-killing factors (*Biomaterials* publication).
- Developing several technologies involving *in vitro* and *in vivo* delivery of therapeutic siRNA, miRNA, mRNA, and DNA with the goal of altering gene expression in human glioblastoma, Schwann cells, and adipose-derived, mesenchymal, and induced pluripotent stem cells for cancer therapy and tissue engineering. (*ACS Nano 2015, Stem Cells, Biomaterials Science* publications)
- Synthesized and characterized a new class of bioreducible polymers for siRNA delivery to primary human glioblastoma and demonstrated their tumor-selective delivery capabilities (*ACS Nano 2014, Chemical Communications* publications, co-inventor on patents)
- Characterized a library of gene delivery polymers including by using Nuclear Magnetic Resonance (*Biomacromolecules* publication)

University of California, Berkeley Chemical and Biomolecular Engineering, Advisor: Dr. David Schaffer (2010)

- Worked on a project using siRNA targeted at multiple regions of the HIV genome in order to prevent HIV infection in T cells.

Johns Hopkins University Biomedical Engineering, Advisor: Dr. Jennifer Elisseeff (2006- 2010)

- Contributed to a project designing a biodegradable poly(ethylene glycol) hydrogel. I assisted in elucidating and fine-tuning the chemical composition of randomly oxidized poly(ethylene glycol). (*Macromolecules* publication*)*
- Cultured primary and stem cells within a 3D hydrogel environment and analyzed their abilities to form cartilage *in vitro*.

Johns Hopkins University Division of Cardiology and Institute for Cell Engineering, Advisor: Dr. Joshua Hare (2005-2006)

- Ran biochemical analyses for a project studying the intracellular effect of heart failure treatment with the drug allopurinol. (*American Journal of Physiology-Heart and Circulatory Physiology* publication*)*

Extracurricular and Volunteer Experience

Johns Hopkins Graduate Women's Empowerment Network (GWEN) (2013-present)

GWEN was formed when fellow female colleagues and I realized how disconnected we were from other women at Hopkins and that the disparity of women in leadership roles often begins just after graduate school. Since founding GWEN in October 2013, we have organized monthly networking events, a speaker series featuring women in leadership roles in JHU, and began a monthly newsletter releasing student highlights and news involving women in science.

Johns Hopkins Translational Tissue Engineering Center (TTEC) Student Association (2011-2014)

The TTEC Student Association was formed to organize course and qualifying exam information for Cell and Tissue Engineering students within the JHU BME department, and to facilitate networking and collaboration within TTEC. As the founding members of TTECSA, fellow students and I have catalogued and clarified course and exam requirements, organized the annual TTEC retreat, coordinated student candidate interviews, and ran several social and networking events. I have served as Treasurer (2011-2013) and Vice President (2013-2014).

Johns Hopkins Center for Global Health, Tanzania (2011)

Two coworkers and I designed and built a bicycle-powered grain mill specific to the needs of subsistence farmers in East Africa. Through funding from JHU, we were able to travel to Kongwa, Tanzania to train locals to build, operate, and troubleshoot the grain mill.

Johns Hopkins Varsity Volleyball Team (2006-2010)

Maria Immaculata Children's Education Center of Nairobi (2008)

Maria Immaculata is an orphanage and school for orphaned and underprivileged children from the slums surrounding Nairobi, Kenya. While there, I taught geometry, algebra, and high school level biology in the secondary school and ran after school athletic activities for the students.

Johns Hopkins University Interfaith Center Katrina Relief Project (2007 and 2008)

I participated in construction projects to rebuild houses destroyed or damaged by Hurricane Katrina.

Johns Hopkins University Society of Women Engineers (2007-2010)

Teaching Assistant Experiences

Computing for Engineers and Scientists (2009)

This course employs MATLAB to teach programming and numerical computation for solving problems in engineering. I held weekly office hours, planned and lead review sessions, and organized and ran a lecture.

Cellular Engineering (2013)

This is an upper level undergraduate and graduate course teaching advanced topics in cell engineering such as gene delivery, synthetic biology, and modeling of cellular processes. I held weekly office hours, organized review sessions, and graded student's homeworks and exams.

Cell and Tissue Engineering Lab: Gene Delivery Lab Module (2014)

This is a laboratory-based course where students learn fundamental techniques required to work in a cell or tissue engineering lab such as cell culture, gene delivery, and encapsulating cells in

scaffolds. I ran the gene delivery lab module which involved preparing all lab materials, assisting students during experiments, and evaluating lab reports.

Molecules and Cells (2014)

This is a Biomedical Engineering undergraduate core course in which students learn fundamental topics in cell biology, genetics, and macromolecules. I held weekly office hours, planned and ran weekly course sections, graded exams, and organized review sections.

Mentoring

Bolivia Hurtado de Mendoza (2013)

Bolivia was an REU student from Columbus State University. She worked with me during the summer of 2013, work which led to her authorship on an *ACS Nano* paper and a conference poster. She has since been a research assistant at the Texas Tech University Health Sciences Center, and is currently a Dental Assistant and aspires to go to Dental School.

Barbara Kim (2013 – present)

Barbara is a Biomedical Engineering undergraduate at Johns Hopkins University. She has been working with me since her freshman year, and this work has led to authorship on 2 posters and 4 conference oral sessions. She will be applying to graduate school this coming fall.

Hannah Vaughan (2014)

Hannah is a Biomedical Engineering undergraduate at Duke University. She worked with me for the summer of 2014 doing research which has led to authorship on 2 posters and 4 talks. Hannah will be a Ph.D. student in the Johns Hopkins University Biomedical Engineering Program starting Fall 2016.

Casey Vantucci (2015)

Casey is an REU student from the University of Maryland majoring in Materials Science and Engineering who is worked for me the summer of 2015. She assisted me in analyzing *in vivo* experiments dealing with siRNA and DNA delivery to human brain cancer models. Casey will be a Ph.D. student in the Georgia Institute of Technology Biomedical Engineering Program starting Fall 2016.

Marissa Gionet-Gonzalez (2015)

Marissa is an REU student from the University of California Riverside studying Chemistry. She assisted me in optimizing nanoparticles for intravenous delivery by making them more stable in the bloodstream. Marissa will be a Ph.D. student in the UC Davis Biomedical Engineering Program starting Fall 2016.